COENZYME BIOSYNTHESIS AND DELIVERY IN THE ETHANOLAMINE UTILIZATION METABOLOSOME

by

FLAVIA GISELA COSTA

(Under the Direction of Jorge C. Escalante-Semerena)

ABSTRACT

Corrinoids are characterized by a tetrapyrrole ring coordinating a central cobalt ion. The coenzymic form adenosylcobalamin (AdoCbl) is required by species in all domains of life. However, only a few prokaryotes including *S. enterica* can produce AdoCbl *de novo*. Additionally, organisms that scavenge incomplete corrinoids must encode an ATP:Co(I)rrinoid adenosyltransferase (ACAT) to activate the vitamin form to the coenzymic form.

There are three families of ACATs, which are named CobA, PduO and EutT. Structural and mechanistic understanding of the CobA and PduO families of ACATs is extensive, however relatively little is known about the EutT family of ACATs. In *S. enterica,* EutT (*Se*EutT) is a metalloenzyme, and requires Fe(II). The residues that bind Fe(II) in *Se*EutT are not conserved in the EutT homologues of *Firmicutes* such as *Listeria monocytogenes*. Biochemical characterization of the metal-less EutT from *L. monocytogenes* (*Lm*EutT) revealed that *Lm*EutT belongs to a second class of EutT-type ACATs whose mechanism proceeds in a metal-independent manner.

Analysis of *Lm*EutT revealed sequence homology to the *Lactobacillus reuteri* PduO (*Lr*PduO) corresponding to residues that form the ATP-binding site and formation of an intersubunit salt bridge in *Lr*PduO. Mutation analyses of these residues in *Lm*EutT and

characterization of the resulting variants suggests a substrate binding mechanism for *Lm*EutT analogous to *Lr*PduO.

The product of EutT, AdoCbl, is required in the catabolism of ethanolamine. The ability to utilize this metabolite provides *S. enterica* a competitive advantage over the course of infection. *S. enterica* metabolizes ethanolamine in a proteinaceous compartment (metabolosome) that sequesters the reactive intermediate acetaldehyde. In *S. enterica,* the functions for ethanolamine catabolism are encoded in the ethanolamine utilization (*eut*) operon, including EutT, the AdoCbl-dependent enzyme ethanolamine ammonia-lyase (EAL), and the reactivase EutA. *In vivo* and *in vitro* studies described herein suggest that EutT, EutA and EAL are localized to the metabolosome, and that EutA and EAL interact.

INDEX WORDS: Cobalamin, ATP:Co(I)rrinoid adenosyltransferases, cobalt reduction, *Listeria monocytogenes, Salmonella enterica,* ethanolamine metabolism, chaperone

COENZYME BIOSYNTHESIS AND DELIVERY IN THE ETHANOLAMINE UTILIZATION METABOLOSOME

by

FLAVIA GISELA COSTA

B.S., University of Minnesota, 2013

A Dissertation Submitted to the Graduate Faculty of The University of Georgia in Partial Fulfillment of the Requirements for the Degree

DOCTOR OF PHILOSOPHY

ATHENS, GEORGIA

2020

COENZYME BIOSYNTHESIS AND DELIVERY IN THE ETHANOLAMINE UTILIZATION METABOLOSOME

by

FLAVIA G. COSTA

Major Professor: Jorge Escalante-Semerena

Committee: Diana Downs
Timothy Hoover
Zachary Lewis

Electronic Version Approved:

Ron Walcott
Dean of the Graduate School
The University of Georgia
December 2020

DEDICATION

To my parents, who worked incredibly hard and made many sacrifices so that I could have better opportunities. Thank you for your continuous support, and for raising me with the core values of perseverance, integrity, and kindness.

Also, to my partner, Andrew, who has been supportive of my growth both personally and professionally.

ACKNOWLEDGEMENTS

Research is a collaborative pursuit, and this work would not be possible without the feedback, advice, collaboration, and support of my advisors, mentors, and colleagues. First, thank to my committee; Dr. Jorge Escalante-Semerena, Dr. Diana Downs, Dr. Timothy Hoover, and Dr. Zachary Lewis. Your feedback was instrumental to the development of this work. A special thank you to my advisor, Dr. Jorge Escalante-Semerena. You never wavered in your support of my work, and belief in my potential. I will greatly miss our brainstorming sessions and discussions. Additionally, thank you to Dr. Diana Downs, who encouraged my professional growth.

Thank you as well to all of the Escalab members, both past and present. I am so lucky to have worked alongside such great people and scientists who have provided feedback, support, ideas, and friendship. In particular, the feedback and advice from Dr. Theodore Moore, Dr. Norbert Tavares, and Dr. Chelsey Vandrisse, and Dr. Rachel Burckhardt were instrumental to this work. Many members of the Downs lab and Szymanski lab were also helpful in these aspects, and I am thankful for that as well.

Thank you to our collaborator at the University of Wisconsin-Madison, Dr. Thomas Brunold, and his graduate students Dr. Nuru Stracey, Elizabeth Greenhalgh, and Laura Elmendorf. The collaboration was both productive and exciting, and I enjoyed working together despite the long distance.

Thank you to my undergraduate research advisor Dr. Jeffrey Gralnick, and his post-doctoral fellow at the time Dr. Evan Brutinel. Their mentorship changed my career trajectory for

the better. Additionally, thank you to Dr. Dianne Newman, who offered an opportunity to advance my research skills, and encouraged me to apply to graduate school.

TABLE OF CONTENTS

Page

CHAPTER 1

INTRODUCTION

Corrinoids are complex macromolecules comprised of a cobalt-containing tetrapyrrole and an upper and lower ligand. The most well-studied corrinoid adenosylcobalamin (AdoCbl) is required in humans, and defects in transport or activation results in severe metabolic disorders.[1] Additionally, corrinoids play important roles in modulating the gut community, detoxification processes, and bacterial pathogenesis.[2-6] Despite the requirement for AdoCbl by many organisms, only a handful of prokaryotes such as *Salmonella enterica* are known to synthesize AdoCbl *de novo*.[7] The study of AdoCbl biosynthesis and use in *S. enterica* has provided a biochemical and genetic framework for understanding the diversity of AdoCbl-producing and AdoCbl-utilizing enzymes. While much is known about these processes, key questions regarding structure, mechanism, and localization of processes involved in AdoCbl biosynthesis and use remain unanswered. This introduction and the following literature review provides an overview of the biosynthesis and use of AdoCbl in *Salmonella enterica*, with emphasis on the corrinoid adenosylation step and its role in ethanolamine metabolism. The work that follows describes a second class of EutT-type ATP:Co(I)rrinoid adenosyltransferases, and identifies substrate-binding residues for this structurally uncharacterized family of enzymes. Then, the delivery of AdoCbl from EutT to the recipient enzyme ethanolamine ammonia-lyase is investigated.

1.1 ATP:CO(I)RRINOID ADENOSYLTRANSFERASES

ATP:Co(I)rrinoid adenosyltransferases (ACATs) refer to a group of enzymes that transfer the adenosyl group from ATP to a corrinoid substrate, forming a Co–C organometallic bond.[8] The reaction requires Co(I) cobamide substrate, however in solution the Co(II) → Co(I) cannot be performed by physiological reductants.[9] ACAT enzymes facilitate this reduction step by displacing the lower ligand, raising the redox potential of Co(II) → Co(I) from approximately -610 mV to approximately -360 mV.[10, 11] Thus, ACATs both prepare the corrinoid substrate for reduction, and position the corrinoid and ATP substrate for the adenosylation reaction.

There are three families of ACATs that are known, namely CobA, PduO and EutT. *S. enterica* encodes a homolog from each of these families of ACATs, and much of our knowledge of these enzymes stems from *S. enterica.* In *S. enterica,* CobA is the "housekeeping" corrinoid adenosyltransferase, and is required for *de novo* corrinoid biosynthesis and adenosylation of scavenged corrinoids.[12] CobA activity is also required for activation of transcription of the ethanolamine utilization (*eut*) operon.[13] In *S. enterica,* PduO is dedicated to propanediol utilization (*pdu*).[14-16] PduO adenosylates Cbl for use by the propanediol dehydratase.[17] Both CobA and PduO have been studied in detail, and structures with the substrates bound have been elucidated.[18, 19]

EutT is associated with ethanolamine metabolism in *S. enterica*. To date, a structure of EutT has not been reported, although insights into the mechanism of the *S. enterica* enzyme have been published.[20-22]. Unlike CobA and PduO, *S. enterica* EutT (*Se*EutT) requires ferrous ions for activity. It is known that Fe(II) binds to a cysteine-rich binding motif of *Se*EutT $HX_{11}CCXXC$,[20, 23] and recent work suggests that the metal promotes the formation of the DMB-off, four-coordinate Co(II)Cbl substrate bound to the active site of *Se*EutT.[21, 22]

1.2 ETHANOLAMINE METABOLISM

Ethanolamine is a by-product of phospholipid degradation, and is abundant in the intestinal environment.[24] Several prokaryotes catabolize ethanolamine as a source of carbon, nitrogen and energy [reviewed in [25]]. This metabolic pathway and its regulation has been well studied in *Salmonella enterica*, and its role in pathogenesis and food microbiology has been documented.[26, 27] In *S. enterica* and other *Enterobacteriaceae,* ethanolamine metabolism is encoded in the 17-gene *eut* operon.[28, 29] Together, these functions regulate operon expression, transport and catabolize ethanolamine, and form a proteinaceous compartment called the metabolosome.[30, 31] During ethanolamine catabolism, the metabolosome maintains private cofactor pools, and sequesters the toxic acetaldehyde intermediate.[31, 32]

The first step of ethanolamine catabolism is performed by the AdoCbl-dependent enzyme ethanolamine ammonia-lyase (EAL).[33-35] EAL binds to AdoCbl (adenosylcobalamin, AdoCbl) and homolytically cleaves the Co - C bond, forming an adenosyl radical that carries out the molecular rearrangement of ethanolamine to acetaldehyde.[36, 37] This radical can become quenched, resulting in EAL bound to inactive Cbl (cobalamin, Cbl).[38] Encoded in the *eut* operon, a reactivase EutA promotes EAL's release of Cbl and binding of AdoCbl, restoring EAL's activity.[39] As mentioned earlier, EutT is also encoded in the operon. It is currently unknown if EutA or EutT are localized to the metabolosome, and the mechanism of delivery of AdoCbl to EAL has not been defined.

1.3 DISSERTATION OUTLINE

In the content that follows, I describe my efforts to advance our understanding of the EutT family of ATP:Co(I)rrinoid adenosyltransferases (ACATs) and the delivery and recycling of AdoCbl in the context of ethanolamine metabolism.

Chapter 2 provides a comprehensive literature review of AdoCbl biosynthesis and utilization in *S. enterica*, with an emphasis on ACAT enzymes and ethanolamine utilization.

Chapter 3 describes a second class of EutT-type ACATs found in *Firmicutes*. Unlike the *S. enterica* EutT characterized previously, the EutT from *Listeria monocytogenes* (*Lm*EutT) does not contain a cysteine motif for binding metal and does not require a metal for function. Additional biochemical characterization determined aspects such as substrate specificity and oligomerization were unique from previously studied ACATs. This work expands the biochemical diversity of the EutT family of ACATs and develops our understanding of a novel class of EutTs.

Chapter 4 compiles the results of a mutagenic analysis of *Lm*EutT. These data suggest that the nucleotide-binding site and intersubunit salt bridge residues are conserved between the PduO family of ACATs and the EutT family of ACATs. These results also suggest that the PduO and EutT ACAT families are evolutionarily related. Despite these similarities in the core structure, a key residue involved in the mechanism of base displacement in EutT was not identified, suggesting this mechanism is different between PduO and EutT ACATs.

Chapter 5 includes the results of microscopic and biochemical approaches aimed at understanding the location and interactions of EutT, EutA and EAL. Localization studies using immunogold-labeling and transmission electron microscopy show that EAL, EutA and EutT are localized to the metabolosome. *In vivo* and *in vitro* evidence of interactions between EutA and EAL are also described. Together, these results suggest that AdoCbl may be recycled in the *eut* metabolosome.

Appendix I investigates the mechanism of *Lm*EutT spectroscopically in order to better understand the Co(II) → Co(I) reduction and adenosyltransferase mechanism of this class of EutT ACATs. These studies found that like PduO, *Lm*EutT binds ATP prior to binding cobalamin (Cbl).

However, like *Se*EutT, *Lm*EutT can bind to the incomplete corrinoid cobinamide (Cbi) but it cannot convert Cbi to a 4C Co(II) species.

1.4 REFERENCES

1. Fowler, B.; Leonard, J. V.; Baumgartner, M. R., Causes of and diagnostic approach to methylmalonic acidurias. *J. Inherited Metab. Dis.* **2008,** *31*, 350-360.

2. Degnan, P. H.; Barry, N. A.; Mok, K. C.; Taga, M. E.; Goodman, A. L., Human gut microbes use multiple transporters to distinguish vitamin B_{12} analogs and compete in the gut. *Cell Host Microbe* **2014,** *15*, 47-57.

3. Degnan, P. H.; Taga, M. E.; Goodman, A. L., Vitamin B_{12} as a modulator of gut microbial ecology. *Cell Metab.* **2014,** *20*, 769-778.

4. Thiennimitr, P.; Winter, S. E.; Winter, M. G.; Xavier, M. N.; Tolstikov, V.; Huseby, D. L.; Sterzenbach, T.; Tsolis, R. M.; Roth, J. R.; Baumler, A. J., Intestinal inflammation allows *Salmonella* to use ethanolamine to compete with the microbiota. *Proc. Natl. Acad. Sci. U.S.A.* **2011,** *108*, 17480-17485.

5. Fetzner, S.; Lingens, F., Bacterial dehalogenases: biochemistry, genetics, and biotechnological applications. *Microbiol. Rev.* **1994,** *58*, 641-685.

6. Yoo, W.; Kim, D.; Yoon, H.; Ryu, S., Enzyme IIA^{Ntr} regulates *Salmonella* invasion via 1,2-propanediol And propionate catabolism. *Sci. Rep.* **2017,** *7*, 44827.

7. Roth, J. R.; Lawrence, J. G.; Bobik, T. A., Cobalamin (coenzyme B_{12}): synthesis and biological significance. *Annu. Rev. Microbiol.* **1996,** *50*, 137-181.

8. Mera, P. E.; Escalante-Semerena, J. C., Multiple roles of ATP:Cob(I)alamin adenosyltransferases in the conversion of B_{12} to coenzyme B_{12}. *Appl. Microbiol. Biotechnol.* **2010,** *88*, 41-48.

9. Mera, P. E.; Escalante-Semerena, J. C., Dihydroflavin-driven adenosylation of 4-coordinate Co(II) corrinoids: are cobalamin reductases enzymes or electron transfer proteins? *J. Biol. Chem.* **2010,** *285*, 2911-2917.

10. Stich, T. A.; Buan, N. R.; Escalante-Semerena, J. C.; Brunold, T. C., Spectroscopic and computational studies of the ATP:Corrinoid adenosyltransferase (CobA) from *Salmonella enterica*: Insights into the mechanism of adenosylcobalamin biosynthesis. *J. Am. Chem. Soc.* **2005,** *127*, 8710-8719.

11. Lexa, D.; Saveant, J.-M., The electrochemistry of vitamin B_{12}. *Acc. Chem. Res.* **1983,** *16*, 235-243.

12. Escalante-Semerena, J. C.; Suh, S. J.; Roth, J. R., *cobA* function is required for both *de novo* cobalamin biosynthesis and assimilation of exogenous corrinoids in *Salmonella typhimurium*. *J. Bacteriol.* **1990,** *172*, 273-280.

13. Buan, N. R.; Suh, S. J.; Escalante-Semerena, J. C., The *eutT* gene of *Salmonella enterica* encodes an oxygen-labile, metal-containing ATP:corrinoid adenosyltransferase enzyme. *J. Bacteriol.* **2004,** *186*, 5708-5714.

14. Jeter, R. M., Cobalamin-dependent 1,2-propanediol utilization by *Salmonella typhimurium*. *Journal of General Microbiology* **1990,** *136*, 887-896.

15. Kerfeld, C. A.; Heinhorst, S.; Cannon, G. C., Bacterial microcompartments. *Annu. Rev. Microbiol.* **2010,** *64*, 391-408.

16. Chowdhury, C.; Sinha, S.; Chun, S.; Yeates, T. O.; Bobik, T. A., Diverse bacterial microcompartment organelles. *Microbiol. Mol. Biol. Rev.* **2014,** *78*, 438-468.

17. Johnson, C. L.; Pechonick, E.; Park, S. D.; Havemann, G. D.; Leal, N. A.; Bobik, T. A., Functional genomic, biochemical, and genetic characterization of the *Salmonella pduO* gene, an ATP:cob(I)alamin adenosyltransferase gene. *J. Bacteriol.* **2001,** *183*, 1577-1584.

18. Moore, T. C.; Newmister, S. A.; Rayment, I.; Escalante-Semerena, J. C., Structural insights into the mechanism of four-coordinate cob(II)alamin formation in the active site of the *Salmonella enterica* ATP:co(I)rrinoid adenosyltransferase (CobA) enzyme: Critical role of residues Phe91 and Trp93. *Biochemistry* **2012,** *51*, 9647-9657.

19. St Maurice, M.; Mera, P. E.; Taranto, M. P.; Sesma, F.; Escalante-Semerena, J. C.; Rayment, I., Structural characterization of the active site of the PduO-type ATP:Co(I)rrinoid adenosyltransferase from *Lactobacillus reuteri*. *J. Biol. Chem.* **2007,** *282*, 2596-2605.

20. Moore, T. C.; Mera, P. E.; Escalante-Semerena, J. C., the EutT enzyme of *Salmonella enterica* is a unique ATP:Cob(I)alamin adenosyltransferase metalloprotein that requires ferrous ions for maximal activity. *J. Bacteriol.* **2014,** *196*, 903-910.

21. Pallares, I. G.; Moore, T. C.; Escalante-Semerena, J. C.; Brunold, T. C., Spectroscopic studies of the EutT adenosyltransferase from *Salmonella enterica*: Mechanism of four-coordinate Co(II)Cbl formation. *J. Am. Chem. Soc.* **2016,** *138*, 3694-3704.

22. Pallares, I. G.; Moore, T. C.; Escalante-Semerena, J. C.; Brunold, T. C., Spectroscopic studies of the EutT adenosyltransferase from *Salmonella enterica*: Evidence of a tetrahedrally coordinated divalent transition metal cofactor with cysteine ligation. *Biochemistry* **2017,** *56*, 364-375.

23. Buan, N. R.; Escalante-Semerena, J. C., Purification and initial biochemical characterization of ATP:Cob(I)alamin adenosyltransferase (EutT) enzyme of *Salmonella enterica*. *J. Biol. Chem.* **2006,** *281*, 16971-16977.

24. Larson, T. J.; Ehrmann, M.; Boos, W., Periplasmic glycerophosphodiester phosphodiesterase of *Escherichia coli*, a new enzyme of the *glp* regulon. *J. Biol. Chem.* **1983,** *258*, 5428-5432.

25. Kaval, K. G.; Garsin, D. A., Ethanolamine utilization in bacteria. *mBio* **2018,** *9*.

26. Anderson, C. J.; Kendall, M. M., Location, location, location. *Salmonella* senses ethanolamine to gauge distinct host environments and coordinate gene expression. *Microb. Cell* **2016,** *3*, 89-91.

27. Srikumar, S.; Fuchs, T. M., Ethanolamine utilization contributes to proliferation of *Salmonella enterica* serovar Typhimurium in food and in nematodes. *Appl. Environ. Microbiol.* **2011,** *77*, 281-290.

28. Roof, D. M.; Roth, J. R., Functions required for vitamin B_{12}-dependent ethanolamine utilization in *Salmonella typhimurium*. *J. Bacteriol.* **1989,** *171*, 3316-3323.

29. Kofoid, E.; Rappleye, C.; Stojiljkovic, I.; Roth, J., The 17-gene ethanolamine (*eut*) operon of *Salmonella typhimurium* encodes five homologues of carboxysome shell proteins. *J. Bacteriol.* **1999,** *181*, 5317-5329.

30. Chowdhury, C.; Sinha, S.; Chun, S.; Yeates, T. O.; Bobik, T. A., Diverse bacterial microcompartment organelles. *Microbiol. Mol. Biol. Rev.* **2014,** *78*, 438-468.

31. Brinsmade, S. R.; Paldon, T.; Escalante-Semerena, J. C., Minimal functions and physiological conditions required for growth of *Salmonella enterica* on ethanolamine in the absence of the metabolosome. *J. Bacteriol.* **2005,** *187*, 8039-8046.

32. Huseby, D. L.; Roth, J. R., Evidence that a metabolic microcompartment contains and recycles private cofactor pools. *J. Bacteriol.* **2013,** *195*, 2864-2879.

33. Chang, G. W.; Chang, J. T., Evidence for the B_{12}-dependent enzyme ethanolamine deaminase in *Salmonella*. *Nature* **1975,** *254*, 150-151.

34. Mori, K.; Oiwa, T.; Kawaguchi, S.; Kondo, K.; Takahashi, Y.; Toraya, T., Catalytic roles of substrate-binding residues in coenzyme B_{12}-dependent ethanolamine ammonia-lyase. *Biochemistry* **2014,** *53*, 2661-2671.

35. Jones, A. R.; Rentergent, J.; Scrutton, N. S.; Hay, S., Probing reversible chemistry in coenzyme B_{12}-dependent ethanolamine ammonia lyase with kinetic isotope effects. *Chemistry* **2015,** *21* (24), 8826-8831.

36. Banerjee, R., *Chemistry and Biochemistry of B_{12}*. John Wiley & Sons: 1999; p 3-6.

37. Nforneh, B.; Bovell, A. M.; Warncke, K., Electron spin-labelling of the EutC subunit in B_{12}-dependent ethanolamine ammonia-lyase reveals dynamics and a two-state conformational equilibrium in the N-terminal, signal-sequence-associated domain. *Free Radical Research* **2018,** *52*, 307-318.

38. Kaplan, B. H.; Stadtman, E. R., Ethanolamine deaminase, a cobamide coenzyme-dependent enzyme. I. Purification, assay, and properties of the enzyme. *J. Biol. Chem.* **1968,** *243*, 1787-1793.

39. Mori, K.; Bando, R.; Hieda, N.; Toraya, T., Identification of a reactivating factor for adenosylcobalamin-dependent ethanolamine ammonia lyase. *J. Bacteriol.* **2004,** *186*, 6845-6854.

CHAPTER 2: LITERATURE REVIEW

BIOSYNTHESIS AND USE OF ADENOSYLCOBALAMIN IN *SALMONELLA ENTERICA*

2.1 INTRODUCTION

The term cobamide (Cba) refers to a group of brightly pigmented, cobalt-containing tetrapyrroles. The most well-studied cobamide and the focus of this work, cobalamin (Cbl), was initially discovered in 1948 in liver extracts, and its structure was determined in 1956. Since then, multi-disciplinary scientific contributions have revealed the diverse strategies for the assembly and use of these complex macromolecules.[1] Despite the widespread requirement for cobamides in all domains of life, the *de novo* biosynthesis of these macromolecules is restricted to a few genera of prokaryotes and archaea.[2]

Although a handful of organisms produce corrinoids *de novo*, the complete set of genes encoding the functions involved in cobamide assembly has not yet been identified in any one organism. The biosynthetic pathway for cobalamin begins at uroporphyrinogen, from which the biosynthesis of heme, coenzyme F_{430}, siroheme, and heme d_1 are also derived.[3] From uroporphyrinogen, the biosynthetic pathway of adenosylcobalamin (AdoCbl) commits to one of two pathways. In the anaerobic pathway, the cobalt is inserted into the tetrapyrrole ring early in the pathway, prior to modification of the tetrapyrrole ring. In the other pathway, the cobalt is inserted into the tetrapyrrole ring once the tetrapyrrole ring modifications are completed. These pathways converge into the pathway where the nucleotide loop is synthesized and attached to the corrin ring, ultimately producing adenosylcobalamin (AdoCbl). In humans, AdoCbl delivery to

the AdoCbl-dependent enzyme is mediated through direct protein-protein interactions. In prokaryotes, the mechanism of AdoCbl is transfer is unknown.[4] In *Salmonella enterica,* AdoCbl is synthesized *de novo,* and there are three known AdoCbl-dependent enzymes; epoxyqueuosine reductase, ethanolamine ammonia-lyase, and 1,2-propanediol dehydratase. Cobalamin also acts as a methyl carrier in the biosynthesis of methionine in *S. enterica*.[5] The AdoCbl-dependent enzymes generate an adenosyl radical from the coenzyme, which mediates some of the most chemically challenging reactions in the cell.[6-8]

The ability of *S. enterica* to produce AdoCbl *de novo* and its genetic tractability has proved to be a useful framework for understanding the biosynthesis and use of this coenzyme in other organisms. This review details the biosynthesis of AdoCbl in *S. enterica* and the AdoCbl-dependent processes in *S. enterica* as the backdrop for the subsequent studies detailed in this dissertation.

2.2 ADENOSYLCOBALAMIN STRUCTURE

Adenosylcobalamin (AdoCbl) is a complex macromolecule with several terms that describe aspects of the structure or precursors. The structure of AdoCbl and the labeling of its components are depicted in Figure 2.1. The upper face of the ring is known as the beta (*Coβ*) face, the lower face is known as the alpha (*Coα*) face. Likewise, the β ligand is attached to the Co on the upper face of the ring, and the α ligand is attached to Co on the lower face of the ring. Cobyric acid (Cby) refers to the decorated tetrapyrrole ring with the cobalt center (Fig. 2.1). Attachment of an aminopropanol-phosphate (AP-P) moiety to the propionyl substituent of ring D produces cobinamide-phosphate (Cbi-P), which when dephosphorylated is termed cobinamide (Cbi).[9] The completed corrinoid, cobalamin (Cbl) contains a nucleotide loop attached to the aminopropanol linker, where 5,6-dimethylbenzimidazole is the base (α-ligand) of the nucleotide loop. For

adenosylcobalamin (AdoCbl), the upper (*Coβ*) ligand is 5' deoxyadenosyl, forming a Co – C organometallic bond. Other ligands can be attached, such as CN– (forms cyanocobalamin, CNCbl) or HO– (forms hydroxocobalamin, HOCbl).

2.3 *DE NOVO* BIOSYNTHESIS: FROM UROPORPHYRINOGEN III TO ADENOSYLCOBYRINIC ACID

There are two major pathways for the biosynthesis of the corrin component of cobamides, which are referred to as the aerobic and anaerobic pathways.[10] The aerobic route has a requirement for molecular oxygen, and cannot operate under anaerobic conditions.[11] Additionally, in the aerobic route cobalt is inserted later in the pathway.[12] In contrast, the anaerobic route does not require molecular oxygen, and can operate anaerobically.[13] In the anaerobic pathway, the cobalt is inserted early in the pathway, before ring contraction.[14-18] Due to this, many of the intermediates of the anaerobic pathway are particularly susceptible to damage by oxygen, and so the pathway operates more efficiently in the absence of oxygen.[13] *S. enterica* utilizes the anaerobic route, which is shown in Figure 2.2. *S. enterica* represses the corrinoid biosynthesis genes in the presence of cobalamin or oxygen, so *de novo* ring formation in AdoCbl biosynthesis is restricted to anaerobic conditions in this organism.[19] Aside from these key differences, the methylations, decarboxylations, amidations, and adenosylations are similar, and these similarities are reflected in the homologous enzymes present between these two pathways.[20]

Cobyric acid is synthesized from uroporphyrinogen III via a pathway that ultimately results in contraction of the ring.[21, 22] As outlined in Figure 2.2, the conversion of uroporphyrinogen III into adenosylcobyric acid involves several modifications. Notably, the addition of 7 SAM-derived methyl groups, loss of the C20 position, decarboxylation of the acetic acid side chain attached to C12, cobalt insertion, and amidation of the *a, b, c, d, e* and *g* side chains occur in this

portion of the pathway.[3] Overall, the conversion of porphyrinogen to adenosylcobyric acid involves 15 enzymatic steps.

From uroporphyrinogen III to adenosylcobyric acid, corrin ring construction requires a total of 8 methylations donated from *S*-adenosyl-L-methionine (SAM, Fig 2.2). These methyl groups are added in a specific order to the tetrapyrrole.[20, 23, 24] The synthesis of precorrin-2 involves the enzyme CysG.[25] The CysG enzyme methylates uroporphyrinogen III initially at the C2 position, to generate precorrin-1, and subsequently at C7 to give precorrin-2.[26] CysG utilizes SAM as the methyl donor at each step, and generates *S*-adenosyl-L-homocysteine (SAH). SAH binds tightly as a competitive inhibitor, regulating the biosynthetic process.[27] In *S. enterica,* siroheme is also synthesized from uroporphyrinogen by CysG, and in the absence of the cobaltochelatase CbiK, CysG can also insert the Co(II) ion.[25, 27, 28] While the structure of CysG highlights how the methylation and dehydrogenation steps occur, it is not clear how the enzyme is able to facilitate metal insertion.[27]

In the next step, precorrin-2 is oxidized by the NAD^+-dependent dehydrogenase SirC to form sirohydrochlorin, or factor II.[29] This introduces a double bond into the ring and stabilizes the framework into which the Co(II) ion is inserted. The insertion involves the cobaltochelatase CbiK, which inserts Co(II) through the removal of two protons from the pyrrole nitrogens in the central cavity of the macrocycle.[14, 17, 18, 30] The insertion of Co(II) into sirohydrochlorin generates Co(II)-sirohydrochlorin, also named Co(II)-factor II (Fig. 2.2). The structure of the protein shows an intersubunit active site, similar to the ferrochelatases associated with heme synthesis.[18, 31] Structures have been solved with both sirohydrochlorin and Co(II) bound to the protein, revealing two conserved histidine residues that are located above the central cavity of the bound sirohydrochlorin. These histidine residues help to position the Co(II) ion for insertion, and likely

help in the deprotonation of the pyrrole-nitrogens, thereby facilitating the insertion of the metal ion.[18]

The SAM-dependent methyltransferase, CbiL, methylates Co(II)-sirohydrochlorin at the C20 position, forming Co(II)-factor III.[32-34] This methylation is essential for the subsequent ring contraction, where the methylated C20 is ultimately released as acetaldehyde.[35-38] The enzyme can methylate Co(II)-sirohydrochlorin and Co(II)-precorrin-2.[34] The following step involves the methyltransferase CbiH, which methylates at the C17 position, converting Co(II)-factor III into Co(II)-precorrin-4.[13, 37] Another SAM-dependent methyltransferase reaction catalyzed by CbiF, converts Co(II)-precorrin-4 to Co(II)-precorrin-5A.[13, 33, 36, 39] CbiF was the first methyltransferase where the structure was determined, and it is active as a homodimer.[36, 40] Co(II)-precorrin-5A is the substrate of CbiG, which breaks the delta-lactone ring and releases the methylated C20 as acetaldehyde, generating Co(II)-precorrin-5B.[13, 36]

The subsequent step is catalyzed by the non-canonical methyltransferase CbiD.[13, 41] CbiD methylates Co(II)-precorrin-5B at the C1 position, resulting in Co(II)-precorrin-6A.[13] Co(II)-precorrin-6A reduced by CbiJ using NADH. This reduction removes the double bond between C18-C19, generating Co(II)-precorrin-6B [13]. The removal of this double bond provides greater flexibility to the corrin macrocycle, and forms a helical macrocycle structure dependent on the coordination state of the central cobalt ion.[42] This helicity is a key facet of cobalamin, and enhances the catalytic properties of the central cobalt ion. Co(II)-precorrin-6B is converted into Co(II)-precorrin-8 by the action of a fusion enzyme CbiET, which in some organisms consists of two separate enzymes (CbiE and CbiT).[43] CbiET carries out two methylation reactions at C5 and C15, as well as a decarboxylation of the acetic acid side chain attached to C12. While CbiE has a conical class III methyltransferase fold, CbiT has a class I fold.[44] Although the function of the fused CbiET

protein was confirmed, the individual roles of CbiE and CbiT have not been determined. It was hypothesized that CbiE performed a methylation at C5 while the CbiT component performed both the decarboxylation of the acetic acid side chain at C12 as well as the methylation at C15.[44]

Co(II)-precorrin-8 is the substrate for CbiC, which migrates the methyl group from C11 to C12.[13] The methyl migration from C11-C12 results in cobyrinic acid, which is the first stable intermediate of the anaerobic pathway.[13] Then, CbiA amidates the *c* side chain followed by the *a* side chain, to give cobyrinic *a,c*-diamide.[45] The CbiA enzyme belongs to the family of glutamine amidotransferases whereby ammonia is removed to form glutamate.[43, 45] The synthesis of cobyrinic acid *a,c*-diamide represents the point at which the aerobic and anaerobic corrin pathways re-join.

From the point of cobyrinic acid *a,c*-diamide synthesis, the corrinoid proceeds through the nucleotide loop biosynthesis pathway (Fig. 2.2). Enzymes in this pathway require an adenosylated intermediate, thus prior to entering this pathway, the corrinoid must be adenosylated.[46] In *de novo* biosynthesis of AdoCbl, CobA is the ATP:Co(I)rrinoid adenosyltransferase (ACAT) responsible for the adenosylation of cobyrinic acid prior to nucleotide loop biosynthesis.[46] CobA and the other two encoded ACATs in *S. enterica,* PduO and EutT, are discussed later in this chapter.

2.4 NUCLEOTIDE LOOP BIOSYNTHESIS AND ATTACHMENT

The nucleotide loop of cobalamin is characterized by some unique chemistry. Notably, there is an α-*N*-glycosidic bond between the ribose and the base, and a phosphodiester bond between the 3′-hydroxyl group of the ribosyl moiety of the nucleotide and the aminopropanol linker (Fig. 2.1). Only two other coenzymes, F_{420} and methanopterin, are known to contain this phosphodiester bond.[47-49]

The nucleotide loop is connected to the corrin ring via this phosphodiester bond by an aminopropanol-phosphate linker (Fig. 2.1). Aminopropanol-phosphate is generated from L-Thr-P

in *S. enterica* in two steps (Figure 2.2).[9, 50, 51] First, the threonine kinase PduX uses ATP to phosphorylate L-threonine, producing L-threonine-P.[51] PduX belongs to a class of kinases that shares a unique ATP-binding loop that is not found in other kinase families.[52] The enzyme PduX forms an ordered ternary complex by binding ATP first, then L-threonine, and may promote catalysis by transition state stabilization.[52] Then, the PLP-dependent enzyme L-Thr *O*-3-phosphate decarboxylase, CobD, converts L-Thr-P to aminopropanol-P (AP-P).[9] Structural determination of CobD revealed a large and small subunit that are connected by a section of random coil. Although CobD functions as a decarboxylase, the fold type and sequence of CobD is similar to PLP-dependent aminotransferases, suggesting a common evolutionary origin.[50] The PduX and CobD pair of enzymes is found in organisms that use the early-Co-insertion pathway for *de novo* adenosylcobamide (AdoCba) biosynthesis.[53] Adenosyl cobyric acid (AdoCby) enters the nucleotide loop assembly (NLA) pathway and is activated by attachment of this AP-P by the integral membrane protein CbiB to form the intermediate AdoCbi-P.[54, 55]

AdoCbi-P is then guanylylated by a bifunctional NTP:AdoCbl kinase/GTP:AdoCbi-P guanylyltransferase CobU, releasing pyrophosphate and AdoCbi-GDP (AdoCbi-GDP).[56, 57] The guanylyltransferase reaction is proposed to occur in two steps, where CobU guanylylates a histidine residue, forming a CobU-GMP covalent phosphoramidate bond, prior to the transfer of the GMP moiety to AdoCbi-P to generate AdoCbi-GDP.[57, 58] Structural information obtained of the CobU trimer and the CobU-GMP trimer intermediate demonstrate a significant change in the conformation of CobU upon guanylylation that forms a GMP-specific binding pocket for the second half of the reaction.[58] CobU only recognizes corrinoids with a nucleoside upper ligand, restricting the attachment of the nucleotide loop and synthesis of cobalamin to adenosylated intermediates.[46, 56, 59]

In the case of cobalamin, the nucleotide loop is attached to the base 5,6-dimethylbenzimidazole (DMB), which coordinates with the cobalt on the α face of the ring. In *S. enterica*, DMB is incorporated under microaerophillic conditions.[60] However, this is not the only corrinoid that *S. enterica* can produce. In the anoxic environment required for *de novo* Cbl biosynthesis, *S. enterica* will incorporate adenine, forming pseudo-cobalamin.[37] While *S. enterica* can synthesize DMB *de novo*, the enzymatic pathway has not been elucidated.[60, 61] Whether synthesized intracellularly or obtained from the extracellular environment, in *S. enterica*, DMB is activated by the (NaMN):DMB phosphoribosyltransferase CobT, which attaches the ribosyl-5'-phosphate moiety from nicotinate mononucleotide (NaMN) to DMB to form α-ribazole-5'-P (α-RP) and the by-product nicotinate (Fig. 2.2).[62, 63] *S. enterica* CobT (*Se*CobT) has broad substrate specificity for the base substrate, and is not only able to phosphoribosylate the preferred substrate DMB, but also other benzimidazoles and purines.[64]

Once activated to α-ribazole-5'-P, the nucleotide loop and base is attached to Ado-Cbi-GDP by the cobalamin 5'-phosphate synthase CobS in *S. enterica*.[65] CobS catalyzes the penultimate step in the pathway, forming AdoCbl-P.[66] Interestingly, CobS is an integral membrane protein, which raises questions about the localization of enzymes associated with the late steps of the AdoCba biosynthesis pathway.[65, 67, 68] The AdoCbl-P product is then dephosphorylated by the AdoCbl phosphatase CobC in bacteria, producing AdoCbl.[66, 69]

2.5 CORRINOID TRANSPORT AND SCAVENGING

Although *S. enterica* can synthesize AdoCbl *de novo*, the biosynthesis of AdoCbl is limited to anoxic conditions, while the biosynthesis of DMB is observed in microaerophilic conditions.[2, 60] Additionally, the biosynthetic pathway requires approximately 26 enzymes, making it an energetically expensive endeavor.[1] For uptake of corrinoids from the environment, *S. enterica*

encodes the corrinoid-specific outer membrane transporter BtuB, as well as the periplasmic chaperon and inner membrane transporter BtuCDF.[70] BtuB is a TonB-dependent outer membrane transporter that actively imports corrinoids into the periplasm.[71] The expression of *btuB* is controlled at the transcriptional level by a riboswitch that binds AdoCbl.[72-74] This transporter's affinity for corrinoids is greatly enhanced by calcium, where in the presence of calcium, the K_d decreases by approximately three logs to 5 nM.[75] Once the corrinoid is transported to the periplasm, the periplasmic protein BtuF captures the corrinoid with high affinity, and binds to the inner membrane transporter BtuCD.[76, 77] BtuCD then couples the transport of corrinoids into the cytoplasm with the hydrolysis of ATP.[70, 78]

Once the corrinoid is transported to the cytoplasm, *S. enterica* modulates the corrinoid for incorporation into the biosynthetic pathway. For example, cobinamide (Cbi) is an incomplete corrinoid that is salvaged by many organisms from their environments.[79] While Cbi is stable in the environment, it is not an intermediate of AdoCbl biosynthesis. To incorporate Cbi into the biosynthetic pathway, *S. enterica* CobA adenosylates Cbi to form AdoCbi (Figure 2.2).[46, 80, 81] This product is subsequently phosphorylated by the bifunctional NTP:AdoCbi kinase/GTP:AdoCbi-P guanylyltransferase CobU, after which it can enter the biosynthetic pathway as AdoCbi-P (Figure 2.2).[57, 82]

2.6 CORRINOID ADENOSYLATION

A variety of ligands can be covalently attached to the Co ion on the β face of the corrin ring. However, the biologically active form of cobalamin is adenosylcobalamin (AdoCbl).[83] Adenosylcobalamin utilized as a radical generator, and is required for several metabolic pathways that involve intramolecular rearrangements, dehydrations, deaminations, and reductive dehalogenations.[83] The adenosyl ligand is also required for the attachment of the nucleotide loop

to AdoCbi-P to produce AdoCbl.[46] Scavenged corrinoids are also adenosylated to incorporate into the biosynthetic pathway, or to regenerate AdoCbl.[84]

Corrinoid adenosylation is performed by a family of enzymes collectively called ATP:Co(I)rrinoid adenosyltransferases (ACATs).[46, 85, 86] These enzymes are categorized into three families named CobA, PduO, and EutT. Characterization of these ACAT families was done most extensively in *Salmonella enterica,* which encodes an ACAT homologue from each of these families.[46, 85-91] Studies of ACAT homologues from other organisms have also shed light onto the structures and mechanisms of these ACATs in *S. enterica*.[92-94] Despite the structural and biochemical diversity among the studied members of these ACAT families, the general mechanism is conserved across the ACAT families, which is summarized in Figure 2.3.

For the adenosylation reaction to occur, the cobalt ion in the corrinoid must be reduced in two consecutive reduction steps: from Co(III) to Co(II), and then from Co(II) to Co(I). In many organisms including *S. enterica*, the intracellular reducing environment drives the reduction of the Co(III) state to the five-coordinate (5C) Co(II) state non-enzymatically by free dihydroflavins.[95] The Co(II) to Co(I) reduction however, has a redox potential of -610 mV, lower than any known physiological reductant in the cell.[96] To solve this problem, the ACAT facilitates the formation of a 4-coordinate (4C) corrinoid within the active site, precluding the lower ligand from coordinating with the Co(II) ion (Fig. 2.3).[97-100] This conformation raises the redox potential of Co(II) → Co(I) by ~250 mV, making the reduction step accessible to dihydroflavins (Fig. 2.3).[97, 101] Once reduced, the Co(I)-cobamide acts as a nucleophile, attacking the 5'C of ATP and resulting in the adenosylated corrinoid and a phosphate by-product. The adenosylated corrinoid product then enters the nucleotide loop biosynthesis pathway as AdoCby acid or AdoCbi. If cobalamin, the AdoCbl is delivered to the target AdoCbl-dependent enzyme.[4, 102]

2.7 COBA

In *S.* enterica, *de novo* cobamide biosynthesis and scavenging of exogenous incomplete corrinoids requires corrinoid adenosylation by the ACAT CobA (*Se*CobA) prior to nucleotide loop attachment (Fig. 2.2).[46, 68, 87] CobA can also adenosylate scavenged incomplete corrinoids such as cobyric acid, cobinamide, as well as cobalamin (Figure 2.2).[46] In *S. enterica*, CobA provides a base level of AdoCbl for activities such as transcriptional activation of the ethanolamine utilization operon. In this manner, CobA in *S. enterica* is viewed as the housekeeping ACAT.[103] A CobA homologue from the methanogenic archaeon *Methanosarcina mazei* (*Mm*CobA) has also been characterized, highlighting differences in ion preference and nucleotide substrate specificity between these homologues.[104] *Se*CobA specific activity is higher with the nucleotide substrates CTP and UTP over ATP *in vitro.* Additionally, *Se*CobA demonstrates an absolute requirement for the 2'-OH of the ribose. On the other hand, *Mm*CobA prefers ATP as the nucleotide substrate and can also utilize deoxyribonucleotides, which lack the 2'-OH group.[88, 104] These differences in substrate affinity suggest that these two homologues bind the nucleotide substrate slightly differently. Both homologues release an inorganic triphosphate byproduct.[104]

While CobA from *S. enterica* adenosylates both complete and incomplete corrinoids, the formation of the 4C Co(II)-corrinoid substrate is improved for *Se*CobA with incomplete corrinoid substrates.[105] In contrast, *Mm*CobA adenosylates Cbl better than it adenosylates incomplete corrinoids.[104] Unlike other ACATs, which are able to utilize free dihydroflavins to accomplish the Co(II)→ Co(I) reduction, *Se*CobA utilizes reduced flavodoxin A ($FldA_{red}$) *in vitro*.[106, 107] The elucidated structure of *Se*CobA bound to ATP and 5C-Cbl or 4C-Cbl product reveals that *Se*CobA possesses an unusual inverted P-loop motif to bind the ATP substrate in a conformation that favors transfer of the Ado moiety instead of the γ-phosphate (Figure 2.4).[87, 108] *Se*CobA accomplishes

displacement of the α-ligand with residues Phe91 and Trp93, which position themselves in place of the α-ligand by movement of an entire loop of the structure, forming a closed conformation at the site.[87] Spectroscopic analysis of the interactions of *Se*CobA with its substrates provided the first mechanistic insight into how ACATs facilitate the reduction of Co(II)-cobamides.[105] In the presence of ATP, cobinamide bound to CobA exhibited a unique paramagnetic species that was interpreted as the 4C-Co(II)cobinamide state. In this state, the $3d_z^2$ molecular orbital is likely more stabilized, lowering the thermodynamic barrier for Co(II) → Co(I) reduction.[101]

2.8 PDUO

1,2-propanediol (1,2-PDL) metabolism is one of the AdoCbl-dependent processes in *S. enterica* discussed later in this review.[109] In *S. enterica,* the propanediol utilization (*pdu*) operon, which encodes functions for 1,2-PDL metabolism, is located adjacent to the *cbi*/*cob* operon that encodes functions for AdoCbl biosynthesis.[110, 111] The ACAT PduO is located in the *pdu* operon, and in *S. enterica,* PduO is the ACAT associated with 1,2-PDL metabolism. It is notable that in many organisms, PduO homologues function as the sole ACAT, or appear in a 1,2-propanediol-independent genetic context.[92, 112] Structural and biochemical information of PduO homologues has been elucidated from organisms such as *S. enterica* (*Se*PduO)*, Lactobacillus reuteri* (*Lr*PduO)*, Bacillus cereus*, *Burkholderia thailandensis, Sulfolobus tokodaii,* and the PduO homologue from *Homo sapiens* hATR.[92, 112-115] Notably, the *Lr*PduO homologue adenosylation of Cbl and Cbi supports AdoCbl-dependent growth *in vivo*, whereas the *Se*PduO homologue can only adenosylate Cbl sufficiently to support growth.[116] Interestingly, *Se*PduO and *Lr*PduO possess an extended C-terminal domain that is absent in hATR, and removal of this C-terminal domain does not affect the adenosyltransferase activity of either *Se*PduO or *Lr*PduO.[90, 117] Recently, the C-terminus of *Se*PduO was co-crystallized with heme, which it binds with high affinity. Although the

physiological role of this domain is unclear, it is speculated to have a role in electron transfer or redox sensing.[91]

The order of substrate binding for any ACAT was first determined with *Lr*PduO, which bound the nucleotide substrate first. The PduO homologues to date characterized prefer ATP as the nucleotide substrate.[90, 92] *Lr*PduO also demonstrates activity with other ribonucleotides with exception for TTP, and can also adenosylate with 2'-deoxy-ATP.[92] As a by-product of corrinoid adenosylation, *Lr*PduO, like CobA, releases inorganic triphosphate.[90] All PduO homologues characterized to date form biologically active trimers, where the substrate binding site is located in each intersubunit cleft.[116] Crystal structures of *Lr*PduO and other homologues reveal that the ATP-binding motif is unique, and requires side chains located throughout the amino acid sequence, including in the core alpha-helices of the enzyme, which together form the active site at the intersubunit cleft.[116] In the crystal structure, an intersubunit Asp – Arg salt bridge was identified in the active site.[116] The most common mutation of the PduO homologue human adenosyltransferase (hATR) resulting in methylmalonic aciduria occurs at the corresponding arginine in the *Lr*PduO salt bridge in hATR.[92] Mutational analysis of this salt bridge suggests that the arginine plays a critical role in ATP affinity, even though it is relatively distant from the nucleotide substrate.[92] A double mutation that switched the position of the aspartate and arginine residues preserved the salt bridge, but resulted in an inactive enzyme. These results suggest that the arginine is somehow involved in the reaction, however its exact involvement is still unclear.[92]

Structural, spectroscopic and biochemical studies of *Lr*PduO confirmed that LrPduO facilitates the conformation of 4C Co(II)-cobalamin by displacing the α-ligand with a phenylalanine residue (Fig. 2.5, panel B).[93, 98] Variants with mutations at the Phe112 residue were also crystallized and demonstrated that absence of the bulky phenylalanine residue resulted in Cbl

bound to the active site with the DMB base still coordinating with the Co(II), preventing the Co(II) → Co(I) reduction, thus preventing the adenosylation reaction from proceeding (Figure 2.5, panel C and D). Replacement with a histidine resulted in a conformation where the DMB ligand was displaced, however the coordination of the histidinyl residue with Co(II) again prevented the reaction from proceeding.[93]

2.9 EUTT

In *S. enterica,* the ACAT EutT is encoded in the ethanolamine utilization (*eut*) operon, and is thought to provide AdoCbl to the AdoCbl-dependent ethanolamine ammonia-lyase (EAL).[86] As mentioned earlier, CobA maintains the basal concentration of AdoCbl that is needed for transcriptional activation of the *eut* operon.[84, 86] In *S. enterica,* CobA can replace the function of EutT when the Cbl concentration in ethanolamine minimal media is high (100 nM Cbl or higher) but in growth conditions with limited Cbl, a growth defect is observed in *eutT* strains, suggesting that EutT is necessary for optimal growth on ethanolamine.[84] Despite the lack of structural information, valuable insights into the function of the EutT-type ACAT family have been reported.[94, 97, 100, 118-120] Like PduO, *Se*EutT has highest specific activity when ATP is the nucleotide substrate.[103] *Se*EutT dimerizes, and adenosylates cobalamin but not cobinamide.[89, 103] *Se*EutT is unique from CobA and PduO ACATs in that it cleaves the triphosphate byproduct of the adenosylation reaction, producing *ortho* and *pyro* phosphate.[103]

Analysis of the primary amino acid sequence of *S. enterica* EutT revealed a cysteine and histidine-rich binding motif (H_{11}CCXXC).[86] These residues bind a divalent cation metal *in vitro* that is critical for enzyme activity.[89] Mutational analysis of the putative metal-binding residues showed that residues C80 and C83 are the key residues for metal binding and activity.[89] Although *Se*EutT is active with several divalent cations *in vitro*, evidence that the divalent cation is likely

Fe(II) stems from two observations, one being that *Se*EutT demonstrates maximum specific activity *in vitro* with Fe(II), and the other is that anoxically purified *Se*EutT is oxygen-labile.[86, 89] To better understand the ligand environment of the Fe(II) binding site, Fe(II) was replaced with the paramagnetic Co(II) in the metal-binding site. Using this species, it was observed that the divalent metal cation is tetrahedrally coordinated, likely by the two critical cysteine residues from each subunit of the *Se*EutT dimer.[119]

Spectroscopic studies of both the Co(II) ion in the corrin ring and a Co(II) ion at the metal-binding site offered insight into the mechanism of this family of ACATs.[118, 119] Interestingly, while CobA and PduO require ATP to be present to observe 4C-Co(II) corrinoid in the active site, *Se*EutT can bind cobalamin in a base off, 5C-Co(II)Cbl coordination in the absence of ATP.[98, 105] Multiple circular dichroism (MCD) spectra suggested that CobA and PduO bind 4C-Co(II)Cbl in a way that results in a relatively planar ring with the lower ligand unbound and exposed to the solvent. However, the MCD spectra for *Se*EutT suggests a different active site environment, potentially one where the lower ligand is sequestered in a specific binding site.[118] Additionally, *Se*EutT can bind Co(II)Cbi but cannot remove the lower ligand. This is intriguing, as water, the lower ligand for Co(II)Cbi, forms a weaker axial bond than DMB.[99] Together, these data suggest that *Se*EutT recognizes and sequesters the nucleotide loop or base from the active site through an unidentified mechanism.[118]

Recently, a EutT homologue from the *Firmicutes* was characterized that lacked the metal-binding motif in *Se*EutT. The purified EutT from *Listeria monocytogenes* (*Lm*EutT) did not bind a Fe(II) or Zn(II) metal, nor did it require one for activity.[120] It was observed that this EutT homologue formed a tetramer, which is a unique oligomerization state among the ACATs studied.[120] Somewhat surprisingly, *Lm*EutT demonstrated higher specific activity with dATP than

with ATP, which may provide clues about the nucleotide binding site of this EutT homologue.[120] Spectroscopic characterization of this homologue suggests that the active site environment is also different from CobA and PduO, as observed in *Se*EutT.[100] However, unlike *Se*EutT, *Lm*EutT does not generate a base-off, 5C-Co(II)Cbl species in the active site in the absence of ATP.[100] Thus, the characterization of *Lm*EutT and bioinformatic analysis of EutT homologues across *Enterobacterales* and *Firmicutes* suggested that the EutT family of ACATs can be separated into two classes based on their requirement for Fe(II).[120]

Further analysis of the class II ACAT, *Lm*EutT, suggested some sequence similarity with the PduO homologue from *Lactobacillus reuteri*.[94] Further analysis of these similarities revealed conserved residues across all PduO and EutT homologues, and it was noted that all EutT homologues had an extended 70-80 amino acids at the N-terminus that did not align with *Lr*PduO.[94] Many of the conserved residues aligned with residues that formed the nucleotide-binding site and an inter-subunit salt bridge in *Lr*PduO. Mutations of these residues and biochemical analysis of the resulting variants supported that the corresponding conserved residues in *Lm*EutT also formed the nucleotide-binding site and intersubunit salt bridge.[94] The phenylalanine residue that displaces the lower ligand in *Lr*PduO was not conserved, nor was a phenylalanine or tryptophan residue with this role identified in *Lm*EutT. However, mutational analysis of F72 in *Lm*EutT suggested that this residue contributed to access to the substrate-binding site.[94] *Lm*EutT residue W238 was also studied in detail, and mutational analysis of this residue affected binding of cobalamin to the active site.[94] Together, these data suggested that EutT and PduO ACATs have a common evolutionary ancestor, or at least have a common core structure. With these data, structural of *Lm*EutT and *Se*EutT were modeled by threading the aligned portions of *Lm*EutT and *Se*EutT into the *Lr*PduO structure (Figure 2.6). These structural models visualize

the striking similarities, including conserved residue positioning, between these families of ACATs.[94]

2.10 COENZYME DELIVERY

The *de novo* AdoCba biosynthetic pathway is an energy-intensive process, requiring the synthesis of ~26 enzymes in *S. enterica*. Under some physiological conditions, Cbl is required in very small quantities (~100 Cbl molecules) by the organism.[121] To prevent loss of the coenzyme, high affinity to the coenzyme or a direct delivery system may be required to successfully transfer the coenzyme to the AdoCbl-dependent enzyme. There is evidence of a direct delivery mechanism observed with the PduO-type adenosyltransferase and methylmalonyl-CoA mutase in humans, as well as between the adenosyltransferase and the AdoCbl-dependent enzyme IcmF in *Methylobacterium extorquens,* however a similar mechanism has not been reported in *S. enterica*.[4, 122]

2.11 ADOCBL UTILIZATION IN *S. ENTERICA*

S. enterica encodes a Cbl-dependent process where Co(I)Cbl acts as a methyl carrier in the biosynthesis of methionine.[5] There are also three known AdoCbl-dependent processes in *S. enterica*: reduction of epoxyqueuosine in tRNA synthesis, catabolism of 1,2-propanediol, and catabolism of ethanolamine.

2.12 METHIONINE SYNTHASE

Methionine synthases catalyze the transfer of a methyl group from Me-THF to homocysteine (Hcy), forming methionine and THF. In *S. enterica,* the Cbl-dependent methionine synthase is encoded by the gene locus *metH*, while the Cbl-independent methionine synthase is encoded by the gene locus *metE* [5, 123]. Both MetE and MetH utilize Me–THF, however MetH can use both the monoglutamate and polyglutamate forms while MetE is restricted to the triglutamate form.[124] The mechanism of MetH has been elucidated by several structural and mechanistic

studies.[125-127] MetH contains four modular regions that each bind Hcy, Me-THF, Cbl, and AdoMet. During turnover, MetH transfers the methyl group from methyl-cobalamin to homocysteine, and remains bound to Co(I)balamin which is then remethylated by CH_3-THF. Structural analysis reveals the enzyme contains a Rossman-fold domain that binds to the lower face of MeCbl, and a four-helix bundle that covers the Cba upper face, which protects the reactive cofactor from oxidation. Even so, at every 100-2000 turnovers, the Co(I)balamin species is oxidized to Co(II)balamin.[128] To regenerate methyl-cobalamin from Co(II)balamin, a reductive methylation is required where an electron from reduced flavodoxin and a methyl group from S-adenosylmethionine regenerates methyl-cobalamin.[129]

2.13 EPOXYQUEUOSINE REDUCTASE

Modified nucleosides are often found in the structures of tRNAs. The nucleoside queuosine, which is found in the wobble position of the tRNAs for histidine, aspartate, asparagine, and tyrosine, is such a nucleoside.[130] The epoxyqueuosine reductase, QueG (oQ), was recently discovered to perform the final epoxide reduction to form queuosine.[131] QueG forms specific interactions with the anticodon at positions conserved across all four tRNAs that contain queuosine.[132] The enzyme QueG binds two [4Fe – 4S] clusters, as well as a AdoCbl coenzyme, and is distantly related to the Cbl-dependent reductive dehalogenases.[8, 131] Spectroscopic characterization of QueG confirmed that like the reductive dehalogenases, the coenzyme is bound in the base-off conformation, and coordination of an alternative lower ligand is blocked by an arginine in a similar manner to the role of glutamine in CblC.[132] Mechanistically, it has been proposed that Co(I)balamin acts as the nucleophile, and reduction of the Co(II) → Co(I) state is facilitated by the two [4Fe – 4S] clusters.[132]

2.14 1,2-PROPANEDIOL UTILIZATION

1,2-propanediol (1,2-PDL) is an end-product of rhamnose and fucose fermentation (methyl sugars common in plant cells) and is utilized in mammalian intestinal epithelial cells as a glycoconjugate.[110, 133] 1,2-PDL can also be catabolized by several enteric microorganisms, such as *S. enterica* and *Klebsiella pneumonia*.[110, 134] The propanediol utilization (*pdu*) operon in *S. enterica* is adjacent to the operon that encodes most of the cobalamin biosynthetic genes (the *cob* operon), and encodes 22 functions for the metabolism of 1,2-propanediol, including carboxysome shell-like proteins and the AdoCbl-dependent enzyme propanediol dehydratase (PDD) (Figure 2.6).[110, 134] There has been great interest in this pathway, as the carboxysome shell-like proteins encoded form a proteinaceous compartment, termed the metabolosome, that could potentially be utilized in several industrial applications (Figure 2.6).[135] In the presence of 1,2-PDL, *S. enterica* assembles these metabolosomes, which sequester the aldehyde intermediate, preventing damage to the cell (Figure 2.7).[136-139] In these metabolosomes, PDD converts 1,2-PDL to propionaldehyde, which is then converted to either propionyl-CoA or propanol (Figure 2.7).[137] Purification of the Pdu metabolosome has identified that many of the functions, including the ACAT PduO, are associated with the Pdu metabolosome.[140]

The *pdu* and *cob* operons are transcribed divergently from distinct promoters (Figure 2.6).[109, 141] Transcription of both operons is induced by the regulator PocR when it is bound to 1,2-propanediol.[142] Both operons and transcription of PocR are also subject to regulation by the global regulators Crp and ArcA.[121, 142]

PDD is an AdoCbl-dependent enzyme that converts 1,2-propanediol to propionaldehyde. PDD is encoded by three genes, *pduCDE,* in the propanediol utilization (*pdu*) operon (Figre 2.6).[134] While AdoCbl-dependent enzymes that were studied up until PDD utilized a histidinyl residue to

coordinate as the a-ligand in lieu of the DMB base (termed 'base off, His on'), PDD lacked the conserved DXHXXG motif required for this conformation. Experiments using ^{15}N-labeled dehydratase apoenzyme indicated that in PDD, AdoCbl was bound in a conformation where the DMB base is preserved as the α-ligand in the active site (termed 'base on'), highlighting a different method of binding AdoCbl.[143] It was also found that AdoCbl binding activates the Co - C bond cleaving activity of the dehydratase, but cleavage of the bond does not occur until 1,2-PD is also bound.[144, 145] The binding of AdoCbl and cleavage of the Co - C bond also requires a monovalent cation such as K^+.[146]

PDD can be inactivated either by O_2 in the absence of substrate, or by glycerol in the holoenzyme, resulting in irreversibly cleaved Co(II)-Cbl and 5'-deoxyadenosine that cannot be displaced *in vitro* by AdoCbl in solution.[147] This inactivation could be reversed by incubation of the enzyme with cell lysates, leading to the identification of an ATP-dependent reactivase for PDD, PduGH (Figure 2.7).[148] This reactivase drives the release of inactive coenzyme that can then be replaced by intact AdoCbl, and this system requires the regeneration of Cbl by an ACAT enzyme. Recently, it was shown that the activity of the ACAT PduO is the most effective for diol dehydratase activation with its corresponding reactivase, however the question of whether these functions interact directly remains open.[149]

2.15 ETHANOLAMINE UTILIZATION

Ethanolamine is a component of the common phospholipid phosphatidylethanolamine and is present in the intestinal environment due to degradation and regeneration of the intestinal epithelial layer.[150] Ethanolamine is broken down to acetyl-CoA, ammonia, and ethanol, thus producing a source of carbon, energy and nitrogen source for the organism.[2] *S. enterica* can respire

ethanolamine anaerobically utilizing tetrathionate as an electron acceptor, and this ability is critical for the successful colonization of *S. enterica* in the intestinal tract.[151-153]

The functions for ethanolamine metabolism are encoded in the 18-gene ethanolamine utilization (*eut*) operon (Figure 2.7).[154] While in *S. enterica* this operon is distant from the *cob, pdu* and *cbi* operons, in some organisms the *eut* operon is located in proximity to, and even intermingled with the *pdu* and *cob* operons.[155] Expression of the *eut* operon in *S. enterica* is controlled by two promoters. One promoter, located at the beginning of the operon, is recognized by the regulator EutR when EutR is bound to both EA and AdoCbl.[156] EutR is encoded in the last gene of the operon, and a second promoter specifically controls the transcription of *eutR*. This second promoter allows for constitutive but low transcription of *eutR*.[156] When EutR binds to both ethanolamine and AdoCbl, it activates transcription of the *eut* operon.[156] Thus, initiation of transcription of the *eut* operon is controlled by the availability of the substrate and the coenzyme required to metabolize the substrate. Recent work showed that EutR also activates transcription at other promoters, including the promoter of *Salmonella* pathogenicity island 2 (SPI-2), suggesting that ethanolamine also acts as an environmental signal for *S. enterica*.[157] EutR is not the only regulator of the *eut* operon, as *eut* operon expression is subject to catabolite repression.[156] Recent work found that the regulator of the *pdu* and cobalamin (*cob*) operons, PocR, mediates repression of the *eut* operon in the presence of 1,2-PDL.[158] Maintaining metabolosome synthesis separate for different metabolic pathways proved important for function, as allowing expression of both metabolosomes resulting in mixed and nonfunctional metabolosomes.[158]

Ethanolamine (EA) metabolism shares striking parallels with the metabolism of 1,2-PDL (Figure 2.6). The first step of EA metabolism is a deamination reaction performed by the AdoCbl-dependent enzyme ethanolamine ammonia-lyase (EAL), resulting in the product acetaldehyde.[159]

Like 1,2-PDL, the metabolism of EA also occurs in a metabolosome to sequester the reactive aldehyde intermediate, mitigating damage to cellular components.[138, 139, 160] From acetaldehyde, an alcohol dehydrogenase (EutG) or an acetaldehyde dehydrogenase (EutE) converts acetaldehyde to ethanol or acetyl-CoA, respectively (Figure 2.6).[161] *S. enterica* already encodes a bifunctional aldehyde/alcohol dehydrogenase as well as a secondary aldehyde dehydrogenase, suggesting that this redundancy is to address the compartmentalization of this pathway. In this manner, a localized pool of NADH can be maintained in the metabolosome.[162] Additionaly, EutD converts acetyl-CoA to acetyl-P, which also permits recycling of CoA in the metabolosome.[162]

Are all the functions of ethanolamine metabolism localized to the metabolosome? There is evidence that at least some functions are localized to the metabolosome. The small subunit of EAL has an N-terminal localization tag that directs EAL to the Eut metabolosome.[163] There is also some evidence that EutE has an N-terminal localization tag.[164] Suppressor mutations of *S. enterica* strains lacking *eutG* or *eutD,* both redundant enzymes in *S. enterica,* were mapped to *eut* shell proteins, suggesting that the Eut metabolosome maintains private coenzyme pools in the metabolosome and EutG and EutD are both localized to the metabolosome.[162] However, a systematic analysis of localization and interactions has not been undertaken for the Eut metabolosome to the same extent as with the Pdu metabolosome.[140]

EAL, which is encoded by the genes *eutB* and *eutC,* is the only known ammonia-lyase that is AdoCbl-dependent. EAL binds AdoCbl in the 'base on' conformation described earlier.[6] In the presence of substrate, EAL homolytically cleaves the Co - C bond of bound AdoCbl, producing the adenosyl radical and Co(II)-Cbl.[6] The mechanism as shown in Figure 2.8 involves a hydrogen abstraction and rearrangement. Specifically, the deoxyadenosine radical abstracts a hydrogen radical from C1 of ethanolamine, and the substrate undergoes a rearrangement where the amine

travels from C2 to C1, producing a hemiaminal that abstracts the hydrogen from the 5'-deoxyadenosine radical.[165] Finally, a deamination results in the products ammonia and acetaldehyde.[165]

The 5'-deoxyadenosine and Co(II)-Cbl radical pair in EAL can be inactivated *in vitro* by ethanol, a downstream product of the reaction.[6] This inactivation results in the binding of Co(II)-Cbl by EAL in such a way that addition of AdoCbl to the reaction *in vitro* does not reactivate EAL function.[166] Instead, EAL reactivation is catalyzed by EutA, which replaces the inactive Co(II)-Cbl coenzyme with AdoCbl at the expense of ATP.[167] The specifics of this mechanism are not clear, as a structure of EutA has not been elucidated.

2.16 CONCLUSIONS AND FUTURE PERSPECTIVES

Adenosylcobalamin is a required coenzyme by many organisms in all domains of life. However, only a handful of prokaryotes are capable of making AdoCbl *de novo*. For decades, *S. enterica* has served as a model for understanding AdoCbl biosynthesis and utilization, which has provided a foundational understanding of these processes in other organisms. Our understanding of *S. enterica* AdoCbl biosynthesis and utilization is extensive, although there are some intriguing questions that warrant further investigation.

The biosynthesis of AdoCbl starts at uroporphyrinogen, where it enters the anaerobic pathway. In this portion of the pathway, the cobalt is inserted into the tetrapyrrole ring early, and several enzymatic steps result in a puckered, decorated, and cobalt-containing tetrapyrrole ring. Then, the corrinoid is adenosylated by the housekeeping ACAT CobA prior to attachment of the nucleotide loop and base. Aside from *de novo* AdoCbl biosynthesis, CobA is also responsible for adenosylation of incomplete corrinoids that are scavenged from the environment, as well as providing AdoCbl for activation of the *eut* operon.

The attachment of the nucleotide loop to form AdoCbl is catalyzed by several enzymatic processes. Notably, two enzymes, CbiB and CobS, are integral membrane proteins, suggesting that the attachment of the nucleotide loop is associated with the membrane. Why CbiB and CobS are in the membrane, and how these functions interact with CobU and CobC in the pathway, is currently unknown and should be investigated in further detail.

Once AdoCbl is produced, there are four cobalamin-dependent processes in *S. enterica* that can utilize this coenzyme, being the methionine synthase (MetH), the epoxyqueuosine reductase (QueG), the 1,2-propanediol dehydratase (PDD, PduCDE), and the ethanolamine ammonia-lyase (EAL, EutBC). Both PDD and EAL are localized to their respective metabolosomes, where they turn over 1,2-propanediol and ethanolamine to propionaldehyde and acetaldehyde, respectively. Both PDD and EAL can be inactivated by the quenching of the Ado• radical, resulting in the enzyme irreversibly bound to Co(II)Cbl. Reactivation of these enzymes require an ATP-dependent reactivase, which are PduGH for PDD and EutA for EAL. These enzymes do not regenerate AdoCbl, rather they exchange Co(II)Cbl for AdoCbl to reactivate PDD or EAL. Each metabolosome is also associated with an ACAT that does regenerate AdoCbl, which are PduO for the Pdu metabolosome and EutT for the Eut metabolosome. Successful purification of intact Pdu metabolosomes showed that PDD, PduGH, and PduO are all in the Pdu metabolosome. While a similar approach has not been published for the Eut metabolosome, EAL does localize to the Eut metabolosome. Whether EutT and EutA also localize to the Eut metabolosome, and whether this results in localized recycling of the AdoCbl coenzyme, has not been published.

While *S. enterica* is a model organism for the study of AdoCbl biosynthesis and utilization, the biochemical diversity of cobamide biosynthesis and utilization is still being uncovered. As sequencing technology has become more widespread and affordable, we are able to identify genes

of interest in other microorganisms. By expanding our studies to other organisms, our understanding of AdoCbl-producing enzymes and AdoCbl-utilizing pathways, will continue to expand.

2.17 REFERENCES

1. Banerjee, R., *Chemistry and Biochemistry of B_{12}*. John Wiley & Sons: 1999; p 3-6.

2. Roth, J. R.; Lawrence, J. G.; Bobik, T. A., Cobalamin (coenzyme B_{12}): synthesis and biological significance. *Annu. Rev. Microbiol.* **1996,** *50*, 137-181.

3. Blanche, F.; Cameron, B.; Crouzet, J.; Debussche, L.; Thibaut, D.; Vuilhorgne, M.; Leeper, F. J.; Battersby, A. R., Vitamin B_{12} - How the problem of its biosynthesis was solved. *Angew. Chem.* **1995,** *34*, 383-411.

4. Padovani, D.; Labunska, T.; Palfey, B. A.; Ballou, D. P.; Banerjee, R., Adenosyltransferase tailors and delivers coenzyme B_{12}. *Nat. Chem. Biol.* **2008,** *4*, 194-196.

5. Taylor, R. R., B_{12}-dependent methionine synthesis. In *B_{12}*, Dolphin, D., Ed. John Wiley & Sons: New York, 1982; Vol. 2, pp 307-356.

6. Abend, A.; Bandarian, V.; Nitsche, R.; Stupperich, E.; Retey, J.; Reed, G. H., Ethanolamine ammonia-lyase has a "base-on" binding mode for coenzyme B_{12}. *Arch. Biochem. Biophys.* **1999,** *370*, 138-141.

7. Toraya, T., Enzymatic radical catalysis: coenzyme B_{12}-dependent diol dehydratase. *The Chemical Record* **2002,** *2*, 352-366.

8. Miles, Z. D.; Myers, W. K.; Kincannon, W. M.; Britt, R. D.; Bandarian, V., Biochemical and spectroscopic studies of epoxyqueuosine reductase: A novel iron-sulfur cluster and cobalamin-containing protein Involved in the biosynthesis of queuosine. *Biochemistry* **2015,** *54*, 4927-4935.

9. Brushaber, K. R.; O'Toole, G. A.; Escalante-Semerena, J. C., CobD, a novel enzyme with L-threonine-*O*-3-phosphate decarboxylase activity, is responsible for the synthesis of (*R*)-1-amino-2-propanol *O*-2-phosphate, a proposed new intermediate in cobalamin biosynthesis in *Salmonella typhimurium* LT2. *J. Biol. Chem.* **1998,** *273*, 2684-2691.

10. Raux, E.; Schubert, H. L.; Warren, M. J., Biosynthesis of cobalamin (vitamin B_{12}): a bacterial conundrum. *Cell. Mol. Life Sci.* **2000,** *57*, 1880-1893.

11. Deery, E.; Schroeder, S.; Lawrence, A. D.; Taylor, S. L.; Seyedarabi, A.; Waterman, J.; Wilson, K. S.; Brown, D.; Geeves, M. A.; Howard, M. J.; Pickersgill, R. W.; Warren, M. J., An enzyme-trap approach allows isolation of intermediates in cobalamin biosynthesis. *Nat. Chem. Biol.* **2012,** *8*, 933-940.

12. Debussche, L.; Thibaut, D.; Cameron, B.; Crouzet, J.; Blanche, F., Purification and characterization of cobyrinic acid *a,c*-diamide synthase from *Pseudomonas denitrificans*. *J. Bacteriol.* **1990,** *172*, 6239-6244.

13. Moore, S. J.; Lawrence, A. D.; Biedendieck, R.; Deery, E.; Frank, S.; Howard, M. J.; Rigby, S. E.; Warren, M. J., Elucidation of the anaerobic pathway for the corrin component of cobalamin (vitamin B12). *Proc. Natl. Acad. Sci. U.S.A.* **2013,** *110*, 14906-14911.

14. Beck, R.; Raux, E.; Thermes, C.; Rambach, A.; Warren, M., CbiX: a novel metal-binding protein involved in sirohaem biosynthesis in *Bacillus megaterium*. *Biochem. Soc. Trans.* **1997,** *25*, 77S.

15. Leech, H. K.; Raux, E.; McLean, K. J.; Munro, A. W.; Robinson, N. J.; Borrelly, G. P.; Malten, M.; Jahn, D.; Rigby, S. E.; Heathcote, P.; Warren, M. J., Characterization of the cobaltochelatase CbiXL: evidence for a 4Fe-4S center housed within an MXCXXC motif. *J. Biol. Chem.* **2003,** *278*, 4190-4197.

16. Müller, G.; Zipfel, F.; Hliney, K.; Savvidis, E.; Hertle, R.; Traub-Eberhard, U.; Scott, A. I.; Williams, H. J.; Stolowich, N. J.; Santander, P. J.; Warren, M.; Blanche, F.; Thibaut, D., Timing of cobalt insertion in vitamin B12 biosynthesis. *J. Am. Chem. Soc.* **1991,** *113*, 9893-9895.

17. Raux, E.; Thermes, C.; Heathcote, P.; Rambach, A.; Warren, M. J., A role for *Salmonella typhimurium cbiK* in cobalamin (vitamin B_{12}) and siroheme biosynthesis. *J. Bacteriol.* **1997,** *179*, 3202-3212.

18. Romao, C. V.; Ladakis, D.; Lobo, S. A.; Carrondo, M. A.; Brindley, A. A.; Deery, E.; Matias, P. M.; Pickersgill, R. W.; Saraiva, L. M.; Warren, M. J., Evolution in a family of chelatases facilitated by the introduction of active site asymmetry and protein oligomerization. *Proc. Natl. Acad. Sci. U.S.A.* **2011,** *108*, 97-102.

19. Escalante-Semerena, J. C.; Roth, J. R., Regulation of cobalamin biosynthetic operons in *Salmonella typhimurium*. *J. Bacteriol.* **1987,** *169*, 2251-2258.

20. Scott, A. I.; MacKenzie, N. E.; Santander, P. J.; Fagerness, P. E.; Muller, G.; Schneider, E.; Sedlmeier, R.; Worner, G., Biosynthesis of vitamin B_{12}: timing of the methylation steps between uro'gen III and cobyrinic acid. *Bioorg. Chem.* **1984,** *12*, 356-362.

21. Battersby, A. R., How nature builds the pigments of life: the conquest of vitamin B_{12}. *Science* **1994,** *264*, 1551-1557.

22. Scott, A. I., Discovering nature's diverse pathways to Vitamin B_{12}: A 35-year odyssey. *The Journal of Organic Chemistry* **2003,** *68*, 2529-2539.

23. Scott, A. I.; Clemens, K. R.; Stolowich, N. J.; Santander, P. J.; Gonzalez, M. D.; Roessner, C. A., Reconstitution of apo-porphobilinogen deaminase: structural changes induced by cofactor binding. *FEBS Lett.* **1989,** *242*, 319-324.

24. Uzar, H. C.; Battersby, A. R.; Carpenter, T. A.; Leeper, F. J., Biosynthesis of porphyrins and related macrocycles. 28. Development of a pulse labeling method to determine the C-methylation sequence for vitamin B_{12}. *J. Chem. Soc. [Prekin 1]* **1987**, 1689-1696.

25. Fazzio, T. G.; Roth, J. R., Evidence that the CysG protein catalyzes the first reaction specific to B_{12} synthesis in *Salmonella typhimurium*, insertion of cobalt. *J. Bacteriol.* **1996,** *178*, 6952-6959.

26. Vevodova, J.; Graham, R. M.; Raux, E.; Schubert, H. L.; Roper, D. I.; Brindley, A. A.; Ian Scott, A.; Roessner, C. A.; Stamford, N. P.; Elizabeth Stroupe, M.; Getzoff, E. D.; Warren, M. J.; Wilson, K. S., Structure/function studies on a S-adenosyl-L-methionine-dependent uroporphyrinogen III C methyltransferase (SUMT), a key regulatory enzyme of tetrapyrrole biosynthesis. *J. Mol. Biol.* **2004,** *344*, 419-433.

27. Stroupe, M. E.; Leech, H. K.; Daniels, D. S.; Warren, M. J.; Getzoff, E. D., CysG structure reveals tetrapyrrole-binding features and novel regulation of siroheme biosynthesis. *Nat. Struct. Biol.* **2003,** *10*, 1064-1073.

28. Warren, M. J.; Bolt, E. L.; Roessner, C. A.; Scott, A. I.; Spencer, J. B.; Woodcock, S. C., Gene dissection demonstrates that the *Escherichia coli cysG* gene encodes a multifunctional protein. *Biochem. J.* **1994,** *302*, 837-844.

29. Spencer, J. B.; Stolowich, N. J.; Roessner, C. A.; Min, C.; Scott, A. I., Biosynthesis of vitamin B_{12}: Ring contraction is preceded by incorporation of molecular oxygen into precorrin-3. *J. Am. Chem. Soc.* **1993,** *115*, 11610-11611.

30. Brindley, A. A.; Raux, E.; Leech, H. K.; Schubert, H. L.; Warren, M. J., A story of chelatase evolution: identification and characterization of a small 13-15-kDa "ancestral" cobaltochelatase (CbiXS) in the archaea. *J. Biol. Chem.* **2003,** *278*, 22388-22395.

31. Schubert, H. L.; Raux, E.; Wilson, K. S.; Warren, M. J., Common chelatase design in the branched tetrapyrrole pathways of heme and anaerobic cobalamin synthesis. *Biochemistry* **1999,** *38*, 10660-10669.

32. Frank, S.; Deery, E.; Brindley, A. A.; Leech, H. K.; Lawrence, A.; Heathcote, P.; Schubert, H. L.; Brocklehurst, K.; Rigby, S. E.; Warren, M. J.; Pickersgill, R. W., Elucidation of substrate specificity in the cobalamin (vitamin B_{12}) biosynthetic methyltransferases. Structure and function of the C20 methyltransferase (CbiL) from *Methanothermobacter thermautotrophicus*. *J. Biol. Chem.* **2007,** *282*, 23957-23969.

33. Roessner, C. A.; Warren, M. J.; Santander, P. J.; Atshaves, B. P.; Ozaki, S.; Stolowich, N. J.; Iida, K.; Scott, A. I., Expression of 9 *Salmonella typhimurium* enzymes for cobinamide synthesis. Identification of the 11-methyl and 20-methyl transferases of corrin biosynthesis. *FEBS Lett.* **1992,** *301*, 73-78.

34. Spencer, P.; Stolowich, N. J.; Sumner, L. W.; Scott, A. I., Definition of the redox states of cobalt-precorrinoids: investigation of the substrate and redox specificity of CbiL from *Salmonella typhimurium*. *Biochemistry* **1998,** *37*, 14917-14927.

35. Frank, S.; Brindley, A. A.; Deery, E.; Heathcote, P.; Lawrence, A. D.; Leech, H. K.; Pickersgill, R. W.; Warren, M. J., Anaerobic synthesis of vitamin B_{12}: characterization of the early steps in the pathway. *Biochem. Soc. Trans.* **2005,** *33*, 811-814.

36. Kajiwara, Y.; Santander, P. J.; Roessner, C. A.; Perez, L. M.; Scott, A. I., Genetically engineered synthesis and structural characterization of cobalt-precorrin 5A and -5B, two new intermediates on the anaerobic pathway to vitamin B_{12}: definition of the roles of the CbiF and CbiG enzymes. *J. Am. Chem. Soc.* **2006,** *128*, 9971-9978.

37. Santander, P. J.; Roessner, C. A.; Stolowich, N. J.; Holderman, M. T.; Scott, A. I., How corrinoids are synthesized without oxygen: nature's first pathway to vitamin B_{12}. *Chem. Biol.* **1997,** *4*, 659-666.

38. Wang, J.; Stolowich, N. J.; Santander, P. J.; Park, J. H.; Scott, A. I., Biosynthesis of vitamin B_{12}: concerning the identity of the two-carbon fragment eliminated during anaerobic formation of cobyrinic acid. *Proc. Natl. Acad. Sci. U.S.A.* **1996,** *93*, 14320-14322.

39. Ozaki, S. I.; Roessner, C. A.; Stolowich, N. J.; Atshaves, B. P.; Hertle, R.; Muller, G.; Scott, A. I., Multienzyme synthesis and structure of Factor-S3. *J. Am. Chem. Soc.* **1993,** *115* (1), 7935-7938.

40. Schubert, H. L.; Wilson, K. S.; Raux, E.; Woodcock, S. C.; Warren, M. J., The X-ray structure of a cobalamin biosynthetic enzyme, cobalt-precorrin-4 methyltransferase. *Nat. Struct. Biol.* **1998,** *5*, 585-592.

41. Roessner, C. A.; Williams, H. J.; Scott, A. I., Genetically engineered production of 1-desmethylcobyrinic acid, 1-desmethylcobyrinic acid *a,c*-diamide, and cobyrinic acid *a,c*-diamide in *E. coli* implies a role for CbiD in C-1 methylation in the anaerobic pathway to cobalamin. *J. Biol. Chem.* **2005,** *280*, 16748-16753.

42. Kieninger, C.; Deery, E.; Lawrence, A. D.; Podewitz, M.; Wurst, K.; Nemoto-Smith, E.; Widner, F. J.; Baker, J. A.; Jockusch, S.; Kreutz, C. R.; Liedl, K. R.; Gruber, K.; Warren, M. J.; Krautler, B., The hydrogenobyric acid structure reveals the corrin ligand as an entatic state module empowering B_{12} cofactors for catalysis. *Angew. Chem.* **2019**.

43. Rodionov, D. A.; Vitreschak, A. G.; Mironov, A. A.; Gelfand, M. S., Comparative genomics of the vitamin B_{12} metabolism and regulation in prokaryotes. *J. Biol. Chem.* **2003,** *278*, 41148-41159.

44. Keller, J. P.; Smith, P. M.; Benach, J.; Christendat, D.; deTitta, G. T.; Hunt, J. F., The crystal structure of MT0146/CbiT suggests that the putative precorrin-8w decarboxylase is a methyltransferase. *Structure* **2002,** *10*, 1475-1487.

45. Fresquet, V.; Williams, L.; Raushel, F. M., Mechanism of cobyrinic acid *a,c*-diamide synthetase from *Salmonella typhimurium* LT2. *Biochemistry* **2004,** *43*, 10619-10627.

46. Escalante-Semerena, J. C.; Suh, S. J.; Roth, J. R., *cobA* function is required for both *de novo* cobalamin biosynthesis and assimilation of exogenous corrinoids in *Salmonella typhimurium*. *J. Bacteriol.* **1990,** *172*, 273-280.

47. Hodgkin, D. C.; Kamper, J.; Lindsey, J.; MacKay, M.; Pickworth, J.; Robertson, J. H.; Shoemaker, C. B.; White, J. G.; Prosen, R. J.; Trueblood, K. N., The structure of vitamin B_{12}. I. An outline of the crystallographic investigation of vitamin B_{12}. *Proc. R. Soc. Lond* **1957,** *A242*, 228-263.

48. van Beelen, P.; Stassen, A. P.; Bosch, J. W.; Vogels, G. D.; Guijt, W.; Haasnoot, C. A., Elucidation of the structure of methanopterin, a coenzyme from *Methanobacterium thermoautotrophicum*, using two-dimensional nuclear-magnetic-resonance techniques. *Eur. J. Biochem.* **1984,** *138*, 563-571.

49. Eirich, L. D.; Vogels, G. D.; Wolfe, R. S., Proposed structure for coenzyme F_{420} from Methanobacterium. *Biochemistry* **1978,** *17*, 4583-4593.

50. Cheong, C. G.; Escalante-Semerena, J. C.; Rayment, I., Structural studies of the L-threonine-*O*-3-phosphate decarboxylase (CobD) enzyme from *Salmonella enterica*: the apo, substrate, and product-aldimine complexes. *Biochemistry* **2002,** *41*, 9079-9089.

51. Fan, C.; Bobik, T. A., The PduX enzyme of *Salmonella enterica* is an L-threonine kinase used for coenzyme B_{12} synthesis. *J. Biol. Chem.* **2008,** *283*, 11322-11329.

52. Fan, C.; Fromm, H. J.; Bobik, T. A., Kinetic and functional analysis of L-threonine kinase, the PduX enzyme of *Salmonella enterica*. *J. Biol. Chem.* **2009,** *284*, 20240-20248.

53. Tavares, N. K.; Zayas, C. L.; Escalante-Semerena, J. C., The *Methanosarcina mazei* MM2060 gene encodes a bifunctional kinase/decarboxylase enzyme involved in cobamide biosynthesis. *Biochemistry* **2018,** *57*, 4478-4495.

54. Woodson, J. D.; Zayas, C. L.; Escalante-Semerena, J. C., A new pathway for salvaging the coenzyme B_{12} precursor cobinamide in archaea requires cobinamide-phosphate synthase (CbiB) enzyme activity. *J. Bacteriol.* **2003,** *185*, 7193-7201.

55. Zayas, C. L.; Claas, K.; Escalante-Semerena, J. C., The CbiB protein of *Salmonella enterica* is an integral membrane protein involved in the last step of the *de novo* corrin ring biosynthetic pathway. *J. Bacteriol.* **2007,** *189*, 7697-7708.

56. O'Toole, G. A.; Escalante-Semerena, J. C., *cobU*-dependent assimilation of nonadenosylated cobinamide in cobA mutants of *Salmonella typhimurium*. *J. Bacteriol.* **1993,** *175*, 6328-6336.

57. O'Toole, G. A.; Escalante-Semerena, J. C., Purification and characterization of the bifunctional CobU enzyme of *Salmonella typhimurium* LT2. Evidence for a CobU-GMP intermediate. *J. Biol. Chem.* **1995,** *270*, 23560-23569.

58. Thompson, T. B.; Thomas, M. G.; Escalante-Semerena, J. C.; Rayment, I., Three-dimensional structure of adenosylcobinamide kinase/adenosylcobinamide phosphate guanylyltransferase (CobU) complexed with GMP: evidence for a substrate-induced transferase active site. *Biochemistry* **1999,** *38*, 12995-13005.

59. Glusker, J. P., X-Ray crystallography of B_{12} and cobaloximes. In *B_{12}*, Dolphin, D., Ed. John Wiley & Sons: New York, 1982; Vol. 1, pp 23-106.

60. Johnson, M. G.; Escalante-Semerena, J. C., Identification of 5,6-dimethylbenzimidazole as the *Coα* ligand of the cobamide synthesized by *Salmonella typhimurium*. Nutritional characterization of mutants defective in biosynthesis of the imidazole ring. *J. Biol. Chem.* **1992,** *267*, 13302-13305.

61. Mattes, T. A.; Deery, E.; Warren, M. J.; Escalante-Semerena, J. C., Cobalamin Biosynthesis and Insertion. In *Encyclopedia of Inorganic and Bioinorganic Chemistry*, Scott, R. A., Ed. John Wiley & Sons, Ltd: Chichester, UK, 2017; pp 1-24.

62. Trzebiatowski, J. R.; O'Toole, G. A.; Escalante-Semerena, J. C., The *cobT* gene of *Salmonella typhimurium* encodes the NaMN: 5,6-dimethylbenzimidazole phosphoribosyltransferase responsible for the synthesis of N^1-(5-phospho-alpha-D-ribosyl)-5,6-dimethylbenzimidazole, an intermediate in the synthesis of the nucleotide loop of cobalamin. *J. Bacteriol.* **1994,** *176*, 3568-3575.

63. Cheong, C. G.; Escalante-Semerena, J. C.; Rayment, I., The three-dimensional structures of nicotinate mononucleotide:5,6- dimethylbenzimidazole phosphoribosyltransferase (CobT) from *Salmonella typhimurium* complexed with 5,6-dimethybenzimidazole and its reaction products determined to 1.9Å resolution. *Biochemistry* **1999,** *38*, 16125-16135.

64. Cheong, C. G.; Escalante-Semerena, J. C.; Rayment, I., Structural investigation of the biosynthesis of alternative lower ligands for cobamides by nicotinate mononucleotide: 5,6-dimethylbenzimidazole phosphoribosyltransferase from *Salmonella enterica*. *J. Biol. Chem.* **2001,** *276*, 37612-37620.

65. Maggio-Hall, L. A.; Claas, K. R.; Escalante-Semerena, J. C., The last step in coenzyme B_{12} synthesis is localized to the cell membrane in bacteria and archaea. *Microbiology* **2004,** *150*, 1385-1395.

66. Zayas, C. L.; Escalante-Semerena, J. C., Reassessment of the late steps of coenzyme B_{12} synthesis in *Salmonella enterica*: Evidence that dephosphorylation of adenosylcobalamin-5'-phosphate by the CobC phosphatase is the last step of the pathway. *J. Bacteriol.* **2007,** *189*, 2210-2218.

67. O'Toole, G. A.; Rondon, M. R.; Escalante-Semerena, J. C., Analysis of mutants of defective in the synthesis of the nucleotide loop of cobalamin. *J. Bacteriol.* **1993,** *175*, 3317-3326.

68. Maggio-Hall, L. A.; Escalante-Semerena, J. C., *In vitro* synthesis of the nucleotide loop of cobalamin by *Salmonella typhimurium* enzymes. *Proc. Natl. Acad. Sci. U.S.A.* **1999,** *96*, 11798-11803.

69. O'Toole, G. A.; Trzebiatowski, J. R.; Escalante-Semerena, J. C., The *cobC* gene of *Salmonella typhimurium* codes for a novel phosphatase involved in the assembly of the nucleotide loop of cobalamin. *J. Biol. Chem.* **1994,** *269*, 26503-26511.

70. DeVeaux, L. C.; Kadner, R. J., Transport of vitamin B_{12} in *Escherichia coli*: cloning of the *btuCD* region. *J. Bacteriol.* **1985,** *162*, 888-896.

71. Kadner, R. J.; McElhaney, G., Outer membrane-dependent transport systems in *Escherichia coli*: turnover of TonB function. *J. Bacteriol.* **1978,** *134*, 1020-1029.

72. Lundrigan, M. D.; De Veaux, L. C.; Mann, B. J.; Kadner, R. J., Separate regulatory systems for the repression of *metE* and *btuB* by vitamin B_{12} in *Escherichia coli*. *Mol. Gen. Genet.* **1987,** *206*, 401-407.

73. Lundrigan, M. D.; Kadner, R. J., Altered cobalamin metabolism in *Escherichia coli btuR* mutants affects *btuB* gene regulation. *J. Bacteriol.* **1989,** *171*, 154-161.

74. Lundrigan, M. D.; Koster, W.; Kadner, R. J., Transcribed sequences of the *Escherichia coli* btuB gene control its expression and regulation by vitamin B_{12}. *Proc. Natl. Acad. Sci. U.S.A.* **1991,** *88*, 1479-1483.

75. Cadieux, N.; Barekzi, N.; Bradbeer, C., Observations on the calcium dependence and reversibility of cobalamin transport across the outer membrane of *Escherichia coli*. *J. Biol. Chem.* **2007,** *282*, 34921-34928.

76. Cadieux, N.; Bradbeer, C.; Reeger-Schneider, E.; Koster, W.; Mohanty, A. K.; Wiener, M. C.; Kadner, R. J., Identification of the periplasmic cobalamin-binding protein BtuF of *Escherichia coli*. *J. Bacteriol.* **2002,** *184*, 706-717.

77. Mireku, S. A.; Ruetz, M.; Zhou, T.; Korkhov, V. M.; Krautler, B.; Locher, K. P., Conformational change of a tryptophan residue in BtuF facilitates binding and transport of cobinamide by the vitamin B_{12} transporter BtuCDF. *Sci. Rep.* **2017,** *7*, 41575.

78. Borths, E. L.; Poolman, B.; Hvorup, R. N.; Locher, K. P.; Rees, D. C., *In vitro* functional characterization of BtuCDF, the *Escherichia coli* ABC transporter for vitamin B_{12} uptake. *Biochemistry* **2005,** *44*, 16301-16309.

79. Degnan, P. H.; Barry, N. A.; Mok, K. C.; Taga, M. E.; Goodman, A. L., Human gut microbes use multiple transporters to distinguish vitamin B_{12} analogs and compete in the gut. *Cell Host Microbe* **2014,** *15*, 47-57.

80. Suh, S. J.; Escalante-Semerena, J. C., Cloning, sequencing and overexpression of *cobA* which encodes ATP:corrinoid adenosyltransferase in *Salmonella typhimurium*. *Gene* **1993,** *129*, 93-97.

81. Suh, S.; Escalante-Semerena, J. C., Purification and initial characterization of the ATP:corrinoid adenosyltransferase encoded by the *cobA* gene of *Salmonella typhimurium*. *J. Bacteriol.* **1995,** *177*, 921-925.

82. Blanche, F.; Debussche, L.; Famechon, A.; Thibaut, D.; Cameron, B.; Crouzet, J., A bifunctional protein from *Pseudomonas denitrificans* carries cobinamide kinase and cobinamide phosphate guanylyltransferase activities. *J. Bacteriol.* **1991,** *173*, 6052-6057.

83. Banerjee, R.; Ragsdale, S. W., The many faces of vitamin B_{12}: catalysis by cobalamin-dependent enzymes. *Annu. Rev. Biochem.* **2003,** *72*, 209-247.

84. Sheppard, D. E.; Penrod, J. T.; Bobik, T.; Kofoid, E.; Roth, J. R., Evidence that a B_{12}-adenosyl transferase is encoded within the ethanolamine operon of *Salmonella enterica*. *J. Bacteriol.* **2004,** *186*, 7635-7644.

85. Johnson, C. L.; Pechonick, E.; Park, S. D.; Havemann, G. D.; Leal, N. A.; Bobik, T. A., Functional genomic, biochemical, and genetic characterization of the *Salmonella pduO* gene, an ATP:cob(I)alamin adenosyltransferase gene. *J. Bacteriol.* **2001,** *183*, 1577-1584.

86. Buan, N. R.; Suh, S. J.; Escalante-Semerena, J. C., The *eutT* gene of *Salmonella enterica* encodes an oxygen-labile, metal-containing ATP:corrinoid adenosyltransferase enzyme. *J. Bacteriol.* **2004,** *186*, 5708-5714.

87. Moore, T. C.; Newmister, S. A.; Rayment, I.; Escalante-Semerena, J. C., Structural insights into the mechanism of four-coordinate cob(II)alamin formation in the active site of the *Salmonella enterica* ATP:co(I)rrinoid adenosyltransferase (CobA) enzyme: Critical role of residues Phe91 and Trp93. *Biochemistry* **2012,** *51*, 9647-9657.

88. Fonseca, M. V.; Buan, N. R.; Horswill, A. R.; Rayment, I.; Escalante-Semerena, J. C., The ATP:Co(I)rrinoid adenosyltransferase (CobA) enzyme of *Salmonella enterica* requires the

2'-OH Group of ATP for function and yields inorganic triphosphate as its reaction byproduct. *J. Biol. Chem.* **2002,** *277*, 33127-33131.

89. Moore, T. C.; Mera, P. E.; Escalante-Semerena, J. C., the EutT enzyme of *Salmonella enterica* is a unique ATP:Cob(I)alamin adenosyltransferase metalloprotein that requires ferrous ions for maximal activity. *J. Bacteriol.* **2014,** *196*, 903-910.

90. Johnson, C. L.; Buszko, M. L.; Bobik, T. A., Purification and initial characterization of the *Salmonella enterica* PduO ATP:Cob(I)alamin adenosyltransferase. *J. Bacteriol.* **2004,** *186*, 7881-7887.

91. Ortiz de Orue Lucana, D.; Hickey, N.; Hensel, M.; Klare, J. P.; Geremia, S.; Tiufiakova, T.; Torda, A. E., The crystal structure of the C-terminal domain of the *Salmonella enterica* PduO protein: An old fold with a new heme-binding mode. *Front. Microbiol.* **2016,** *7*, 1010.

92. Mera, P. E.; Maurice, M. S.; Rayment, I.; Escalante-Semerena, J. C., Structural and functional analyses of the human-type corrinoid adenosyltransferase (PduO) from *Lactobacillus reuteri*. *Biochemistry* **2007,** *46*, 13829-13836.

93. Mera, P. E.; St Maurice, M.; Rayment, I.; Escalante-Semerena, J. C., Residue Phe112 of the human-type corrinoid adenosyltransferase (PduO) enzyme of *Lactobacillus reuteri* is critical to the formation of the four-coordinate Co(II) corrinoid substrate and to the activity of the enzyme. *Biochemistry* **2009,** *48*, 3138-3145.

94. Costa, F. G.; Greenhalgh, E. D.; Brunold, T. C.; Escalante-Semerena, J. C., Mutational and functional analyses of substrate binding and catalysis of the *Listeria monocytogenes* EutT ATP:Co(I)rrinoid adenosyltransferase. *Biochemistry* **2020,** *59*, 1124-1136.

95. Fonseca, M. V.; Escalante-Semerena, J. C., Reduction of cob(III)alamin to cob(II)alamin in *Salmonella enterica* Serovar Typhimurium LT2. *J. Bacteriol.* **2000,** *182*, 4304-4309.

96. Lexa, D.; Saveant, J.-M., The electrochemistry of vitamin B_{12}. *Acc. Chem. Res.* **1983,** *16*, 235-243.

97. Pallares, I. G.; Moore, T. C.; Escalante-Semerena, J. C.; Brunold, T. C., Spectroscopic studies of the *Salmonella enterica* adenosyltransferase enzyme *Se*CobA: Molecular-level insight into the mechanism of substrate cob(II)alamin activation. *Biochemistry* **2014,** *53*, 7969-7982.

98. Park, K.; Mera, P. E.; Escalante-Semerena, J. C.; Brunold, T. C., Spectroscopic characterization of active-site variants of the PduO-type ATP:Corrinoid adenosyltransferase from *Lactobacillus reuteri*: Insights into the mechanism of four-coordinate Co(II)corrinoid formation. *Inorg. Chem.* **2012,** *51*, 4482-4494.

99. Park, K.; Mera, P. E.; Moore, T. C.; Escalante-Semerena, J. C.; Brunold, T. C., Unprecedented mechanism employed by the *Salmonella enterica* EutT ATP:Co(I) rrinoid adenosyltransferase precludes adenosylation of incomplete Co(II)rrinoids. *Angew. Chem.* **2015,** *54*, 7158-7161.

100. Stracey, N. G.; Costa, F. G.; Escalante-Semerena, J. C.; Brunold, T. C., Spectroscopic study of the EutT adenosyltransferase from *Listeria monocytogenes*: Evidence for the formation of a four-coordinate cob(II)alamin intermediate. *Biochemistry* **2018,** *57* (34), 5088-5095.

101. Stich, T. A.; Yamanishi, M.; Banerjee, R.; Brunold, T. C., Spectroscopic evidence for the formation of a four-coordinate Co^{2+} cobalamin species upon binding to the human ATP:Cobalamin adenosyltransferase. *J. Am. Chem. Soc.* **2005,** *127*, 7660-7661.

102. Jost, M.; Cracan, V.; Hubbard, P. A.; Banerjee, R.; Drennan, C. L., Visualization of a radical B_{12} enzyme with its G-protein chaperone. *Proc. Natl. Acad. Sci. U.S.A.* **2015,** *112*, 2419-2424.

103. Buan, N. R.; Escalante-Semerena, J. C., Purification and initial biochemical characterization of ATP:Cob(I)alamin adenosyltransferase (EutT) enzyme of *Salmonella enterica*. *J. Biol. Chem.* **2006,** *281*, 16971-16977.

104. Buan, N. R.; Rehfeld, K.; Escalante-Semerena, J. C., Studies of the CobA-type ATP:Co(I)rrinoid adenosyltransferase enzyme of *Methanosarcina mazei* strain Gö1. *J. Bacteriol.* **2006,** *188*, 3543-3550.

105. Stich, T. A.; Buan, N. R.; Escalante-Semerena, J. C.; Brunold, T. C., Spectroscopic and computational studies of the ATP:Corrinoid adenosyltransferase (CobA) from *Salmonella enterica*: Insights into the mechanism of adenosylcobalamin biosynthesis. *J. Am. Chem. Soc.* **2005,** *127*, 8710-8719.

106. Buan, N. R.; Escalante-Semerena, J. C., Computer-assisted docking of flavodoxin with the ATP:Co(I)rrinoid adenosyltransferase (CobA) enzyme reveals residues critical for protein-protein interactions but not for catalysis. *J. Biol. Chem.* **2005,** *280*, 40948-40956.

107. Mera, P. E.; Escalante-Semerena, J. C., Dihydroflavin-driven adenosylation of 4-coordinate Co(II) corrinoids: are cobalamin reductases enzymes or electron transfer proteins? *J. Biol. Chem.* **2010,** *285*, 2911-2917.

108. Bauer, C. B.; Fonseca, M. V.; Holden, H. M.; Thoden, J. B.; Thompson, T. B.; Escalante-Semerena, J. C.; Rayment, I., Three-dimensional structure of ATP:corrinoid adenosyltransferase from *Salmonella typhimurium* in its free state, complexed with MgATP, or complexed with hydroxycobalamin and MgATP. *Biochemistry* **2001,** *40*, 361-374.

109. Jeter, R. M., Cobalamin-dependent 1,2-propanediol utilization by *Salmonella typhimurium*. *Journal of General Microbiology* **1990,** *136*, 887-896.

110. Bobik, T. A.; Havemann, G. D.; Busch, R. J.; Williams, D. S.; Aldrich, H. C., The propanediol utilization (*pdu*) operon of *Salmonella enterica* serovar Typhimurium LT2 includes genes necessary for formation of polyhedral organelles involved in coenzyme B_{12}-dependent 1, 2-propanediol degradation. *J. Bacteriol.* **1999,** *181*, 5967-5975.

111. Chen, P.; Ailion, M.; Bobik, T.; Stormo, G.; Roth, J., Five promoters integrate control of the *cob/pdu* regulon in *Salmonella typhimurium*. *J. Bacteriol.* **1995,** *177*, 5401-5410.

112. Schubert, H. L.; Hill, C. P., Structure of ATP-bound human ATP:cobalamin adenosyltransferase. *Biochemistry* **2006,** *45*, 15188-15196.

113. Moon, J. H.; Park, A. K.; Jang, E. H.; Kim, H. S.; Chi, Y. M., Crystal structure of a PduO-type ATP:cobalamin adenosyltransferase from *Burkholderia thailandensis*. *Proteins* **2008,** *72*, 1066-1070.

114. Tanaka, Y.; Sasaki, T.; Kumagai, I.; Yasutake, Y.; Yao, M.; Tanaka, I.; Tsumoto, K., Molecular properties of two proteins homologous to PduO-type ATP:cob(I)alamin adenosyltransferase from *Sulfolobus tokodaii*. *Proteins* **2007,** *68*, 446-457.

115. Park, A. K.; Chi, Y. M.; Moon, J. H., Crystal structure of PduO-Type ATP:Cob(I)alamin adenosyltransferase from *Bacillus cereus* in a complex with ATP. *Biochem. Biophys. Res. Commun.* **2011,** *408*, 417-421.

116. St Maurice, M.; Mera, P. E.; Taranto, M. P.; Sesma, F.; Escalante-Semerena, J. C.; Rayment, I., Structural characterization of the active site of the PduO-type ATP:Co(I)rrinoid adenosyltransferase from *Lactobacillus reuteri*. *J. Biol. Chem.* **2007,** *282*, 2596-2605.

117. St Maurice, M.; Mera, P.; Park, K.; Brunold, T. C.; Escalante-Semerena, J. C.; Rayment, I., Structural characterization of a human-type corrinoid adenosyltransferase confirms that coenzyme B_{12} is synthesized through a four-coordinate intermediate. *Biochemistry* **2008,** *47*, 5755-5766.

118. Pallares, I. G.; Moore, T. C.; Escalante-Semerena, J. C.; Brunold, T. C., Spectroscopic studies of the EutT adenosyltransferase from *Salmonella enterica*: Mechanism of four-coordinate Co(II)Cbl formation. *J. Am. Chem. Soc.* **2016,** *138*, 3694-3704.

119. Pallares, I. G.; Moore, T. C.; Escalante-Semerena, J. C.; Brunold, T. C., Spectroscopic studies of the EutT adenosyltransferase from *Salmonella enterica*: Evidence of a tetrahedrally coordinated divalent transition metal cofactor with cysteine ligation. *Biochemistry* **2017,** *56*, 364-375.

120. Costa, F. G.; Escalante-Semerena, J. C., A new class of EutT ATP:Co(I)rrinoid adenosyltransferases found in *Listeria monocytogenes* and other *Firmicutes* does not require a metal ion for activity. *Biochemistry* **2018,** *57* (34), 5076-5087.

121. Andersson, D. I.; Roth, J. R., Mutations affecting regulation of cobinamide biosynthesis in *Salmonella typhimurium*. *J. Bacteriol.* **1989,** *171*, 6726-6733.

122. Li, Z.; Kitanishi, K.; Twahir, U. T.; Cracan, V.; Chapman, D.; Warncke, K.; Banerjee, R., Cofactor Editing by the G-protein Metallochaperone Domain Regulates the Radical B_{12} Enzyme IcmF. *J. Biol. Chem.* **2017,** *292*, 3977-3987.

123. Foster, M. A.; Dilworth, M. J.; Woods, D. D., Cobalamin and the synthesis of methionine by *Escherichia coli*. *Nature* **1964,** *201*, 39-42.

124. Whitfield, C. D.; Steers, E. J., Jr.; Weissbach, H., Purification and properties of 5-methyltetrahydropteroyltriglutamate-homocysteine transmethylase. *J. Biol. Chem.* **1970,** *245*, 390-401.

125. Bandarian, V.; Ludwig, M. L.; Matthews, R. G., Factors modulating conformational equilibria in large modular proteins: a case study with cobalamin-dependent methionine synthase. *Proc. Natl. Acad. Sci. U.S.A.* **2003,** *100*, 8156-8163.

126. Drennan, C. L.; Matthews, R. G.; Ludwig, M. L., Cobalamin-dependent methionine synthase: the structure of a methylcobalamin-binding fragment and implications for other B_{12}-dependent enzymes. *Curr. Opin. Struct. Biol.* **1994,** *4*, 919-929.

127. Drennan, C. L.; Huang, S.; Drummond, J. T.; Matthews, R. G.; Ludwig, M. L., How a protein binds B_{12}: A 3.0Å X-ray structure of B_{12}-binding domains of methionine synthase. *Science* **1994,** *266*, 1669-1674.

128. Goulding, C. W.; Postigo, D.; Matthews, R. G., Cobalamin-dependent methionine synthase is a modular protein with distinct regions for binding homocysteine, methyltetrahydrofolate, cobalamin, and adenosylmethionine. *Biochemistry* **1997,** *36*, 8082-8091.

129. Vetter, H., Jr.; Knappe, J., Flavodoxin and ferredoxin of *Escherichia coli*. *Hoppe-Seyler's Zeitschrift fur Physiologische Chemie* **1971,** *352*, 433-446.

130. Nishimura, S., Structure, biosynthesis, and function of queuosine in transfer RNA. *Prog. Nucleic Acid Res. Mol. Biol.* **1983,** *28*, 49-73.

131. Miles, Z. D.; McCarty, R. M.; Molnar, G.; Bandarian, V., Discovery of epoxyqueuosine (oQ) reductase reveals parallels between halorespiration and tRNA modification. *Proc. Natl. Acad. Sci. U.S.A.* **2011,** *108*, 7368-7372.

132. Dowling, D. P.; Miles, Z. D.; Kohrer, C.; Maiocco, S. J.; Elliott, S. J.; Bandarian, V.; Drennan, C. L., Molecular basis of cobalamin-dependent RNA modification. *Nucleic Acids Res.* **2016,** *44*, 9965-9976.

133. Badia, J.; Ros, J.; Aguilar, J., Fermentation mechanism of fucose and rhamnose in *Salmonella typhimurium* and *Klebsiella pneumoniae*. *J. Bacteriol.* **1985,** *161*, 435-437.

134. Bobik, T. A.; Xu, Y.; Jeter, R. M.; Otto, K. E.; Roth, J. R., Propanediol utilization genes (*pdu*) of *Salmonella typhimurium*: three genes for the propanediol dehydratase. *J. Bacteriol.* **1997,** *179*, 6633-6639.

135. Frank, S.; Lawrence, A. D.; Prentice, M. B.; Warren, M. J., Bacterial microcompartments moving into a synthetic biological world. *J. Biotechnol.* **2013,** *163*, 273-279.

136. Leal, N. A.; Havemann, G. D.; Bobik, T. A., PduP is a coenzyme-A-acylating propionaldehyde dehydrogenase associated with the polyhedral bodies involved in B_{12}-dependent 1,2-propanediol degradation by *Salmonella enterica* serovar Typhimurium LT2. *Arch. Microbiol.* **2003,** *180*, 353-361.

137. Sampson, E. M.; Bobik, T. A., Microcompartments for B_{12}-dependent 1,2-propanediol degradation provide protection from DNA and cellular damage by a reactive metabolic intermediate. *J. Bacteriol.* **2008,** *190*, 2966-2971.

138. Rondon, M. R.; Kazmierczak, R.; Escalante-Semerena, J. C., Glutathione is required for maximal transcription of the cobalamin biosynthetic and 1,2-propanediol utilization (*cob/pdu*) regulon and for the catabolism of ethanolamine, 1,2-propanediol, and propionate in *Salmonella typhimurium* LT2. *J. Bacteriol.* **1995,** *177*, 5434-5439.

139. Brinsmade, S. R.; Paldon, T.; Escalante-Semerena, J. C., Minimal functions and physiological conditions required for growth of *Salmonella enterica* on ethanolamine in the absence of the metabolosome. *J. Bacteriol.* **2005,** *187*, 8039-8046.

140. Havemann, G. D.; Bobik, T. A., Protein content of polyhedral organelles involved in coenzyme B_{12}-dependent degradation of 1,2-propanediol in *Salmonella enterica* serovar Typhimurium LT2. *J. Bacteriol.* **2003,** *185*, 5086-5095.

141. Jeter, R. M.; Roth, J. R., Cobalamin (vitamin B_{12}) biosynthetic genes of S*almonella typhimurium*. *J. Bacteriol.* **1987,** *169*, 3189-3198.

142. Bobik, T. A.; Ailion, M.; Roth, J. R., A single regulatory gene integrates control of vitamin B_{12} synthesis and propanediol degradation. *J. Bacteriol.* **1992,** *174*, 2253-2266.

143. Yamanishi, M.; Yamada, S.; Muguruma, H.; Murakami, Y.; Tobimatsu, T.; Ishida, A.; Yamauchi, J.; Toraya, T., Evidence for axial coordination of 5,6-dimethylbenzimidazole to the cobalt atom of adenosylcobalamin bound to diol dehydratase. *Biochemistry* **1998,** *37*, 4799-4803.

144. Abeles, R. H.; Dolphin, D., The vitamin B_{12} coenzyme. *Acc. Chem. Res.* **1976,** *9*, 114-120.

145. Payne, K. A. P.; Quezada, C. P.; Fisher, K.; Dunstan, M. S.; Collins, F. A.; Sjuts, H.; Levy, C.; Hay, S.; Rigby, S. E. J.; Leys, D., Reductive dehalogenase structure suggests a mechanism for B_{12}-dependent dehalogenation. *Nature* **2015,** *517*, 513-516.

146. Toraya, T.; Fukui, S., Ternary complex formation of 1,2-propanediol dehydratase, cobamide coenzyme and substrate analogue. *Biochem. Biophys. Res. Commun.* **1969,** *36* (3), 469-474.

147. Bachovchin, W. W.; Eagar Jr, R. G.; Moore, K. W.; Richards, J. H., Mechanism of action of adenosylcobalamin: glycerol and other substrate analogs as substrates and inactivators

for propanediol dehydratase-kinetics, stereospecificity, and mechanism. *Biochemistry* **1977,** *16*, 1082-1092.

148. Mori, K.; Toraya, T., Mechanism of reactivation of coenzyme B_{12}-dependent diol dehydratase by a molecular chaperone-like reactivating factor. *Biochemistry* **1999,** *38*, 13170-13178.

149. Toraya, T.; Tanokuchi, A.; Yamasaki, A.; Nakamura, T.; Ogura, K.; Tobimatsu, T., Diol dehydratase-reactivase Is essential for recycling of Coenzyme B_{12} in diol dehydratase. *Biochemistry* **2015**.

150. Bertin, Y.; Girardeau, J. P.; Chaucheyras-Durand, F.; Lyan, B.; Pujos-Guillot, E.; Harel, J.; Martin, C., Enterohaemorrhagic *Escherichia coli* gains a competitive advantage by using ethanolamine as a nitrogen source in the bovine intestinal content. *Environ. Microbiol.* **2011,** *13*, 365-377.

151. Price-Carter, M.; Tingey, J.; Bobik, T. A.; Roth, J. R., The alternative electron acceptor tetrathionate supports B_{12}-dependent anaerobic growth of *Salmonella enterica* serovar Typhimurium on ethanolamine or 1,2-propanediol. *J. Bacteriol.* **2001,** *183*, 2463-2475.

152. Thiennimitr, P.; Winter, S. E.; Winter, M. G.; Xavier, M. N.; Tolstikov, V.; Huseby, D. L.; Sterzenbach, T.; Tsolis, R. M.; Roth, J. R.; Baumler, A. J., Intestinal inflammation allows *Salmonella* to use ethanolamine to compete with the microbiota. *Proc. Natl. Acad. Sci. U.S.A.* **2011,** *108*, 17480-17485.

153. Srikumar, S.; Fuchs, T. M., Ethanolamine utilization contributes to proliferation of *Salmonella enterica* serovar Typhimurium in food and in nematodes. *Appl. Environ. Microbiol.* **2011,** *77*, 281-290.

154. Roof, D. M.; Roth, J. R., Ethanolamine utilization in *Salmonella typhimurium*. *J. Bacteriol.* **1988,** *170*, 3855-3863.

155. Kaval, K. G.; Gebbie, M.; Goodson, J. R.; Cruz, M. R.; Winkler, W. C.; Garsin, D. A., Ethanolamine utilization and bacterial microcompartment formation are subject to carbon catabolite repression. *J. Bacteriol.* **2019,** *201*, e00703-18.

156. Roof, D. M.; Roth, J. R., Autogenous regulation of ethanolamine utilization by a transcriptional activator of the *eut* operon in S*almonella typhimurium*. *J. Bacteriol.* **1992,** *174*, 6634-6643.

157. Anderson, C. J.; Kendall, M. M., Location, location, location. *Salmonella* senses ethanolamine to gauge distinct host environments and coordinate gene expression. *Microb. Cell* **2016,** *3*, 89-91.

158. Sturms, R.; Streauslin, N. A.; Cheng, S.; Bobik, T. A., In *Salmonella enterica*, ethanolamine utilization is repressed by 1,2-propanediol to prevent detrimental mixing of components of two different bacterial microcompartments. *J. Bacteriol.* **2015,** *197*, 2412-2421.

159. Bradbeer, C., The clostridial fermentation of choline and ethanolamine. II. Requirement for a cobamide coenzyme by an ethanolamine deaminase. *J. Biol. Chem.* **1965,** *240*, 4675-4681.

160. Rondon, M. R.; Horswill, A. R.; Escalante-Semerena, J. C., DNA polymerase I function is required for the utilization of ethanolamine, 1,2-propanediol, and propionate by *Salmonella typhimurium* LT2. *J. Bacteriol.* **1995,** *177*, 7119-7124.

161. Stojiljkovic, I.; Baumler, A. J.; Heffron, F., Ethanolamine utilization in *Salmonella typhimurium*: nucleotide sequence, protein expression, and mutational analysis of the *cchA cchB eutE eutJ eutG eutH* gene cluster. *J. Bacteriol.* **1995,** *177*, 1357-1366.

162. Huseby, D. L.; Roth, J. R., Evidence that a metabolic microcompartment contains and recycles private cofactor pools. *J. Bacteriol.* **2013,** *195*, 2864-2879.

163. Choudhary, S.; Quin, M. B.; Sanders, M. A.; Johnson, E. T.; Schmidt-Dannert, C., Engineered protein nano-compartments for targeted enzyme localization. *PLoS One* **2012,** *7*, e33342.

164. Jakobson, C. M.; Kim, E. Y.; Slininger, M. F.; Chien, A.; Tullman-Ercek, D., Localization of proteins to the 1,2-propanediol utilization microcompartment by non-native signal sequences is mediated by a common hydrophobic motif. *J. Biol. Chem.* **2015,** *290*, 24519-24533.

165. Bandarian, V.; Reed, G. H., Analysis of the electron paramagnetic resonance spectrum of a radical intermediate in the coenzyme B_{12}-dependent ethanolamine ammonia-lyase catalyzed reaction of *S*-2-aminopropanol. *Biochemistry* **2002,** *41*, 8580-8588.

166. Kaplan, B. H.; Stadtman, E. R., Ethanolamine deaminase, a cobamide coenzyme-dependent enzyme. I. Purification, assay, and properties of the enzyme. *J. Biol. Chem.* **1968,** *243*, 1787-1793.

167. Mori, K.; Bando, R.; Hieda, N.; Toraya, T., Identification of a reactivating factor for adenosylcobalamin-dependent ethanolamine ammonia lyase. *J. Bacteriol.* **2004,** *186*, 6845-6854.

2.18 FIGURES

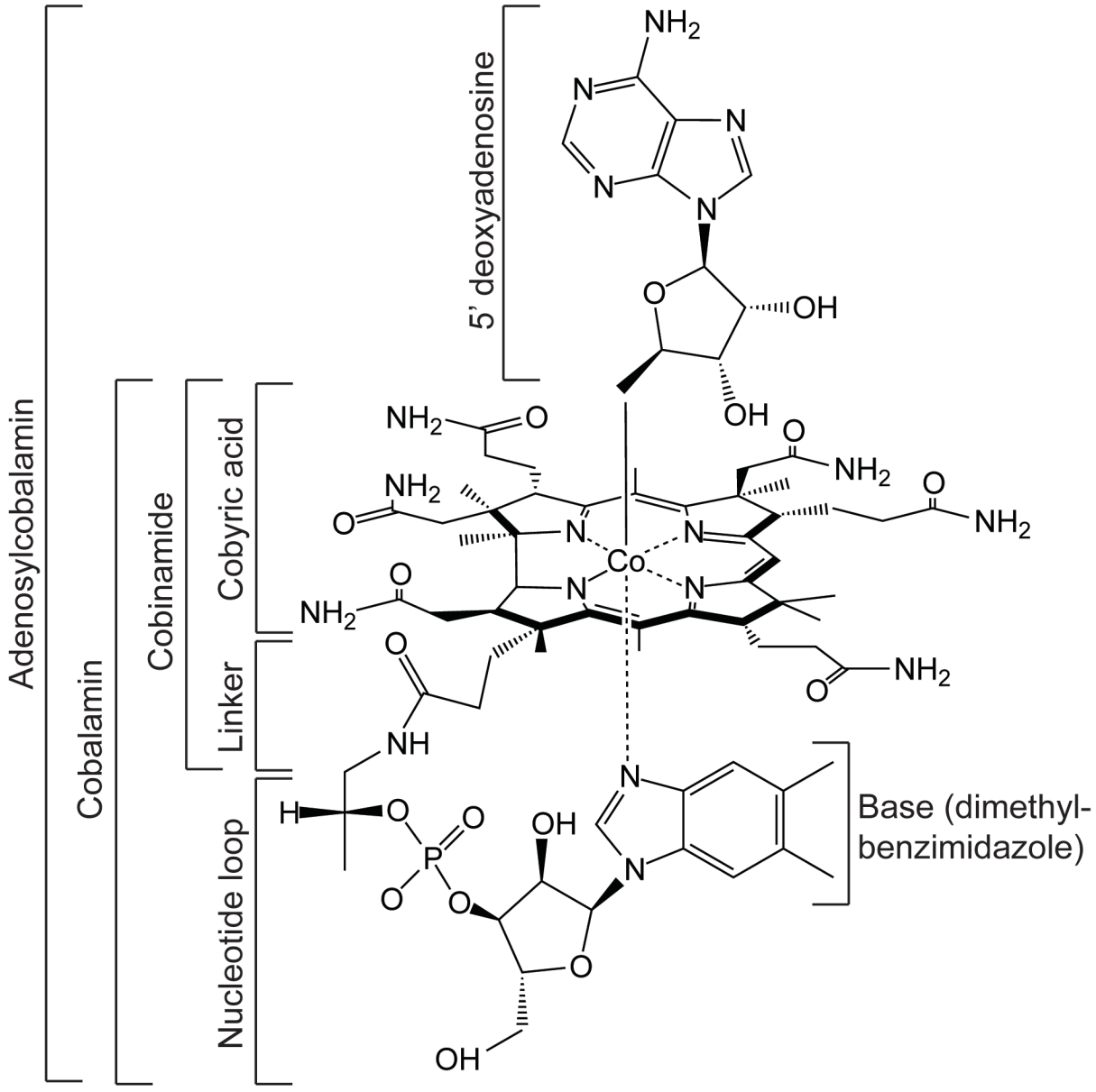

Figure 1.2. **Structure of adenosylcobalamin (AdoCbl)**. The fully amidated corrin ring is cobyric acid (Cby). An aminopropanol linker is added, forming cobinamide. The aminopropanol linker connects the nucleotide loop and base to the corrin ring, forming cobalamin. The base is 5,6-dimethylbenzimidazole (DMB), which forms a coordination bond with the Co ion, ie the *Coa* ligand of the ring. The covalent organometallic bond between 5'deoxyadenosine and the Co ion, *i.e*, the *Co* ligand of the ring, is critical to the function of the coenzyme.

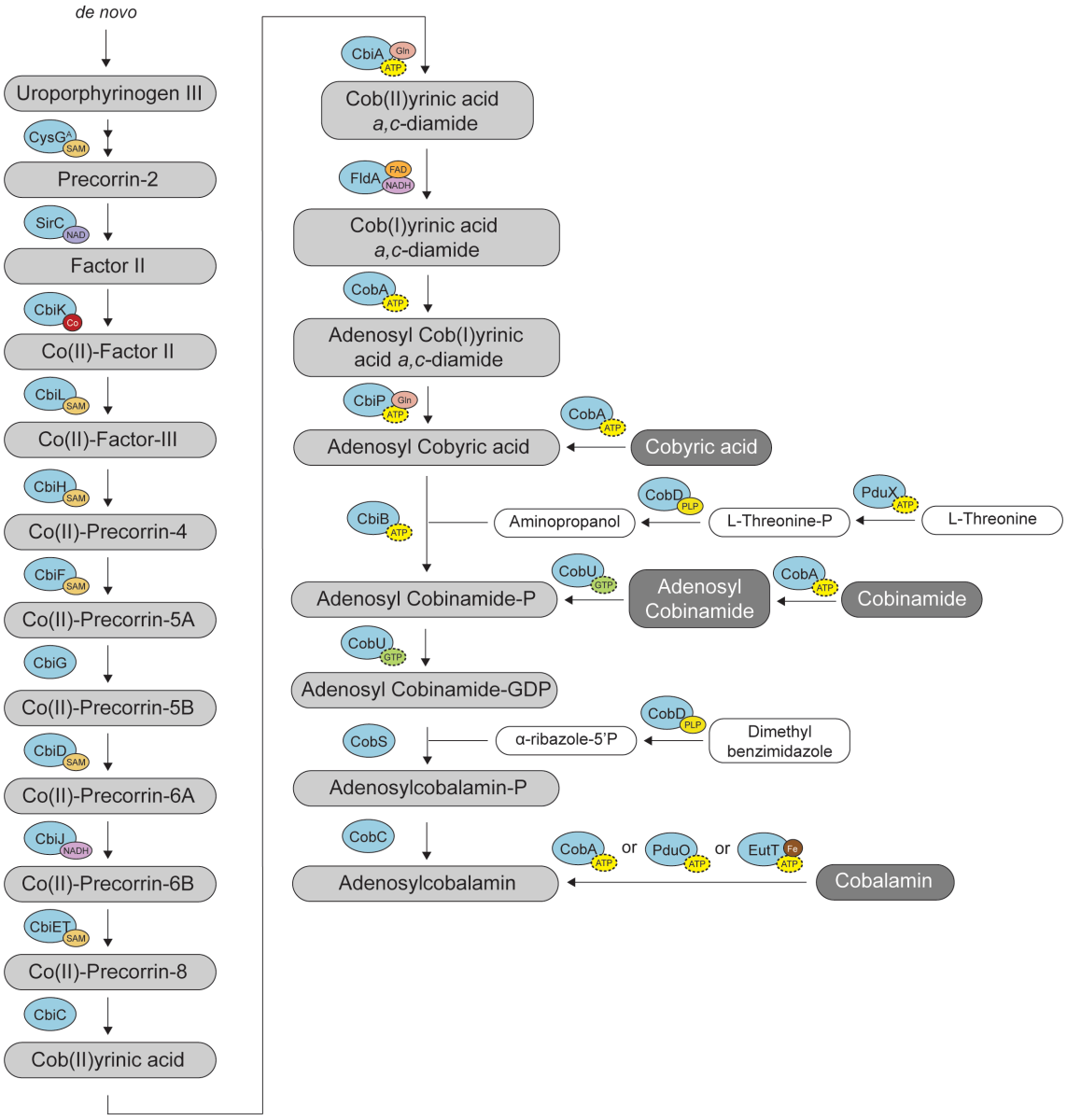

Figure 2.2. Biosynthesis of AdoCbl in *S. enterica.* Enzymes are in blue, and associated cofactors or substrates are depicted in the smaller oval associated with the enzyme. In light gray, the *de novo* pathway from uroporphyrinogen III to adenosylcobalamin (AdoCbl) is shown. In dark gray are pathways indicating corrinoids that *S. enterica* can scavenge from the environment and incorporate into the biosynthetic pathway. The enzymatic steps that form the aminopropanol linker and the nucleotide loop are indicated in white at the location where they enter the pathway

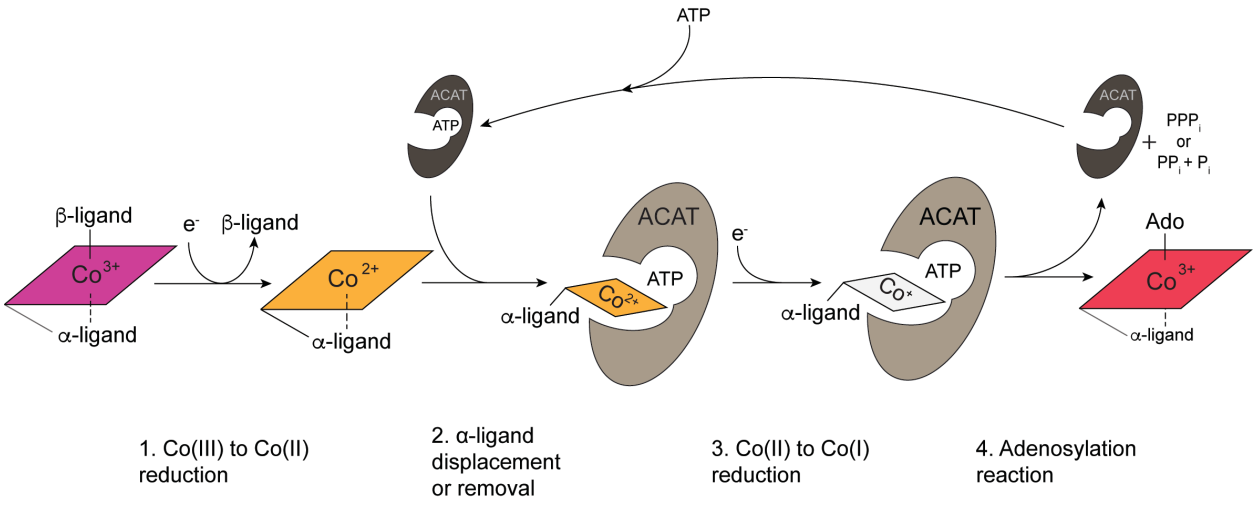

Figure 2.3 General mechanism of ATP:Co(I)rrinoid adenosyltransferases (ACATs). In the extracellular environment, corrinoids are coordinated by ligands at both faces of the ring in addition to the equatorial coordination by the tetrapyrrole ring, forming six-coordinate (6C) corrinoid. In the intracellular environment, free dihydroflavins or flavin reductase (represented by e^-) reduce Co(III) to Co(II), removing the b-ligand and forming five-coordinate (5C) corrinoid. The ACAT enzyme, typically already bound to ATP, binds to the corrinoid substrate and facilitates the displacement of the a-ligand, forming four-coordinate (4C) corrinoid. Then, reduction of Co(II) to Co(I) is performed with free dihydroflavins or flavin reductase (represented by e^-), quickly followed by the adenosylation of the corrinoid.

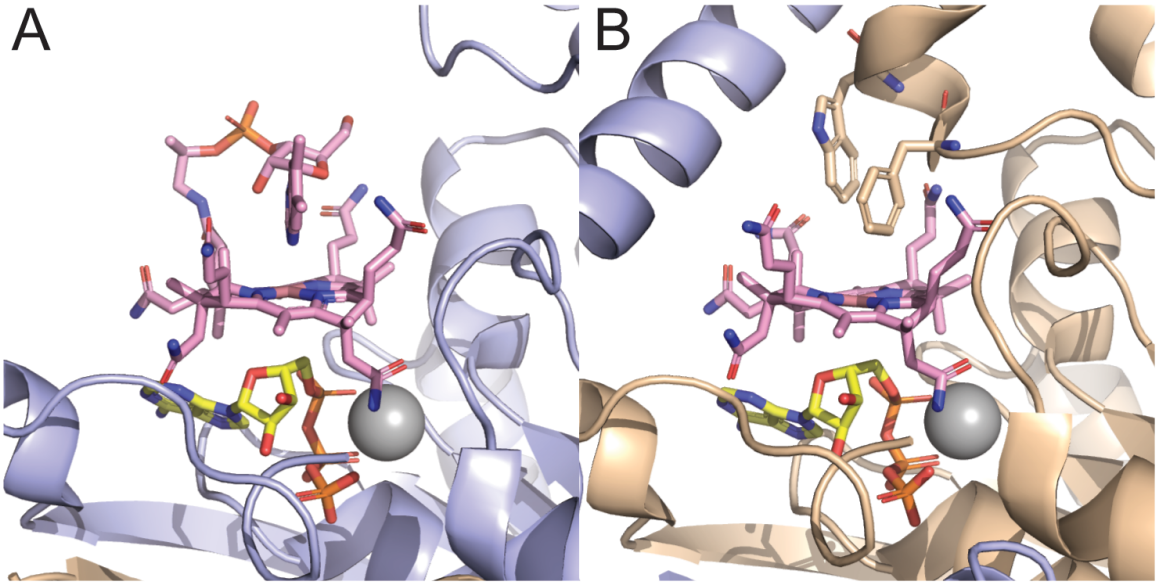

Figure 2.4 X-Ray crystallography structure of CobA from *Salmonella enterica.* Each panel shows a close-up view of each binding site, in which one substrate binding site has cobalamin in the A) five-coordinate state and the active site is "open", while the other substrate binding site has cobalamin in the B) four-coordinate state, and the active site is "closed". In both panels, ATP is shown in yellow, the Mg(II) ion in gray, and cobalamin in pink. In panel B, Phe91 and Trp93 are shown precluding coordination of a ligand at the *Coa* face of the corrin ring.

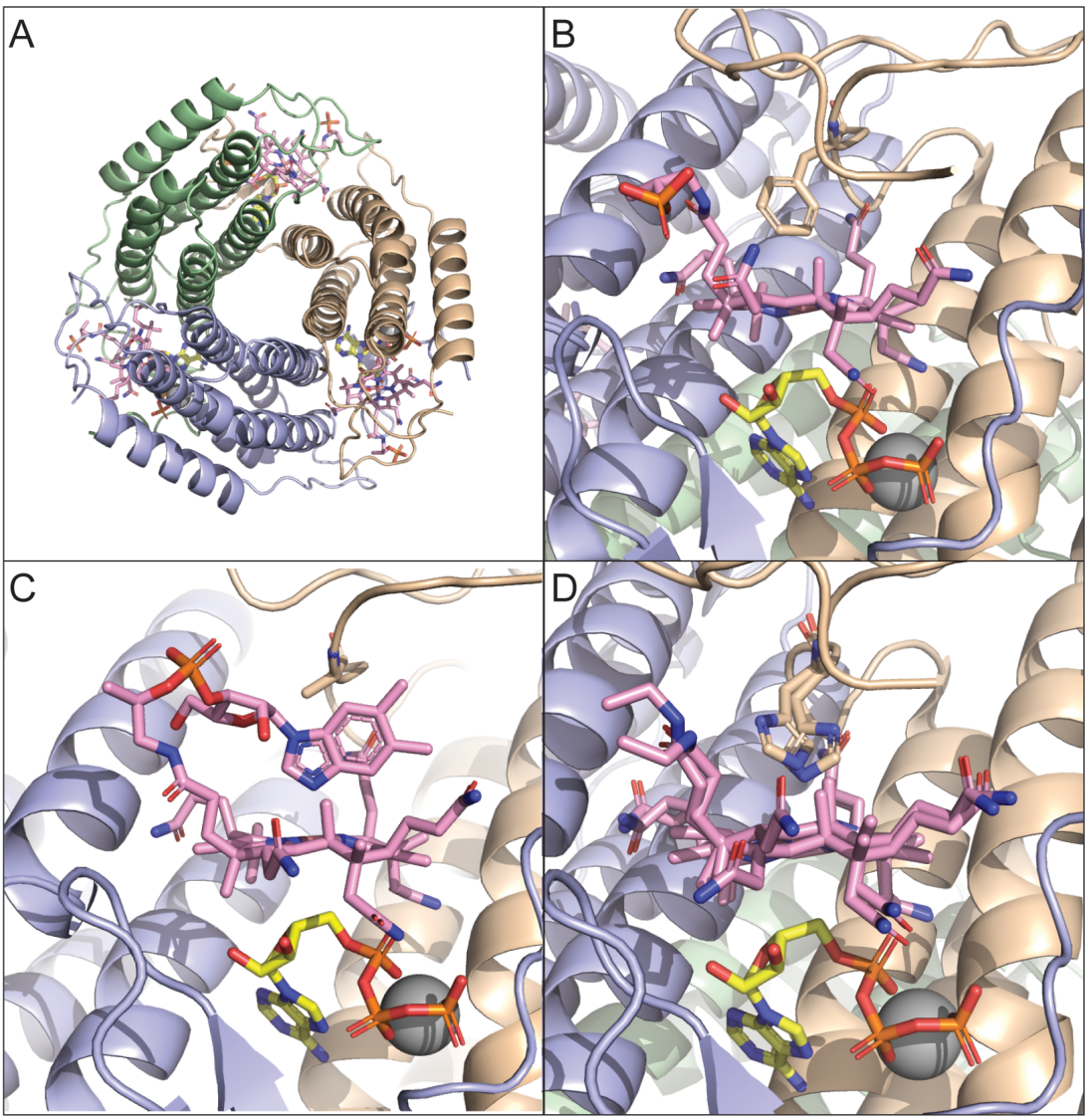

Figure 2.5 X-Ray crystallography structures of PduO from *Lactobacillus reuteri.* In all panels, ATP is shown in yellow, the Mg(II) ion in gray, and cobalamin in pink. A) Top-down view of the *Lr*PduO trimer. Each subunit is highlighted with a different color. B) Close-up of one of the intersubunit active sites of *Lr*PduO bound to Co(II)Cbl and ATP. Here, the F112 residue precludes coordination of a ligand at the *Coa* face of the ring. C) The intersubunit active site of a *Lr*PduO variant with a F112A mutation. The absence of the bulky side chain permits binding of the lower ligand, preventing Co(II) → Co(I) reduction and subsequent adenosylation. D) The intersubunit active site of a *Lr*PduO variant with a F112H mutation. The histidine can form a coordination bond in lieu of a lower ligand, also preventing the Co(II) → Co(I) reduction and subsequent adenosylation.

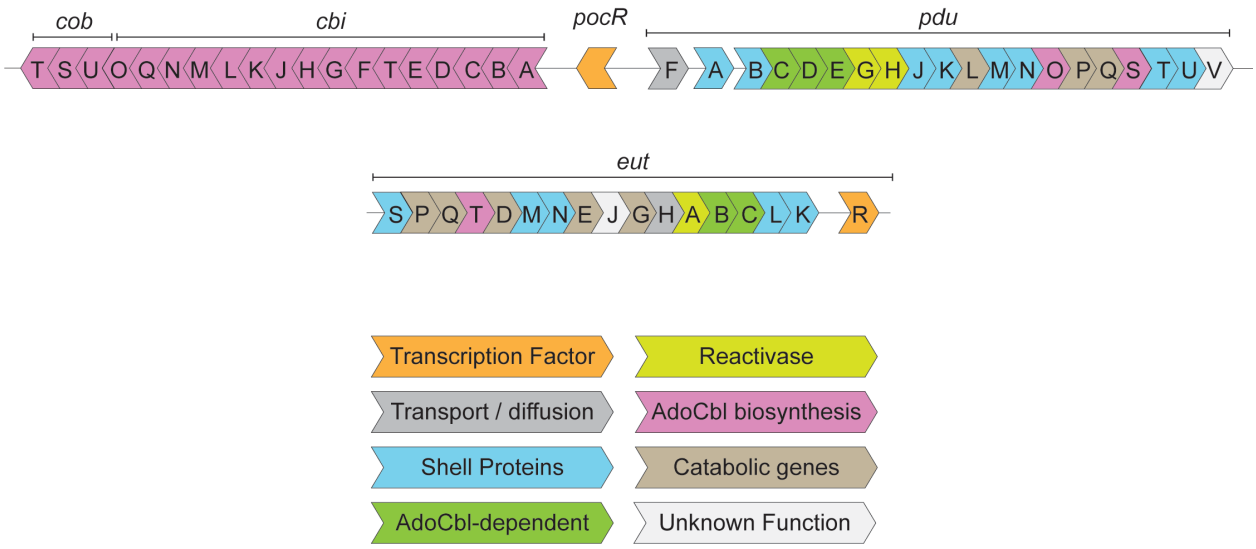

Figure 2.6 Genetic organization of the operons encoding cobalamin biosynthesis, 1,2-propanediol catabolism and ethanolamine catabolism genes in *S. enterica*. The genes are color-coded to denote their function and the color coding is labeled in the figure.

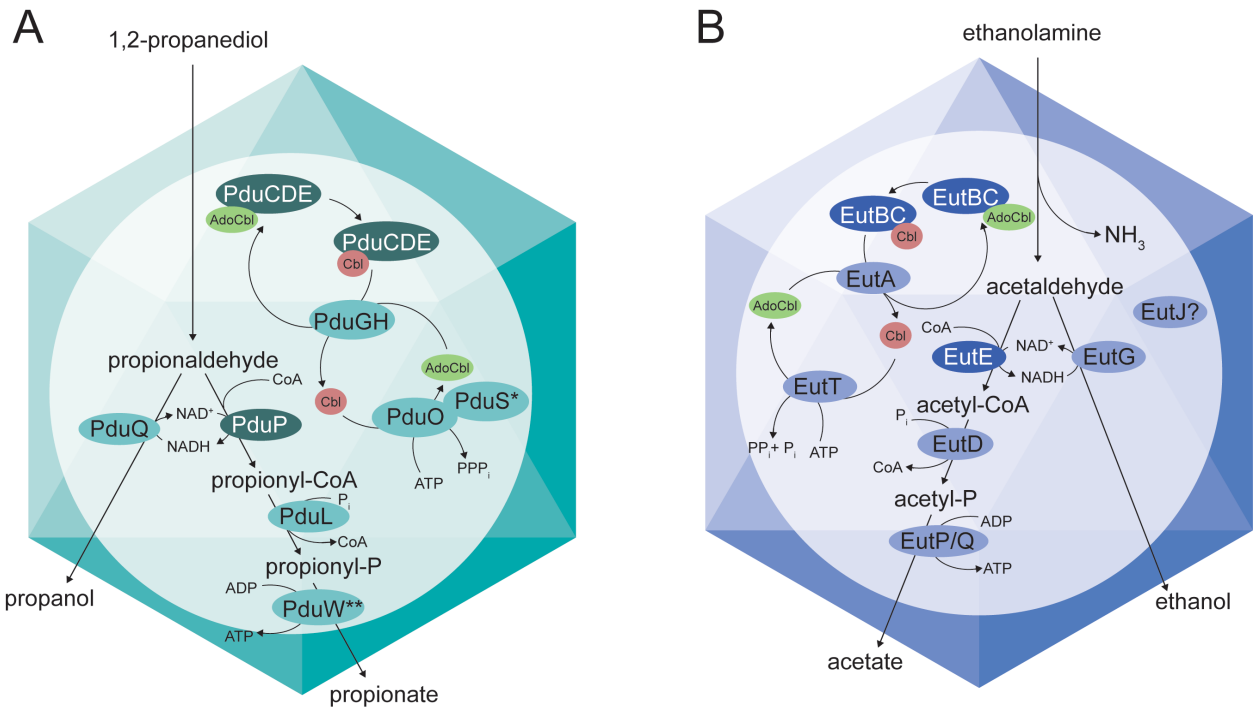

Figure 2.7 Metabolism of 1,2-propanediol (A) and ethanolamine (B) in *S. enterica.* Pathways are denoted by arrows, with intermediates and cofactors labeled. Enzymes are depicted in larger ovals. Enzymes denoted with white font encode an N-terminal amino acid sequence that localizes that enzyme to the metabolosome. AdoCbl is depicted as a green oval, and Cbl is depicted as a red circle. In both pathways, the intermediate is an aldehyde product that is sequestered by the metabolosome shell. The aldehyde intermediate is then oxidized to propionyl-CoA, which can undergo phosphorylation followed by formation of ATP. To balance NADH/NAD^+, aldehyde can also be reduced to an alcohol.
*PduS is suggested to be a corrinoid reductase
**PduW has not been detected in purified 1,2-propanediol metabolosomes

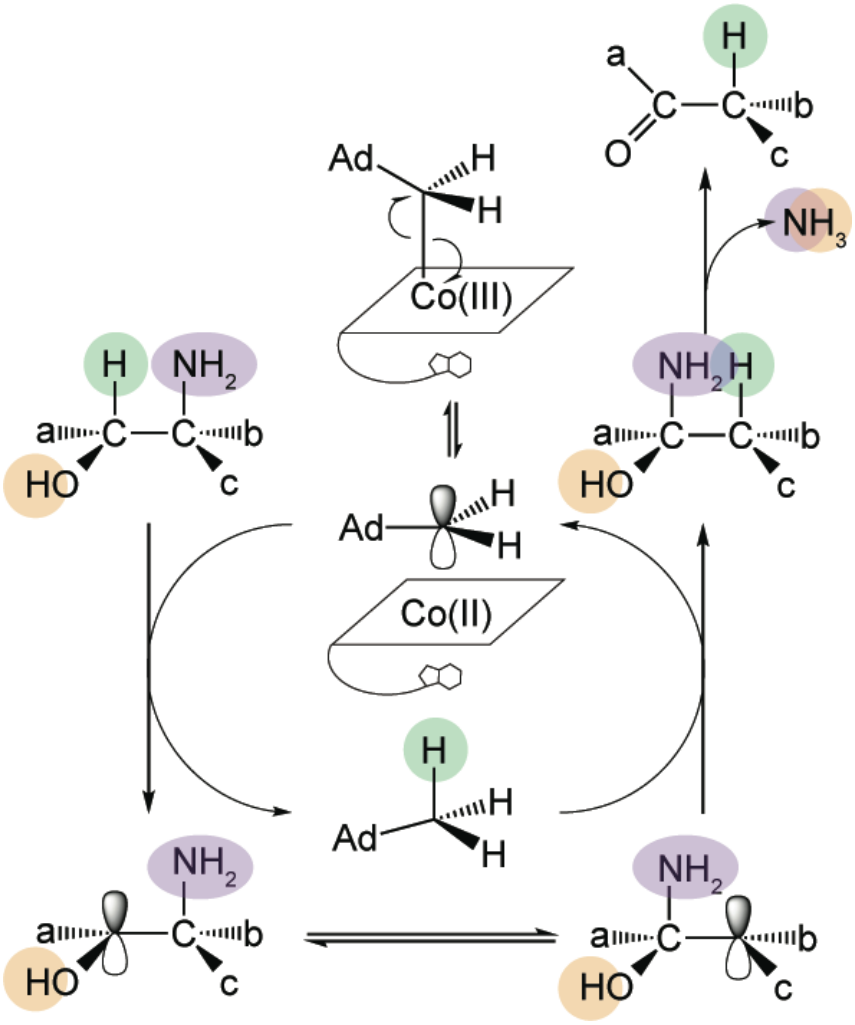

Figure 2.8. Mechanism of action of ethanolamine ammonia-lyase (EAL). When bound to ethanolamine, EAL homolytically cleaves the Co - C bond of AdoCbl, producing an Ado• radical. The Ado• radical abstracts a hydrogen (highlighted in green, and the amine group (highlighted in purple) travels from C2 to C1. The hydrogen (highlighted in green) is abstracted from the adenosyl group, and subsequent deamination results in ammonia and acetaldehyde.

CHAPTER 3

A NEW CLASS OF EUTT ATP:CO(I)RRINOID ADENOSYLTRANSFERASES FOUND IN *LISTERIA MONOCYTOGENES* AND OTHER *FIRMICUTES* DOES NOT REQUIRE A METAL ION FOR ACTIVITY[1]

[1]Costa, F. G., & Escalante-Semerena, J. C. (2018). A new class of EutT ATP: Co(I)rrinoid adenosyltransferases found in *Listeria monocytogenes* and other *Firmicutes* does not require a metal ion for activity. *Biochemistry*, *57*(34), 5076-5087. Copyright (2018) American Chemical Society. Author link: https://pubs.acs.org/articlesonrequest/AOR-SCUZk6rdiDstSrXbT8qY. Reprinted here with permission of publisher.

3.1 ABSTRACT

ATP:Co(I)rrinoid adenosyltransferases (ACATs) are involved in *de novo* adenosylcobamide (AdoCba) biosynthesis, and in salvaging complete and incomplete corrinoids from the environment. The ACAT enzyme family is comprised of three classes of structurally and evolutionarily distinct proteins (*i.e.,* CobA, PduO, EutT). The structure of EutT is unknown, and an understanding of its mechanism is incomplete. The *Salmonella enterica* EutT (*Se*EutT) enzyme is the best-characterized member of its class and is known to be a ferroprotein. Here, we report the identification and initial biochemical characterization of an enzyme representative of a new class of EutTs that does not require a metal ion for activity. *In vivo* and *in vitro* evidence shows that the metal-less EutT homologue from *Listeria monocytogenes* (*Lm*EutT) has ACAT activity, and that unlike other ACATs, the biologically active form of *Lm*EutT is a tetramer. *In vitro* studies revealed that *Lm*EutT was more efficient than *Se*EutT and displayed positive cooperativity. *Lm*EutT adenosylated cobalamin but not cobinamide, showed specificity for ATP and 2'-deoxyATP, and released a triphosphate by-product. Bioinformatics analyses suggest that metal-less EutT ACATs are also present in other *Firmicutes*.

3.2 INTRODUCTION

Like most vitamins, vitamin B_{12} (a.k.a. cyanocobalamin, CNB_{12}) needs to be converted to its coenzymic, biologically active form. In coenzyme B_{12} (a.k.a. adenosylcobalamin, AdoCbl), the upper ligand is a 5'-deoxyadenosine (Ado) group that is attached to the corrin ring via a unique covalent organometallic C-Co bond (Fig. 3.1, panel A). AdoCbl is used by cells to perform carbon-based radical chemistry, which is initiated by the homolysis of the C-Co bond. Ado• radicals are used to extract non-acidic hydrogen atoms to accelerate the cleavage of C-C, C-N, and C-O bonds to allow group migrations within the molecule [reviewed in [3]]. *Salmonella enterica* is an enterobacterium that synthesizes AdoCbl *de novo* or from precursors found in its environment [reviewed in [4]]. Corrinoid adenosylation has been extensively studied in this bacterium.

Enzymes responsible for the attachment of the Ado upper ligand of the ring are known as ATP:Co(I)rrinoid adenosyltransferases (hereafter ACATs; PF01923). With the exception of plants and fungi, ACATs are found in cells from all domains of life [reviewed in [5]]. ACATs facilitate the reduction of Co(II)balamin to Co(I)balamin by the generation of a Co(II)balamin four-coordinate intermediate in the enzyme active site (Fig. 3.1, panel B).[6-10] Three classes of ACATs have been identified, namely CobA, PduO, and EutT. All three classes of ACATs are present in *S. enterica* and have been studied in detail. In *S. enterica*, CobA is the "housekeeping" ACAT, and its activity is required for *de novo* corrin ring biosynthesis and adenosylation of scavenged complete and incomplete corrinoids.[11] PduO is encoded by the *pduO* gene that is part of a 21-gene operon whose functions are used to catabolize 1,2-propanediol.[12-14] AdoCbl is the coenzyme of the 1,2-propanediol dehydratase that converts 1,2-propanediol to propionaldehyde.[15] In-depth studies of CobA and PduO have been reported, and structures with substrates bound to them have been elucidated.[8, 16-18] EutT class of ACATs are not as well understood. In *S. enterica*, EutT is encoded

by the *eutT* gene of the 17-gene ethanolamine utilization (*eut*) operon that encodes functions necessary for the AdoCbl-dependent catabolism of ethanolamine [reviewed in [19]].[20-23]

To date, a structure of a EutT class ACAT has not been reported, but insights into the mechanism of the *S. enterica* enzyme have been published.[10, 24, 25] Unlike CobA and PduO, *S. enterica* EutT (*Se*EutT) requires ferrous ions for optimal activity, but substantial activity is observed when Zn(II) ions substitute for Fe(II) ions. It is known that Fe(II) binds to a cysteine-rich binding motif of *Se*EutT $HX_{11}CCXXC$, and recently published work suggests that the metal promotes the formation of the DMB-off, four-coordinate Co(II)Cbl substrate bound to the active site of *Se*EutT.[24-26]

Here, we report results of bioinformatics analyses of *Se*EutT homologues that revealed a group of EutT homologues in the *Firmicutes* that lack the metal-binding motif present in *Se*EutT. We also report the initial biochemical characterization of a metal-less EutT homologue from *Listeria monocytogenes* 10403S. Our data indicate that metal-less EutT homologues comprise a new class of EutT enzymes.

The accompanying paper by Stracey *et al* (Appendix I) reports spectroscopic evidence that the mechanism of catalysis of *Lm*EutT proceeds via a four-coordinate Co(II)balamin intermediate. Consistemt with our findings, spectroscopic evidence reported by Stracey *et al* show that the enzyme does not adenosylate Co(II)binamide.[27]

3.3 MATERIALS AND METHODS

Bacterial strains and growth media. Strains used in this study were all derivatives of *Salmonella enterica* sv Typhimurium LT2 (Table 3.1). MudJ is an abbreviation of the MudI1734 transposon.[28] Mutant strains were constructed using the lRed recombinase system as described.[29] Transductional crosses needed for strain construction were performed using a high-frequency, general transducing mutant of bacteriophage P22.[30]

Difco nutrient broth (NB) (8 g/L) with NaCl (5 g/L) was used as rich medium. All chemicals were purchased from Sigma-Aldrich Chemical Company unless otherwise stated. All chemicals were reagent grade and were used without further purification. Cyanocobalamin (CNCbl) was added as such to culture media. Hydroxycobalamin (HOCbl) was used in *in vitro* activity assays, dicyanocobinamide [$(CN)_2$Cbi] was decyanated as described elsewhere,[31] and commercially available adenosylcobalamin (AdoCbl) was used as a standard. Two minimal media were used in this work, one medium was no-carbon E (NCE),[32] which contained a source of nitrogen but not a source of carbon, and a second medium lacked nitrogen and carbon (NCN) supplemented with $MgSO_4$ (1 mM), and Wolfe's trace minerals.[33-35] When NCN medium was used, ethanolamine was added as the source of nitrogen. When used as a carbon and energy source ethanolamine was present at 90 mM; the medium was supplemented with CNCbl (200 nM), and IPTG (100 mM). When lactose was used as carbon and energy, it was present at 29 mM. Ethanolamine (1 mM) and CNCbl (50 nM) were added to allow EutR-dependent activation of the *eut* operon, and IPTG (100 mM) to induce expression of plasmid-encoded *Lm*EutT or *Se*EutT. When ethanolamine was used as nitrogen source, NCN medium was supplemented with glycerol (22 mM), ethanolamine (30 mM), Cbl (200 nM) and IPTG (100 mM). For plasmid maintenance, 100 mg/mL or 20 mg/mL ampicillin was added to rich and minimal medium, respectively.

Plasmid construction. All plasmids were constructed using described protocols.[36, 37] *Listeria monocytogenes* 10403S *eutT*$^+$ and *Salmonella enterica eutT*$^+$ genes were amplified from genomic DNA and codon-optimized synthesized DNA (GeneScript) and cloned into the NcoI and SalI sites of vector pTAC-85.[37] *L.m. eutT*$^+$ was also cloned into the expression vector pTEV18 using primers listed in Table S1 and protocols are described elsewhere.[36]

Phenotypic analysis. Strains were grown in biological triplicate in nutrient broth (NB, Difco) medium with ampicillin (100 mg/mL) at 37°C overnight (~16 h) shaking at 155 rpm. Overnight cultures were sub-cultured with a 2.5% inoculum (v/v) into a microtiter plate containing 200 mL of medium per well. Cultures were grown in a plate reader (Biotek, model ELx808) whose chamber was set at 37°C for 48 h with continuous shaking.

Protein purification. BL21-CodonPlus cells (Agilent) containing plasmid pEUT140 (Table 3.2) were grown to an OD_{600} = 0.5 - 0.6 at 37°C in 4 L flasks containing 2 L of Terrific Broth (TB) medium [tryptone (24 g/L), yeast extract (24 g/L), glycerol (4 mL/L), KH_2PO_4 (17 mM), K_2HPO_4 (72 mM), $MgSO_4$ (2 mM)].[38] Metal springs were placed in the flasks to increase aeration. To maintain the plasmids, ampicillin (100 mg/mL) and chloramphenicol (25 mg/mL) were added to the medium. Gene expression was induced by the addition of IPTG (1 mM), and protein over production proceeded for 36 h at 15ºC and shaking (150 rpm). Cells were harvested by centrifugation at 6,000 x *g* for 15 min at 4ºC in a refrigerated Avanti J-20 XPI equipped with a JLA 8.1 rotor. Cell pellets (~1 g of wet cell mass) were resuspended in 5 mL of buffer A [(4-(2-hydroxyethyl)-1-piperazineethanesulfonic acid (HEPES, 50 mM, pH 7.5 at 4 °C), NaCl (0.5 M), imidazole (20 mM), and *tris*(2-chloroethyl)phosphate (TCEP, 1 mM)]. Cell suspensions were incubated at 4 °C for 10 min with lysozyme (1 mg/mL) and DNase (0.1 mg/mL), after which the cell slurry was passed once through a cell disruptor (Constant Systems) at 1.91 kPa; serine protease inhibitor phenylmethanesulfonyl fluoride (PMSF, 1 mM) was added to the cell lysate immediately after lysis. Lysates were centrifuged at 40,000 x *g* for 30 min at 4ºC in an Avanti J-25I centrifuged equipped with a JA 25.50 rotor. Supernatants were filtered with a 0.45 mm polyethersulfone (PES) filter (Millipore). Clarified cell lysate was loaded onto a 5 mL HisTrap Fast Flow (FF) column equilibrated with buffer A. Protein was eluted off the column with an imidazole gradient (20-500

mM). The His_6 tag was cleaved with in-house-purified recombinant tobacco etch virus (rTEV) protease[39] for three hours at room temperature, and protein was dialyzed thrice in buffer A at 4 °C. Protein was re-loaded onto a 5 mL HisTrap FF column and flow-through was collected. Flow-through material was dialyzed against HEPES buffer (50 mM, pH 7.5 at 4 °C), with NaCl (500 mM) and TCEP (1 mM), concentrated using an Amicon Ultra 15 centrifugal filter unit (10 kDa molecular mass cut off), and stored in liquid nitrogen at -80 °C until used.

Purification of LmEutT under anoxic conditions. Protocols for protein overexpression and cell harvesting remained unchanged. Cell pellets were moved into an anoxic chamber (Coy) and resuspended in N_2-sparged buffer A. Lysozyme (1 mg/mL), DNase (0.1 mg/mL) and PMSF (1 mM) were added to the lysate, and the cell slurry was sonicated on ice thrice (2 s on, 2 s off, 1 min total) with five-minute intervals between sonications. Samples were transferred into 50-ml stainless steel centrifuge tubes with an airtight seal and removed from the chamber. Samples were centrifuged at 40,000 x *g* for 30 min at 4 ºC, and the centrifuge tube was returned to the anoxic chamber. Cell lysates were applied to a Ni-NTA affinity chromatography resin (1 mL, Qiagen) equilibrated with buffer A. Five-mL fractions of flow-through were collected, followed by washes with buffer A, buffer A and 5% buffer B [HEPES (50 mM, pH 7.5 at 25 °C), NaCl (500 mM), imidazole (500 mM), and TCEP (1 mM)], buffer A and 6% buffer B, and buffer B. The His_6 tag was cleaved with rTEV protease for two hours at room temperature and the protein was dialyzed thrice against buffer A at 25 °C. Protein was re-loaded onto the Ni-NTA column and fractions of the flow-through, the buffer A wash, and the buffer B wash were collected. Fractions from the buffer A wash were collected and dialyzed against HEPES buffer (50 mM, pH 7.5 at 25 °C) containing NaCl (500 mM) and TCEP (1 mM), and finally against HEPES buffer (20 mM, pH 7.5 at 25 °C) containing NaCl (100 mM) and TCEP (1 mM). Protein was dispensed into 10-mL glass

Balch vials, sealed with a butyl rubber stopper and aluminum seal; samples were stored at -80 °C until used.

Assessment of *Lm*EutT activity in the absence and presence of metals. Purified *Lm*EutT was thawed on ice and dialyzed in 1 L of buffer (50 mM HEPES, 500 mM NaCl, 1 mM TCEP pH 7.5 at 4 ºC) with 1 mM EDTA for 1 h at 4 ºC. *Lm*EutT was then dialyzed thrice in 1 L of buffer treated with Chelex (4 g L^{-1}) to remove the EDTA but maintain the protein demetallated. *Lm*EutT was then assayed for activity in the absence of metal and the presence of Fe(II), Ni(II), Co(II), and Zn(II) (400 nM each) with the microtiter Co(I)balamin assay described below. All buffers and solutions used in the assay were Chelex treated, and all glassware was acid washed with 1 N HCl and rinsed with MilliQ H_2O prior to use.

Assessment of protein homogeneity. To quantify the homogeneity of *Lm*EutT, purified *Lm*EutT samples were loaded onto a 12% (w/v) SDS-PAGE[40] gel containing varying amounts of protein (0.25 to 5.0 mg) and the gel was developed by applying 200 V for 50 min. Protein was visualized using a Coomassie Blue R staining solution (25% isopropanol, 10% acetic acid, 0.05% Coomassie Brilliant Blue R) [41]. The gel was submerged in the staining solution and microwaved for 45 s. After heating, the gel was rinsed and excess dye was removed using acetic acid (10%, v/v). The destaining procedure was repeated twice and the gel was placed in fresh destaining solution and rocked overnight at room temperature. The gel image shown in Figure 3.2 was captured using a FotoDyne digital imaging system and analyzed by TotalLab 1D gel analysis software. The protein purity was calculated by interpolation into a calibration curve obtained by plotting the pixel intensity of the protein of interest in each lane to the protein concentration in each lane. The purity of *Lm*EutT protein used in this work was ~90% as shown in Figure 3.2.

Inductively coupled plasma optical emission spectroscopy (ICP-OES). For both normoxically and anoxically purified protein, *Lm*EutT was dialyzed in buffer with the lowest concentration of buffer and salt possible for the purpose of this experiment. HEPES buffer (20 mM, pH 7.0 at 25 °C) containing NaCl (100 mM) and TCEP (0.25 mM). The protein was then loaded onto a microfuge concentrator and diluted with Chelex 100-treated buffer (0.4% w/v Chelex, BioRad Laboratories). Protein was centrifuged in the concentrator, and the wash was collected and stored; these steps were repeated twice. Two samples of the wash, two samples of the Chelex-treated buffer, and four samples of the *Lm*EutT protein solution were submitted to the Center for Applied Isotope Studies (CAIS) at the University of Georgia for ICP-OES analysis of twenty elements including iron and zinc.

ACAT activity assays. *Lm*EutT activity was assayed using the Co(I) and Co(II) assays described elsewhere in either a microtiter plate or cuvette under anoxic conditions.[17, 24] For both methods the assay buffer [Tris•HCl (100 mM, pH 7.5 at 37 °C), KCl (500 mM), $MgCl_2$ (1 mM) and Ti(III)citrate stock (200 mM)] were each prepared and N_2-sparged in Balch vials.[35] Ti(III)citrate was prepared as described elsewhere.[26] Other substrates were weighed out and transferred into the anoxic chamber before being suspended in anoxic buffer or anoxic water. Aquacobinamide was synthesized using a protocol described elsewhere, and was resuspended in anoxic water.[31]

Microtiter plate setup for LmEutT activity assays. When assays were performed in microtiter dishes, the total volume of the reaction mixture was 300 mL. To set up the reaction, the buffer volume was split into two wells containing a final volume of 150 mL each. Corrinoid and reducing system were incubated in one well, and $MgCl_2$, protein, and ATP were incubated in a second well. This allowed for both pre-incubation of the enzyme with the substrate that binds first, and reduction of Co(III) to Co(II) or Co(I). Both wells were equilibrated at 37°C for 20 min before the reaction

components were mixed together and absorbance was monitored for 45 min at 525 nm for cobalamin (ε = 7877 M^{-1} cm^{-1}) or 458 nm for hydroxocobinamide (ε = 9300 M^{-1} cm^{-1}).

Cuvette setup for Lm*EutT activity assays*. For these assays we used a 1.0-mL quartz cuvette capped with a rubber butyl stopper. The headspace of the cuvette was flushed with O_2-free nitrogen gas for 5 min prior to the addition of reaction mixture components. After flushing, assay buffer (1 mL), Ti(III)citrate (2.5 mM), HOCbl (50 μM), and protein (varied concentrations) were added to the cuvette using pre-flushed Hamilton syringes. Reaction mixtures were then incubated at 37°C for 30 min. The reaction was started by the addition of ATP (1 mM) and formation of AdoCbl was spectrophotometrically monitored at 525 nm.

Determination of kinetic parameters. Pseudo-first order kinetic data were obtained at a range of Cbl concentrations (1-30 mM) with a saturating concentration of ATP (1 mM). Pseudo-first order kinetic data were obtained at a range of concentrations for ATP (1-30 mM) and dATP (1-30 mM) at a saturating concentration of HOCbl (50 mM). The data displayed positive cooperativity and was fit to a sigmoidal equation to obtain the maximum velocity (V_{max}), the K_{half} ($K_{0.5}$), and the Hill constant (h):

$$Y = \frac{V_{max} \times X^h}{(K_{0.5}{}^h + X^h)} \qquad (1)$$

To obtain the turnover constant (k_{cat}), the following equation was used, where the enzyme concentration is represented by E:

$$k_{cat} = \frac{V_{max}}{E} \qquad (2)$$

Catalytic efficiencies were obtained by dividing k_{cat} / $K_{0.5}$.

*Bioassays. Se*EutT and *Lm*EutT proteins were incubated in assay buffer (1 mL) containing $MgCl_2$ (1 mM), Ti(III)citrate (2.5 mM), HOCbl (50 mM), ATP (1 mM) and EutT oligomer (50 nM). A

reaction mixture lacking enzyme, and a reaction mixture lacking ATP were used as controls. Reaction mixtures were kept in the dark for two hours at 37°C, then filtered with a 0.22-mm filter (Amicon). Some reactions were exposed to light for 15 min after the two-hour incubation. AdoCbl and HOCbl standards (Sigma) were prepared at the same concentration as the HOCbl concentration present in the enzyme reaction mixture (50 mM). The reactions were filtered, and 8 mL of the filtered reactions were added to each well of a 96-well plate containing 200 mL of NCE medium containing Wolfe's trace minerals,[35] $MgSO_4$ (1 mM), ethanolamine hydrochloride (90 mM, pH 7), L-methionine (0.5 mM), and a 2.5% (v/v) inoculum of strain JE23613 (Δ*pduO* Δ*cobA* Δ*eutT*) grown overnight in NB with ampicillin (100 mg/mL) medium. Microtiter plates were incubated shaking at 37°C and growth was monitored spectrophotometrically at 630 nm every 90 min. UV-vis scans (250-700 nm) of the product of the *Lm*EutT reaction mixtures were obtained before and after irradiation. Samples were irradiated using a bank of 8x60W incandescent light bulbs placed 30 cm away from the sample. Spectra of the authentic AdoCbl and irradiated AdoCbl were also obtained.

Determination of the phosphate by-product of the *Lm*EutT reaction. A 1-mL cuvette reaction mixture containing assay buffer, $MgCl_2$ (2 mM), Ti(III)citrate (1 mM), HOCbl (100 mM), ATP (3 mM), and *Lm*EutT (20 mg/mL) was incubated in the presence of light to continuously regenerate the Co(II)Cbl substrate and maximize ATP usage. After 5 h, ethylenediaminetetraacetic acid (EDTA) was added to each reaction to a final concentration of 20 mM. Deuterated water (D_2O) was added to the reaction to a final concentration of 17% (v/v). ^{1}H-Decoupled ^{31}P-NMR spectra of the samples were obtained using a Bruker AVANCE III 400 MHz spectrometer (Chemical Sciences Magnetic Resonance Facility at the University of Georgia) set at the default parameters of the spectrometer with the following modifications: a spectral width of 40 ppm, centered on -10

ppm. The data was collected in 512 scans per sample. A phosphoric acid standard was also analyzed to normalize the chemical shift between samples.

Gel permeation liquid chromatography. Purified *Lm*EutT was dialyzed against 1 L of HEPES buffer (50 mM, pH 7.5 at 4 °C), NaCl (500 mM), and TCEP (1 mM), three times. The first two dialyses lasted 1 h, the third dialysis was performed overnight (~14 h). All *Lm*EutT samples were quantified using a Nanodrop 1000 (Thermo Scientific). The column (Superose 12 10/300 GL, GE) was equilibrated with four column volumes of dialysis buffer at a rate of 0.75 mL/min. A sample of *Lm*EutT (100 mL) at a concentration of 4.1 mg/mL was loaded onto the column and the column was developed until the sample was eluted off. After *Lm*EutT was eluted, the column was washed with two column volumes before a new sample was loaded. This procedure was repeated with three samples. The mobile phase was applied at a rate of 0.75 mL min^{-1} and peak fractionation was set to 10 mAU (280 nm) min^{-1}. One major peak eluted, and the eluents from each experiment were collected separately. These eluents were concentrated with a 0.5 mL centrifugal filter (Amicon), quantified using the protein's extinction coefficient (17,400 M^{-1} cm^{-1}) and absorbance at 280 nm, and diluted to 0.582 mg/mL. These samples were assayed for activity using the Co(I)balamin assay mentioned above with HOCbl (50 mM) and ATP (1 mM).

3.4 RESULTS

Bioinformatics and phylogenetic analyses reveal EutT homologues without a metal-binding site. Iterative pBLAST searches identified putative EutT homologues and were aligned using Geneious software and annotated with ESPript (Fig. 3.4).[42,43,44]

Assembly of a phylogenetic tree revealed two distinct groups of EutT homologues (Fig. 3.5). We found that these EutT homologues could be split into two classes, class I and class II. Class I homologues were found in *Enterobacteriaceae*, including *S. enterica*. Notably, all

members of class I EutT proteins contained the critical residues of the metal-binding motif $HX_{11}CCXXC$ found in *Se*EutT (Fig. 3.4).[23, 24] Class II EutT homologues were found in several *Firmicutes* (*e.g., Clostridia, Listeria, Brevibacillus* and *Paenibacillus* species) and did not contain any of the metal-binding residues found in class-I enzymes (Fig. 3.4). Results of *in vivo* and *in vitro* assays showed that class-II EutT homologues from *Clostridium tetani* E88 *and Listeria monocytogenes* subs. 10403S had ATP-Co(I)rrinoid adenosyltransferase activity (data not shown). *L. monocytogenes* EutT (*Lm*EutT) was analyzed further.

Purified *Lm*EutT does not contain a metal. The metal content of normoxically and anoxically purified *Lm*EutT samples were analyzed by inductively coupled plasma-optical emission spectrometry (ICP-OES), probing for the presence of twenty elements including Zn and Fe (Table 3.3). Unlike *Se*EutT. neither iron nor zinc were detected in significant quantities in the proteinaceous solution, a result that was consistent with the absence of the metal-binding motif found in class-I EutT homologues.[24]

***Lm*EutT does not require a metal for activity.** Purified *Lm*EutT was dialyzed in buffer containing EDTA to remove any bound divalent metal ions. EDTA was subsequently dialyzed away in buffer treated with Chelex to maintain a metal-free enzyme and buffer. Various metals were incubated in a reaction mixture with *Lm*EutT protein, and the activity of *Lm*EutT was assayed using the Co(I)balamin assay [23]. *Lm*EutT was active without the addition of metal (sp. act. = 39 nmol AdoCbl/min/mg of protein) and did not show an improvement in activity with the addition of ferrous iron, zinc, cobalt, or nickel, with specific acidity values ranging from 37- 39 nmol of AdoCbl/min/mg of protein. This is in contrast to *Se*EutT, which is inactive without the addition of Zn(II) or Fe(II) ions [24].

***In vivo* evidence that *Lm*EutT has ATP:Co(I)rrinoid adenosyltransferase (ACAT) activity**. The *L. monocytogenes* 10403S *eutT*$^+$ allele was cloned into vector pTAC-85, placing the gene under the control of the isopropyl b-D-1-thiogalactopyranoside (IPTG)-inducible promoter. Primers used to amplify *eutT* are described in Table 3.2. The resulting plasmid (pEUT159) was transformed into a *S. enterica* strain lacking all ACATs known to exist in this bacterium, *i.e.,* CobA, PduO, EutT (hereafter referred to as the ΔACAT strain JE23613, Table 3.1). Plasmids encoding *Se*EutT or *Lm*EutT restored growth with ethanolamine as a carbon and energy source to different degrees, with *Lm*EutT being noticeably less efficient than *Se*EutT (Fig 3.5, panel A, black *vs* gray triangles). To rule out problems with inefficient mRNA translation due to differences in codon usage between *L. monocytogenes and* S. *enterica*, the *L. monocytogenes eutT*$^+$ gene was synthesized (GenScript) for optimal expression in *S. enterica.* Although expression of codon-optimized *L. monocytogenes eutT*$^+$ resulted in improved growth, we observed an ~10-h lag before the onset of exponential growth and limited cell yield (Figure 3.5, panel A, gray diamonds).

To test a condition with a lower cellular requirement for AdoCbl, the same strains were grown in minimal medium containing glycerol as the carbon and energy source and ethanolamine as the nitrogen source. Under these growth conditions all EutT homologues restored growth at similar rates, but exponential growth of the strain that synthesized *Lm*EutT was delayed for ~8h, a delay that was not observed with the strain synthesizing *Se*EutT (Fig. 3.5 panel B, diamonds and inverted triangles *vs* gray triangles). These data suggested that while *Lm*EutT was active *in vivo* and did to a certain extent support ethanolamine ammonia-lyase function, an unidentified problem prevented *Lm*EutT-supported wild-type growth with ethanolamine in this heterologous system. Experiments described below attempted to determine whether *Lm*EutT synthesized sufficient AdoCbl to grow on lactose as a result of the expression of a *lacZ*$^+$ transcriptional fusion under the

control of the *eut* promoter, a condition that requires AdoCbl synthesis but not a functional ethanolamine metabolosome.

***In vivo* assessment of *Lm*EutT function independent of ethanolamine catabolism.** We used an alternative approach to determine the level of *Lm*EutT activity *in vivo* independent of ethanolamine catabolism. For this purpose, the vector encoding *Lm*EutT was transformed into a ΔACAT strain carrying a chromosomal MudJ (*lacZ*$^{+}$) transcriptional fusion in the *eut* operon (strain JE22174).[23, 28] The rationale for this approach was centered on the AdoCbl requirement for the EutR-dependent expression of the *eut* operon.[22, 23] We reasoned that if *Lm*EutT synthesized AdoCbl *in vivo,* it would bind to the EutR/ethanolamine binary complex triggering the transcription of the *eut* operon and the concomitant synthesis of LacZ (*i.e.,* b-galactosidase). Growth with lactose as the source of carbon and energy would mean that *Lm*EutT synthesized sufficiently high levels of AdoCbl to ensure high levels of *eut* operon expression. We observed that the native and codon-optimized *L. monocytogenes eutT*$^{+}$ genes, and the *S. enterica eutT*$^{+}$ gene supported robust growth with lactose (Fig. 3.6, gray diamonds and gray triangles). These results suggested that *Lm*EutT synthesized sufficient AdoCbl. These results also suggested that the observed ethanolamine phenotypes (Fig. 3.5) were probably caused by a reason other than insufficient AdoCbl.

***Lm*EutT is a *bona fide* ATP:Co(I)rrinoid adenosyltransferase (ACAT).** *Lm*EutT was purified to ~90% purity in HEPES buffer (50 mM, pH 7.5 at 4 °C) containing NaCl (0.5 M) and TCEP (1 mM) (Fig. 3.2). The optimal buffer for the ACAT activity assay was determined to be Tris•HCl (0.1 M, pH 7.5) containing KCl (0.5 M). To confirm that the product of the reaction was AdoCbl, *Lm*EutT and *Se*EutT were assayed for activity. The reaction products were filter-sterilized and spotted into wells containing a ΔACAT strain whose growth required AdoCbl. Growth was assessed using NCE minimal medium supplemented with 90 mM ethanolamine without AdoCbl.

Supplementation of the reaction product from both *Se*EutT and *Lm*EutT supported growth on ethanolamine (Fig. 3.7, panel A). A portion of the *Lm*EutT reaction was exposed to light for 15 min before it was added to the bioassay. The ΔACAT indicator strain inoculated into medium containing irradiated AdoCbl did not grow, further confirmation that the product formed was AdoCbl (Fig. 3.7, panel B). When *Lm*EutT was incubated with Cbl without any added ATP, the reaction conferred some growth to the ΔACAT indicator strain compared to the Cbl standard, suggesting that purified *Lm*EutT might have had ATP bound to it.

Specificity of *Lm*EutT for its NTP and corrinoid substrates. To gain insights into the specificity of *Lm*EutT for its NTP substrate, enzyme activity was assayed as a function of the NTP added to the reaction mixture. Unexpectedly, the specific activity of *Lm*EutT when ATP and HOCbl were used as substrates (360 nmol AdoCbl min^{-1} mg^{-1} of protein) was somewhat lower than the specific activity of the enzyme when 2'-deoxy-ATP (hereafter dATP) substituted for ATP (450 nmole AdoCbl min^{-1} mg^{-1} of protein) (Fig. 3.8). No enzyme activity significant from the baseline was detected when ADP, AMP, TTP, GTP, CTP, UTP, or ITP substituted for ATP (Fig. 3.8).

The substrate specificity for HOCbl and aquacobinamide were also tested for *Lm*EutT. The Co(I) assay uses Ti(III)citrate, which reduces the corrinoid directly to the supernucleophillic state required for the adenosylation step. Thus, the Co(I) assay solely determines whether *Lm*EutT can bind and position the substrates correctly, but it does not provide information on its ability to facilitate the reduction of the corrinoid from Co(II) → Co(I). In contrast, the Co(II) assay is used to reduce Co(III) to Co(I), and requires that an ACAT facilitate the second reduction step.[45] Previous work established that CobA interacts with reduced flavodoxin A (FldA) to drive the reduction of Co(II)Cbl to Co(I)Cbl. In contrast to CobA, *Se*EutT can use free dihydroflavins to drive the reduction of Co(II)Cbl to Co(I)Cbl.[24, 46] *Lm*EutT adenosylated both HOCbl and

aquacobinamide when the substrate was reduced to the Co(I) state using Ti(III)citrate, indicating that *Lm*EutT can bind both corrinoids in the substrate binding pocket (Fig. 3.9, third set of columns). However, *Lm*EutT only adenosylated HOCbl when the substrate was reduced to the Co(II), whether FldA-mediated or by free dihydroflavins (Fig. 3.9, first two set of columns).

Triphosphate is the by-product of the *Lm*EutT reaction. We used ^{31}P-NMR to analyze the products of the *Lm*EutT reaction. Signals observed in the spectrum of the complete reaction mixture indicated that triphosphate was the by-product of the reaction (Fig. 3.10, panel A). *Lm*EutT did not cleave ATP in the absence of cobalamin (Fig. 3.10, panel B). The signals observed in the above spectra were compared to authentic standards resuspended in the same buffer (Fig. 3.10, panel C).

Pseudo-first order kinetics analysis of the reaction catalyzed by LmEutT. Kinetic parameters for the reaction catalyzed by *Lm*EutT were obtained with Cbl when MgATP (1 mM) was saturating. Under these conditions, the enzyme displayed positive cooperativity (Fig. 3.11). The analysis was repeated under conditions when cobalamin (50 mM) was saturating and ATP or dATP concentrations were varied. We observed positive cooperativity under all conditions tested, as observed with *Se*EutT previously (Fig. 3.11, panel B and C).[24] A summary of the kinetic parameters is reported in Table 3.4.

***Lm*EutT forms a tetramer**. We determined the oligomeric state of active *Lm*EutT using gel permeation liquid chromatography. The retention time of *Lm*EutT was consistent with a molecular mass of 121 kDa, a mass that closely matched that of tetrameric *Lm*EutT (118 kDa) (Fig. 3.12). We assayed the activity of the *Lm*EutT tetramer collected from the column and compared its activity to that of the protein loaded onto the column. We used the Co(I) assay to compare the activity of the protein after elution from the column to that of the protein loaded onto the column.

The measured specific activities were 309 ± 23 nmol min^{-1} mg-1 and 311 ± 28 nmol min^{-1} mg^{-1}, respectively. These results indicated confirmed that the major peak was *Lm*EutT.

3.5 DISCUSSION

***Listeria monocytogenes* and other *Firmicutes* synthesize a new sub-class of metal-less EutT ATP:Co(I)rrinoid adenosyltransferases**. The EutT homologue encoded by the *L. monocytogenes* genome shares only 29% end-to-end amino acid identity with *Se*EutT (Fig. 3.3). In spite of such limited identity, the *Lm*EutT protein has *bona fide* ACAT activity (Fig. 3.7). Importantly, *Lm*EutT and EutT homologues from other *Firmicutes* lack the metal-binding motif that is critical for metal binding and function in *Se*EutT (Fig. 3.3).

The absence of the metal in *Lm*EutT was confirmed by results of ICP-OES analysis of ~90% homogeneous, enzymatically active *Lm*EutT enzyme (Fig. 3.3, Table 3.3). Consistent with the idea that *Lm*EutT does not require a metal ion for activity, EDTA-treated *Lm*EutT was active as untreated enzyme. The lack of metal in *Lm*EutT is of interest, because in *Se*EutT Fe(II) somehow disrupts the coordination bond between DMB and the Co(II) ion of the ring. The resulting DMB-off form of the corrinoid substrate results in a Co(II) four-coordinate species whose redox potential is within physiological range and can be readily reduced to Co(I) cobalamin by dihydroflavins.[24, 25, 45] At present, it is unclear how *Lm*EutT generates the Co(II) four-coordinate species of the cobalamin in the absence of a metal ion.

***Lm*EutT is a *bona fide* ATP:Co)I)rrinoid adenosyltransferase.** Three lines of evidence support this conclusion. First, *Lm*EutT compensated for the absence of *Se*EutT in a *S. enterica* strain devoid of ACAT activities during growth on NCE plus ethanolamine minimal medium (Fig. 3.5), Second, *Lm*EutT supported robust growth of a *S. enterica* strain lacking all three known ATP:Co(I)rrinoid adenosyltransferases (*i.e.,* CobA, PduO, EutT) with lactose as the sole source of carbon and

energy. The β-galactosidase enzyme needed to grow on lactose was encoded by a *lacZ* transcriptional reporter inserted within the *eut* operon of *S. enterica* (Fig. 3.6). Hence, growth on lactose could only happen if *Lm*EutT synthesized sufficient AdoCbl to trigger the expression of the *eut* operon. Furthermore, *in vitro* activity data indicate that *Lm*EutT has as strong, if not stronger, ACAT activity than *Se*EutT (Table 3.4). Third, results from bioassays further confirmed that the product of the *Lm*EutT reaction was AdoCbl (Fig. 3.7).

In spite of having strong ACAT activity, *Lm*EutT does not support robust growth of a *S. enterica eutT* strain with ethanolamine. It is of interest that when ethanolamine was provided as the sole source of carbon and energy, *Lm*EutT did not support growth of a ΔACAT strain as well as *Se*EutT did (Fig. 3.5). These results are inconsistent with those from experiments that demanded growth on lactose (Fig. 3.6). Hence, transcriptional and translational issues do not explain the growth differences between strains expressing *Se*EutT or *Lm*EutT with ethanolamine as carbon and energy source. We speculate that the limited growth of strains that synthesized *Lm*EutT may be the result of sub-optimal interactions of *Lm*EutT with other *S. enterica* Eut proteins, or alternatively, the inability for *Lm*EutT to localize to the metabolosome. These possibilities merit further investigation.

***Lm*EutT prefers dATP as its nucleotide substrate, and unlike *Se*EutT, it releases triphosphate as its by-product.** Our data indicate that *Lm*EutT uses only ATP or dATP *in vitro* (Fig. 3.8). Comparison of the catalytic efficiencies of *Lm*EutT when ATP or dATP were used as co-substrates supports this conclusion (Fig. 3.11, Table 3.4). While this is an interesting result, it may not be physiologically relevant since it is unclear whether the lumen of the metabolosome contains any dATP. An additional difference between class I and class II EutT enzymes is the

phosphate by-product. While class-I *Se*EutT releases PP_i and P_i,[26] class-II *Lm*EutT releases PPP_i, which is also the phosphate by-product of CobA and PduO ACATs.[47, 48]

Concluding remarks. This study of *Lm*EutT sheds light on the enzymatic properties of a previously unknown sub-class of EutT homologues belonging to ethanolamine-utilizing *Firmicutes*, and expands the functional diversity of ATP:Co(I)rrinoid adenosyltransferases.

3.6 REFERENCES

1. Letunic, I.; Bork, P., Interactive Tree Of Life (iTOL): an online tool for phylogenetic tree display and annotation. *Bioinformatics* **2007,** *23*, 127-128.

2. Robert, X.; Gouet, P., Deciphering key features in protein structures with the new ENDscript server. *Nucleic Acids Res.* **2014,** *42* (Web Server issue), W320-4.

3. Banerjee, R., Radical carbon skeleton rearrangements: catalysis by coenzyme B_{12}-dependent mutases. *Chemical Reviews* **2003,** *103*, 2083-2094.

4. Mattes, T. A.; Deery, E.; Warren, M. J.; Escalante-Semerena, J. C., Cobalamin Biosynthesis and Insertion. In *Encyclopedia of Inorganic and Bioinorganic Chemistry*, Scott, R. A., Ed. John Wiley & Sons, Ltd: Chichester, UK, 2017; pp 1-24.

5. Mera, P. E.; Escalante-Semerena, J. C., Multiple roles of ATP:Cob(I)alamin adenosyltransferases in the conversion of B_{12} to coenzyme B_{12}. *Appl. Microbiol. Biotechnol.* **2010,** *88*, 41-48.

6. Stich, T. A.; Yamanishi, M.; Banerjee, R.; Brunold, T. C., Spectroscopic evidence for the formation of a four-coordinate Co^{2+} cobalamin species upon binding to the human ATP:Cobalamin adenosyltransferase. *J. Am. Chem. Soc.* **2005,** *127*, 7660-7661.

7. Stich, T. A.; Buan, N. R.; Escalante-Semerena, J. C.; Brunold, T. C., Spectroscopic and computational studies of the ATP:Corrinoid adenosyltransferase (CobA) from *Salmonella*

enterica: Insights into the mechanism of adenosylcobalamin biosynthesis. *J. Am. Chem. Soc.* **2005,** *127*, 8710-8719.

8. Mera, P. E.; St Maurice, M.; Rayment, I.; Escalante-Semerena, J. C., Residue Phe112 of the human-type corrinoid adenosyltransferase (PduO) enzyme of *Lactobacillus reuteri* is critical to the formation of the four-coordinate Co(II) corrinoid substrate and to the activity of the enzyme. *Biochemistry* **2009,** *48*, 3138-3145.

9. Moore, T. C.; Newmister, S. A.; Rayment, I.; Escalante-Semerena, J. C., Structural insights into the mechanism of four-coordinate cob(II)alamin formation in the active site of the *Salmonella enterica* ATP:co(I)rrinoid adenosyltransferase (CobA) enzyme: Critical role of residues Phe91 and Trp93. *Biochemistry* **2012,** *51*, 9647-9657.

10. Pallares, I. G.; Moore, T. C.; Escalante-Semerena, J. C.; Brunold, T. C., Spectroscopic studies of the EutT adenosyltransferase from *Salmonella enterica*: Mechanism of four-coordinate Co(II)Cbl formation. *J. Am. Chem. Soc.* **2016,** *138*, 3694-3704.

11. Escalante-Semerena, J. C.; Suh, S. J.; Roth, J. R., *cobA* function is required for both *de novo* cobalamin biosynthesis and assimilation of exogenous corrinoids in *Salmonella typhimurium*. *J. Bacteriol.* **1990,** *172*, 273-280.

12. Jeter, R. M., Cobalamin-dependent 1,2-propanediol utilization by *Salmonella typhimurium*. *Journal of General Microbiology* **1990,** *136*, 887-896.

13. Kerfeld, C. A.; Heinhorst, S.; Cannon, G. C., Bacterial microcompartments. *Annu. Rev. Microbiol.* **2010,** *64*, 391-408.

14. Chowdhury, C.; Sinha, S.; Chun, S.; Yeates, T. O.; Bobik, T. A., Diverse bacterial microcompartment organelles. *Microbiol. Mol. Biol. Rev.* **2014,** *78*, 438-468.

15. Johnson, C. L.; Pechonick, E.; Park, S. D.; Havemann, G. D.; Leal, N. A.; Bobik, T. A., Functional genomic, biochemical, and genetic characterization of the *Salmonella pduO* gene, an ATP:cob(I)alamin adenosyltransferase gene. *J. Bacteriol.* **2001,** *183*, 1577-1584.

16. St Maurice, M.; Mera, P. E.; Taranto, M. P.; Sesma, F.; Escalante-Semerena, J. C.; Rayment, I., Structural characterization of the active site of the PduO-type ATP:Co(I)rrinoid adenosyltransferase from *Lactobacillus reuteri*. *J. Biol. Chem.* **2007,** *282*, 2596-2605.

17. Mera, P. E.; Maurice, M. S.; Rayment, I.; Escalante-Semerena, J. C., Structural and functional analyses of the human-type corrinoid adenosyltransferase (PduO) from *Lactobacillus reuteri*. *Biochemistry* **2007,** *46*, 13829-13836.

18. Ortiz de Orue Lucana, D.; Hickey, N.; Hensel, M.; Klare, J. P.; Geremia, S.; Tiufiakova, T.; Torda, A. E., The crystal structure of the C-terminal domain of the *Salmonella enterica* PduO protein: An old fold with a new heme-binding mode. *Front. Microbiol.* **2016,** *7*, 1010.

19. Kaval, K. G.; Garsin, D. A., Ethanolamine utilization in bacteria. *mBio* **2018,** *9*.

20. Roof, D. M.; Roth, J. R., Functions required for vitamin B_{12}-dependent ethanolamine utilization in *Salmonella typhimurium*. *J. Bacteriol.* **1989,** *171*, 3316-3323.

21. Kofoid, E.; Rappleye, C.; Stojiljkovic, I.; Roth, J., The 17-gene ethanolamine (*eut*) operon of *Salmonella typhimurium* encodes five homologues of carboxysome shell proteins. *J. Bacteriol.* **1999,** *181*, 5317-5329.

22. Sheppard, D. E.; Penrod, J. T.; Bobik, T.; Kofoid, E.; Roth, J. R., Evidence that a B_{12}-adenosyl transferase is encoded within the ethanolamine operon of *Salmonella enterica*. *J. Bacteriol.* **2004,** *186*, 7635-7644.

23. Buan, N. R.; Suh, S. J.; Escalante-Semerena, J. C., The *eutT* gene of *Salmonella enterica* encodes an oxygen-labile, metal-containing ATP:corrinoid adenosyltransferase enzyme. *J. Bacteriol.* **2004,** *186*, 5708-5714.

24. Moore, T. C.; Mera, P. E.; Escalante-Semerena, J. C., the EutT enzyme of *Salmonella enterica* is a unique ATP:Cob(I)alamin adenosyltransferase metalloprotein that requires ferrous ions for maximal activity. *J. Bacteriol.* **2014,** *196*, 903-910.

25. Pallares, I. G.; Moore, T. C.; Escalante-Semerena, J. C.; Brunold, T. C., Spectroscopic studies of the EutT adenosyltransferase from *Salmonella enterica*: Evidence of a tetrahedrally coordinated divalent transition metal cofactor with cysteine ligation. *Biochemistry* **2017,** *56*, 364-375.

26. Buan, N. R.; Escalante-Semerena, J. C., Purification and initial biochemical characterization of ATP:Cob(I)alamin adenosyltransferase (EutT) enzyme of *Salmonella enterica*. *J. Biol. Chem.* **2006,** *281*, 16971-16977.

27. Stracey, N. G.; Costa, F. G.; Escalante-Semerena, J. C.; Brunold, T. C., Spectroscopic study of the EutT adenosyltransferase from *Listeria monocytogenes*: Evidence for the formation of a four-coordinate cob(II)alamin intermediate. *Biochemistry* **2018,** *57* (34), 5088-5095.

28. Castilho, B. A.; Olfson, P.; Casadaban, M. J., Plasmid insertion mutagenesis and *lac* gene fusion with mini-Mu bacteriophage transposons. *J. Bacteriol.* **1984,** *158*, 488-495.

29. Datsenko, K. A.; Wanner, B. L., One-step inactivation of chromosomal genes in *Escherichia coli* K-12 using PCR products. *Proc. Natl. Acad. Sci. U.S.A.* **2000,** *97*, 6640-6645.

30. Schmieger, H.; Backhaus, H., The origin of DNA in transducing particles in P22-mutants with increased transduction-frequencies (HT-mutants). *Mol. Gen. Genet.* **1973,** *120*, 181-190.

31. Fonseca, M. V.; Escalante-Semerena, J. C., An *in vitro* reducing system for the enzymic conversion of cobalamin to adenosylcobalamin. *J. Biol. Chem.* **2001,** *276*, 32101-32108.

32. Berkowitz, D.; Hushon, J. M.; Whitfield, H. J., Jr.; Roth, J.; Ames, B. N., Procedure for identifying nonsense mutations. *J. Bacteriol.* **1968,** *96*, 215-220.

33. Ratzkin, P.; Roth, J. R., Cluster of genes controlling proline degradation in *Salmonella typhimurium*. *J. Bacteriol.* **1978,** *133*, 744-754.

34. Vogel, H. J.; Bonner, D. M., Acetylornithinase of *Escherichia coli*: partial purification and some properties. *J. Biol. Chem.* **1956,** *218*, 97-106.

35. Balch, W. E.; Wolfe, R. S., New approach to the cultivation of methanogenic bacteria: 2-mercaptoethanesulfonic acid (HS-CoM)-dependent growth of *Methanobacterium ruminantium* in a pressurized atmosphere. *Appl. Environ. Microbiol.* **1976,** *32*, 781-791.

36. VanDrisse, C. M.; Escalante-Semerena, J. C., New high-cloning-efficiency vectors for complementation studies and recombinant protein overproduction in *Escherichia coli* and *Salmonella enterica*. *Plasmid* **2016,** *86*, 1-6.

37. Marsh, P., pTAC-85, an *E. coli* vector for expression of non-fusion proteins. *Nucleic Acids Res.* **1986,** *14*, 3603.

38. Sambrook, J.; Fritsch, E. F.; Maniatis, T., *Molecular Cloning: A Laboratory Manual*. Second ed.; Cold Spring Harbor Laboratory: Cold Spring Harbor, N.Y., 1989.

39. Blommel, P. G.; Becker, K. J.; Duvnjak, P.; Fox, B. G., Enhanced bacterial protein expression during auto-induction obtained by alteration of *lac* repressor dosage and medium composition. *Biotechnol. Prog.* **2007,** *23*, 585-598.

40. Laemmli, U. K., Cleavage of structural proteins during the assembly of the head of bacteriophage T4. *Nature* **1970,** *227*, 680-685.

41. Sasse, J., Detection of proteins. In *Current Protocols in Molecular Biology*, Ausubel, F. A.; Brent, R.; Kingston, R. E.; Moore, D. D.; Seidman, J. G.; Smith, J. A.; Struhl, K., Eds. Wiley Interscience: New York, 1991; Vol. 1, pp 10.6.1-10.6.8.

42. Robert, X.; Gouet, P., Deciphering key features in protein structures with the new ENDscript server. *Nucleic Acids Res.* **2014,** *42* (Web Server issue), W320-4.

43. Altschul, S. F.; Gish, W.; Miller, W.; Myers, E. W., Basic local alignment search tool. *J. Mol. Biol.* **1990,** *215*, 403-410.

44. Kearse, M.; Moir, R.; Wilson, A.; Stones-Havas, S.; Cheung, M.; Sturrock, S.; Buxton, S.; Cooper, A.; Markowitz, S.; Duran, C.; Thierer, T.; Ashton, B.; Meintjes, P.; Drummond, A., Geneious Basic: an integrated and extendable desktop software platform for the organization and analysis of sequence data. *Bioinformatics* **2012,** *28*, 1647-1649.

45. Mera, P. E.; Escalante-Semerena, J. C., Dihydroflavin-driven adenosylation of 4-coordinate Co(II) corrinoids: are cobalamin reductases enzymes or electron transfer proteins? *J. Biol. Chem.* **2010,** *285*, 2911-2917.

46. Buan, N. R.; Escalante-Semerena, J. C., Computer-assisted docking of flavodoxin with the ATP:Co(I)rrinoid adenosyltransferase (CobA) enzyme reveals residues critical for protein-protein interactions but not for catalysis. *J. Biol. Chem.* **2005,** *280*, 40948-40956.

47. Fonseca, M. V.; Buan, N. R.; Horswill, A. R.; Rayment, I.; Escalante-Semerena, J. C., The ATP:Co(I)rrinoid adenosyltransferase (CobA) enzyme of *Salmonella enterica* requires the 2'-OH Group of ATP for function and yields inorganic triphosphate as its reaction byproduct. *J. Biol. Chem.* **2002,** *277*, 33127-33131.

48. Johnson, C. L.; Buszko, M. L.; Bobik, T. A., Purification and initial characterization of the *Salmonella enterica* PduO ATP:Cob(I)alamin adenosyltransferase. *J. Bacteriol.* **2004,** *186*, 7881-7887.

3.7 TABLES

Table 3.1. A list of strains and plasmids used in this study

Strain	Organism	Genotype	Source, reference
JE4846	*E. coli*	BL21 Codon Plus – RIL (cat$^+$)	Stratagene
JE6583	*S. enterica*[a]	*metE205 ara-9*	laboratory collection
Derivatives of JE6583			
JE22174		Δ*pduO522* Δ*cobA1465* Δ*eutT1141* *eutE*::MudJ(*kan*$^+$)	this work
JE23613		Δ*pduO522* Δ*cobA1465* Δ*eutT1141*	this work
Plasmid	**Cloning vector**	**Protein encoded**	**Source, reference**
pTAC-85	control	none	[37]
pEUT140	pTEV18	*Lm*EutT^{WT}	this work
pEUT159	pTAC-85	*Lm*EutT^{WT}	this work
pEUT160	pTAC-85	*Se*EutT^{WT}	this work
pEUT176	pTAC-85	*Lm*EutT$^{WT\ codon\ optimized}$	this work

[a]All *S. enterica* strains were derivatives of *S. enterica* subsp *enterica* sv. Typhimurium strain LT2

Table 3.2. Primers used in this study

Primer name	Sequence
SeEutT 5' NcoI pTAC-85	5’-NNNNCCATGGATGAACGATTTCATCACCGAA-3’
SeEutT 3' SalI pTAC-85	5’-NNNNGTCGACTCATGGCTTCTCTCCCAAC-3’
LmEutT 5' NcoI pTAC-85	5’-NNNNCCATGGATGGCTATTTTGACAGAAGATGAGTTAC-3’
LmEutT 3' SalI pTAC85	5’-NNNNGTCGACTTACTTTTTATATTCATTAGTTCTCACGCGGAAC-3’
LmEutT 5’ pTEV18	5’-NNGCTCTTCNTTCATGGCTATTTTGACAG-3’
LmEutT 3’ pTEV18	5’-NNGCTCTTCNTTATTACTTTTTATATTCAT-3’

Table 3.3. ICP-OES analysis of *Lm*EutT purified under normoxic and anoxic conditions. *BD: below detection, numbers in parenthesis in these columns reflect the detection limits reported by the Center for Applied Isotope Studies (CAIS) at the University of Georgia (UGA). Values reflect the average concentrations of metal found in the protein sample and the standard error between samples.

	[Protein]	[Iron]	[Zinc]
*Lm*EutT normoxic purification	15 ± 0.4 mM	*BD (<0.4 mM)	*BD (<0.2 mM)
*Lm*EutT anoxic purification	9 ± 0.6 mM	0.9 ± 0.4 mM	*BD (<0.2 mM)

Table 3.4. Kinetic parameters of *Lm*EutT. The kinetic parameters were obtained from data in Figure 8. Units for each parameter are in parentheses where applicable. The k_{cat} was calculated assuming four active sites per *Lm*EutT tetramer.

	$K_{0.5}$ (mM)	h	V_{max} (nM s^{-1})	k_{cat} (s^{-1})	$k_{cat} / K_{0.5}$ (mM s^{-1})
Cbl	4.2 ± 0.2	1.9 ± 0.2	41.8 ± 1.3	0.21 ± 0.01	5.00 x 10^{-2}
ATP	4.4 ± 0.3	2.3 ± 0.3	47.7 ± 1.7	0.24 ± 0.01	5.45 x 10^{-2}
dATP	3.8 ± 0.2	1.8 ± 0.2	55.7 ± 1.4	0.28 ± 0.01	7.37 x 10^{-2}

3.8 FIGURES

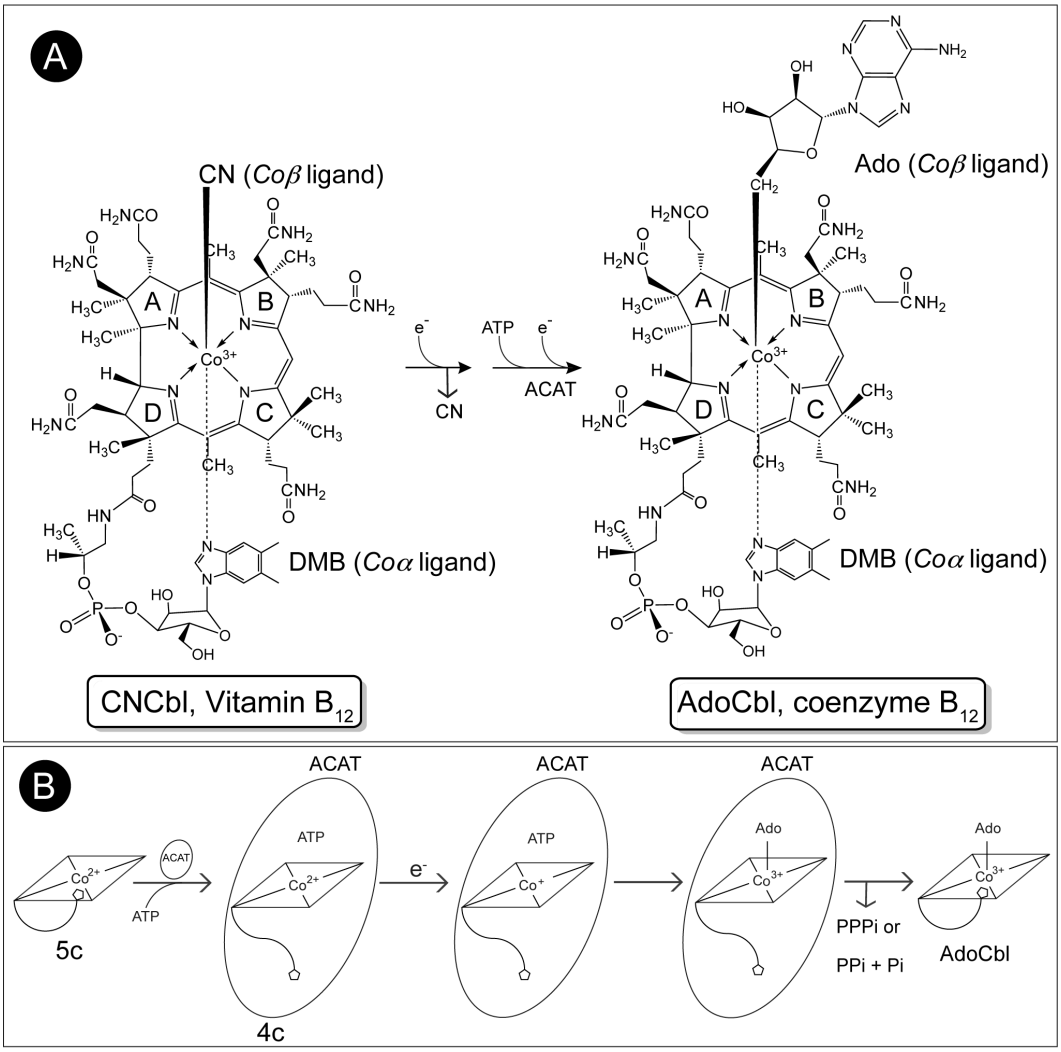

Figure 3.1. Chemical structures of vitamin B_{12}, coenzyme B_{12}, and the pathway that converts the vitamin to the coenzyme. A. Structures of cyanocobalamin (a.k.a. CNCbl, vitamin B_{12}) and adenosylcobalamin a.k.a. AdoCbl, coenzyme B_{12}). Vitamin B_{12} is converted to coenzyme B_{12} in two one-electron reduction steps. In prokaryotes, the first step is likely non-enzymatic, and can be driven by dihydroflavins; the second electron can also be donated by dihydroflavins once ATP and the corrinoid substrate are bound to the active site of the ATP:Co(I)rrinoid adenosyltranferase (ACAT) that catalyzes the nucleophilic attack of Co(I) to the 5' C of ATP. B. Corrinoid adenosylation pathway catalyzed by ACATs. ATP binds before the 5-coordinate (5c) Co(II)balamin substrate. The latter is converted to four-coordinate (4c) Co(II)balamin upon binding by displacement of the lower ligand base. The 4c Co(II)balamin species is reduced by dihydroflavins to generate the Co(I)balamin supernucleophile that attacks ATP releasing a phosphate byproduct.

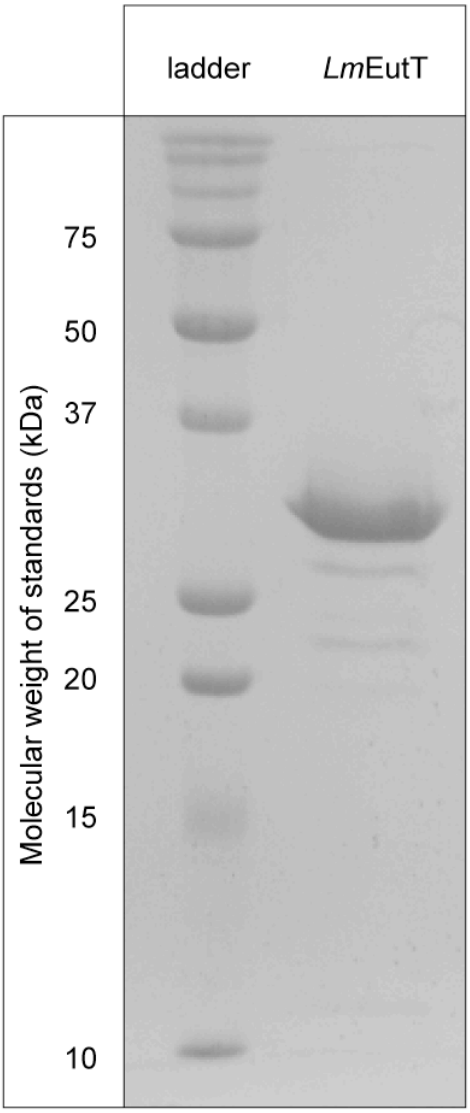

Figure 3.2. Assessment of *Lm*EutT homogeneity. *Lm*EutT (2 µg) was resolved on a 15% SDS-PAGE gel and protein was visualized with a Coomassie Blue R stain. The percentage of each protein species in each lane was analyzed using TotalLab 1D analysis software. The purity of *Lm*EutT was calculated at 90% of the total protein detected in the lane.

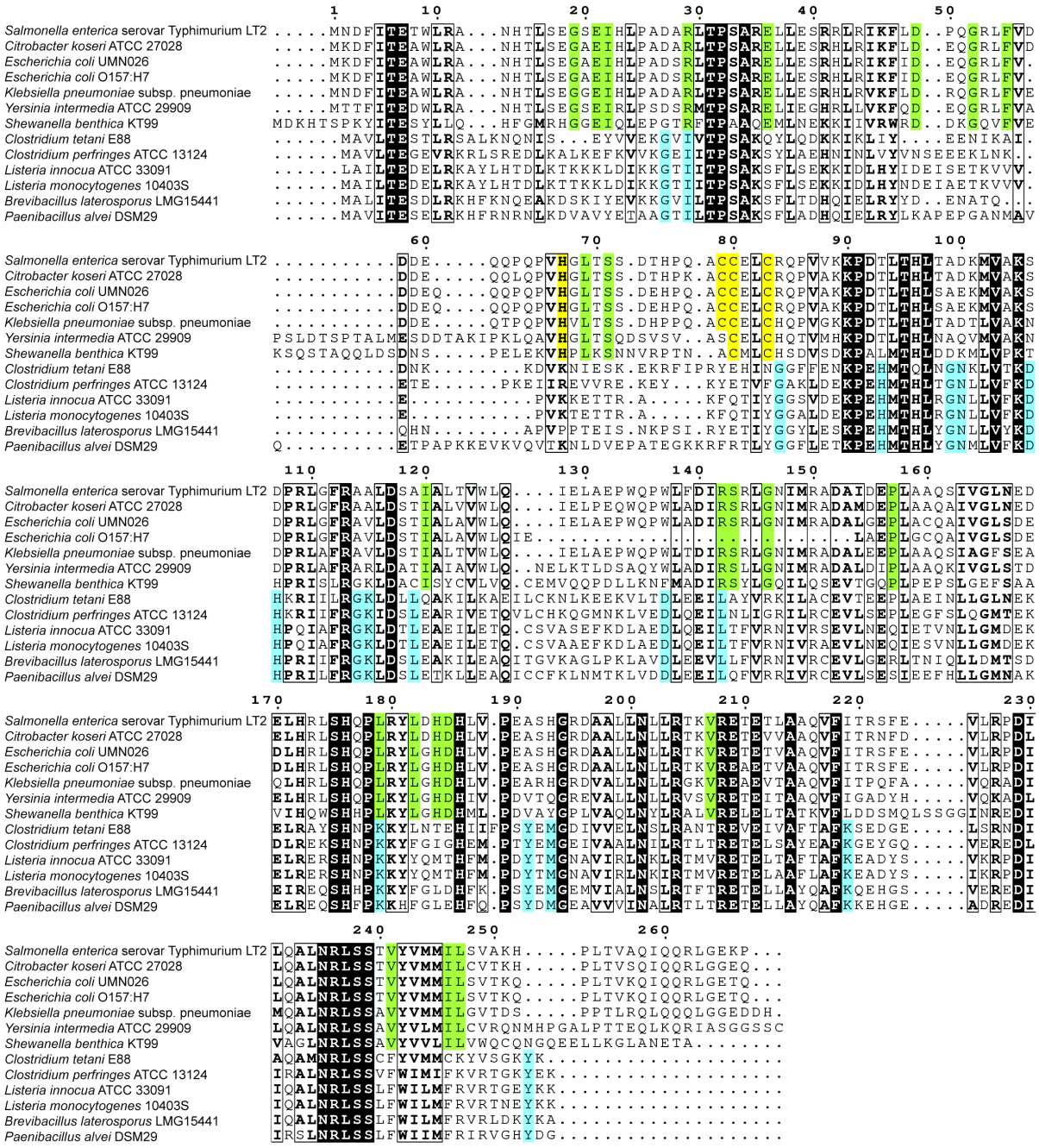

Figure 3.3. A sequence alignment of EutT homologues reveals two sub-classes of EutTs. This sequence alignment was assembled in Geneious using the BLOSUM62 algorithm and annotated using ESPript 3.0[2]. Residues that are identical across all EutT homologues are in black with white lettering. Highly similar (>0.7) residues are boxed and in bold. In addition to these annotations, the metal-binding residues are shown in yellow, and residues identical within each EutT type are shown in green for the type I homologues and blue for the type II homologues.

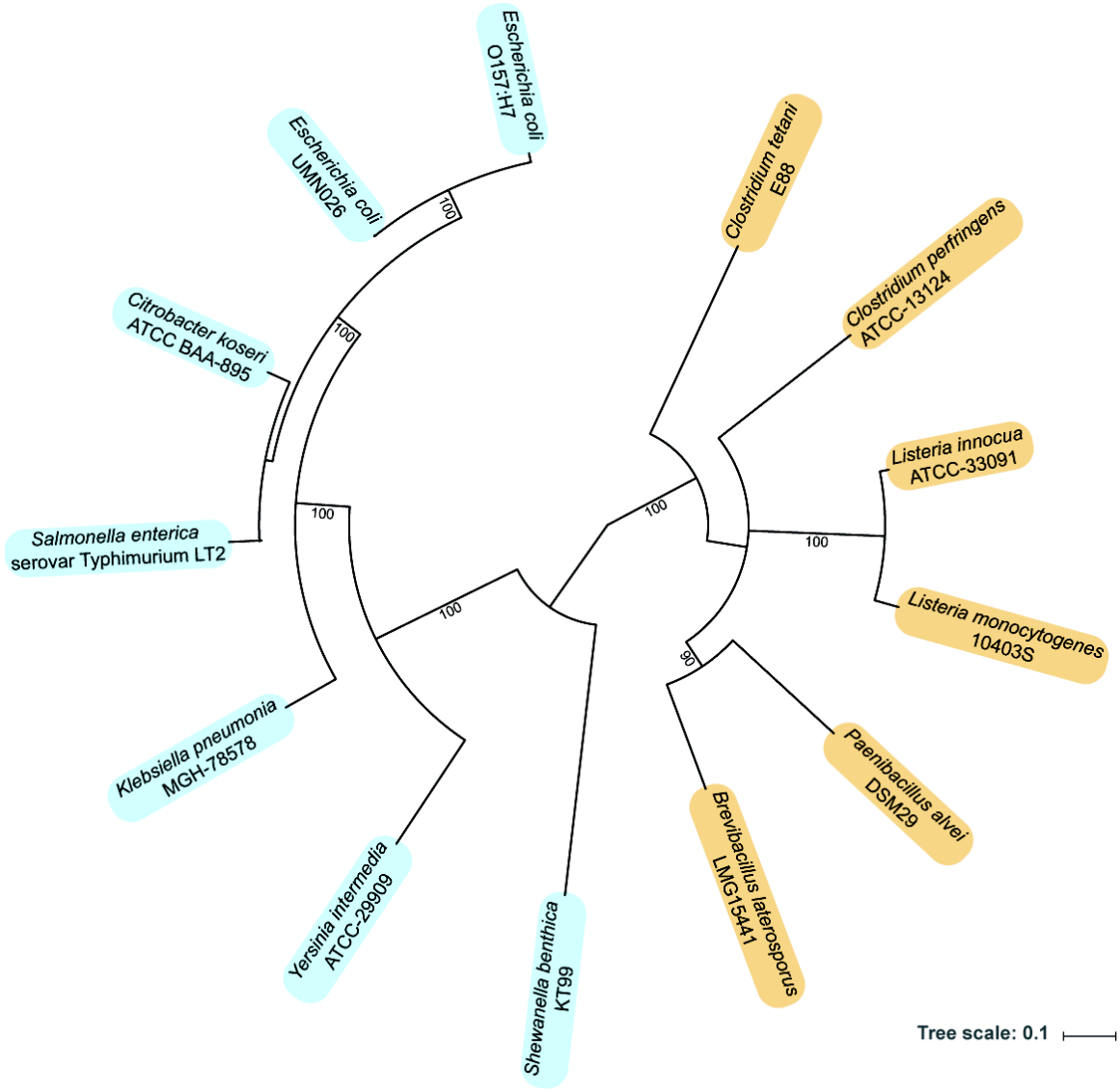

Figure 3.4. A phylogenetic tree of the aligned EutT homologues. The phylogenetic tree was generated in Geneious and processed in ITOL[1]. Metallated EutT homologues are highlighted in blue, and non-metal EutT homologues are highlighted in orange. Bootstrap values higher than 80% are annotated on the branches.

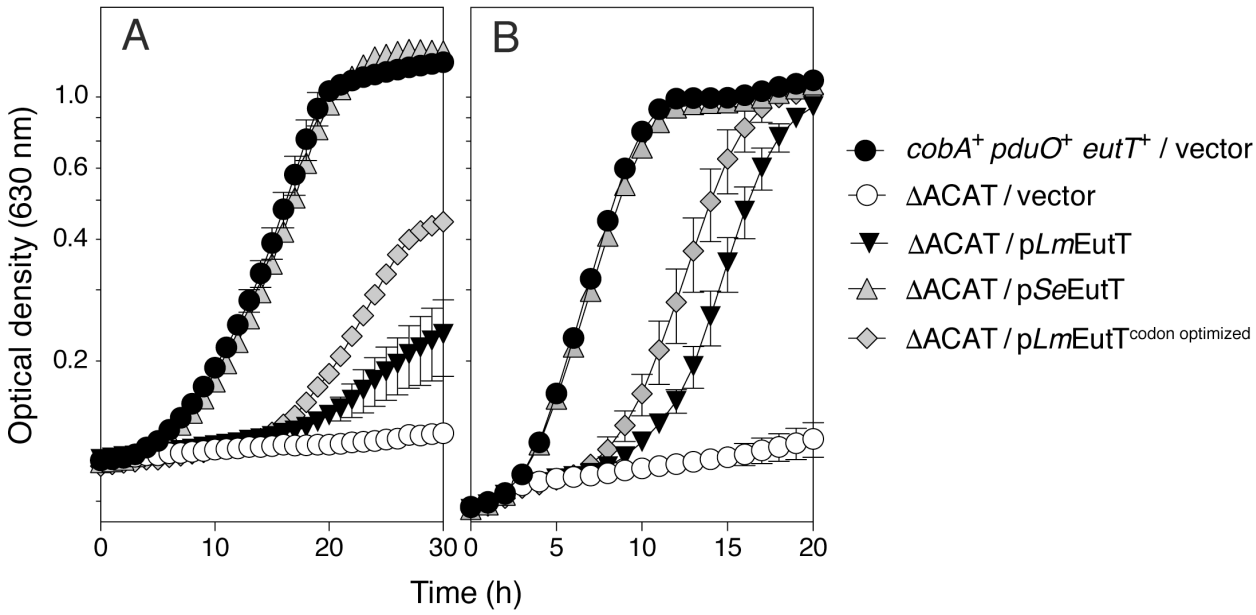

Figure 3.5. *Lm*EutT is active *in vivo*. *S. enterica* strains were grown in minimal medium with ethanolamine as carbon and energy source (A) or minimal medium with glycerol as carbon and energy source and ethanolamine as nitrogen source (B). Strains were grown in 200 μL of medium in microtiter dishes and growth was monitored at 630 nm with a plate reader. The experiment was repeated three times, and the error bars represent the standard error between three biological replicates of one experiment.

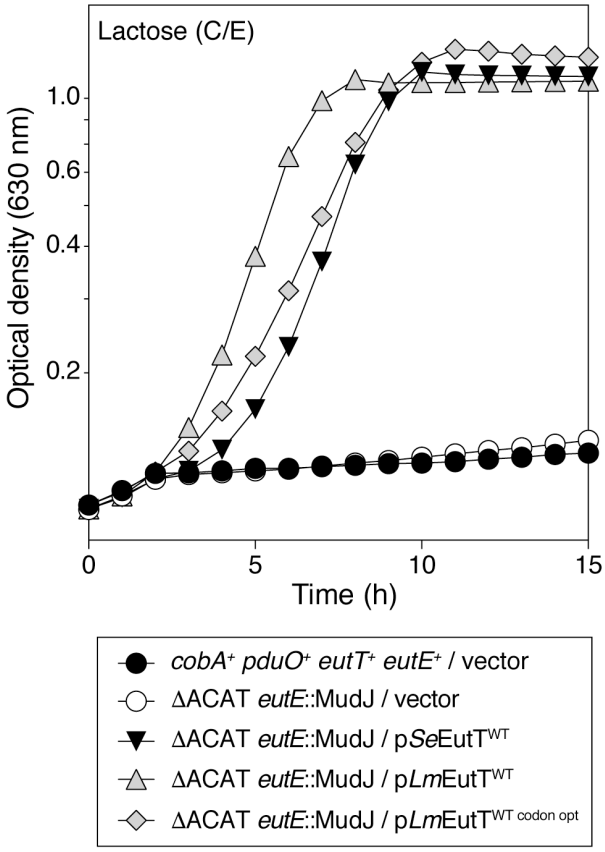

Figure 3.6. *Lm*EutT synthesized sufficient AdoCbl to activate the transcription of the *eut* operon. All strains were grown in NCE plus lactose minimal medium. Strains were grown in 200 μL of medium as described in Figure 3. The experiment was repeated three times, and the error bars represent the standard error between three biological replicates. The ΔACAT *eutE*::MudJ (*lacZ*$^+$) strain did not grow with lactose as the carbon and energy source (closed circles, open circles respectively). Strains carrying a chromosomal *eutE*::MudJ (*lacZ*$^+$) fusion and a plasmid encoding an active EutT grew with lactose as carbon and energy source.

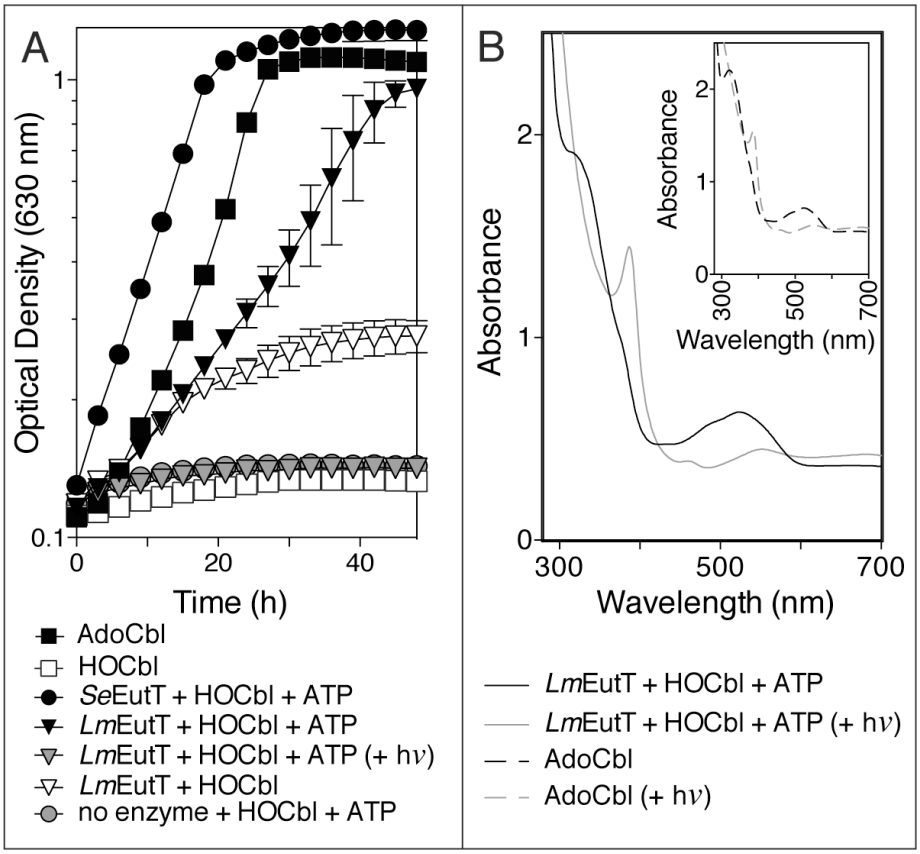

Figure 3.7. *Lm*EutT is active *in vitro.* A. The product of reaction mixtures containing *Se*EutT and *Lm*EutT proteins incubated with the indicated substrates was fed to a strain that required AdoCbl for growth on ethanolamine (Δ*cobA* Δ*pdu* Δ*eutT*). Authentic AdoCbl and HOCbl standards were added as controls; + hν indicates that the reaction was exposed to light. Growth was monitored in a 96-well plate reader. The experiment was repeated twice, and error bars represent the standard error of a biological triplicate. B. UV-vis spectra of the AdoCbl product of the *Lm*EutT-catalyzed reaction, before (dark gray line) and after (light gray line) irradiation. Authentic AdoCbl (Sigma) was used for comparison before (dark gray dotted line) and after (light gray dotted line) irradiation (inset graph).

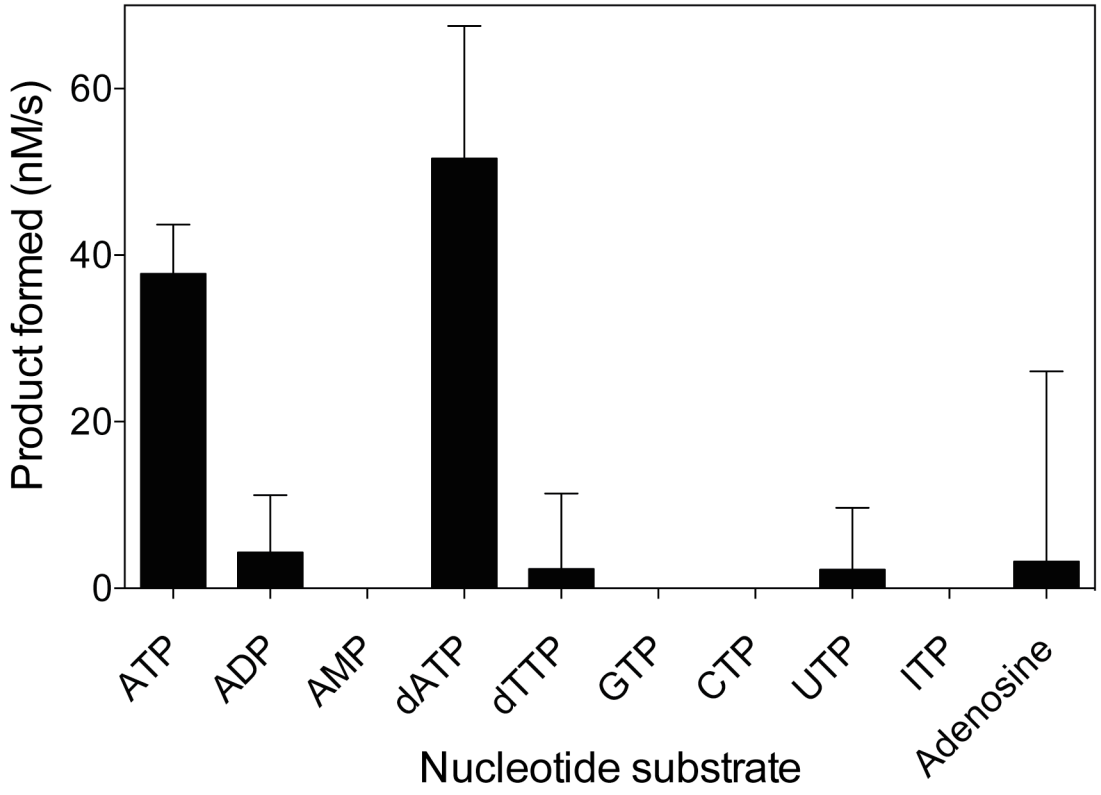

Figure 3.8. *Lm*EutT adenosylates cobalamin with ATP or dATP. The nucleotide substrate specificity of *Lm*EutT was tested with the Co(I)balamin assay. The average specific activity of *Lm*EutT for each substrate is shown with error bars representing the confidence interval ($p<0.05$).

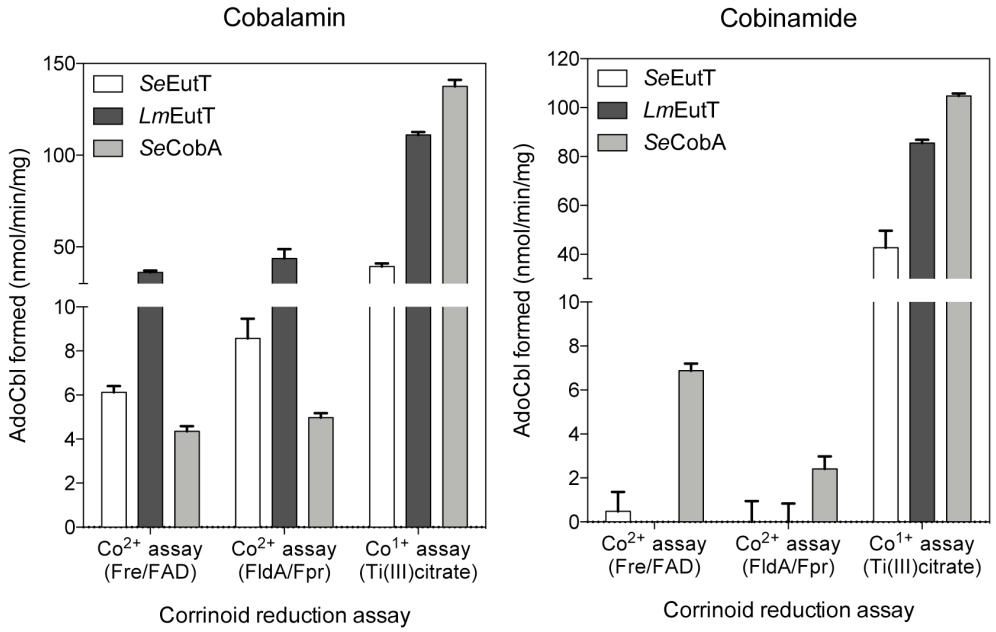

Figure 3.9. *Lm*EutT is specific for cobalamin. *Lm*EutT activity with cobalamin or cobinamide were tested using the Co(I) assay [Ti(III)citrate)], the Fre-dependent Co(II) assay, or the FldA-dependent Co(II) assay. *Se*EutT and *Se*CobA were also assayed as controls. *Lm*EutT adenosylated HOCbl under all assay conditions, but only adenosylated Co(I)aquacobinamide.

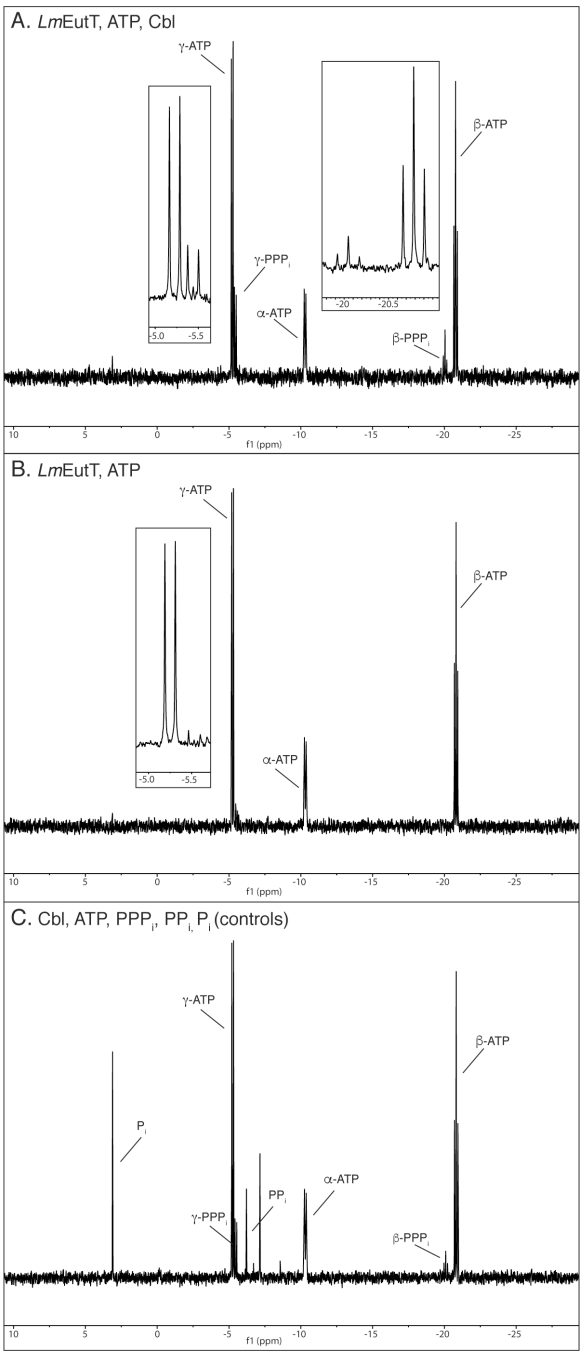

Figure 3.10. *Lm*EutT releases triphosphate as the by-product. All samples were in Tris•HCl buffer (100 mM Tris, pH 7.5 at 37 °C) containing KCl (500 mM), $MgCl_2$ (2 mM) and Ti(III)citrate (1 mM). (A) In the presence of *Lm*EutT (20 μg mL^{-1}), HOCbl (100 μM) and ATP (3 mM) the formation of a triphosphate product was evident, (-6.03, -6.15; -20.57, -20.70, and -20.82 ppm). (B) This triphosphate product was not present when HOCbl was omitted from the reaction. Regions of interest are magnified in the NMR spectra inset. (C) ATP and HOCbl concentrations were as in the experiment shown in panel A, but phosphate product standards were each added to a final concentration of 1 mM.

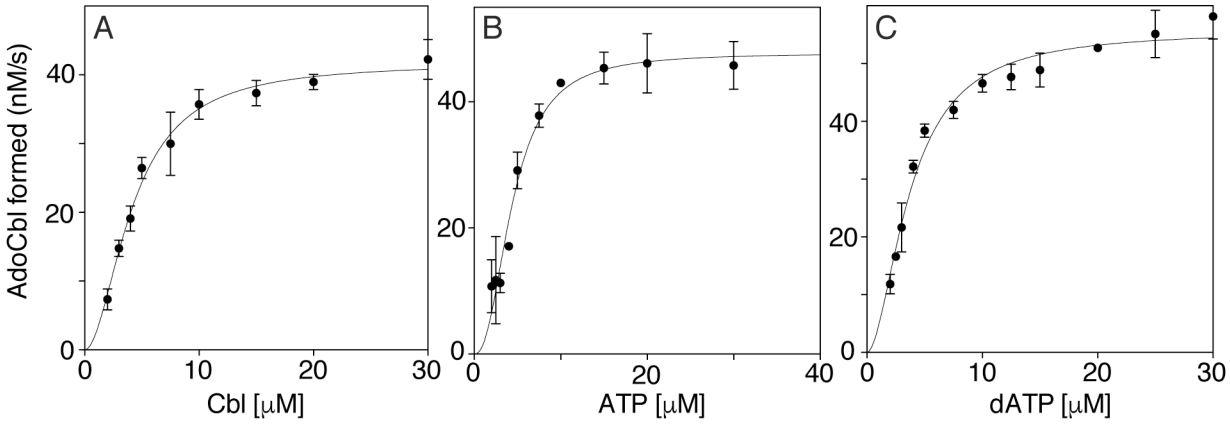

Figure 3.11. *Lm*EutT kinetics. The kinetics of AdoCbl formation was analyzed with (A) Varying concentrations of Cbl (x-axis) and saturating ATP (1 mM); (B) Varying concentrations of ATP (x-axis) and saturating Cbl (50 μM); (C) Varying concentrations of dATP (x-axis) and saturating Cbl (50 μM).

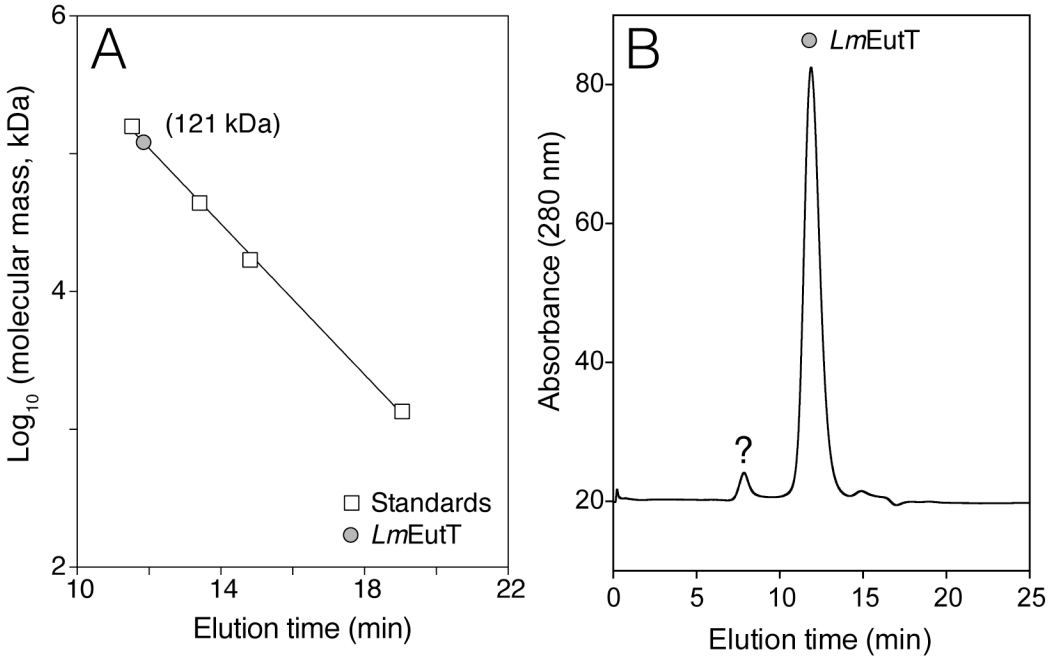

Figure 3.12. *Lm*EutT forms a tetramer. Purified *Lm*EutT was applied onto a size exclusion chromatography column (Superose 12 10/300 GL, GE) and the elution time was compared to markers of known molecular masses (α-globulin, 158 kDa; ovalbumin, 44 kDa; myoglobin, 17 kDa, vitamin B_{12}, 1.35 kDa). (A) Data were plotted as the $\log_{10}$ of the molecular mass as a function of elution time. The white squares denote the standards, and the gray circle represents the mean elution time of *Lm*EutT in three different experiments. (B) A sample trace of *Lm*EutT eluting from the size exclusion chromatography column is shown. The large peak corresponds to an *Lm*EutT tetramer. The small peak appears to be a protein aggregate >1000 kDa. The identity of the aggregated protein was not established.

CHAPTER 4

MUTATIONAL AND FUNCTIONAL ANALYSES OF SUBSTRATE BINDING AND CATALYSIS OF THE *LISTERIA MONOCYTOGENES* EUTT ATP:CO(I)RRINOID ADENOSYLTRANSFERASE[2]

[2]Costa, F. G., Greenhalgh, E. D., Brunold, T. C., & Escalante-Semerena, J. C. (2020). Mutational and functional analyses of substrate binding and catalysis of the Listeria monocytogenes EutT ATP:Co(I)rrinoid adenosyltransferase. *Biochemistry*, *59*(10), 1124-1136. Copyright (2020) American Chemical Society. Author link: https://pubs.acs.org/articlesonrequest/AOR-GADNMVT59ZNKRTHB5FRC. Reprinted here with permission of publisher.

4.1 ABSTRACT

ATP:Co(I)rrinoid adenosyltransferases (ACATs) catalyze the transfer of the adenosyl moiety from co-substrate ATP to a corrinoid substrate. ACATs are grouped into three families, namely CobA, PduO, and EutT. The EutT family of enzymes is further divided into two classes, depending on whether they require a divalent metal ion for activity (Class I and Class II). To date, a structure has not been elucidated for either class of the EutT family of ACATs. In this work, results of bioinformatics analyses revealed several conserved residues between the *C*-terminus of EutT homologues and the structurally characterized *Lactobacillus reuteri* PduO (*Lr*PduO) homologue. In *Lr*PduO, these residues are associated with ATP-binding and formation of an inter-subunit salt bridge. These residues were substituted, and *in vivo* and *in vitro* data support the conclusion that the equivalent residues in the metal-free (i.e., Class II) *Listeria monocytogenes* EutT (*Lm*EutT) enzyme affect ATP binding. Results of *in vivo* and *in vitro* analyses of *Lm*EutT variants with substitutions at phenylalanine and tryptophan residues revealed that replacement of the phenylalanine residue at position 72 affects access to the substrate binding site and replacement of a tryptophan residue at position 238 affected binding of the Cbl substrate to the active site. Unlike the PduO family of ACATs, a single phenylalanine residue is not responsible for displacement of the a-ligand. Together, these data suggest that while EutT enzymes share a conserved ATP-binding motif and an inter-subunit salt bridge with PduO family ACATs, Class II EutT family ACATs utilize an unidentified mechanism for Cbl lower ligand displacement and reduction that is different from that of PduO and CobA family ACATs.

4.2 INTRODUCTION

Cobamides (Cbas) are structurally complex cyclic tetrapyrroles produced exclusively by some prokaryotes and required by organisms from all domains of life.[1] The best-studied cobamide is cobalamin (Cbl), whose vitamin form is cyanocobalamin (CNCbl), and biologically active form is adenosylcobalamin (AdoCbl). AdoCbl is required by several enzymes, such as methylmalonyl-CoA mutase (EC 5.4.99.2), class II ribonucleotide reductase (EC 1.17.4.2), diol dehydratase EC 4.2.1.28), and ethanolamine ammonia-lyase (EAL, EC 4.3.1.7).[2-4] *Salmonella enterica* and several other prokaryotes produce EAL in order to use ethanolamine as a source of carbon, nitrogen, and energy.[5] EAL is encoded by the *eutBC* genes in the ethanolamine utilization (*eut*) operon,[6] which in *S. enterica* is comprised of 16 genes (*eutSPQTDMNEJGHABCLK*) followed by an independently expressed regulator (*eutR*).[7] The *eutT* gene encodes an ATP:Co(I)rrinoid adenosyltransferase (ACAT) that generates the AdoCbl coenzyme used by EAL.[8, 9] In general, ACATs facilitate the adenosylation of corrinoids via the displacement of the lower axial ligand (a-ligand) of cobamides (Cbas) generating a four-coordinate (4C) Co(II)corrinoid intermediate that can be reduced by free or protein-bound dihydroflavins (Fig. 4.1).[10, 11]

Three families of ACATs have been described, namely CobA, PduO, and EutT, all of which have been genetically well characterized in *S. enterica.* CobA is considered the housekeeping ACAT of *S. enterica*, and is involved in *de novo* cobalamin biosynthesis, adenosylation of incomplete corrinoids, transcriptional activation of the *eut* operon, and post-transcriptional regulation of the gene encoding the outer membrane corrinoid transporter, *btuB*.[8, 12, 13] Structural and spectroscopic analysis of *S. enterica* CobA demonstrated that the enzyme binds 4C-Co(II)Cbl, prior to its reduction to Co(I)Cbl and subsequent transfer of the adenosyl (Ado) moiety of ATP to the Co ion of the corrinoid substrate.[14, 15] In CobA, five-coordinate (5C)-

Co(II)Cbl is converted to 4C-Co(II)Cbl by displacement of the a-ligand of the corrinoid by residues F91 and W93, which are located within a disordered loop that swings into place under the corrin ring upon binding of 5C-Co(II)Cbl to the active site. The ATP-binding site of CobA is comprised of an inverted P-loop that positions the C-5' of ATP proximal to Co(I) allowing the formation of the Co–C organometallic bond.

In *S. enterica,* PduO is important for the metabolism of 1,2-propanediol; however, many organisms (including humans) only encode PduO-type ACATs and utilize these enzymes in a 1,2-propanediol-independent manner.[16-18] Of note, humans encode a PduO homologue that delivers AdoCbl to methylmalonyl-CoA mutase (MCM).[19-21] In all homologues where structural information has been elucidated, PduO forms a trimer.[22-24] In the PduO trimer, each active site is located at the interface of two subunits, and residues from both subunits contribute to substrate binding. Additionally, the well-conserved R128 residue from the *Lactobacillus reuteri* PduO homologue (*Lr*PduO), which is essential for adenosylation activity, appears to form an inter-subunit salt bridge with residue D35.[16]

In *S. enterica*, EutT is encoded as a member of the *eut* operon and plays an important role in the catabolism of ethanolamine. To date, X-ray structural data of members of the EutT family enzymes have not been reported; however, *in vivo* and *in vitro* characterization of EutT homologues have provided insights into the mechanism of this family of ACATs.[25-30] EutT family ACATs can be divided into two classes, one class of enzymes that binds and requires Fe(II) or other divalent transition metal ions for activity (Class I),[27, 31] and another class that lacks a metal-binding site and does not require Fe(II) for activity (Class II).[26, 28] *S. enterica* EutT (*Se*EutT), the best studied Class I EutT, binds Fe(II) using a conserved $HX_{11}CCXXC$ motif at the dimer interface.[27] Spectroscopic analysis of *Se*EutT, where the Fe(II) ion was replaced with Co(II),

demonstrated that the metal is tetrahedrally coordinated by four cysteines, two from each subunit.[31] Interestingly, *Se*EutT initially generates a 5C-Co(II)Cbl intermediate, whereas the Class II EutT from *Listeria monocytogenes* (*Lm*EutT) binds 4C-Co(II)Cbl, similar to PduO and CobA family enzymes.[28] *Lm*EutT also forms a tetramer, a unique oligomeric state in all ACATs studied to date.[26]

In this work, we describe the results of a directed mutagenic analysis of the Class II EutT ACAT from *Listeria monocytogenes* (*Lm*EutT). This analysis was guided by the finding that primary sequences of PduO family ACATs align with EutT family ACATs, except EutT homologues have a ~70 aa N-terminal extension that PduO homologues lack. The results suggest that EutT family ACATs bind the ATP substrate and form an inter-subunit salt bridge similarly to *Lr*PduO.

4.3 MATERIALS AND METHODS

Bioinformatics analysis. Amino acid sequences of crystallized PduO homologues, EutT homologues from both classes that demonstrated activity *in vitro*, and the human adenosyltransferase (hATR) were aligned in Geneious (version 8.1.9) using the ClustalW BLOSUM cost matrix, with a gap open cost = 9 and gap extension = 1. This alignment was annotated in ESPript 3.0 incorporating the secondary structure of *Lactobacillus reuteri* PduO, with an identity cutoff of 0.7.

Site-directed mutagenesis. Plasmids pEUT140 and pEUT159 encoding *Lm*EutT (UniProt accession code A0A0H3GFM5)[26] were mutagenized using the QuikChange II site-directed mutagenesis protocol (Agilent), with the changes noted: 150 ng of template DNA (pEUT140 or pEUT159) was used for the amplification, and the DpnI digestion was incubated at 37 °C for six hours. Primers used for the amplification of each variant are listed in Table 4.1. Candidate plasmids

were sequenced to confirm the presence of the correct mutation. A list of the plasmids used in this work can be found in Table 4.2.

Strains and growth media. For protein expression, pTEV18[32] vector-based plasmids encoding *Lm*EutT variants were transformed into BL21-CodonPlus cells (Agilent) and grown as previously described.[26] For analysis of ACAT activity *in vivo*, pTAC-85[33] vector-based plasmids encoding *Lm*EutT variants were transformed into the reporter strain JE22174. Strains were grown in 1 mL of nutrient broth (NB, Difco) (8 g/L) containing NaCl (5 g/L) and were incubated overnight at 37 °C. These cultures were subcultured into minimal medium containing lactose as the sole source of carbon and energy, as described elsewhere.[26]

Protein purification. Purification of *Lm*EutT variants and analysis of their purity was performed as described elsewhere[26] If variants were unstable, as in the case of *Lm*EutT^{R200D} and *Lm*EutT$^{D110R\ R200D}$, some protein precipitated and was removed by centrifugation at 2,000 x *g* for 10 minutes at 4 ºC in an Eppendorf Centrifuge 5810R centrifuge. The remaining soluble protein was decanted and filtered through a 0.45-mm filter (VWR) to remove particulates before storage at -80 ºC until used.

Western blotting. Strains were grown on 5 mL NCE medium [34] containing Wolfe's trace minerals [35] and $MgSO_4$ (1 mM) supplemented with lactose (22 mM), glycerol (22 mM), ethanolamine (1 mM), cyanocobalamin (CNCbl, 25 nM), ampicillin (20 mM) and isopropyl b-D-thiogalatopyranoside (IPTG, 10 mM). Strains were grown to an optical density (OD) of 0.6-0.8 at 600 nm. Cells were pelleted by centrifugation at 4,000 x *g* using an Beckman Avanti^{TM} refrigerated centrifuge furnished with a JA25.50 rotor. Cell pellets were stored at –80 °C until used. Cell pellets were resuspended in 300 mL of B-PER^{TM} reagent (Thermo Fisher Scientific) and insoluble debris was centrifuged at 16,000 x *g* for 5 minutes on a Eppendorf Centrifuge Model 5425. Cell lysates

were quantified with the Pierce BCA protein assay kit (Thermo Fisher Scientific) and 100 mg of each lysate was loaded into two 15% polyacrylamide SDS-PAGE gels in duplicate.[36] One gel was loaded with a Precision Plus Protein Standards (Bio-Rad Laboratories) and the other gel was loaded with SuperSignal™ Molecular Weight Protein Ladder (Thermo Fisher). A constant voltage of 200 V was applied for 50 min to separate the proteins in each lysate by size on the gel. One gel was stained with Coommassie Brilliant R dye to visualize the protein content of each sample. The other gel was transferred to a PVDF membrane using the Bio-Rad Laboratories Trans-Blot Turbo transfer system. After blocking the membrane with 1X Phosphate-Buffered Saline with 0.1% (v/v) Tween (PBST) solution and 0.5% (w/v) non-fat milk for one hour, the membrane was incubated with the same blocking buffer with rabbit polyclonal antibodies against *Lm*EutT (Envigo, PA) that were precleared with lysate from the background strain harboring the empty cloning vector grown under the same conditions; the antibody dilution used was 1:500 for the primary antibody. The membrane was washed thrice with PBST, 10 minutes per wash, and a second hour-long incubation was performed with blocking buffer containing goat anti-rabbit IgG, horseradish peroxidase conjugate (Sigma) at a 1:10,000 dilution. The membrane was again washed thrice with PBST before applying 10 mL of SuperSignal™ West Pico PLUS Chemiluminescent Substrate (Thermo Fisher) and incubating for 10 min. The blot was imaged with a UVP ChemStudio (analytikjena) with an exposure time of 10 min.

***In vitro* corrinoid adenosyltransferase activity assays.** Adenosyltransferase activity assays were prepared as described elsewhere with minor changes.[26] Enzyme assays had an enzyme concentration of 400 nM for the determination of the kinetic parameters, and these concentrations were quantified using a NanoDrop 1000 spectrophotometer with the appropriate molecular weight and extinction coefficient for each variant. In the assays comparing the specific activity among

variants in the Co(I)Cbl and Co(II)Cbl assay comparison, the enzyme concentration was 800 nM and this was calculated using the BCA protein assay kit (Pierce), as several variants lacked any tryptophans to reliably quantify their concentration by NanoDrop.

Spectroscopic analysis. Purified *Lm*EutT in buffer containing 20 mM phosphate, 200mM NaCl, and 1 mM TCEP, was mixed with Co(II)Cbl (reduced with saturated sodium formate solution) and ATP under anoxic conditions. Samples were prepared such that the final protein concentration was ~300 μM with a 0.9:1 Co(II)Cbl:Protein ratio and a 10x excess of MgATP. X-Band EPR spectra were collected on a Bruker ESP 300E spectrometer using an Oxford ESR 900 continuous-flow liquid helium cryostat and an Oxford ITC4 temperature controller. All spectra were obtained at 20 K with a modulation amplitude of 5G, modulation frequency of 100kHz, and gain of 60 dB. The EPR data were fit using Mark Nilges' SIMPOW program.[37] All CD spectra were obtained at room temperature using a Jasco J-715 spectropolarimeter.

Structural modeling. Structural models of *Lm*EutT (UniProt accession code A0A0H3GFM5) and *Se*EutT (UniProt accession code Q9ZFV4) were constructed with Phyre[2] one-to-one threading program utilizing the *Lr*PduO structure (UniProt accession code A0A0U5JSW2, PDB code 3CI1) as the template.[38] The model was subsequently downloaded and imported into MacPyMol 1.7.4.4 to generate the surface model and highlight residues of interest.

4.4 RESULTS

EutT shares C-terminal sequence homology with PduO. Amino acid homology between PduO and EutT was initially uncovered between *Lm*EutT and *Lr*PduO, using the NCBI pBLAST algorithm with default parameters. We note that the same program and parameters did not identify significant homology between *Se*EutT and *Lr*PduO. The amino acid sequences of PduO homologues and the sequences of EutT homologues were aligned using Geneious software version

8.1.9 by employing parameters that relaxed the requirement for end-to-end sequence similarity and gap stringency (Fig. 4.2). This analysis revealed that all EutT homologues have an extended N-terminus compared to PduO homologues. The majority of the residues that are conserved between all EutT and PduO homologues used in the alignment correspond to *Lr*PduO residues reported to bind the ATP nucleotide substrate and form an inter-subunit salt bridge.[24]

Notably, the reported ATP-binding motif in *Lr*PduO [T_5-(K/R)-X-G-D-X-G-X-$(T/S)_{13}$] is not conserved across EutT homologues, with the exception of T13 in *Lr*PduO.[24] Importantly, these non-conserved residues are believed to interact with the substrate via *N*a, which could explain why the side chains are not conserved. The residues whose side chains are implicated in the binding of ATP in the *Lr*PduO structure, including T13, are conserved in the EutT and PduO homologues included in the alignment (Fig. 4.2, blue arrows). The only exception to this pattern involves the human adenosyltransferase (hATR), which has serine in lieu of threonine at position 13 in the *Lr*PduO sequence.[24] Additionally, the residues that form a salt bridge in the *Lr*PduO crystal structure, *i.e.,* D35 and R128, are also conserved in the EutT homologues, which correspond to residues D110 and R200 in *Lm*EutT (Fig. 4.2, green arrows). The sequence alignment suggests that EutT ACATs may have a similar mode of ATP-binding as PduO, and may also form an inter-subunit aspartate-arginine salt bridge. This hypothesis was investigated further through site-directed mutagenesis of these residues in *Lm*EutT followed by *in vivo* and *in vitro* analyses.

***In vivo* assessment of nucleotide binding and salt bridge variants.** Variants of *Lm*EutT were constructed to change the residues presumed to be involved in ATP binding and formation of the inter-subunit salt bridge (Table 4.1, 4.2). These variants were tested for their ability to complement an *S. enterica* ΔACAT mutant, using a derivative of the reporter assay ($P_{eut\text{-}lacZ}$ transcriptional fusion) described elsewhere.[8, 26] Interestingly, none of the variants synthesized enough AdoCbl to

support growth under the conditions tested (Fig. 4.3, panel A and B). To confirm that the variants were being produced *in vivo*, a Western blot was performed on lysates grown to mid-log phase in medium supplemented with lactose, glycerol, Cbl and ethanolamine. Although *Lm*EutT was detected in all samples except the vector control sample, the relative detection for all variants was less than that for *Lm*EutT^{WT} and varied from variant to variant (Fig. 4.3, panel C). It was plausible that the reduced amounts of *Lm*EutT variants explained the lack of growth of the *S. enterica* ΔACAT strain. To investigate the effects of the various residue replacements on the catalytic mechanism of *Lm*EutT, wild-type and variant proteins were purified and tested for activity *in vitro.*

***In vitro* activity of putative EutT ATP-binding variants.** The *Lm*EutT variants that were mutagenized at putative ATP-binding residues were purified, and kinetic parameters were obtained for ATP and HOCbl substrates using the Co(I)Cbl assay (Table 4.3).[8] We used the reported crystal structure of *Lr*PduO in complex with Mg(II)ATP (PDB code 3CI1) to identify contacts between the *Lm*EutT and ATP.[24] Variants *Lm*EutT^{R204K} and *Lm*EutT^{N231L} did not have detectable activity *in vitro.* Residue R204 of *Lm*EutT aligned with residue R132 of *Lr*PduO, which we posited to hydrogen bond with the ribose-ring oxygen and the a-phosphate ribose-bridging oxygen.[24] Previous work showed that the *Lr*PduO^{R132K} variant had a ~300-fold decrease in catalytic efficiency (k_{cat}/K_m) for ATP and a ~3000-fold decrease for Cbl.[16] Residue N231 of *Lm*EutT aligned with residue N156 of *Lr*PduO, whose carboxamide oxygen coordinates Mg(II) while its backbone nitrogen hydrogen bonds with the hydroxyl group of the a -phosphate moiety.[24] In *Lr*PduO, residues R132 and N156 coordinate regions of the ATP molecule near the C-5' that must be positioned correctly for the adenosylation reaction to proceed. Residues T88 and K98 of *Lm*EutT aligned with residues T13 and K23 of *Lr*PduO, respectively, and in *Lr*PduO these residues interact with the g phosphate of ATP.[24] We determined increases of ~6-fold and ~22-fold in the K_{half} for

ATP for the *Lm*EutT^{T88V} *Lm*EutT^{K98Q} variants, respectively (Table 4.3). The *Lm*EutT^{E207Q} variant lacked the residue that aligns with residue E135 of *Lr*PduO, which hydrogen bonds with the amino group of adenine in ATP. Consistent with the loss of the negative charge of E207, the K_{half} for ATP of *Lm*EutT^{E207Q} increased ~50-fold. Importantly, the turnover number (k_{cat}) did not significantly decrease for *Lm*EutT^{T88V}, *Lm*EutT^{K98Q} or *Lm*EutT^{E207Q}, suggesting that substrate affinity, not the turnover rate, was affected in these variants. Noteworthy is the fact that *Lm*EutT co-purified with ATP, and when pure protein was incubated with Co(I)Cbl without additional ATP, enough AdoCbl was produced to support growth of a ΔACAT strain.[26] Several attempts to remove the ATP substrate proved unsuccessful, making it difficult to determine the binding constant of *Lm*EutT and its variants for ATP.

***In vitro* analysis of the putative inter-subunit, salt-bridge variants.** Several changes at positions D110 and R200, which align with residues D35 and R128 of *Lr*PduO, were purified and tested *in vitro* (Table 4.4). In *Lr*PduO, these residues form an inter-subunit salt bridge (Figure 4.2).[24] The K_{half} for ATP of *Lm*EutT^{D110N} and *Lm*EutT^{R200K} were not significantly affected by these substitutions compared to *Lm*EutT^{WT}, and the k_{cat} / K_{half} decreased by no more than a log for either variant and substrate (Table 4.4). This finding was surprising, because the corresponding mutations in *Lr*PduO (*i.e., Lr*PduO^{D35N} and *Lr*PduO^{R128K}) significantly perturbed the activity of the enzyme.[16] For example, the *Lr*PduO^{D35N} variant displayed a >50-fold increase in K_m and 230-fold decrease in the catalytic efficiency (k_{cat}/K_m) relative to the wild-type enzyme.[16]

The *Lm*EutT$^{D110R,\ R200D}$ double-substitution variant, which was expected to retain the inter-subunit salt bridge, was inactive. This finding was consistent with the ~6 orders-of-magnitude decrease in the catalytic efficiency of the *Lr*PduO$^{D35R,\ R128D}$ variant.[16]

Oligomerization state of the inter-subunit, salt-bridge variants. We also investigated the effect of substitutions at positions D110 and R200 of *Lm*EutT. Again, the aforementioned positions in *Lm*EutT are equivalent to positions D35 and R128 in *Lr*PduO (Fig. 4.2). To frame our findings, we note that variants *Lr*PduO^{D35R} and *Lr*PduO^{R128D} were not found to play a significant role in oligomerization of PduO, that is, substitutions at the alluded positions did not change the trimeric state of *Lr*PduO.[16] The oligomeric state of *Lm*EutT variants was analyzed by size exclusion chromatography to determine the percentage of each oligomeric state of *Lm*EutT variants normalized to the total amount of protein used for the analysis (Fig. 4.4).

*Lm*EutT^{WT} formed a tetramer as well as a small amount of higher molecular weight aggregate (Fig. 4.4).[26] All *Lm*EutT^{D110} and *Lm*EutT^{R200} variants displayed the same oligomeric properties. However, several of the variants differed from *Lm*EutT^{WT} in the relative abundance of tetrameric versus aggregate form. Variants believed to preserve hydrogen-bonding interactions were not significantly affected in their aggregate to tetramer ratio. However, the *Lm*EutT^{D110R} and *Lm*EutT^{R200D} variants, for which we predicted the salt bridge would be disrupted completely, showed significantly increased aggregation (Fig. 4.4). The residue-swap variant, *Lm*EutT$^{D110R, R200D}$, whose activity was significantly perturbed, displayed a tetramer-to-aggregate ratio equal to *Lm*EutT^{WT}. Altogether, these data supported the hypothesis that the *Lm*EutT^{D110} and *Lm*EutT^{R200} residues interact. Additionally, these results suggested that these residues prevent *Lm*EutT aggregation (Fig. 4.4).

Screening for residues involved in 4C-Co(II)Cbl formation. In *Lr*PduO, residue F112 (see Fig. 4.2) is critical for the formation of the 4C-Co(II)Cbl species, which is required to facilitate the reduction of Co(II) → Co(I) in all ACATs studied to date.[29, 39, 40] Our sequence alignment showed that an equivalent residue to *Lr*PduO F112 was not conserved in EutT family ACATs (Fig. 4.2).

In the absence of a divalent metal like in *Se*EutT, we hypothesized that *Lm*EutT, like PduO and CobA, might also utilize hydrophobic, bulky residues to facilitate the displacement of the lower ligand.[14, 40] We explored this possibility by introducing Phe → Ala and Trp → His substitutions at each phenylalanine and tryptophan residue of *Lm*EutT. The ability of the resulting variants to confer growth was compared to that of *Lm*EutT^{WT} in medium supplemented with 25 nM CNCbl. Some of the *Lm*EutT variants tested (*i.e.,* *Lm*EutT^{F39A}, *Lm*EutT^{F105A}, *Lm*EutT^{F127A}, *Lm*EutT^{F140A}, *Lm*EutT^{F183A}, *Lm*EutT^{F211A}, *Lm*EutT^{F242A}) synthesized AdoCbl that supported growth of the indicator strain that was indistinguishable from that of the same strain that synthesized *Lm*EutT^{WT} (Fig. 4.5, panel A).

Five variants (*Lm*EutT^{F72A}, *Lm*EutT^{F97A}, *Lm*EutT^{F214A}, *Lm*EutT^{F237A}, and *Lm*EutT^{W238H}) displayed a discernable loss of enzymatic activity as seen by the reduction in the rate of growth relative to that of the strain that synthesized *Lm*EutT^{WT} (Fig. 4.5, panel B). To determine whether these variants were defective in displacement of the lower ligand, the variants were purified and characterized *in vitro* using two assays, the Co(II)Cbl assay and the Co(I)Cbl assay.[26] In the Co(II)Cbl assay, the Cbl substrate is reduced from Co(III)Cbl to five-coordinate 5C-Co(II)Cbl with reduced dihydroflavins. Upon binding of the 5C-Co(II)Cbl substrate to the ACAT enzyme, the lower ligand is displaced, forming 4C-Co(II)Cbl needed for the reduction to Co(I)Cbl. In contrast, in the Co(I)Cbl assay, HOCbl is converted to Co(I)Cbl in the presence of the strong reductant Ti(III)citrate. Thus, in the Co(I)Cbl assay, the enzyme only needs to bind and position the substrates properly for the reaction to proceed. Previous work found that when CobA and PduO residues critical for lower ligand displacement were mutated to alanine, these variant enzymes were active in the Co(I)Cbl assay, but had undetectable activity in the Co(II)Cbl assay.[14, 40] When *Lm*EutT^{WT} and the five variants identified *in vivo* were purified and screened using the Co(II)Cbl

and Co(I)Cbl assays, three variants showed significant deviations in activity compared to *Lm*EutT^{WT} (Fig. 4.6).

*Lm*EutT^{F97A} variant had a higher specific activity compared to *Lm*EutT^{WT} in both assays. This phenylalanine is adjacent to the K98 residue involved in ATP binding. Additionally, residue F97 of *Lm*EutT is not conserved across Type II EutTs, and aligns with a conserved alanine in Type I EutTs (Fig. 4.2). We did not pursue this variant further, as the relative activity of *Lm*EutT^{F97A} to *Lm*EutT^{WT} did not suggest a role for F97 in Co(II) to Co(I) reduction.

As seen in figure 4.6, variant *Lm*EutT^{F72A} had similar specific activity to *Lm*EutT^{WT} in the Co(II)Cbl assay, but had significantly higher specific activity than *Lm*EutT^{WT} in the Co(I)Cbl assay (Fig. 4.6). While this did not immediately suggest a role in the displacement of the lower ligand, the difference in relative specific activity in the two assays for *Lm*EutT^{F72A} was intriguing. Additionally, the alignment shown in figure 4.2 indicated that F72 is located in the same region as the metal-binding site of Type I EutTs. Finally, variant *Lm*EutT^{W238H} had significantly diminished activity in both assays, and the activity was nearly undetectable in the Co(I)Cbl assay (Fig. 4.6). In the sequence alignment, this residue is conserved as a hydrophobic, bulky residue and aligns with residue F163 of *Lr*PduO, which is located in the active site proximal to the corrin ring and is involved in corrinoid substrate binding.[40] Additional variants with substitutions of residues W238 and F72 were constructed and tested *in vivo* and *in vitro* in an effort to characterize the possible involvement of these residues in 4C-Co(II)Cbl formation.

***Lm*EutT^{F72} and *Lm*EutT^{W238} contribute to 5C-Co(II)Cbl active-site access and affinity, respectively.** To analyze the contributions of residue F72 to the *Lm*EutT activity, we constructed *Lm*EutT^{F72Y} and *Lm*EutT^{F72H} variants. The *Lm*EutT^{F72Y} variant was expected to maintain the relative size of the residue at position 72, while slightly increasing its polarity. Conversely, the

*Lm*EutT^{F72H} variant was expected to significantly increase the polarity at position 72. When the medium was supplemented with 5 nM CNCbl, the strain that synthesized *Lm*EutT^{F72Y} displayed wild-type growth, while the strain that synthesized *Lm*EutT^{F72H} showed slightly reduced growth as compared to the *Lm*EutT^{WT} control strain (Fig. 4.7, panel A). Both variants allowed for better growth outcomes than *Lm*EutT^{F72A}. When 25 nM CNCbl was supplemented in the medium, only the strain harboring *Lm*EutT^{F72A} showed a visible growth defect, as compared to the *Lm*EutT^{WT} control strain (Fig. 4.7, panel B).

As shown in figure 4.6, the *Lm*EutT^{W238H} variant activity was very low in the Co(II)Cbl and Co(I)Cbl assays. Consistent with this information, *Lm*EutT^{W238H} failed to synthesize enough AdoCbl to support growth (Fig. 4.5, Fig. 4.7). If we assume that in *Lm*EutT the W238 residue is positioned under the cobalt, then substituting the indole side chain of tryptophan for the imidazole side chain of histidine could allow for the formation of a coordination bond between a nitrogen of the imidazolyl moiety of histidine and the cobalt ion of Co(II)Cbl, as it occurs with "base off/His on" AdoCbl-dependent isomerases.[41] To determine whether this was the case, the tryptophan residue was replaced with an alanine or a leucine residue. Neither *Lm*EutT^{W238A} nor *Lm*EutT^{W238L} allowed growth in the presence of 5 nM or 25 nM exogenous CNCbl (Fig. 4.7), suggesting that the residue W238 was critical for activity, as these substitutions to other nonpolar residues did not improve activity *in vivo*. Shown in figure 4.8, are the results of Co(I) and Co(II) activity assays performed with *Lm*EutT^{F72} and *Lm*EutT^{W238} variants.

Substitution of the bulky phenyl group at position 72 by an alanine (F72A) resulted in an enzyme that had comparable activity to *Lm*EutT^{WT} in the Co(II)Cbl assay, but had >2-fold increased specific activity relative to *Lm*EutT^{WT} in the Co(I)Cbl assay (Fig. 4.8, panel A). In contrast, replacement of F72 with other bulky residues (*e.g.,* Tyr or His) resulted in variants with

slightly lower specific activity in both assays, relative to *Lm*EutT^{WT}. The reaction rate of ACATs belonging to the CobA and PduO families are limited by the rate of corrinoid reduction. Once the corrinoid is reduced, the nucleophilic attack occurs quickly, and this is reflected in the increase in specific activity in the Co(I) assay compared to the Co(II) assay. Assuming that this is the case for *Lm*EutT, these results suggested that residue F72 might restrict access to the active site, since replacement with a less bulky residue (*e.g.,* Ala) increased the specific activity of the variant only in the fast step of the reaction, *i.e.*, the nucleophilic attack (compare F72A in Fig. 4.8, panel A *vs* panel B).

*Lm*EutT^{W238A} and *Lm*EutT^{W238L} variants showed reduced specific activity in both assays, as compared to *Lm*EutT^{WT}. However, the activity of *Lm*EutT^{W238H} was reduced to a greater extent in both assays (Fig. 4.8). The alignment of this region with *Lr*PduO suggested that residue W238 might enhance the affinity of the enzyme for the corrinoid substrate.[40]

Spectroscopic analysis of the F72X and W238H variants. Previous studies revealed that *Lm*EutT^{WT} complexed with ATP converts Co(II)Cbl to a four-coordinate species, so as to facilitate the thermodynamically-challenging Co(II) → Co(I) reduction.[28] As the single unpaired electron in Co(II)Cbl resides in the Co-d_z^2-based molecular orbital that is oriented along the α-ligand–Co bond axis, X-band electron paramagnetic (EPR) spectroscopy provides a uniquely sensitive probe of perturbations to the axial ligation of Co(II)Cbl. Therefore, EPR studies were conducted to assess if the F72X and W238H *Lm*EutT variants were able to displace the α-ligand in 5C-Co(II)Cbl to form 4C-Co(II)Cbl.

Consistent with the observation that the replacement of F72 with other residues decreased the specific activity in the *in vitro* Co(II)Cbl assay, our EPR spectra (Fig. 4.9, Table 4.5) show

that the F72A, F72Y, and F72H substitutions reduce the ability of *Lm*EutT to convert 5C-Co(II)Cbl to 4C-Co(II)Cbl relative to the WT enzyme (which achieves a >98% 5C→4C conversion.)[28]

The EPR spectrum of Co(II)Cbl in the presence of *Lm*EutT^{F72A} (Fig. 4.9, part C) shows that the F72A substitution results in a mixture of base-off 5C-Co(II)Cbl and 4C-Co(II)Cbl in the enzyme active site. While the g values for the 5C fraction are more reminiscent of base-on 5C-Co(II)Cbl (Fig. 4.9, part A) than its base-off analogue (Figure 4.9, part B), the lack of ^{14}N (I = 1) superhyperfine splittings in the 3000-4000 G region indicates that a solvent-derived water molecule rather than the intramolecular DMB base serves as the α-ligand in this species. The unexpectedly small g spread displayed by this species likely reflects a compressed Co–O(H_2) bond relative to free base-off 5C-Co(II)Cbl, as this would destabilize the Co-d_z^2-based molecular orbital and thus decrease the extent of spin-orbit mixing between the ground and ligand field excited states.[42] The fraction of 4C-Co(II)Cbl bound to *Lm*EutT^{F72A} gives rise to a series of weak features across the entire 1000-4500 G range, as reported previously for *Lm*EutT^{WT} and other ACATs.[28, 29, 39, 43] This 4C-Co(II)Cbl signal is more easily identified in the EPR spectrum of Co(II)Cbl bound to the F72Y variant (Fig. 4.9, part D), as the F72Y substitution only marginally compromises the ability of *Lm*EutT to convert Co(II)Cbl to a 4c species (~80% 5C→4C conversion, Table 4.5). Notably, the fraction of 5C-Co(II)Cbl that is formed in this variant is characterized by g values that are similar to those of free base-off 5C-Co(II)Cbl, indicating a relatively unperturbed Co–O(H_2) bond. Finally, the EPR spectrum of Co(II)Cbl in the presence of *Lm*EutT^{F72H} (Fig. 4.9, part E) reveals contributions from 4C-Co(II)Cbl (~45%) and two distinct base-off 5C-Co(II)Cbl species, one with a normal Co–O(H_2) bond (~35%) and one in which this bond is compressed (~20%). The fact that a substantial fraction of 4C-Co(II)Cbl is generated in each of these variants

supports the hypothesis that F72 restricts access to the active site and is not essential for the conversion of 5C-Co(II)Cbl to 4C-Co(II)Cbl.

EPR spectroscopy was also used to probe the origin of the low activity of *Lm*EutT^{W238H} displayed in both assays. One cause of low activity could be the replacement of the intramolecular base with His-238 similar to what has been observed for enzymes binding the Cbl cofactor in the base off, His-on form such as MCM. However, the EPR spectrum of Co(II)Cbl in the presence of *Lm*EutT^{W238H} (Fig. 4.9, part F) exclusively has contributions from a base-off 5C-Co(II)Cbl species, indicating that the drastically reduced activity in the Co(II)Cbl assay might arise from an inability of the W238H variant to form appreciable amounts of 4C-Co(II)Cbl. To probe whether the inability of *Lm*EutT^{W238H} to convert 5C-Co(II)Cbl to 4C-Co(II)Cbl was temperature dependent, we also collected room temperature circular dichroism (CD) data. Surprisingly, the room temperature CD spectra of Co(II)Cbl in the absence and presence of *Lm*EutT^{W238H} are nearly identical (Fig. 4.10), suggesting that the significantly decreased specific activity of this variant in both the Co(II)Cbl and Co(I)Cbl assays is due to weak binding of the Cbl substrate to the enzyme active site.

Modeling *Lm*EutT and *Se*EutT sequences to the reported *Lr*PduO structure (PDB code 3CI1) emphasizes similarities in the conserved regions. The amino acid sequences of *Lm*EutT^{WT} and *Se*EutT^{WT} were modeled to the *Lr*PduO structure using Phyre^2 (Fig. 4.11).[38] The software did not align the N-terminal residues of *Lm*EutT or *Se*EutT since they were not present in *Lr*PduO, and these were excluded from the model. However, the models suggest that there are structural similarities between PduO and EutT ACATs, particularly in the substrate-binding region (Fig. 4.11).

4.5 DISCUSSION

EutT and PduO ACATs share conserved residues that bind ATP. The sequence alignment of EutT and PduO ACATs and the subsequent biochemical analysis of variants with substitutions at the conserved ATP-binding residues suggest that EutT and PduO ACATs evolved similar substrate-binding sites. The similarities were not noted before as the identified ATP-binding motif in *Lr*PduO is not conserved in EutT family ACATs. However, the five residues that were noted in *Lr*PduO to bind to the ATP substrate are conserved across the PduO and EutT homologues included in the alignment. Of note is the conserved NRLS(D/S) motif near the C-terminus of both ACAT families; this motif is part of one of the core □-helices in the structure in *Lr*PduO and may suggest that these ACATs are evolutionarily related.

EutT ACATs may form an inter-subunit salt bridge. The stability of the *Lr*PduO oligomer is not dependent on the presence of the salt brige between residues D35 and R128. In contrast, we found that the stability of the *Lm*EutT oligomer is affected by substitutions of these residues. The *Lm*EutT^{D110R} and *Lm*EutT^{R200D} variants formed significantly more aggregate than variants *Lm*EutT^{D110N}, *Lm*EutT^{R200K}, or *Lm*EutT^{WT} (Fig. 4). If formation of the salt bridge was preserved, as in the *Lm*EutT^{D110R,R200D} variant, the oligomeric state mimicked that of *Lm*EutT^{WT}. Contrary to *Lr*PduO, substitutions of residues D35 or R128 for *Lm*EutT affected the K_m of Co(II)Cbl more than the K_m of ATP (Table 2). These observations suggest that the salt bridge may play a greater role in *Lm*EutT in the stability of the oligomer and affinity for Cbl than in *Lr*PduO.

The mechanism of base displacement in *Lm*EutT is unique among ACAT classes. The mechanism of base displacement has been well documented in CoA and PduO type ACATs, where a phenylalanine and/or tryptophan residue is involved.[14, 40] These residues disrupt the (alpha) ligand coordination which allows the reduction of Co(II) to Co(I) to proceed. Analysis of all the

tryptophan and phenylalanine residues in *Lm*EutT did not identify a residue that possessed similar biochemical characteristics to previously studied variants of F112 in *Lr*PduO (Fig.7-8).[40] Based on these observations and the spectroscopic differences between EutT ACATs and the other ACAT families, we suggest that Class II EutT ACATs utilize an alternative mechanism for base displacement. Our phenotypic and biochemical observations suggest that F72 may be located near the entrance of the substrate-binding site and may control Cbl access to the active site, while residue W238 may be located within the substrate-binding pocket and hence contribute to the hydrophobic pocket for corrin ring positioning.

The unique mechanism of ligand displacement by *Lm*EutT as revealed in the present study is consistent with results obtained previously for *Se*EutT and *Lm*EutT^{WT}.[28, 29] Specifically, it was found that these enzymes can bind both Co(II)Cbl and Co(II)Cbi^{+}; however, only Co(II)Cbl is converted to a 4C species and can thus be adenosylated *in vivo* and in the *in vitro* Co(II)Cbl assay. On the basis of this observation, it was concluded that members of the EutT family of ACATs possess a binding pocket for the DMB base to enhance their affinity for the native substrate and promote axial ligand dissociation. The EPR data obtained in the present study provide evidence that in *Lm*EutT, residues F72 and, in particular, W238 are required for maximum 5C → 4C-Co(II)Cbl conversion. Although in the absence of a crystal structure the location of these residues relative to the Cbl substrate cannot be determined, our results for the *Lm*EutT^{W238H} variant are consistent with W238 playing an important role in properly organizing the putative DMB binding pocket.

4.6 CONCLUSIONS.

This work provides insights into how the Class II EutT ACAT from *Listeria monocytogenes* (*Lm*EutT) binds its substrates. The residues that bind ATP and form an inter-

subunit salt bridge in *Lr*PduO are conserved in *Lm*EutT, and *in vitro* studies of *Lm*EutT variants suggest that these residues perform the same roles in *Lm*EutT as they do in *Lr*PduO. Interestingly, mutations to the inter-subunit salt bridge residues D110 and R200 did not affect *Lm*EutT in the same manner as in *Lr*PduO. Differences in oligomeric state (*Lr*PduO forms a trimer and *Lm*EutT a tetramer) may contribute to these differences. Lastly, residues F72 and W238 were identified as needed for Cbl binding, however, unlike in PduO and CobA, *Lm*EutT does not use a canonical residue to generate 4C-Co(I)Cbl. The mechanism of 4C-Co(I)Cbl formation remains unclear.

4.7 AUTHOR CONTRIBUTIONS

F.C. and J.C.E.S devised the project, planned experiments, and lead the writing of the manuscript. F.G. generated the enzyme variants, performed experiments, and analyzed data. E.G. and T.B. planned the spectroscopic experiments. E.G. performed the spectroscopic simulations and experiments. E.G. and T.B. analyzed the spectroscopic data, and contributed to writing and feedback on the manuscript.

4.8 REFERENCES

1. Zhang, Y.; Rodionov, D. A.; Gelfand, M. S.; Gladyshev, V. N., Comparative genomic analyses of nickel, cobalt and vitamin B12 utilization. *BMC Genomics* **2009,** *10*, 78.

2. Nordlund, P.; Reichard, P., Ribonucleotide reductases. *Annu. Rev. Biochem.* **2006,** *75*, 681-706.

3. Toraya, T., Enzymatic radical catalysis: coenzyme B12-dependent diol dehydratase. *Chem Rec* **2002,** *2*, 352-366.

4. Bandarian, V.; Reed, G. H., Analysis of the electron paramagnetic resonance spectrum of a radical intermediate in the coenzyme B(12)-dependent ethanolamine ammonia-lyase catalyzed reaction of S-2-aminopropanol. *Biochemistry* **2002,** *41*, 8580-8588.

5. Roof, D. M.; Roth, J. R., Ethanolamine utilization in *Salmonella typhimurium*. *J. Bacteriol.* **1988,** *170*, 3855-3863.

6. Roof, D. M.; Roth, J. R., Autogenous regulation of ethanolamine utilization by a transcriptional activator of the *eut* operon in S*almonella typhimurium*. *J. Bacteriol.* **1992,** *174*, 6634-6643.

7. Kofoid, E.; Rappleye, C.; Stojiljkovic, I.; Roth, J., The 17-gene ethanolamine (*eut*) operon of *Salmonella typhimurium* encodes five homologues of carboxysome shell proteins. *J. Bacteriol.* **1999,** *181*, 5317-5329.

8. Buan, N. R.; Suh, S. J.; Escalante-Semerena, J. C., The *eutT* gene of *Salmonella enterica* encodes an oxygen-labile, metal-containing ATP:corrinoid adenosyltransferase enzyme. *J. Bacteriol.* **2004,** *186*, 5708-5714.

9. Sheppard, D. E.; Penrod, J. T.; Bobik, T.; Kofoid, E.; Roth, J. R., Evidence that a B12-adenosyl transferase is encoded within the ethanolamine operon of *Salmonella enterica*. *J. Bacteriol.* **2004,** *186*, 7635-7644.

10. Mera, P. E.; Escalante-Semerena, J. C., Dihydroflavin-driven adenosylation of 4-coordinate Co(II) corrinoids: are cobalamin reductases enzymes or electron transfer proteins? *J. Biol. Chem.* **2010,** *285*, 2911-2917.

11. Fonseca, M. V.; Escalante-Semerena, J. C., An in vitro reducing system for the enzymic conversion of cobalamin to adenosylcobalamin. *J. Biol. Chem.* **2001,** *276*, 32101-32108.

12. Escalante-Semerena, J. C.; Suh, S. J.; Roth, J. R., *cobA* function is required for both de novo cobalamin biosynthesis and assimilation of exogenous corrinoids in *Salmonella typhimurium*. *J. Bacteriol.* **1990,** *172*, 273-280.

13. Nou, X.; Kadner, R. J., Adenosylcobalamin inhibits ribosome binding to *btuB* RNA. *Proc. Natl. Acad. Sci. U S A* **2000,** *97*, 7190-7195.

14. Moore, T. C.; Newmister, S. A.; Rayment, I.; Escalante-Semerena, J. C., Structural insights into the mechanism of four-coordinate cob(II)alamin formation in the active site of the *Salmonella enterica* ATP:co(I)rrinoid adenosyltransferase (CobA) enzyme: Critical role of residues Phe91 and Trp93. *Biochemistry* **2012,** *51*, 9647-9657.

15. Pallares, I. G.; Moore, T. C.; Escalante-Semerena, J. C.; Brunold, T. C., Spectroscopic studies of the *Salmonella enterica* adenosyltransferase enzyme *Se*CobA: Molecular-level insight into the mechanism of substrate cob(II)alamin activation. *Biochemistry* **2014,** *53*, 7969-7982.

16. Mera, P. E.; Maurice, M. S.; Rayment, I.; Escalante-Semerena, J. C., Structural and functional analyses of the human-type corrinoid adenosyltransferase (PduO) from *Lactobacillus reuteri*. *Biochemistry* **2007,** *46*, 13829-13836.

17. Johnson, C. L.; Pechonick, E.; Park, S. D.; Havemann, G. D.; Leal, N. A.; Bobik, T. A., Functional genomic, biochemical, and genetic characterization of the *Salmonella pduO* gene, an ATP:cob(I)alamin adenosyltransferase gene. *J. Bacteriol.* **2001,** *183*, 1577-1584.

18. Fan, C.; Bobik, T. A., Functional characterization and mutation analysis of human ATP:Cob(I)alamin adenosyltransferase. *Biochemistry* **2008,** *47*, 2806-2813.

19. Padovani, D.; Labunska, T.; Palfey, B. A.; Ballou, D. P.; Banerjee, R., Adenosyltransferase tailors and delivers coenzyme B12. *Nat. Chem. Biol.* **2008,** *4*, 194-196.

20. Lofgren, M.; Banerjee, R., Loss of allostery and coenzyme B(12) delivery by a pathogenic mutation in adenosyltransferase. *Biochemistry* **2011,** *50*, 5790-5798.

21. Padovani, D.; Banerjee, R., A rotary mechanism for coenzyme B(12) synthesis by adenosyltransferase. *Biochemistry* **2009,** *48*, 5350-5357.

22. Park, A. K.; Chi, Y. M.; Moon, J. H., Crystal structure of PduO-Type ATP:Cob(I)alamin adenosyltransferase from *Bacillus cereus* in a complex with ATP. *Biochem. Biophys. Res. Commun.* **2011,** *408*, 417-421.

23. Moon, J. H.; Park, A. K.; Jang, E. H.; Kim, H. S.; Chi, Y. M., Crystal structure of a PduO-type ATP:cobalamin adenosyltransferase from *Burkholderia thailandensis*. *Proteins* **2008,** *72*, 1066-1070.

24. St Maurice, M.; Mera, P. E.; Taranto, M. P.; Sesma, F.; Escalante-Semerena, J. C.; Rayment, I., Structural characterization of the active site of the PduO-type ATP:Co(I)rrinoid adenosyltransferase from *Lactobacillus reuteri*. *J. Biol. Chem.* **2007,** *282*, 2596-2605.

25. Buan, N. R.; Escalante-Semerena, J. C., Purification and initial biochemical characterization of ATP:Cob(I)alamin adenosyltransferase (EutT) enzyme of *Salmonella enterica*. *J. Biol. Chem.* **2006,** *281*, 16971-16977.

26. Costa, F. G.; Escalante-Semerena, J. C., A new class of EutT ATP:Co(I)rrinoid adenosyltransferases found in *Listeria monocytogenes* and other *Firmicutes* does not require a metal Ion for activity. *Biochemistry* **2018,** *57* (34), 5076-5087.

27. Moore, T. C.; Mera, P. E.; Escalante-Semerena, J. C., the EutT enzyme of *Salmonella enterica* is a unique ATP:Cob(I)alamin adenosyltransferase metalloprotein that requires ferrous ions for maximal activity. *J. Bacteriol.* **2014,** *196*, 903-910.

28. Stracey, N. G.; Costa, F. G.; Escalante-Semerena, J. C.; Brunold, T. C., Spectroscopic study of the EutT adenosyltransferase from *Listeria monocytogenes*: Evidence for the formation of a four-coordinate cob(II)alamin intermediate. *Biochemistry* **2018,** *57* (34), 5088-5095.

29. Pallares, I. G.; Moore, T. C.; Escalante-Semerena, J. C.; Brunold, T. C., Spectroscopic studies of the EutT adenosyltransferase from *Salmonella enterica*: Mechanism of four-coordinate Co(II)Cbl formation. *J. Am. Chem. Soc.* **2016,** *138*, 3694-3704.

30. Park, K.; Mera, P. E.; Moore, T. C.; Escalante-Semerena, J. C.; Brunold, T. C., Unprecedented mechanism employed by the *Salmonella enterica* EutT ATP:Co(I) rrinoid adenosyltransferase precludes adenosylation of incomplete Co(II)rrinoids. *Angew. Chem. Int. Ed. Engl.* **2015,** *54*, 7158-7161.

31. Pallares, I. G.; Moore, T. C.; Escalante-Semerena, J. C.; Brunold, T. C., Spectroscopic studies of the EutT adenosyltransferase from *Salmonella enterica*: Evidence of a tetrahedrally coordinated divalent transition metal cofactor with cysteine ligation. *Biochemistry* **2017,** *56*, 364-375.

32. VanDrisse, C. M.; Escalante-Semerena, J. C., New high-cloning-efficiency vectors for complementation studies and recombinant protein overproduction in *Escherichia coli* and *Salmonella enterica*. *Plasmid* **2016,** *86*, 1-6.

33. Marsh, P., Ptac-85, an *E. coli* vector for expression of non-fusion proteins. *Nucleic Acids Res.* **1986,** *14*, 3603.

34. Berkowitz, D.; Hushon, J. M.; Whitfield, H. J., Jr.; Roth, J.; Ames, B. N., Procedure for identifying nonsense mutations. *J. Bacteriol.* **1968,** *96*, 215-220.

35. Balch, W. E.; Wolfe, R. S., New approach to the cultivation of methanogenic bacteria: 2-mercaptoethanesulfonic acid (HS-CoM)-dependent growth of *Methanobacterium ruminantium* in a pressurized atmosphere. *Appl. Environ. Microbiol.* **1976,** *32*, 781-791.

36. Laemmli, U. K., Cleavage of structural proteins during the assembly of the head of bacteriophage T4. *Nature* **1970,** *227*, 680-685.

37. Nilges, M. J. Electron paramagnetic resonance studies of low symmetry nickel(I) and molybdenum(V) complexes. Ph.D., University of Illinois at Urbana-Champaign, 1979.

38. Kelley, L. A.; Sternberg, M. J., Protein structure prediction on the Web: a case study using the Phyre server. *Nat. Protoc.* **2009,** *4*, 363-371.

39. Stich, T. A.; Buan, N. R.; Escalante-Semerena, J. C.; Brunold, T. C., Spectroscopic and computational studies of the ATP:Corrinoid adenosyltransferase (CobA) from *Salmonella enterica*: Insights into the mechanism of adenosylcobalamin biosynthesis. *J. Am. Chem. Soc.* **2005,** *127*, 8710-8719.

40. Mera, P. E.; St Maurice, M.; Rayment, I.; Escalante-Semerena, J. C., Residue Phe112 of the human-type corrinoid adenosyltransferase (PduO) enzyme of *Lactobacillus reuteri* is critical to the formation of the four-coordinate Co(II) corrinoid substrate and to the activity of the enzyme. *Biochemistry* **2009,** *48*, 3138-3145.

41. Banerjee, R.; Ragsdale, S. W., The many faces of vitamin B12: catalysis by cobalamin-dependent enzymes. *Annu. Rev. Biochem.* **2003,** *72*, 209-247.

42. Stich, T. A.; Buan, N. R.; Brunold, T. C., Spectroscopic and computational studies of Co(2+)corrinoids: spectral and electronic properties of the biologically relevant base-on and base-off forms of Co(2+)cobalamin. *J. Am. Chem. Soc.* **2004,** *126*, 9735-9749.

43. Park, K.; Mera, P. E.; Escalante-Semerena, J. C.; Brunold, T. C., Spectroscopic characterization of active-site variants of the PduO-type ATP:Corrinoid adenosyltransferase from *Lactobacillus reuteri*: Insights into the mechanism of four-coordinate Co(II)corrinoid formation. *Inorg. Chem.* **2012,** *51*, 4482-4494.

44. Marsh, P., pTAC-85, an *E. coli* vector for expression of non-fusion proteins. *Nucleic Acids Res.* **1986,** *14*, 3603.

45. Kearse, M.; Moir, R.; Wilson, A.; Stones-Havas, S.; Cheung, M.; Sturrock, S.; Buxton, S.; Cooper, A.; Markowitz, S.; Duran, C.; Thierer, T.; Ashton, B.; Meintjes, P.; Drummond, A., Geneious Basic: an integrated and extendable desktop software platform for the organization and analysis of sequence data. *Bioinformatics* **2012,** *28*, 1647-1649.

46. Robert, X.; Gouet, P., Deciphering key features in protein structures with the new ENDscript server. *Nucleic Acids Res.* **2014,** *42* (Web Server issue), W320-4.

4.9 TABLES

Table 4.1 Primers used in this study

Primer name	Sequence
*Lm*EutT^{T88V} F	atgagaagccagaacatatggtgcatttgcgtggtaatctgc
*Lm*EutT^{T88V} R	gcagattaccacgcaaatgcaccatatgttctggcttctcat
*Lm*EutT^{K98Q} F	cgatttgtggatggtcctgaaatacaagcagattaccacgcaaatgc
*Lm*EutT^{K98Q} R	gcatttgcgtggtaatctgcttgtatttcaggaccatccacaaatcg
*Lm*EutT^{R204K} F	agctaagaaggcagctaattctgtttccttgaccatcgttcttattttgtttaaacg
*Lm*EutT^{R204K} R	cgtttaaacaaaataagaacgatggtcaaggaaacagaattagctgccttcttagct
*Lm*EutT^{E207Q} F	aagctaagaaggcagctaactgtgtttcacggaccatcgtt
*Lm*EutT^{E207Q} R	aacgatggtccgtgaaacacagttagctgccttcttagctt
*Lm*EutT^{N231L} F	tatccagaataaactcgataatcgtagaagcgcttgaataatgtctggtcgtttaat
*Lm*EutT^{N231L} R	attaaacgaccagacattattcaagcgcttctacgattatcgagtttattctggata
*Lm*EutT^{D110N} F	cagcttccagtgtatttaattttccgcggaaagcgattt
*Lm*EutT^{D110N} R	aaatcgctttccgcggaaaattaaatacactggaagctg
*Lm*EutT^{D110R} F	cagcttccagtgtacgtaattttccgcggaaagcgatttgtg
*Lm*EutT^{D110R} R	cacaaatcgctttccgcggaaaattacgtacactggaagctg
*Lm*EutT^{R200K} F	ttcacggaccatcgtttttatttgtttaaacgaatgacagcattac
*Lm*EutT^{R200K} R	gtaatgctgtcattcgtttaaacaaaataaaaacgatggtccgtgaa
*Lm*EutT^{R200D} F	tgtttcacggaccatcgtatctattttgtttaaacgaatgacagcattacccatcg
*Lm*EutT^{R200D} R	cgatgggtaatgctgtcattcgtttaaacaaaatagatacgatggtccgtgaaaca
*Lm*EutT^{F72A} F	ccaccataaatcgtttgggcttttgctcgagtagtttctgttttcac
*Lm*EutT^{F72A} R	gtgaaaacagaaactactcgagcaaaagcccaaacgatttatggtgg
*Lm*EutT^{F72H} F	ccaccataaatcgtttggtgttttgctcgagtagtttctgttttcac
*Lm*EutT^{F72H} R	gtgaaaacagaaactactcgagcaaaacaccaaacgatttatggtgg
*Lm*EutT^{F72Y} F	aatgctccaccataaatcgtttgatattttgctcgagtagtttctgttttc
*Lm*EutT^{F72Y} R	gaaaacagaaactactcgagcaaaatatcaaacgatttatggtggagcatt
*Lm*EutT^{F97A} F	gcgatttgtggatggtctttagctacaagcagattaccacgcaa
*Lm*EutT^{F97A} R	ttgcgtggtaatctgcttgtagctaaagaccatccacaaatcgc
*Lm*EutT^{F214A} F	tttaatggaataatctgcttccttagcagctaagaaggcagctaattctgtt
*Lm*EutT^{F214A} R	aacagaattagctgccttcttagctgctaaggaagcagattattccattaaa
*Lm*EutT^{F237A} F	gaacatcagtatccaggctaaactcgataatcggttaagcgcttgaa
*Lm*EutT^{F237A} R	ttcaagcgcttaaccgattatcgagtttagcctggatactgatgttc
*Lm*EutT^{W238H} F	tagttctcacgcggaacatcagtatatggaataaactcgataatcggttaagc
*Lm*EutT^{W238H} R	gcttaaccgattatcgagtttattccatatactgatgttccgcgtgagaacta
*Lm*EutT^{W238A} F	gcttaaccgattatcgagtttattcgcgatactgatgttccgcgtgagaacta
*Lm*EutT^{W238A} R	tagttctcacgcggaacatcagtatcgcgaataaactcgataatcggttaagc
*Lm*EutT^{W238L} F	gcttaaccgattatcgagtttattcctgatactgatgttccgcgtgagaacta
*Lm*EutT^{W238L} R	tagttctcacgcggaacatcagtatcaggaataaactcgataatcggttaagc

Table 4.2 A list of strains and plasmids used in this study

Strain	Organism	Genotype	Source, reference
JE4846	*E. coli*	BL21-Codon Plus –RIL (cat^+)	Stratagene
JE22174	*S. enterica*	*metE205 ara-9* Δ*pduO522* Δ*cobA1465* Δ*eutT1141 eutE18*::MudJ (kan^+)	[26]
Plasmid	**Vector**	**Protein encoded**	**Source, reference**
pTAC-85	control	none	[44]
pEUT159	pTAC-85	*Lm*EutT^{WT}	[26]
pEUT201	pTAC-85	*Lm*EutT^{T88V}	
pEUT202	pTAC-85	*Lm*EutT^{K98Q}	
pEUT206	pTAC-85	*Lm*EutT^{R204K}	
pEUT209	pTAC-85	*Lm*EutT^{E207Q}	
pEUT208	pTAC-85	*Lm*EutT^{N231L}	
pEUT203	pTAC-85	*Lm*EutT^{D110N}	
pEUT204	pTAC-85	*Lm*EutT^{D110R}	
pEUT205	pTAC-85	*Lm*EutT^{R200K}	
pEUT207	pTAC-85	*Lm*EutT^{R200D}	
pEUT218	pTAC-85	*Lm*EutT^{D110R,R200D}	
pEUT196	pTAC-85	*Lm*EutT^{F72A}	
pEUT197	pTAC-85	*Lm*EutT^{F72H}	
pEUT198	pTAC-85	*Lm*EutT^{F72Y}	
pEUT241	pTAC-85	*Lm*EutT^{F97A}	
pEUT247	pTAC-85	*Lm*EutT^{F214A}	
pEUT217	pTAC-85	*Lm*EutT^{F237A}	
pEUT216	pTAC-85	*Lm*EutT^{W238H}	
pEUT251	pTAC-85	*Lm*EutT^{W238A}	
pEUT252	pTAC-85	*Lm*EutT^{W238L}	
pEUT210	pTEV18	*Lm*EutT^{T88V}	
pEUT211	pTEV18	*Lm*EutT^{K98Q}	
pEUT212	pTEV18	*Lm*EutT^{R204K}	
pEUT213	pTEV18	*Lm*EutT^{E207Q}	
pEUT214	pTEV18	*Lm*EutT^{N231L}	
pEUT220	pTEV18	*Lm*EutT^{D110N}	
pEUT221	pTEV18	*Lm*EutT^{D110R}	
pEUT222	pTEV18	*Lm*EutT^{R200K}	
pEUT223	pTEV18	*Lm*EutT^{R200D}	
pEUT224	pTEV18	*Lm*EutT^{D110R,R200D}	
pEUT225	pTEV18	*Lm*EutT^{F72A}	
pEUT226	pTEV18	*Lm*EutT^{F72H}	
pEUT227	pTEV18	*Lm*EutT^{F72Y}	
pEUT233	pTEV18	*Lm*EutT^{F97A}	
pEUT238	pTEV18	*Lm*EutT^{F214A}	
pEUT230	pTEV18	*Lm*EutT^{F237A}	
pEUT231	pTEV18	*Lm*EutT^{W238H}	
pEUT249	pTEV18	*Lm*EutT^{W238A}	
pEUT250	pTEV18	*Lm*EutT^{W238L}	

Table 4.3. Kinetic parameters of ATP-binding variants. Details of the assay conditions and protocol are described under *Materials and Methods*. Each reaction was performed in triplicate; '±' indicates the standard deviation. To obtain the kinetic parameters for the ATP substrate, ATP was added at a concentration of 2-1000 mM, and HOCbl was fixed at 50 or 100 mM. To obtain the kinetic parameters for the Cbl substrate, HOCbl was added at a concentration of 2-90 mM, and ATP was fixed at 1000 mM.

Enzyme	Corres-ponding residue in *Lr*PduO	Role in PduO	Subs-trate	K_{half} [μM]	Hill coefficient	k_{cat} [s^{-1}]	k_{cat} / K_{half} [M^{-1} s^{-1}]
*Lm*EutT$^{WT(26)}$			ATP	4.4 ± 0.3	2.3 ± 0.3	0.24	5.4 x 10^4
			Cbl	4.2 ± 0.2	1.9 ± 0.2	0.21	5.0 x 10^4
*Lm*EutT^{T88V}	T13	g phosphate	ATP	27.5 ± 3.0	1.2 ± 0.1	0.27	9.8 x 10^3
			Cbl	10.5 ± 0.9	1.8 ± 0.3	0.26	2.5 x 10^4
*Lm*EutT^{K98Q}	K23	g phosphate	ATP	95.4 ± 11	0.9 ± 0.1	0.17	1.8 x 10^3
			Cbl	42.7 ± 6.0	1.7 ± 0.2	0.18	4.2 x 10^3
*Lm*EutT^{R204K}	R132	Ribose and a - phosphate	ND*				
*Lm*EutT^{E207Q}	E135	adenosine	ATP	229.0 ± 13.1	1.7 ± 0.1	0.18	8.0 x 10^2
			Cbl	44.8 ± 3.5	2.4 ± 0.2	0.22	4.9 x 10^3
*Lm*EutT^{N231L}	N156	g phosphate	ND*				
	ND* = no activity detected, rate ≤0 nM/s						

Table 4.4 Kinetics parameters of the putative salt bridge variants. Details of the assay conditions and protocol are described under *Materials and Methods*. Each reaction was performed in triplicate; '±' indicates the standard deviation. To obtain the kinetic parameters for the ATP substrate, ATP was added at a concentration of 2 – 1000 mM, and HOCbl was fixed at 50 mM. To obtain the kinetic parameters for the Cbl substrate, HOCbl was added at a concentration of 2 – 50 mM, and ATP was fixed at 1000 mM.

Corres-ponding residue in *Lr*PduO	Role in PduO	Enzyme	Subs-trate	K_{half} [mM]	Hill coefficient	k_{cat} [s^{-1}]	k_{cat} / K_{half} [M^{-1} s^{-1}]
		*Lm*EutT^{WT}	ATP	4.4 ± 0.3	2.3 ± 0.3	0.24	5.4 x 10^4
			Cbl	4.2 ± 0.2	1.9 ± 0.2	0.21	5.0 x 10^4
D35	salt bridge	*Lm*EutT^{D110N}	ATP	5.3 ± 0.5	1.2 ± 0.2	0.07	1.4 x 10^4
			Cbl	9.2 ± 0.4	2.5 ± 0.3	0.05	5.8 x 10^3
		*Lm*EutT^{D110R}	ND*				
R128	salt bridge	*Lm*EutT^{R200K}	ATP	4.5 ± 0.5	1.3 ± 0.2	0.10	2.2 x 10^4
			Cbl	9.4 ± 0.6	1.9 ± 0.2	0.06	6.5 x 10^3
		*Lm*EutT^{R200D}	ND*				
D35, R200	salt bridge	*Lm*EutT$^{D110R, R200D}$	ND*				
ND* = no activity detected, rate < 0 nM/s							

Table 4.5. Spin-Hamiltonian Parameters for Co(II)Cbl Species in Figure 10 Derived from Spectral Simulations

						A(^{59}Co)			A (^{14}N)
Sample	**Co(II) Cbl Species**	**%**	**g1**	**g2**	**g3**	**A1 (MHz)**	**A2 (MHz)**	**A3 (MHz)**	**Aiso (MHz)**
A-Co(II)Cbl (base-on)	**5C**	**100**	2.27	2.23	2.00	40	30	302	49
B-Co(II)Cbi^{+} (base-off)	**5C**	**100**	2.42	2.32	2.00	226	210	402	N/A
C-*Lm*EutT^{F72A}	**4C**	**65**	3.59	2.60	1.82	1148	534	718	N/A
	5C	**35**	2.27	2.23	2.00	25	22	307	N/A
D-*Lm*EutT^{F72Y}	**4C**	**80**	3.55	2.60	1.79	1179	621	716	N/A
	5C	**20**	2.42	2.24	2.02	230	172	350	N/A
E-*Lm*EutT^{F72H}	**4C**	**45**	3.51	2.60	1.78	1228	621	758	N/A
	5C-I	**35**	2.39	2.27	1.99	212	149	385	N/A
	5C-II	**20**	2.28	2.21	1.99	25	21	317	N/A
F-*Lm*EutT^{W238H}	**5C**	**100**	2.37	2.28	1.99	163	151	356	N/A

4.10 FIGURES

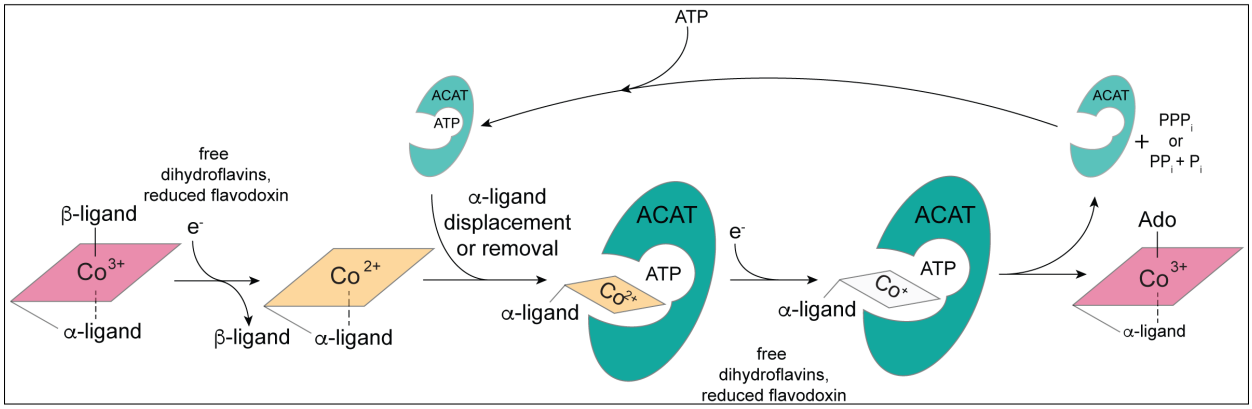

Figure 4.1. Corrinoid adenosylation pathway. To date, all ACATs studied follow a two-step mechanism for adenosylation of corrinoids. If the corrinoid is scavenged from the environment, is is imported as Co(III)Cba and reduced intracellularly to Co(II)Cba, which causes dissociation of the a-ligand. The Co(II) to Co(I) reduction requires displacement or removal of the a-ligand, which is facilitated by the ACAT. Once the cobalt center is coordinated only by the four equatorial pyrroles, the reduction step from Co(II) to Co(I) can occur. The residued Co(I) nucleophile attacks the 5'C of ATP, completing the adenosylation reaction.

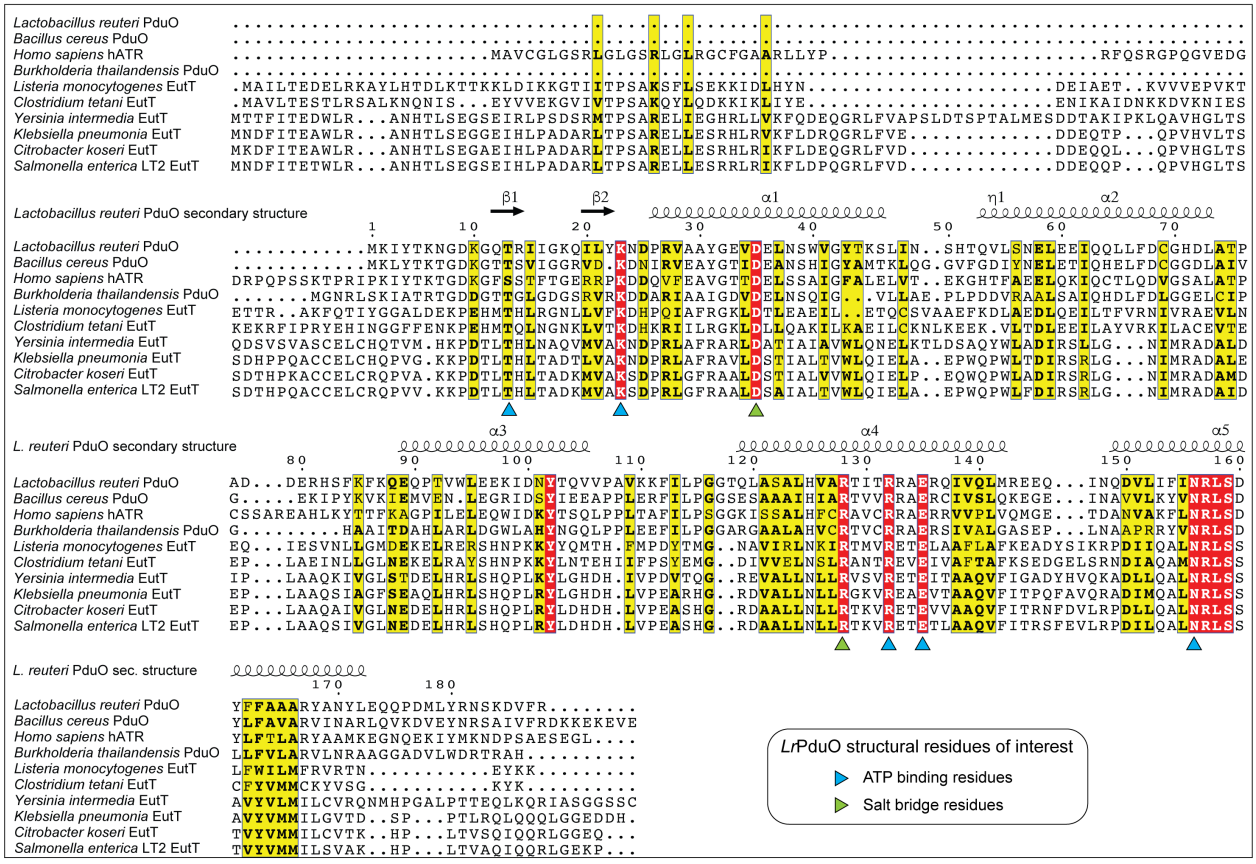

Figure 4.2. Sequence alignment of PduO and EutT homologues. PduO homologues for which structural information is available and EutT homologues that were active *in vitro* were aligned using Geneious and annotated in ESpript 3.0.[45, 46] The percent pairwise identity was 29.2%. The secondary structure of *Lactobacillus reuteri* (*Lr*PduO) is shown above the alignment. Residues highlighted in red are conserved across EutT and PduO ACATs, and residues in yellow are similar with a similarity cut-off value of 0.7. Blue arrows indicate residues that interact with ATP in the active site of *Lr*PduO. Green arrows indicate residues that form the inter-subunit salt bridge in *Lr*PduO.

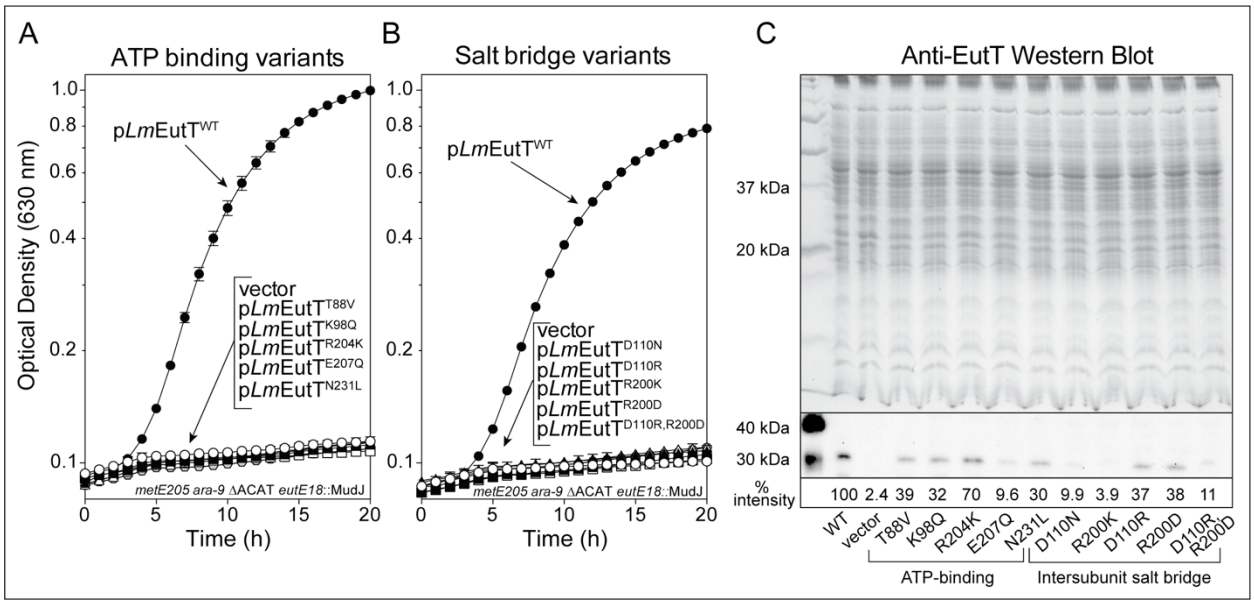

Figure 4.3. **Growth analysis of *Lm*EutT variants.** *Lm*EutT^{WT} and *Lm*EutT variants of residues implicated in ATP binding (A) and forming an inter-subunit salt bridge (B) were expressed *in trans* in a strain lacking ACAT activity and expressing the *lacZ* gene under the control of the *eut* operon promoter. These strains were grown on minimal medium containing lactose as the carbon source. Ethanolamine (1 mM) and CNCbl (200 nM) were also added, as ethanolamine and AdoCbl are needed for EutR-dependent transcriptional activation of the *eut*.[9] Growth on lactose indicated sufficient ACAT-dependent conversion of Cbl to AdoCbl to activate transcription of the *lacZ* fusion. None of the *Lm*EutT variants tested supported growth in these conditions. (C) Western blot of cell lysates grown to mid-log phase under the same conditions supplemented with glycerol (22 mM). Anti-*Lm*EutT polyclonal rabbit antibodies probed for the presence of *Lm*EutT^{WT} or *Lm*EutT variants in the the soluble fraction of cell lysates of each corresponding strain. The molecular mass of *Lm*EutT is 29.1 kDa. The relative intensity of each band was expressed as a percentage of the intensity of the *Lm*EutT variant band compared to the intensity of the *Lm*EutT^{WT} band.

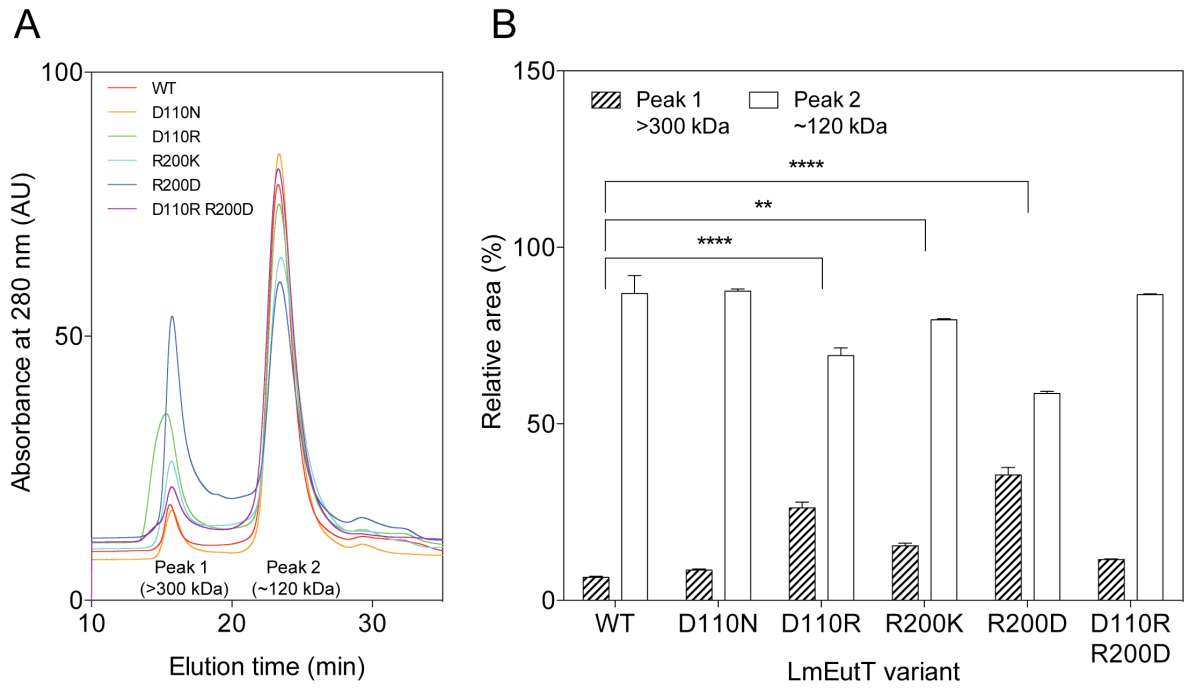

Figure 4.4. Oligomerization states of *Lm*EutT and variants targeting inter-subunit, salt-bridge residues. (A) *Lm*EutT^{WT} (and variants of residues D110 and R200 were resolved over a size exclusion column (Superose 12 10/300 GL, GE). Elution of the complexes were monitored by UV absorption at 280 nm, and the elution time was compared to a set of standards (a-globulin, 158 kDa; ovalbumin, 44 kDa; myoglobin, 17 kDa, vitamin B_{12}, 1.35 kDa) to determine the size of the complex. (B) The area under each peak was quantified and the percentage of each species was calculated by dividing the peak area by the total area. A two-way analysis of variance (ANOVA) comparing the mean of each of the peaks of the variants to *Lm*EutT^{WT} was performed. *Lm*EutT^{D110R}, *Lm*EutT^{R200D} and to a lesser extent *Lm*EutT^{R200K} were significantly different in oligomerization pattern from *Lm*EutT^{WT} (29.1 kDa monomer, 116.4 kDa tetramer). Two-way ANOVA analysis was performed to assess the level of significance, which is denoted by asterisks, where ** is $p \leq 0.01$ and **** is $p \leq 0.0001$. This analysis was performed twice per sample.

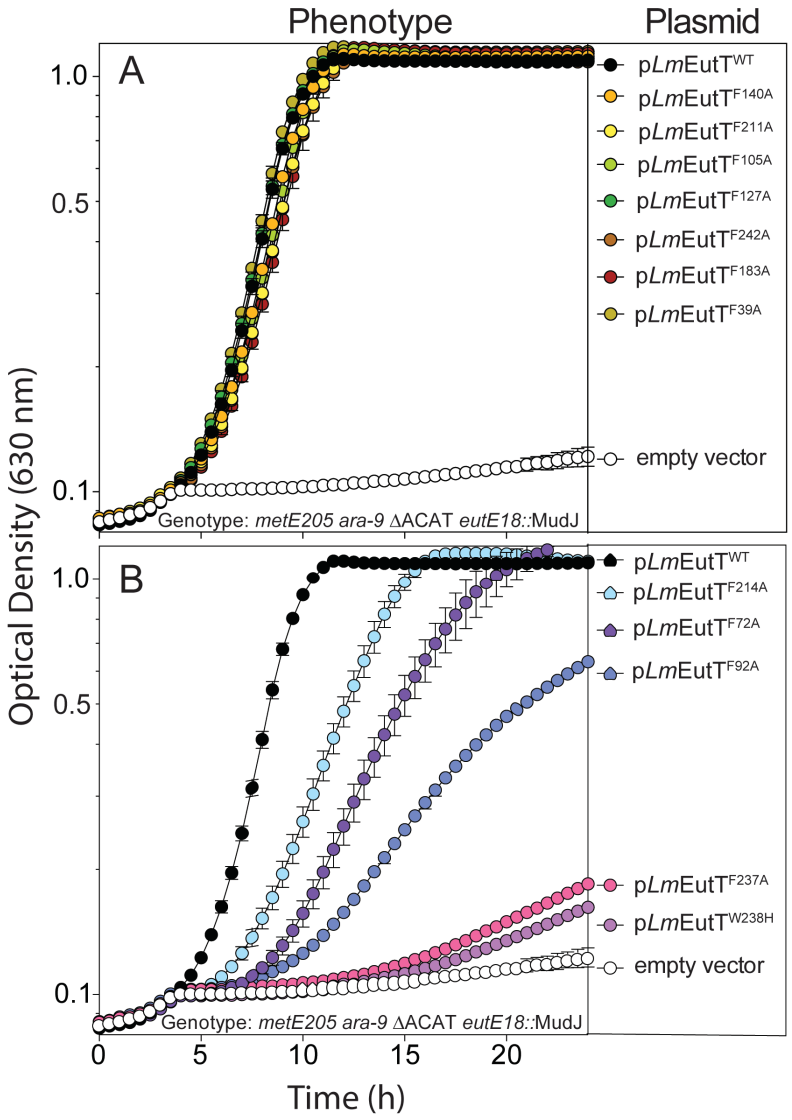

Figure 4.5. ***In vivo*** **screen of phenylalanyl and tryptophanyl variants of *Lm*EutT**. *Lm*EutT^{WT} and *Lm*EutT variants were expressed *in trans* under the same conditions as in Figure 3. (A) Seven variants supported growth of the indicator strain at the same growth rate and yield as the strain that synthesized *Lm*EutT^{WT}. (B) Five variants displayed a range of defects shown by their ability to support growth at different rates, and in some cases yield, relative to *Lm*EutT^{WT}.

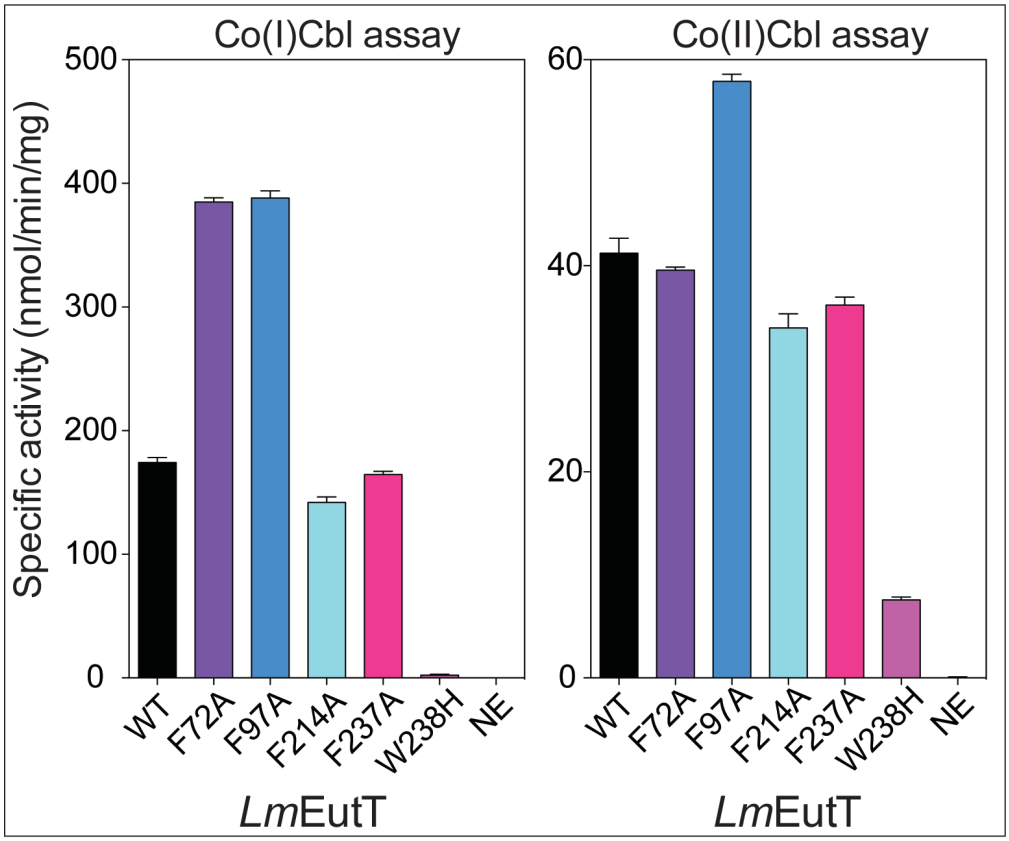

Figure 4.6. *In vitro* analysis of *Lm*EutT phenylalanyl and tryptophanyl variants. Variants with decreased enzymatic activity (Fig. 4.5, panel B) were purified and characterized *in vitro* using two assays: the Co(I)Cbl assay (left panel), and the Co(II)Cbl assay (right panel). The Co(I)Cbl assay only requires the proper positioning of substrates, while the Co(II)Cbl assay additionally requires that *Lm*EutT generates the 4C-Co(II)Cbl to facilitate the reduction of Co(II) to Co(I). Each bar is labeled to indicate the *Lm*EutT variant used; NE stands for the 'No Enzyme' control.

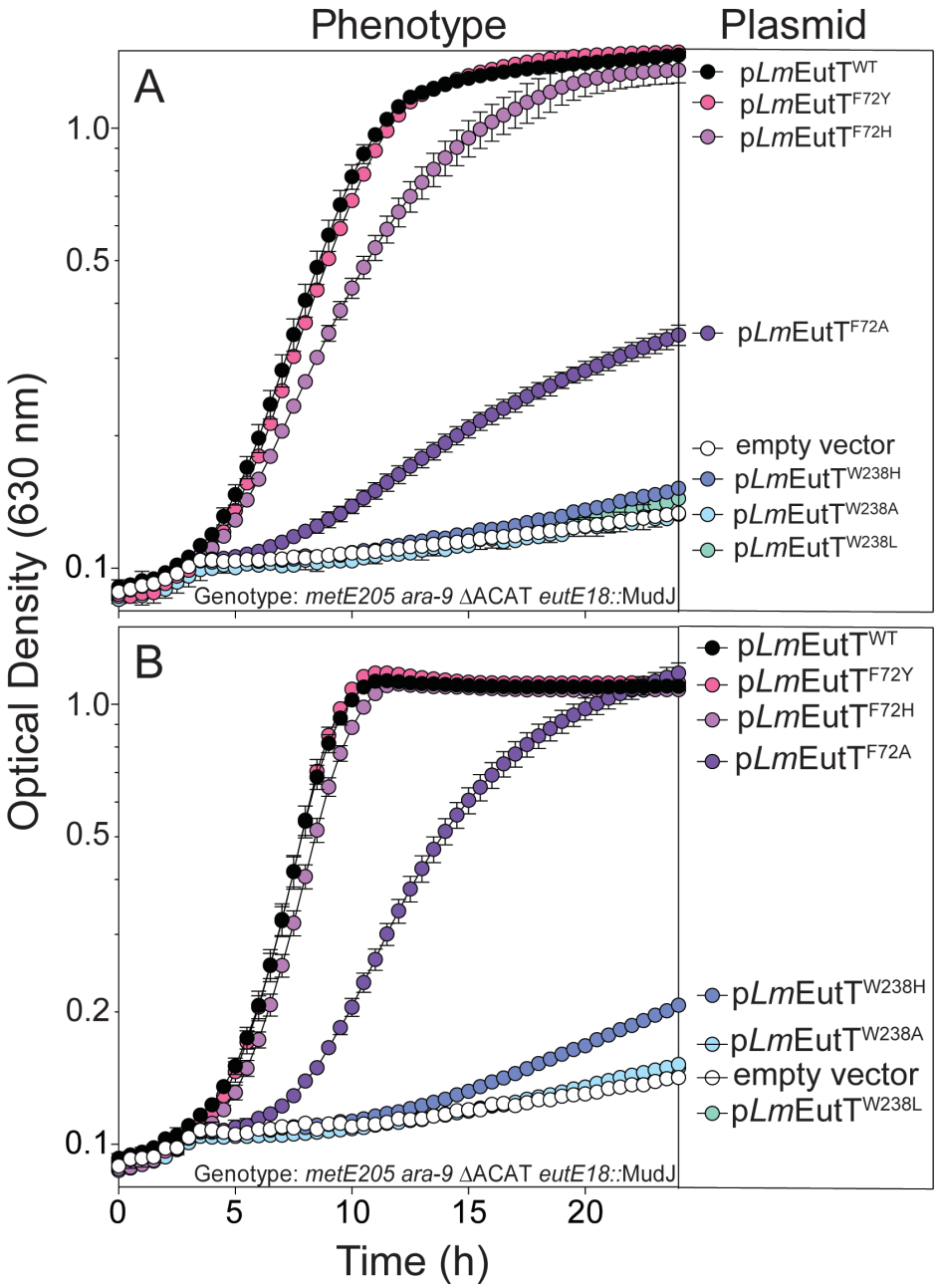

Figure 4.7. *In vivo* analysis of *Lm*EutT variants with substitutions at residues F72 and W238. Several variants of *Lm*EutT with changes at residues F72 and W238 were analyzed *in vivo* in minimal + lactose medium with (A) medium supplemented with 5 nM CNCbl, or (B) medium supplemented with 25 nM CNCbl. Variants *Lm*EutT^{F72H}, *Lm*EutT^{F72A}, and *Lm*EutT^{W238H} synthesized more AdoCbl when the concentration of CNCbl was increased 5-fold. Strains synthesizing *Lm*EutT^{F72Y} or *Lm*EutT^{WT} showed the same growth behavior.

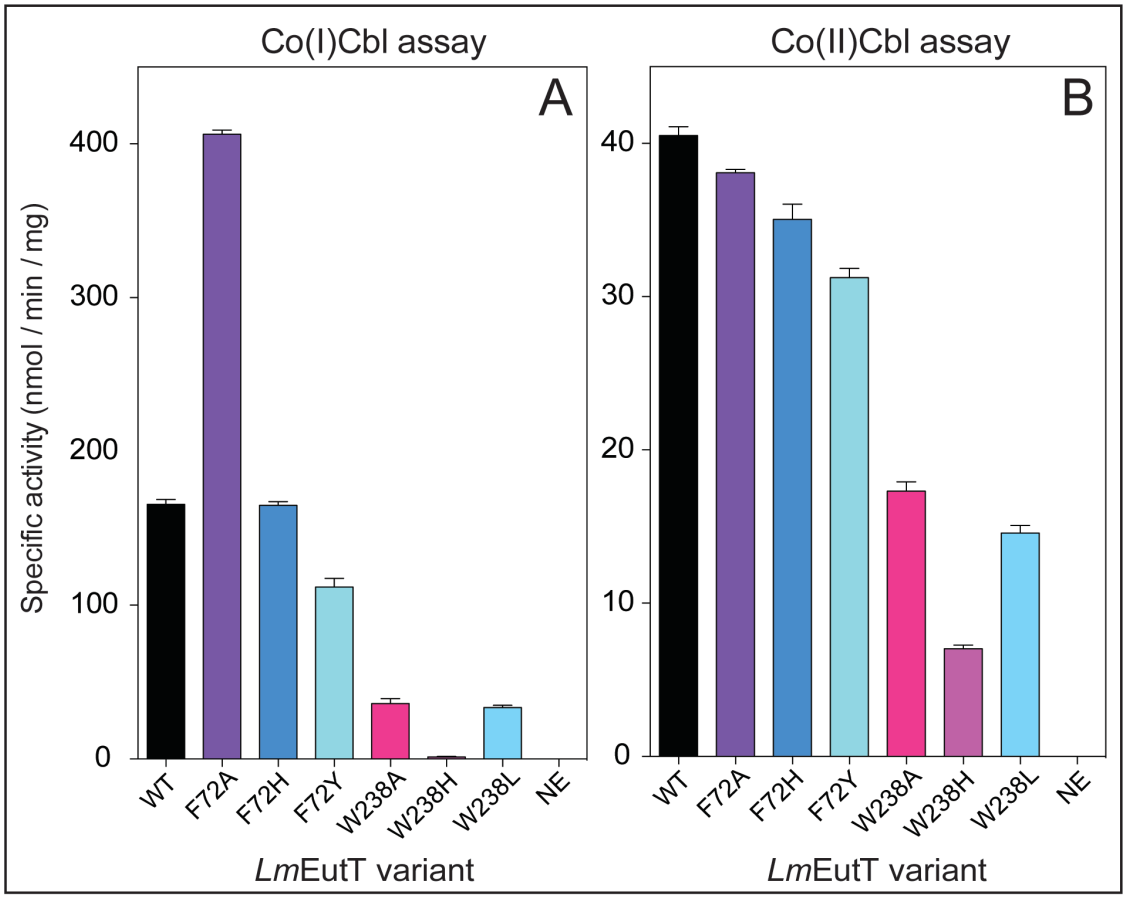

Figure 4.8. *In vitro* analysis of F72 and W238 variants. *Lm*EutT^{WT} and variants were purified and tested for activity in the Co(I)Cbl (A) and Co(II)Cbl (B) assays; NE stands for 'no enzyme' control. *Lm*EutT^{F72A} was the most striking variant, as the specific activity was similar to *Lm*EutT^{WT} in the Co(II)Cbl assay and much higher in specific activity compared to *Lm*EutT^{WT} in the Co(I)Cbl assay. *Lm*EutT^{F72H} and *Lm*EutT^{F72Y} had similar or lower activity compared to *Lm*EutT^{WT} in both assays. All W238 variants had lower activity than *Lm*EutT^{WT}, however, nonpolar amino acid substitutions (*e.g.,* *Lm*EutT^{W238A}, *Lm*EutT^{W238L}) were less detrimental than histidine.

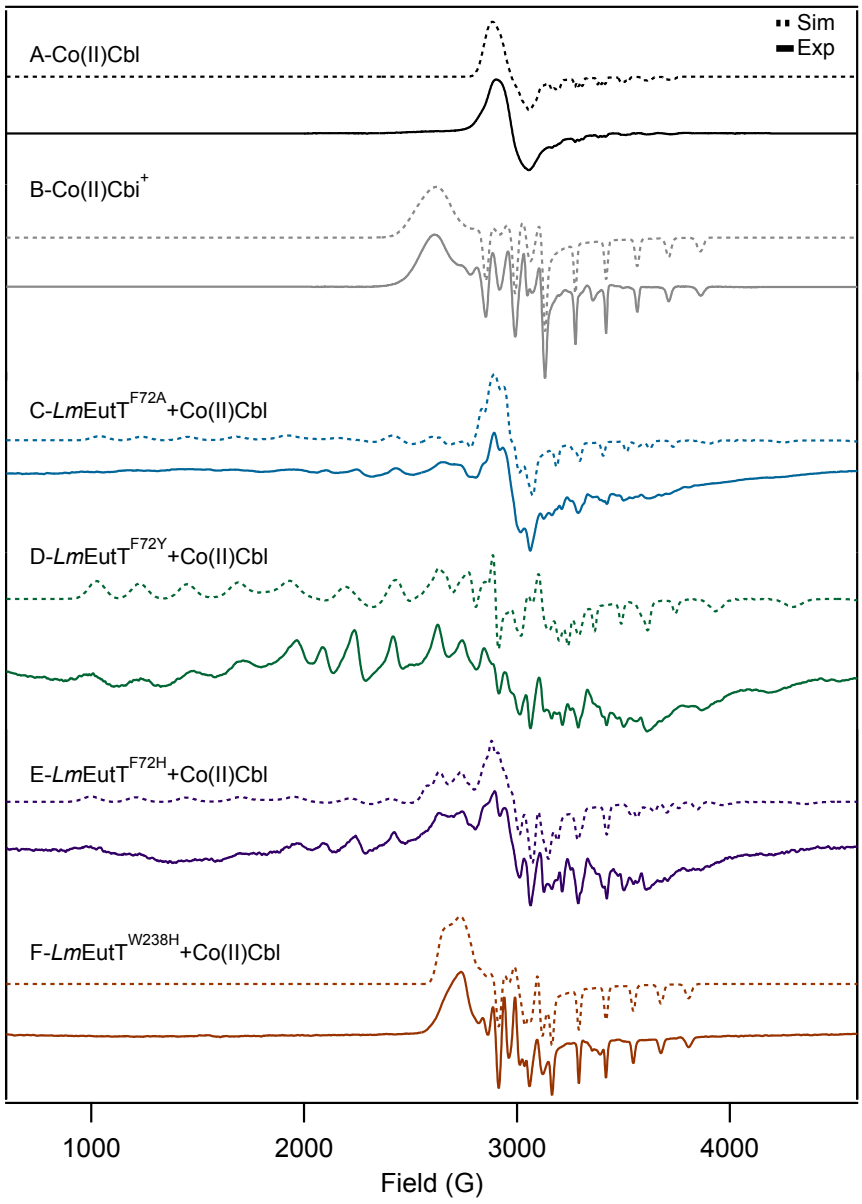

Figure 4.9. X Band EPR data collected at 20 K (solid line) and simulated spectra (dashed line) for (A) Co(II)Cbl, a base-on 5C species, (B) Co(II)Cbi^{+}, which lacks the intramolecular DMB and thus serves as a model of base-off Cbl in solution at neutral pH, and (C-F) Co(II)Cbl in the presence of various *Lm*EutT variants as labeled. The relative contributions from base-off 5C-Co(II)Cbl and 4C-Co(II)Cbl are provided in Table 4.5.

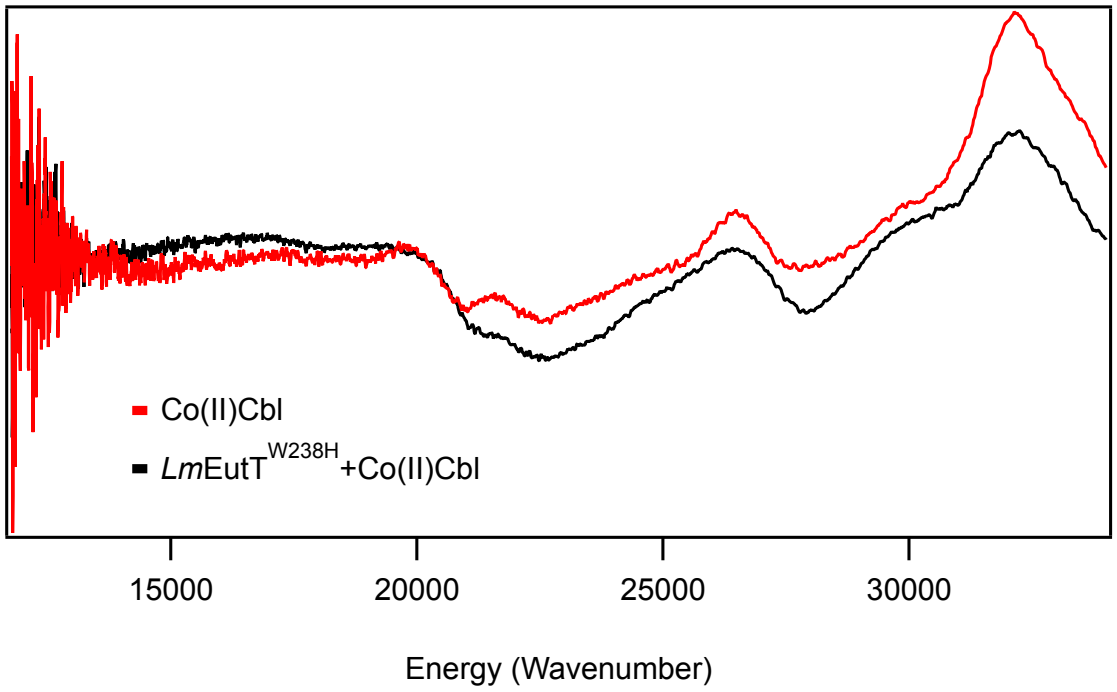

Figure 4.10. Room temperature CD spectra of Co(II)Cbl in the absence (red) and presence (black) of *Lm*EutT^{W238H}.

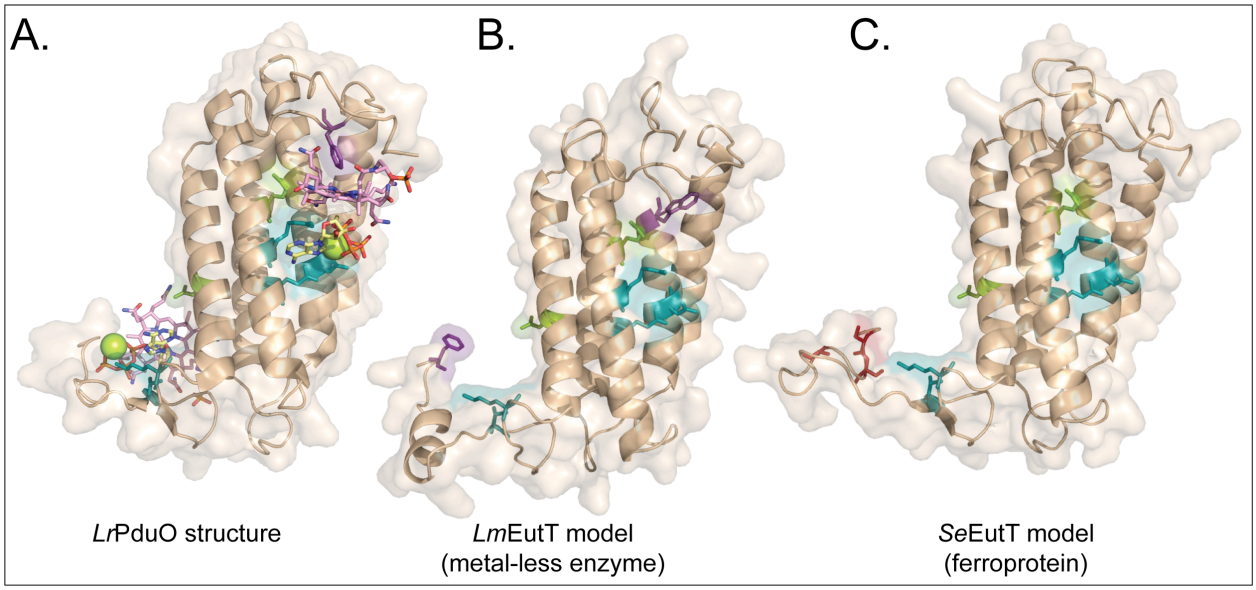

Figure 4.11. *Lm*EutT and *Se*EutT were modeled using the *Lr*PduO structure as a scaffold in the Phyre[2] one-to-one threading program.[38] ATP-binding residues in the *Lr*PduO structure were color-coded in blue, as were the corresponding residues in the *Lm*EutT and *Se*EutT models. The residues involved in the inter-subunit salt bridge are shown in green in the *Lr*PduO structure as well as corresponding residues in the models. The location of the substrates in two of the three active sites of the *Lr*PduO trimer is shown on both sides of a single *Lr*PduO subunit, and residue F112 in *Lr*PduO, the residue that displaces the a - ligand of the cobamide is in magenta. In the *Lm*EutT model, residues F72 and W238 are shown in pink. In the *Se*EutT model, the two cysteines that bind Fe(II), C80 and C83, are shown in orange.

CHAPTER 5

LOCALIZATION AND INTERACTIONS OF ADENOSYLCOBALAMIN-DEPENDENT ETHANOLAMINE AMMONIA-LYASE, ETHANOLAMINE AMMONIA-LYASE REACTIVATING FACTOR, EUTA, AND ATP:CO(I)RRINOID ADENOSYLTRANSFERASE, EUTT[3]

[3]Costa, F.G., and Escalante-Semerena, J.C. To be submitted to *Molecular Microbiology.*

5.1 ABSTRACT

Metabolic compartmentalization has several uses in prokaryotes, including substrate concentration and sequestration of reactive intermediates. In *Salmonella enterica,* the catabolism of ethanolamine is accomplished in a proteinaceous compartment, or the ethanolamine utilization (Eut) metabolosome. The role of this metabolosome is to mitigate potential toxicity associated with generation of the acetaldehyde intermediate via sequestration in the Eut metabolosome. The first step of ethanolamine catabolism is accomplished by the adenosyl-cobalamin (AdoCbl)-dependent ethanolamine ammonia-lyase (EAL) through a radical mechanism. This radical can be inactivated, requiring replacement of the coenzyme by the reactivase EutA. Generation of AdoCbl from cobalamin (Cbl) is accomplished by the ATP:Co(I)rrinoid adenosyltransferase (ACAT) EutT. It is known that EAL localizes to the metabolosome, however it was unclear where EutA and EutT were localized and how they interacted with EAL. Here, we provide evidence that EAL, EutA, and EutT localize to the *eut* metabolosome, and that EutA interacts directly with EAL. No evidence supporting a direct interaction was found between EutT and EAL, or between EutT, EutA and EAL. However, growth phenotypes from a Δ*eutT* mutant strain suggest that, despite the presence of two additional ACATs in the cell, EutT expression is critical for efficient ethanolamine catabolism. Altogether, this work provides a preliminary understanding of the fate of AdoCbl within the Eut metabolosome.

5.2 INTRODUCTION

Ethanolamine is a component of the phospholipid, phosphatidylethanolamine, and is present in the intestinal environment as a result of phospholipid degradation and epithelial cell turnover.[1] Ethanolamine can be utilized as a source of carbon, nitrogen, and energy by several enteric microorganisms, including commensals and pathogens such as *Salmonella enterica, Escherichia coli, Listeria monocytogenes, Enterococcus faecalis,* and *Clostridium difficile*.[2-5] Respiration of ethanolamine coupled to tetrathionate reduction confers a fitness advantage to *S. enterica* in the murine gut.[6] Additionally, it has been shown that *S. enterica* utilizes ethanolamine as a signal to activate transcription of genes required for macrophage survival.[7]

The functions required for ethanolamine catabolism in *S. enterica* are encoded in a single ethanolamine utilization (*eut*) operon (Figure 5.1, panel A).[8] The first step of ethanolamine catabolism begins with the conversion of ethanolamine to the reactive intermediate, acetaldehyde, and ammonia by the adenosylcobalamin (AdoCbl)-dependent ethanolamine ammonia-lyase (EAL). EAL is comprised of two subunits, the large subunit (EutB) and the small subunit (EutC) (EC:4.3.1.7, EAL) (Figure 5.1).[8-10] Ethanolamine ammonia-lyase activity is dependent on the formation of an adenosyl radical produced by the homolytic cleavage of the Co – C bond connecting the adenosyl group to cobalamin.[11, 12] EAL can be inactivated by irreversibly binding to cobalamin (Cbl), which can occur in the event the radical is quenched (Figure 5.1).[13] Inactive Cbl is removed from EAL's active site and replaced with AdoCbl by the ethanolamine ammonia-lyase reactivating factor, EutA, at the expense of ATP,[14] while the ATP:Co(I)rrinoid adenosyltransferase (ACAT), EutT (EC:2.5.1.17), is responsible for generating AdoCbl from Co(II)balamin (Cbl) (Figure 5.1).[14]

The reactive acetaldehyde intermediate produced by EAL can then be converted to acetyl-CoA by the acetaldehyde dehydrogenase (EutE) or to ethanol by the alcohol dehydrogenase (EutG) (Fig. 5.1).[1] Cells have developed several mitigation strategies for circumventing metabolic stress evoked by reactive metabolic intermediates like acetaldehyde.[15-17] In many prokaryotes, including *S. enterica*, the reactive acetaldehyde intermediate produced in the catabolism of ethanolamine is sequestered within a proteinaceous compartment called the ethanolamine utilization (Eut) metabolosome (Figure 5.1, panel B).[2] The metabolosome is made up of five different shell proteins that assemble into pentamers or hexamers containing a central pore, and then self-assemble into the metabolosome structure.[18] The pores function as gates, permitting the ingress of ethanolamine and egress of acetate and ethanol, while preventing the egress of acetaldehyde.[19]

In addition to sequestration of acetaldehyde, the Eut metabolosome maintains its own private cofactor pools.[20] EutE reduces NAD^+ and consumes CoA to produce acetyl-CoA from acetaldehyde. The NADH generated is oxidized back to NAD^+ by EutG, and CoA is regenerated by EutD in the production of acetyl-P (Fig. 5.1, panel B). Deletion of either *eutG* or *eutD* produces a growth defect that is suppressed by mutations in the metabolosome shell proteins, supporting the idea that the native metabolosome is impermeable to NAD^+ and CoA and must recycle these cofactors *in situ*.[20] There is some evidence of enzyme localization to the Eut metabolosome for these purposes. Studies have demonstrated that the N-terminal end of EutC serves as a localization tag to the Eut metabolosome.[16] A localization tag has also been identified on the N-terminal end of EutE, the enzyme responsible for catabolizing acetaldehyde to acetyl-CoA.[21]

In this work, we used localization studies of EAL, EutA, and EutT as a first step to investigating whether AdoCbl is also recycled within the metabolosome. We confirmed that EAL localizes to the metabolosome, and found that EutA and EutT also localize to the *eut*

metabolosome. Additionally, *in vivo* and *in vitro* evidence that EutA and EAL interact directly and are stabilized in solution together are presented. Direct interactions were not found between EutT and EutA or EutT, and EutA in complex with EAL. However, EutT expression is critical for efficient ethanolamine catabolism, despite the presence of two additional cytosolic ACATs.

5.3 MATERIALS AND METHODS

Strains and plasmids. Strains used in this study were all derivatives of *Salmonella enterica* sv. Typhimurium LT2 or *E. coli* BL21 (Table 5.1). Mutant strains were constructed using the λRed recombinase system as described previously.[22] Transductional crosses needed for strain construction were performed using a high-frequency, general transducing mutant of bacteriophage P22.[23] For protein purification, *S. enterica eutA* and *eutBC* genes were cloned into pSAPKO-WT vector as described elsewhere (Table 5.2).[24, 25] For *in vivo* complementation, *eutA, eutBC,* and *eutABC* genes were cloned into pCV3 or pTAC-85 complementation vectors as previously described (Table 5.2).[24, 26]

Growth media. Difco nutrient broth (NB) (8 g/L) with NaCl (5 g/L) or lysogeny broth (LB) (20 g/L) were used as rich media. Solidified media was made with addition of agar (15 g/L). All chemicals were purchased from Millipore-Sigma unless otherwise stated. All chemicals were reagent grade and were used without further purification. The ribose minimal medium used in this work was no-carbon essential medium (NCE),[27] supplemented with $MgSO_4$ (1 mM), Wolfe's trace minerals,[28] ribose (20 mM), and methionine (0.5 mM). Ethanolamine (30 mM) and CNCbl (200 nM) were added when the EutR-dependent transcriptional activation of the *eut* operon was desired. Ethanolamine minimal media was NCE media supplemented with $MgSO_4$ (1 mM), Wolfe's trace minerals, methionine (0.5 mM), ethanolamine (90 mM) and CNCbl (200 nM, 10 nM where indicated). For plasmid maintenance, chloramphenicol (25 μg/mL) for pCV3 vectors, ampicillin

(100 μg/mL) for pTAC-85 vectors, and kanamycin (50 μg/mL) for pSAPKO-WT vectors were added to rich media. For minimal media, all antibiotics were used at 1/5 the concentration that was used in rich media. To induce transcription of the complementation plasmids, L-arabinose (100 μM) for pCV3 vectors or isopropyl β-D-1-thiogalactopyranoside (IPTG, 100 μM) for pTAC-85 vectors were added to the media. Strains were grown in 1 mL NB for 16 h at 37 °C shaking at 150 RPM. These overnight cultures were sub-cultured at 1% v/v in the ribose minimal media, or 2.5% in the ethanolamine minimal media.

Purification of EutA and EAL. EutA and EAL were purified individually or in combination using the following method. *E. coli* BL21-CodonPlus cells were transformed with the plasmid pEUT194 or pEUT195 and plated on LB with kanamycin (50 μg/mL) and chloramphenicol (25 μg/mL) and incubated overnight at 37 °C. 5 mL of LB was added to the plate, and cells were scraped into solution with a sterilized plate spreader. The suspended cells were transferred to a 2 L flask containing a metal spring and 1L TB media supplemented with kanamycin (50 μg/mL) and chloramphenicol (25 μg/mL). Cultures were grown to an OD_{600} = 0.6 - 0.8 at 25 °C, at which point IPTG was added at a final concentration of 1 mM. The induced cells were incubated at 25 °C for 16 hours, at which point they were harvested by centrifugation at 6,000 *x g* for 15 min in a refrigerated Avanti J-20 XPI equipped with a JLA 8.1 rotor. Cell pellet was resuspended in in 50 mL of Buffer A (50 mM Tris pH 7.5 at 4 °C) supplemented with phenylmethylsulfonylfluoride (PMSF,1 mM), lysozyme (1 mg/mL), and DNase (0.1 mg/mL). If EutA and EAL were to be copurified, at this point the cell suspensions were mixed together. The cell suspension was sonicated on ice with a Fisher Scientific/Brandon Sonifier Model 150 Cell Disruptor using the following settings: 2 s on, 2 s off for 30 s at 60% amplitude. This was repeated one more time after a 5 min rest. Cell suspension was then stirred at 4 °C for 30 minutes before centrifugation at 40,000

x g for 30 min. Supernatant was filtered with a 0.45 μm filter and loaded onto a HiPrep DEAE FF 16/10 (GE Healthcare) anion exchange column equilibrated with Buffer A. Column was washed with 20 column volumes (CV) of buffer A, then a gradient was applied of 0-40% of buffer B (50 mM Tris, 2 M NaCl pH 7.5 at 4 °C). Fractions containing EutA and/or EAL were combined and concentrated with 25% w/v NH_4SO_4 at 4 °C and centrifuged at 10,000 *x* g for 30 min. Pellet was incubated in a smaller volume of Buffer A overnight at 4 °C, and the pellet was gently resuspended into solution the next morning. The suspended protein was dialyzed against 1 L of Buffer A three times, and the solution was centrifuged at 16,000 *x* g for 15 min before storing soluble protein at -80 °C.

Antibody preparation. Purified EutT, EutA or EAL protein was provided to Envigo for production of rabbit polyclonal antibodies. Rabbit antiserum was precleared against *S. enterica* strain JE7092 for EutT antibodies, JE8093 for EutA antibodies, and JE8094 for EAL antibodies using the following procedure. *S. enterica* was grown in 5 mL NCE minimal media supplemented with ribose, ethanolamine and CNCbl to an OD_{600} = 1.0 – 1.1. Cell culture was transferred to a 15 mL falcon tube and incubated on ice for 15 min. Tubes were centrifuged in a tabletop centrifuge (Eppendorf 5804R) at 2,000 *x* g for 15 minutes. Cells were resuspended in 100 μL of denaturing buffer (50 mM Tris, pH 7.5, at 4 °C, 2% SDS). Suspension was boiled for 5 min to lyse cells and iced for 10 minutes. 900 μL of buffer (50 mM Tris, pH 7.5, at 4 °C) was added to the lysed cells with 10 μL of anti-serum and incubated at 4 °C for 36 h. The samples were centrifuged at 16,000 *x* g for 10 minutes. The supernatant was flash frozen in aliquots and stored at -80 °C.

Western Blotting. Western blots were prepared as previously described.[29] Pre-cleared primary antibodies were used at a 1:2,000 dilution, and the secondary antibody (goat anti-rabbit peroxidase antibody, Millipore Sigma) was used at a 1:10,000 dilution.

Thin section preparation for transmission electron microscopy. *S. enterica* cells were grown in minimal media with ribose; or minimal media with ribose, ethanolamine and CNCbl to an OD_{600} = 1.0 – 1.1. 5 mL of culture was centrifuged at 6,000 *x g* for 2 minutes and resuspended in 1 mL of Sorenson's phosphate buffer pH 7.4 (0.1 M sodium phosphate) with 4% paraformaldehyde and 0.2% glutaraldehyde. The resuspended cells were fixed at room temperature for 15 minutes and centrifuged at 6,000 *x g* for 2 minutes. Supernatant was removed and cell pellet was washed two times in Sorenson's phosphate buffer pH 7.4 before a final centrifugation of 6,000 *x g* for 2 minutes. Noble agar (4% in Sorenson's buffer pH 7.4) melted and at 60 °C was added to the cell pellet and the cells were enrobed in the agar with a sterile toothpick. A short centrifugation was performed to concentrate the sample at the tip. The fixed and agar-enrobed sample was removed and cut into 2 mm blocks for dehydration and embedding.

All dehydration and embedding steps were incubated at room temperature on a slow rotator set at a 45° angle. The dehydration steps were as follows: 50% EtOH for 15 min, 70% EtOH for 15 min, 80% EtOH for 10 min. Then LR White resin was mixed with 80% EtOH at a 2:1 ratio and the samples were incubated in that mixture for 1 h. Samples were then incubated in 100% LR White resin for 1 h three times. Samples were then embedded in LR White resin in gelatin capsules and incubated at 50 °C for 14-16 h to polymerize. Thin sections of 30-50 nm thickness were cut using a DiATOME Ultra diamond knife mounted on a RMC – MT-X microtome and placed onto copper grids coated with formvar and carbon for uranyl acetate staining or gold grids coated with formvar and carbon for immunogold labeling.

Immunogold labeling. Grids containing sectioned samples were incubated face down on a 25 μL droplet of blocking buffer (20 mM Tris pH 7.4, 150 mM NaCl, 1% w/v bovine serum albumin) for 10 min and dipped repeatedly in a beaker of blocking buffer for 1 min before being transferred

to a 25 µL droplet of blocking buffer containing the primary antibody. For immunogold-labeling of EAL, the primary antibody was at a 1:250 dilution and incubated at room temperature for 4 hours before moving on to the next step. For immunogold-labeling of EutA and EutT, the primary antibody was at 1:100 dilution and incubated at 4 °C for 16 hours. After the primary antibody incubation, the grids were dipped repeatedly in a 10 mL beaker of blocking buffer for 1 min and each grid was incubated on a 25 µL droplet of blocking buffer for 15 min. Grids were transferred to 25 µL droplets of anti-rabbit IgG-gold antibody produced in goat (Millipore-Sigma) and incubated for 1 h at room temperature. The grids were dipped repeatedly in a 10 mL beaker of blocking buffer for 30 seconds followed by dipping repeatedly in a 10 mL beaker of water for 30 seconds immediately followed by post-staining with uranyl acetate as described below.

Uranyl acetate staining. Thin section samples on grids were placed face-down on droplets of filtered 4% aqueous uranyl acetate for 20 minutes, then dipped in a beaker of DI H_2O thirty times before placing face-down on droplets of filtered DI H_2O for 1 min.

Size exclusion chromatography. Purified EutA, EAL, and copurified EutA and EAL were applied in 0.5 mL volumes to a HiLoad 16/600 Superdex 200 pg packed column equilibrated with sizing column buffer (50 mM Tris pH 7.5 at 4 °C, 1 mM TCEP). Individual preparations of EutA and EAL were loaded at a concentration of 1 mg/mL, and the copurified EutA and EAL preparation was loaded at a concentration of 2 mg/mL. Protein standards used were the following: thyroglobulin (8 mg/mL), apoferritin (10 mg/mL), β-amylase (4 mg/mL), alcohol dehydrogenase (5 mg/mL), bovine serum albumin (10 mg/mL), and carbionic anhydrase (3 mg/mL). These protein standards were selected from Millipore Sigma's molecular weight markers for gel filtration chromatography, and the combined solution was prepared in the recommended concentrations. Protein standards were run in quadruplicate and were also applied to the column in 0.5 mL volumes

for each run. The protein sample was run at 1 mL/min, and elution of protein was monitored at 280 nm wavelength. Elution time was recorded in minutes.

5.4 RESULTS AND DISCUSSION

Ribose minimal media supplemented with ethanolamine and cyanocobalamin induce Eut metabolosome formation. Prior work has shown that ethanolamine and AdoCbl are both required for expression of genes encoded within the *eut* operon.[30] Ethanolamine and AdoCbl directly bind to the activator, EutR, which binds to the *eut* operon promoter and to its own promoter (Figure 5.1).[31] EutR is not the only regulator of the operon, as expression of the *eut* operon is also subject to catabolite repression.[4] One challenge in this work was to obtain cell mass for mutant strains unable to utilize ethanolamine, but still capable of producing metabolosomes. Ribose was selected as an alternate carbon source that would circumvent catabolite repression and permit for *eut* operon transcription. To ensure that the Eut metabolosomes are produced in the presence of ribose, wild-type *S. enterica* (JE6583) was grown in ribose minimal medium with or without ethanolamine and cyanocobalamin (CNCbl). These cultures were prepared for transmission electron microscopy (TEM) to confirm formation of Eut metabolosomes when ethanolamine and CNCbl are present. In ribose minimal medium (Fig. 5.2, panel A), no Eut metabolosomes were observed. However, supplementation of the ribose minimal medium with ethanolamine and CNCbl (Fig. 5.2, panel B) allowed for the visualization of Eut metabolosomes within the *S. enterica* cells (Fig. 5.2, panel B, emphasized by a black arrow). These conditions were used to further analyze the localization of EutT, EutA, and EAL, in relation to the Eut metabolosome.

EAL, EutA, and EutT are localized to the *eut* metabolosome. Prior work identified that EAL is localized to the metabolosome, and the first ~35 amino acids of the N-terminus of the small EAL subunit, EutC, binds to the EutS shell protein.[16] While the biochemical activity and physiological

contributions of EAL, EutA, and EutT have been well-studied, the localization of EutA and EutT in *S. enterica* has not been determined.[16] We sought to confirm the localization of EAL to the metabolosome, and determine the localization of EutT and EutA in *S. enterica* cells.

Having established the presence and appearance of the Eut metabolosomes within *S. enterica* cells grown in ribose minimal medium supplemented with ethanolamine and CNCbl, we proceeded to determine the localization of EutT, EutA, and EAL in relation to the *eut* metabolosome by immunogold labeling. *S. enterica* wild-type (*eutT*$^+$ *eutA*$^+$ *eutBC*$^+$, JE6583), Δ*eutA* (JE8093), Δ*eutBC* (JE8094), or Δ*eutT* (JE7092) cells were grown in ribose minimal medium containing ethanolamine and CNCbl. The wild-type cells grown on ribose minimal medium were used as a no metabolosome control.

The primary antibodies used for immunogold labeling were precleared polyclonal antibodies against EAL, EutA, and EutT. The specificity of these EutT, EutA, and EutBC antibodies was confirmed through the visualization of the expected size bands corresponding to 30.2, 49.5, 49.4 and 32.1 kDa for EutT, EutA, EutB, and EutC monomers, respectively (Figure 5.3). Importantly, no band was observed when EutT, EutA, or EutBC antibodies were exposed to lysate derived from the corresponding Δ*eutT,* Δ*eutA,* or Δ*eutBC* mutant strains grown in minimal medium with ribose, ethanolamine, and CNCbl, ruling out nonspecific antibody binding.

A secondary antibody conjugated to a 5 nm gold particle, targeting the primary antibody, was used to visualize the localization of each protein in cross-sectioned cell samples prepared for each strain. All of the samples were then post-stained in uranyl acetate to improve contrast. In the samples of wild-type cells grown in ribose minimal media with ethanolamine and CNCbl, EAL (EutBC) detection clustered to the regions in the cell previously identified as the *eut* metabolosomes (Figure 5.4, panel A and B). These data confirmed earlier findings that EAL is

localized to the Eut metabolosome.[16] Importantly, immunogold labeled EutBC was markedly absent from *eutBC* mutant strain grown in the presence of ethanolamine and CNCbl (Figure 5.4, panel C), and in wild-type cells grown without ethanolamine and CNCbl (Figure 5.4, panel D), confirming that immunogold labeling is specific to EAL and EAL is only expressed in the presence of ethanolamine and CNCbl. These same patterns were also observed when wild-type *S. enterica* was labeled with anti-EutA and anti-EutT antibody, suggesting that EutA and EutT are also localized to the metabolosome (Figure 5.4, panels E and F for EutA antibodies and panels I and J for EutT antibodies). Immunogold labeling was markedly absent in the Δ*eutA* and Δ*eutT* strains (Fig. 5.4, panels G and K, respectively) or when $eutA^+$ and $eutT^+$ strains were grown on ribose minimal medium (Fig. 5.4, panels H and L, respectively).

eutA* from distantly related enteric organisms is unable to complement an *S. enterica eutA* mutant *in vivo. Previous *in vitro* work identified that EutA can facilitate the removal of inactive Co(II)Cbl from EAL's active site and replacement with AdoCbl.[14] Whether EutA directly interacts with EAL *in vivo*, however, has not yet been determined. If EutA specifically interacts with EAL to form an EAL-EutA complex, it is expected that heterologously expressed EutA isozymes from distantly related species would be unable to form such a complex with *S. enterica* EAL. Four EutA homologues from a diversity of Eut metabolosome-encoding enteric organisms, comprising differences in both length and amino acid identity from *Se*EutA (Table 5.3), were assessed for their ability to complement an *S. enterica* Δ*eutA* strain (Figure 5.5). Two homologues from *Citrobacter koseri* and *Klebsiella pneumoniae*, which have the same amino acid length as *S. enterica* EutA and have ~90% amino acid identity, readily complemented the *S. enterica* Δ*eutA* strain, when 100 μM IPTG was used to induce their expression (Figure 5.5). The two EutA homologues from *Enterococcus faecalis* and *Listeria monocytogenes* had ~36% identity to *S. enterica* EutA and were

6 and 15 amino acids longer, respectively. Neither of these homologues were able to complement an *S. enterica* Δ*eutA* strain. Further *in vivo* work using the EutA and EAL homologue from *L. monocytogenes* helped determine whether the inability for this homolog to complement an *S. enterica* Δ*eutA* mutant was due to perturbed EutA-EAL interaction or for some other biological reason.

***In vivo* evidence supports species-specific EutA and EAL interaction.** Previously, we studied the function and mechanism of EutT from *Listeria monocytogenes* (*Lm*EutT) expressed in *S. enterica.*[32] This study showed that *Lm*EutT could complement an *S. enterica* strain lacking ATP:Co(I)rrinoid adenosyltransferase (ACAT) activity. However, when we expanded heterologous complementation to EutA and EAL from *L. monocytogenes,* we found neither homologue could complement an *S. enterica* Δ*eutA* or Δ*eutBC* strain, respectively. In this work, we probed this incompatibility by testing growth of *S. enterica* Δ*eutA,* Δ*eutBC,* and Δ*eutABC* strains on ethanolamine when *L. monocytogenes* EutA (*Lm*EutA) and EAL (*Lm*EAL) were expressed *in trans* individually or in concert (Figure 5.6). An *S. enterica* Δ*eutA* strain is unable to grow in minimal medium supplemented with CNCbl and using ethanolamine as a sole carbon source. Expectedly, *SeeutA* expressed *in trans* can complement the Δ*eutA* mutant, restoring growth (Fig. 5.6, panel A). However, expression of *LmeutA* failed to restore growth, unless *LmeutBC* was also expressed *in trans* (Fig. 5.6, panel A). This suggests that *Lm*EutA is unable to reactivate *Se*EAL, but it can successfully facilitate the reactivation of *Lm*EAL. When *Lm*EAL was expressed alone, it failed to rescue growth for the *S. enterica* Δ*eutA* strain, ruling out the possibility that *Lm*EAL alone restores EAL activity to levels sufficient for growth (Fig.5.6, panel A). Similarly, expression of *LmeutBC* in an *S. enterica* Δ*eutBC* mutant strain confers modest growth, but growth is significantly improved by expression of *LmeutA* (Fig. 5.6, panel B). Importantly, *LmeutBC*

cannot complement an *S. enterica* Δ*eutA* or Δ*eutABC* mutant strain, indicating that *eutA* is still required for modest *LmeutBC* complementation (Figure 5.6, panels A and C). It is notable that *SeeutBC* can complement *S. enterica* Δ*eutA* or Δ*eutABC* mutant strain (Figure 5.6, panel A and C). This suggests that EAL can accomplish several turnovers before it is subject to inactivation, and so overexpression of EAL permits sufficient conversion of ethanolamine to acetaldehyde to support growth. Overall, these data suggest that *Se*EutA can reactivate *Lm*EAL to a small enough degree to allow modest growth, while *LmeutA* cannot sufficiently reactivate *Se*EAL to allow growth on ethanolamine. Importantly, since the inclusion of *LmeutA* or *Lm*EAL fully restores growth to these backgrounds, respectively, these data are consistent with a model where a direct species-specific interaction between *S. enterica* or *L. monocytogenes* EutA-EAL pairs is critical for complete reactivation of either EAL, during ethanolamine catabolism.

***In vitro* evidence that EutA and EAL form an enzyme complex.** The *in vivo* observations of EutA and EAL complementation led to further analysis of the interaction between EutA and EAL *in vitro.* EutA and EAL were purified alone or in combination using a two-step purification, resulting in protein at least 88% pure (Figure 5.7). Notably, when EutA and EAL were purified individually, each enzyme was prone to aggregation, but when copurified, EutA and EAL were less prone to this aggregation behavior. In the purification buffer, EutA could be concentrated to a maximum of approximately 2 mg/mL, and EAL could be concentrated to a maximum of approximately 4 mg/mL before seeing visible aggregation. The mixture of EutA and EAL, however, was stable at much higher concentrations, with the highest concentration measured at 19 mg/mL. The results for EAL were not surprising, as it has been previously reported that EAL solubility improves greatly following deletion of a portion of the N-terminus from EutC.[33] EutA and EAL were run on a gel filtration column individually or in combination, and the elution rate

of the oligomers was recorded and compared to a set of protein standards (Figure 5.8). When 0.5 mg of EutA was added, a large high molecular mass oligomer (~900 kDa) whose size is not accurately captured by the chosen column's size limit of 600 kDa was observed (Figure 5.8, panel B). This supported the finding that EutA has a tendency to aggregate on its own. An additional minor population of EutA was observed at 57 kDa, corresponding closest to the predicted size of a EutA monomer (49.5 kDa). When 0.5 mg of EAL was analyzed on the gel filtration column a high molecular mass oligomer (~1,300 kDa) was also observed, again consistent with the aggregation behavior mentioned above. However, the major population elutes at a calculated mass of 487 kDa, which agrees with the size of the EAL oligomer consisting of a trimer of dimers.[34] When 0.5 mg of EutA and 0.5 mg EAL are combined and run on the gel filtration column, both of the EAL and EutA higher molecular mass oligomers observed in isolation are significantly reduced (Figure 5.8, panel B). Additionally, the major oligomeric state has a molecular mass of 475 kDa, a shift from the 487 kDa oligomer observed with EAL alone. This shift was significant as determined by the 95% confidence intervals for each peak (474.6 – 476.1 kDa and 486.1 – 488.5 kDa, respectively) There are two additional oligomeric states at 241 and 63 kDa, which form in the combined EutA and EAL preparation. Without more information about the oligomeric ratio of EutA to EAL, it is difficult to make predictions regarding the makeup of oligomeric states corresponding to the peaks at 475, 241, and 63 kDa in the EutA and EAL mixed samples.

EutT is conditionally required with low Cbl supplementation. The above work demonstrated *in vivo* and *in vitro* evidence that EutA and EAL interact, further supporting that both components are localized to the metabolosome. Attempts to determine interactions with EutT and EAL, or EutT and EutA + EAL did not reveal interactions between these enzymes *in vitro* (data not shown). Previously published work showed that high (≥100 nM) cobalamin supplementation overcomes

the growth defect of a Δ*eutT* strain. This can be explained by the presence of CobA, the housekeeping ACAT. CobA is required for adenosylation of cobalamin precursors and for production of the AdoCbl required to activate the *eut* operon.[35] When the cobalamin concentration was restricted (10 nM), a Δ*eutT* strain had a growth defect, however this was not complemented using *eutT in trans*.[36] To confirm these data and determine if the phenotype is a result of the absence of *eutT* as opposed to polar effects of the mutation, growth studies were carried out using 200 nM and 10 nM CNCbl, and complementation of the Δ*eutT* deletion was accomplished by expressing *eutT in trans* (Figure 5.9). At 200 nM CNCbl supplementation, all of the strains displayed wild-type growth behavior (Figure 5.9, panel A). At 10 nM CNCbl supplementation, the Δ*eutT* strain showed perturbed growth, as compared to *eutT*$^{+}$ strain (Figure 5.9, panel B). This was complemented by *S. enterica eutT* expressed *in trans*, confirming the growth defect was due to the absence of *eutT* and not polar effects in the *eut* operon. The growth rates for each strain were calculated in the exponential phase (Figure 5.9, panel C). For the 10 nM CNCbl condition, two doubling times were calculated, as there is an inflection point at approximately 15 h where the growth rate for the *eutT*$^{+}$ and the complementation strain (Δ*eutT* / p*eutT*$^{+}$) change. Interestingly, the overall yield for any strains when CNCbl was supplemented at 10 nM did not grow more than to a measured absorbance (measured at 630 nm) of 0.5, suggesting that the amount of cobalamin available to the cell limited growth.

5.5 CONCLUSION

EutT, EutA and EAL are localized to the Eut metabolosome. Prior work demonstrated EAL was localized to the *eut* metabolosome.[16] While the biochemical functions and physiological role of EutA and EutT have been studied, the localization of these enzymes and their potential association with EAL function remain unknown. Immunogold labeling revealed that the

localization patterns of EAL, EutA, and EutT were very similar, and all of these enzymes grouped to locations containing Eut metabolosomes. However, it remains unclear whether EAL, EutA, or EutT are localized inside or outside of the Eut metabolosome, warranting further study. The contents of the Pdu metabolosome were identified by purification of the intact metabolosome followed by gel electrophoresis and identification of protein fragments by mass spectrometry.[37] Unfortunately, this approach has not been successful for purification of intact Eut metabolosomes.

EAL reactivation requires a cognate EutA. A previous heterologous expression system, where EutT from *Listeria monocytogenes* (*Lm*EutT) was expressed in an *S. enterica* strain lacking all ACATs (Δ*cobA* Δ*pduO* Δ*eutT*, or ΔACAT), revealed that *Lm*EutT could supply sufficient AdoCbl for growth, though growth was limited.[32] When this heterologous approach was applied to EutA homologues, complementation depended on the similarity of the EutA homologue to *Se*EutA. The selected EutA homologues with high amino acid identity (*Ck*EutA and *Kp*EutA) were the same amino acid length as *Se*EutA. Notable, these homologues are derived from organisms that encode *eut* operons that are also transcriptionally controlled by EutR. The two EutA homologues with low amino acid identity were longer in amino acid length than *Se*EutA, and are derived from organisms whose *eut* operon is controlled not by EutR, but by a two-component sensor.[3, 4, 38] Notably, *Lm_eutA* and *Lm_eutBC* could not complement an *S. enterica* Δ*eutA* and Δ*eutBC* strain, respectively. While possible that the enzymes were not functional or required codon optimization, co-expression of *Lm_eutA* and *Lm_eutBC* restored growth, suggesting that a specific interaction between EutA and EAL was necessary.

Another line of support for the direct interaction of EutA and EAL is the behavior of the enzymes *in vitro*. Purified EutA could only be concentrated to a maximum of 1-2 mg/mL, while purified EAL could only be concentrated to 4 mg/mL, before aggregation. However, copurification

of EutA with EAL eliminated this aggregation phenotype, allowing concentration to 19 mg/mL, which was supported from the size exclusion chromatography observations. Importantly, the aggregation behavior for *S. enterica* EAL was observed previously and could be overcome through the elimination of a 29 aa long fragment from the N-terminus of EutC without negatively impacting catalysis.[33] This region was later identified as the *eut* metabolosome localization tag. It is possible that the interaction between EutA and EAL occurs at an interface corresponding to the EutC localization tag, such that EutA-EAL interaction changes the solvent accessibility of the EutC N-terminal region, improving EAL solubility dynamics. The same may be true for EutA, though a *eut* metabolosome localization tag for EutA has not been characterized. Further characterization of interactions between enzyme variants with perturbations corresponding to residues making up these localization tags will help determine whether this may be the case.

To our knowledge, this work provides the first evidence of localization of EutA and EutT to the *eut* metabolosome, and of direct interactions between EutA and EAL. While we were able to show that there is a direct interaction between EutA and EAL, the insolubility and instability of purified EutA challenged kinetic analysis of its interaction with EAL. Future work with the EutA + EAL complex, such as structural determination of the complex, cross-linking studies, and substrate-binding studies, will advance our understanding of the mechanism EutA utilizes to facilitate replacement of the coenzyme in EAL.

EutT maximizes efficiency of ethanolamine metabolism. *S. enterica* encodes three ATP:Co(I)rrinoid adenosyltransferases (ACATs) in its genome. This is remarkable, as many organisms only encode one ACAT.[39] It is notable that two of the ACATs, PduO and EutT, are associated with metabolic pathways that are encapsulated in the propanediol utilization (*pdu*), and the ethanolamine utilization (*eut*) metabolosomes, respectively. The growth defect observed with

the Δ*eutT* strain demonstrated that the initial doubling time (between 10 – 15 h) of the Δ*eutT* strain was significantly higher than that of *eutT*$^{+}$ or Δ*eutT* / pEutT^{+}. However, there was an inflection point at approximately 15 h, after which the doubling time between *eutT*$^{+}$ and Δ*eutT* was the same. Additionally, the overall yield of growth for all strains was much lower with 10 nM CNCbl supplementation. These observations may be explained by the affinity of the Cbl transporter, BtuB, which has a dissociation constant of 5 nM for CNCbl in the presence of Ca^{2+}.[40] Overall, the growth defect of Δ*eutT,* which was conditional on the amount of cobalamin supplemented, combined with the localization of EutT to the *eut* metabolosome as observed in the immunogold labeling experiments, suggests that localized adenosylation of cobalamin may provide a growth advantage to *S. enterica* when the availability of cobalamin is limited, and ethanolamine is available.

In this work, interacting partners of EutT were not identified. It is possible that an interaction between EutT and EutA and/or EAL exists and was not detected the *in vitro* conditions tested. It's also possible that maintenance of a localized pool of AdoCbl inside the metabolosome is sufficient for EAL to be loaded with AdoCbl by EutA, and so a direct interaction is not required. Co-immunoprecipitation of EutT from *S. enterica* cells may interacting partners of EutT, if any. Overall, this work lays a foundation for advancements in our understanding of the *eut* enzymes involved in AdoCbl biosynthesis and utilization.

5.6 ACKNOWLEDGEMENTS

We would like to thank Dr. John Shields and Dr. Mary Ard at the Georgia Electron Microscopy facility for their training, advice, and assistance with preparation of samples and use of the electron microscope.

5.7 REFERENCES

1. Kaval, K. G.; Garsin, D. A., Ethanolamine utilization inbacteria. *MBio* **2018,** *9*.

2. Brinsmade, S. R.; Paldon, T.; Escalante-Semerena, J. C., Minimal functions and physiological conditions required for growth of *Salmonella enterica* on ethanolamine in the absence of the metabolosome. *J. Bacteriol.* **2005,** *187*, 8039-8046.

3. Buchrieser, C.; Rusniok, C.; Kunst, F.; Cossart, P.; Glaser, P.; Listeria, C., Comparison of the genome sequences of *Listeria monocytogenes* and *Listeria innocua*: clues for evolution and pathogenicity. *FEMS Immunol. Med. Microbiol.* **2003,** *35*, 207-213.

4. Kaval, K. G.; Gebbie, M.; Goodson, J. R.; Cruz, M. R.; Winkler, W. C.; Garsin, D. A., Ethanolamine utilization and bacterial microcompartment formation are subject to carbon catabolite repression. *J. Bacteriol.* **2019,** *201*, e00703-18.

5. Nawrocki, K. L.; Wetzel, D.; Jones, J. B.; Woods, E. C.; McBride, S. M., Ethanolamine is a valuable nutrient source that impacts *Clostridium difficile* pathogenesis. *Environ. Microbiol.* **2018,** *20*, 1419-1435.

6. Thiennimitr, P.; Winter, S. E.; Winter, M. G.; Xavier, M. N.; Tolstikov, V.; Huseby, D. L.; Sterzenbach, T.; Tsolis, R. M.; Roth, J. R.; Baumler, A. J., Intestinal inflammation allows *Salmonella* to use ethanolamine to compete with the microbiota. *Proc. Natl. Acad. Sci. U.S.A.* **2011,** *108*, 17480-17485.

7. Anderson, C. J.; Clark, D. E.; Adli, M.; Kendall, M. M., Ethanolamine signaling promotes *Salmonella* niche recognition and adaptation during infection. *PLoS Pathog.* **2015,** *11*, e1005278.

8. Roof, D. M.; Roth, J. R., Functions required for vitamin B_{12}-dependent ethanolamine utilization in *Salmonella typhimurium*. *J. Bacteriol.* **1989,** *171*, 3316-3323.

9. Chang, G. W.; Chang, J. T., Evidence for the B_{12}-dependent enzyme ethanolamine deaminase in *Salmonella*. *Nature* **1975,** *254*, 150-151.

10. Faust, L. R.; Connor, J. A.; Roof, D. M.; Hoch, J. A.; Babior, B. M., Cloning, sequencing, and expression of the genes encoding the adenosylcobalamin-dependent ethanolamine ammonia-lyase of *Salmonella typhimurium*. *J. Biol. Chem.* **1990,** *265*, 12462-12466.

11. Krouwer, J. S.; Holmquist, B.; Kipnes, R. S.; Babior, B. M., The mechanisms of action of ethanolamine ammonia-lyase, an adenosylcobalamin-dependent enzyme. Evidence that carbon-cobalt bond cleavage is driven in part by conformational alterations of the corrin ring. *Biochimica et Biophysica Acta* **1980,** *612*, 153-159.

12. Bandarian, V.; Poyner, R. R.; Reed, G. H., Hydrogen atom exchange between 5'-deoxyadenosine and hydroxyethylhydrazine during the single turnover inactivation of ethanolamine ammonia-lyase. *Biochemistry* **1999,** *38*, 12403-12407.

13. Kaplan, B. H.; Stadtman, E. R., Ethanolamine deaminase, a cobamide coenzyme-dependent enzyme. II. Physical and chemical properties and interaction with cobamides and ethanolamine. *J. Biol. Chem.* **1968,** *243*, 1794-1803.

14. Mori, K.; Bando, R.; Hieda, N.; Toraya, T., Identification of a reactivating factor for adenosylcobalamin-dependent ethanolamine ammonia lyase. *J. Bacteriol.* **2004,** *186*, 6845-6854.

15. Hanson, A. D.; Henry, C. S.; Fiehn, O.; de Crecy-Lagard, V., Metabolite Damage and Metabolite Damage Control in Plants. *Annu. Rev. Plant Biol.* **2016,** *67*, 131-152.

16. Choudhary, S.; Quin, M. B.; Sanders, M. A.; Johnson, E. T.; Schmidt-Dannert, C., Engineered protein nano-compartments for targeted enzyme localization. *PLoS One* **2012,** *7*, e33342.

17. Nicolaou, S. A.; Gaida, S. M.; Papoutsakis, E. T., A comparative view of metabolite and substrate stress and tolerance in microbial bioprocessing: From biofuels and chemicals, to biocatalysis and bioremediation. *Metab. Eng.* **2010,** *12*, 307-331.

18. Sutter, M.; Greber, B.; Aussignargues, C.; Kerfeld, C. A., Assembly principles and structure of a 6.5-MDa bacterial microcompartment shell. *Science* **2017,** *356*, 1293-1297.

19. Takenoya, M.; Nikolakakis, K.; Sagermann, M., Crystallographic insights into the pore structures and mechanisms of the EutL and EutM shell proteins of the ethanolamine-utilizing microcompartment of *Escherichia coli*. *J. Bacteriol.* **2010,** *192*, 6056-6063.

20. Huseby, D. L.; Roth, J. R., Evidence that a metabolic microcompartment contains and recycles private cofactor pools. *J. Bacteriol.* **2013,** *195*, 2864-2879.

21. Jakobson, C. M.; Kim, E. Y.; Slininger, M. F.; Chien, A.; Tullman-Ercek, D., Localization of proteins to the 1,2-propanediol utilization microcompartment by non-native signal sequences is mediated by a common hydrophobic motif. *J. Biol. Chem.* **2015,** *290*, 24519-24533.

22. Datsenko, K. A.; Wanner, B. L., One-step inactivation of chromosomal genes in *Escherichia coli* K-12 using PCR products. *Proc. Natl. Acad. Sci. USA* **2000,** *97*, 6640-6645.

23. Schmieger, H.; Backhaus, H., The origin of DNA in transducing particles in P22-mutants with increased transduction-frequencies (HT-mutants). *Mol. Gen. Genet.* **1973,** *120*, 181-190.

24. VanDrisse, C. M.; Escalante-Semerena, J. C., New high-cloning-efficiency vectors for complementation studies and recombinant protein overproduction in *Escherichia coli* and *Salmonella enterica*. *Plasmid* **2016,** *86*, 1-6.

25. Momany, C.; Levdikov, V.; Blagova, L.; Lima, S.; Phillips, R. S., Three-dimensional structure of kynureninase from Pseudomonas fluorescens. *Biochemistry* **2004,** *43* (5), 1193-203.

26. Marsh, P., pTAC-85, an *E. coli* vector for expression of non-fusion proteins. *Nucleic Acids Res.* **1986,** *14*, 3603.

27. Berkowitz, D.; Hushon, J. M.; Whitfield, H. J., Jr.; Roth, J.; Ames, B. N., Procedure for identifying nonsense mutations. *J. Bacteriol.* **1968,** *96*, 215-220.

28. Balch, W. E.; Wolfe, R. S., New approach to the cultivation of methanogenic bacteria: 2-mercaptoethanesulfonic acid (HS-CoM)-dependent growth of *Methanobacterium ruminantium* in a pressurized atmosphere. *Appl. Environ. Microbiol.* **1976,** *32*, 781-791.

29. Costa, F. G.; Greenhalgh, E. D.; Brunold, T. C.; Escalante-Semerena, J. C., Mutational and functional analyses of substrate binding and catalysis of the *Listeria monocytogenes* EutT ATP:Co(I)rrinoid adenosyltransferase. *Biochemistry* **2020,** *59* (10), 1124-1136.

30. Roof, D. M.; Roth, J. R., Ethanolamine utilization in *Salmonella typhimurium*. *J. Bacteriol.* **1988,** *170*, 3855-3863.

31. Garsin, D. A., Ethanolamine utilization in bacterial pathogens: roles and regulation. *Nature Reviews Microbiology* **2010,** *8*, 290-295.

32. Costa, F. G.; Escalante-Semerena, J. C., A new class of EutT ATP:Co(I)rrinoid adenosyltransferases found in *Listeria monocytogenes* and other *Firmicutes* does not require a metal ion for activity. *Biochemistry* **2018,** *57* (34), 5076-5087.

33. Akita, K.; Hieda, N.; Baba, N.; Kawaguchi, S.; Sakamoto, H.; Nakanishi, Y.; Yamanishi, M.; Mori, K.; Toraya, T., Purification and some properties of wild-type and N-terminal-truncated ethanolamine ammonia-lyase of *Escherichia coli*. *J. Biochem.* **2010,** *147*, 83-93.

34. Faust, L. P.; Babior, B. M., Overexpression, purification, and some properties of the AdoCbl-dependent ethanolamine ammonia-lyase from *Salmonella typhimurium*. *Arch. Biochem. Biophys.* **1992,** *294*, 50-54.

35. Buan, N. R.; Suh, S. J.; Escalante-Semerena, J. C., The *eutT* gene of *Salmonella enterica* encodes an oxygen-labile, metal-containing ATP:corrinoid adenosyltransferase enzyme. *J. Bacteriol.* **2004,** *186*, 5708-5714.

36. Sheppard, D. E.; Penrod, J. T.; Bobik, T.; Kofoid, E.; Roth, J. R., Evidence that a B_{12}-adenosyl transferase is encoded within the ethanolamine operon of *Salmonella enterica*. *J. Bacteriol.* **2004,** *186*, 7635-7644.

37. Havemann, G. D.; Bobik, T. A., Protein content of polyhedral organelles involved in coenzyme B_{12}-dependent degradation of 1,2-propanediol in *Salmonella enterica* serovar Typhimurium LT2. *J. Bacteriol.* **2003,** *185*, 5086-5095.

38. Del Papa, M. F.; Perego, M., Ethanolamine activates a sensor histidine kinase regulating its utilization in *Enterococcus faecalis*. *J. Bacteriol.* **2008,** *190*, 7147-71456.

39. Shelton, A. N.; Seth, E. C.; Mok, K. C.; Han, A. W.; Jackson, S. N.; Haft, D. R.; Taga, M. E., Uneven distribution of cobamide biosynthesis and dependence in bacteria predicted by comparative genomics. *ISME J.* **2019,** *13*, 789-804.

40. Cadieux, N.; Barekzi, N.; Bradbeer, C., Observations on the calcium dependence and reversibility of cobalamin transport across the outer membrane of *Escherichia coli*. *J. Biol. Chem.* **2007,** *282*, 34921-34928.

41. Buan, N. R.; Suh, S. J.; Escalante-Semerena, J. C., The *eutT* gene of *Salmonella enterica* encodes an oxygen-labile, metal-containing ATP:corrinoid adenosyltransferase enzyme. *J. Bacteriol.* **2004,** *186*, 5708-5714.

42. Brinsmade, S. R.; Paldon, T.; Escalante-Semerena, J. C., Minimal functions and physiological conditions required for growth of *Salmonella enterica* on ethanolamine in the absence of the metabolosome. *J. Bacteriol.* **2005,** *187*, 8039-8046.

43. Moore, T. C.; Escalante-Semerena, J. C., The EutQ and EutP proteins are novel acetate kinases involved in ethanolamine catabolism: physiological implications for the function of the ethanolamine metabolosome in *Salmonella enterica*. *Mol. Microbiol.* **2016,** *99*, 497-511.

5.8 TABLES

Table 5.1. List of strains used in this study

Strain #	Strain	Reference
E. coli strains		
JE13737	BL21-CodonPlus (DE3)-RIL	
S. enterica sv. Typhimurium LT2 strains		
JE7092	*metE205 ara-9* Δ*eutT1141*	[41]
JE8093	*metE205 ara-9* Δ*eutA1155*	[2]
JE8094	*metE205 ara-9* Δ*eutBC1156*	[2]
JE10323	*metE205 ara-9* / pTAC-85 *bla*$^+$	[42]
JE24578	*metE205 ara-9* Δ*eutT1141* / pTAC-85 *bla*$^+$	[32]
JE24579	*metE205 ara-9* Δ*eutT1141* / pEUT160 *bla*$^+$ *SeeutT*$^+$	[32]
JE25513	*metE205 ara-9* Δ*eutA1155* / pTAC-85 *bla*$^+$	This work
JE25514	*metE205 ara-9* Δ*eutA1155* / pEUT261 *bla*$^+$ *SeeutA*$^+$	This work
JE25515	*metE205 ara-9* Δ*eutA1155* / pEUT262 *bla*$^+$ *LmeutA*$^+$	This work
JE25516	*metE205 ara-9* Δ*eutA1155* / pEUT263 *bla*$^+$ *CkeutA*$^+$	This work
JE25517	*metE205 ara-9* Δ*eutA1155* / pEUT264 *bla*$^+$ *EfeutA*$^+$	This work
JE25518	*metE205 ara-9* Δ*eutA1155* / pEUT265 *bla*$^+$ *KpeutA*$^+$	This work
JE22072	*metE205 ara-9* / pCV3$^+$ *cat*$^+$	This work
JE25599	*metE205 ara-9* Δ*eutA1155* / pCV3$^+$ *cat*$^+$	This work
JE25600	*metE205 ara-9* Δ*eutA1155* / pEUT181 *SeeutA*$^+$ *cat*$^+$	This work
JE25601	*metE205 ara-9* Δ*eutA1155* / pEUT182 *LmeutA*$^+$ *cat*$^+$	This work
JE25602	*metE205 ara-9* Δ*eutA1155* / pEUT133 Se*eutABC*$^+$ *cat*$^+$	This work
JE25603	*metE205 ara-9* Δ*eutA1155* / pEUT135 *LmeutABC*$^+$ *cat*$^+$	This work
JE25908	*metE205 ara-9* Δ*eutA1155* / pEUT134 *SeeutBC*$^+$ *cat*$^+$	This work
JE25909	*metE205 ara-9* Δ*eutA1155* / pEUT136 *LmeutBC*$^+$ *cat*$^+$	This work
JE22348	*metE205 ara-9* Δ*eutBC1156* / pCV3 *cat*$^+$	This work
JE22349	*metE205 ara-9* Δ*eutBC1156* / pEUT134 *SeeutBC*$^+$ *cat*$^+$	This work
JE22351	*metE205 ara-9* Δ*eutBC1156* / pEUT136 *LmeutBC*$^+$ *cat*$^+$	This work
JE25604	*metE205 ara-9* Δ*eutBC1156* / pEUT133 *SeeutABC*$^+$ *cat*$^+$	This work
JE22350	*metE205 ara-9* Δ*eutBC1156* / pEUT135 *LmeutABC*$^+$ *cat*$^+$	This work
JE24189	*metE205 ara-9* Δ*eutABC1157* / pCV3 *cat*$^+$	This work
JE25605	*metE205 ara-9* Δ*eutABC1157* / pEUT134 *SeeutBC*$^+$ *cat*$^+$	This work
JE25606	*metE205 ara-9* Δ*eutABC1157* / pEUT136 *LmeutBC*$^+$ *cat*$^+$	This work
JE24190	*metE205 ara-9* Δ*eutABC1157* / pEUT133 *SeeutABC*$^+$ *cat*$^+$	This work
JE24191	*metE205 ara-9 eutABC1157* / pEUT135 *LmeutABC*$^+$ *cat*$^+$	This work

Table 5.2. List of plasmids used in this study.

Plasmid	Vector	Gene(s) encoded	Reference
pEUT133	pCV3	*SeeutABC*$^{+}$, *cat*$^{+}$	This work
pEUT134	pCV3	*SeeutBC*$^{+}$, *cat*$^{+}$	This work
pEUT135	pCV3	*LmeutABC*$^{+}$, *cat*$^{+}$	This work
pEUT136	pCV3	*LmeutBC*$^{+}$, *cat*$^{+}$	This work
pEUT160	pTAC-85	*SeeutT*$^{+}$, *bla*$^{+}$	[32]
pEUT181	pCV3	*SeeutA*$^{+}$, *cat*$^{+}$	This work
pEUT182	pCV3	*LmeutA*$^{+}$, *cat*$^{+}$	This work
pEUT194	pSAPKO-WT	*SeeutA*$^{+}$, *kan*$^{+}$	This work
pEUT195	pSAPKO-WT	*SeeutBC*$^{+}$, *kan*$^{+}$	This work
pEUT261	pTAC-85	*SeeutA*$^{+}$, *bla*$^{+}$	This work
pEUT262	pTAC-85	*LmeutA*$^{+}$, *bla*$^{+}$	This work
pEUT263	pTAC-85	*CkeutA*$^{+}$, *bla*$^{+}$	This work
pEUT264	pTAC-85	*EfeutA*$^{+}$, *bla*$^{+}$	This work
pEUT265	pTAC-85	*KpeutA*$^{+}$, *bla*$^{+}$	This work

Table 5.3. EutA homologues from enteric bacterial species. EutA homologues from *Citrobacter koseri, Klebsiella pneumonia, Listeria monocytogenes,* and *Enterococcus faecalis* were selected to assay their ability to complement an *S. enterica eutA* strain. Their amino acid identity to *S. enterica* EutA, and the amino acid length of each homologue are detailed below.

Organism	Amino acid identity to *S. enterica*	Length (amino acids)
S. enterica		468
C. koseri	90.15%	468
K. pneumoniae	89.23%	468
E. faecalis	36.50%	474
L. monocytogenes	35.52%	483

5.9 FIGURES

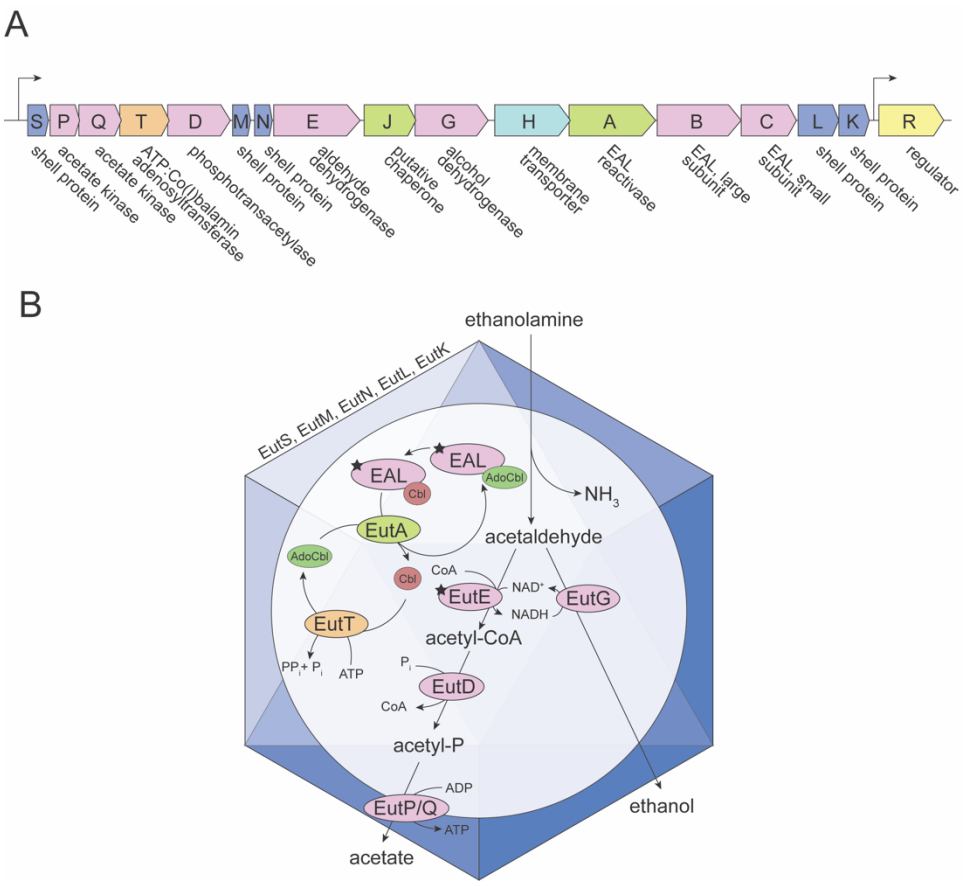

Figure 5.1. (A) Representation of the ethanolamine utilization (*eut*) operon. Functions are color coded by purpose in the cell. Genes in purple indicate shell proteins, and genes in pink indicate enzymes involved in ethanolamine catabolism. ATP-dependent chaperones/reactivases are in green. The regulator is in yellow. The membrane transporter is in blue, and the ATP:Co(I)rrinoid adenosyltransferase is in orange.
(B) Model of the ethanolamine utilization (*eut*) metabolosome. The metabolosome shell is represented in this figure by the icosahedron and is made us of five different shell proteins; EutS, EutM, EutN, EutL, and EutK. Ethanolamine is converted to acetaldehyde and ammonia by the adenosylcobalamin (AdoCbl, in green)-dependent ethanolamine ammonia-lyase (EAL), encoded by *eutB* and *eutC*. In the event EAL is bound to cobalamin (Cbl, in red) and rendered inactive, EutA facilitates the replacement of the incomplete coenzyme with AdoCbl. EutT is an ATP:Co(I)rrinoid adenosyltransferase that generates AdoCbl from Cbl. From EAL, acetaldehyde is then converted to acetyl-CoA by the acetaldehyde dehydrogenase EutE, or to ethanol by the alcohol dehydrogenase EutG to regenerate NAD^+.[20] Acetyl-CoA is then phosphorylated by EutD. EutP and EutQ have acetate kinase activity *in vitro,* and EutQ is required for acetate production in anaerobic conditions.[43] The starred functions encode localization tags that have been demonstrated to localize to the metabolosome.[16]

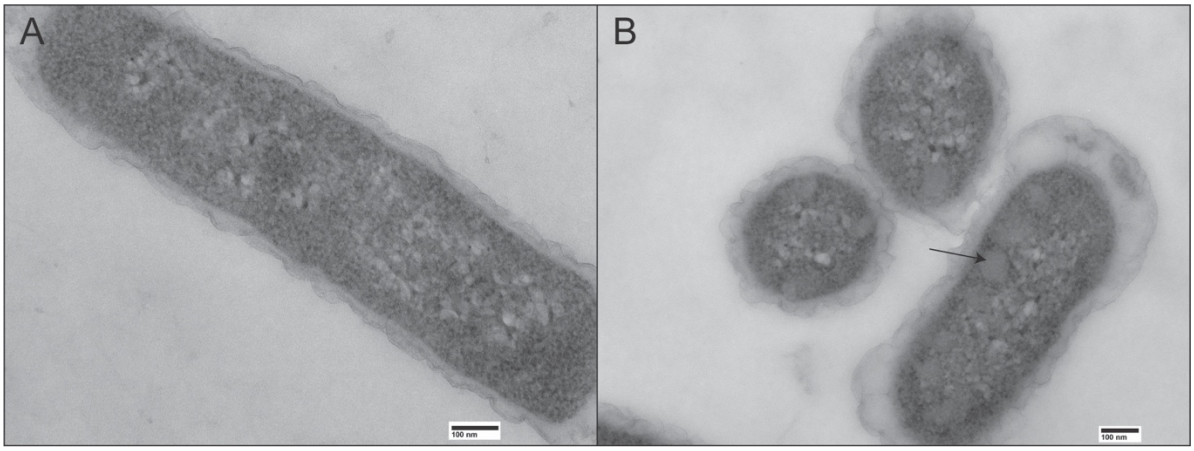

Figure 5.2. *S. enterica* grown on minimal medium with ribose as a carbon source (A), and ribose as a carbon source with ethanolamine and CNCbl as inducers of the *eut* operon (B) were grown to an OD_{600} = 1.0-.1.1 and fixed in 4% paraformaldehyde and 0.2% glutaraldehyde. Samples were enrobed in 4% noble agar and embedded in LR white resin. Thin sections were post-stained with uranyl acetate. Photos were taken on a JEOL JEM1011 transmission electron microscope. The black bar denotes 100 nm length on the respective image. The *eut* metabolosomes were observed when ethanolamine and CNCbl were present as inducers (B, black arrow).

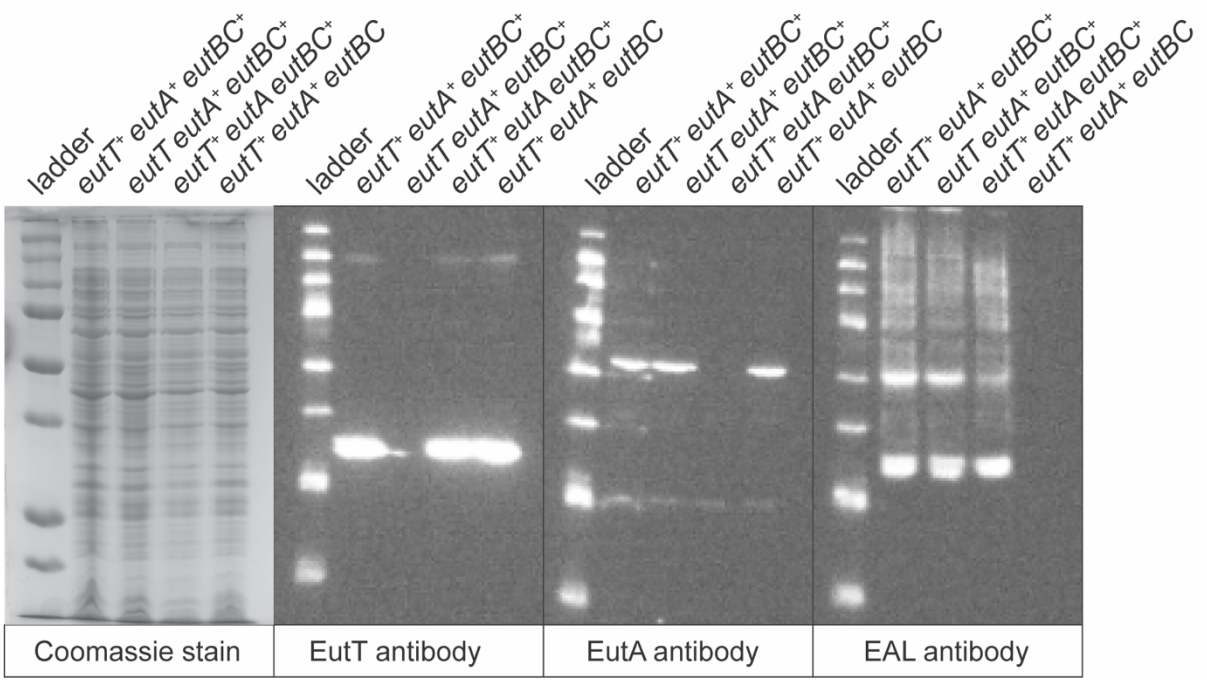

Figure 5.3. Precleared antibodies are specific for EutT, EutA, and EAL. Polyclonal antibodies were pre-cleared against *S. enterica eutT, eutA,* or *eutBC* strains and tested against these same strains grown on NCE minimal medium with ribose, ethanolamine and CNCbl added. 100 ug of each cell lysates was loaded onto 12% SDS-PAGE gels in quadruplicate. The ladder used for the Coomassie stained gel was Precision Plus Protein (BioRad), while the gels that were used for Western blots used the SuperSignal Molecular Weight ladder (ThermoFisher). Precleared antibodies were used at a 1:2,000 concentration, and secondary antibodies were used at a 1:10,000 dilution (anti-rabbit IgG, peroxidase antibody produced in goat, Millipore Sigma). The antibodies were determined to be sufficiently specific to their respective target for immunogold labeling.

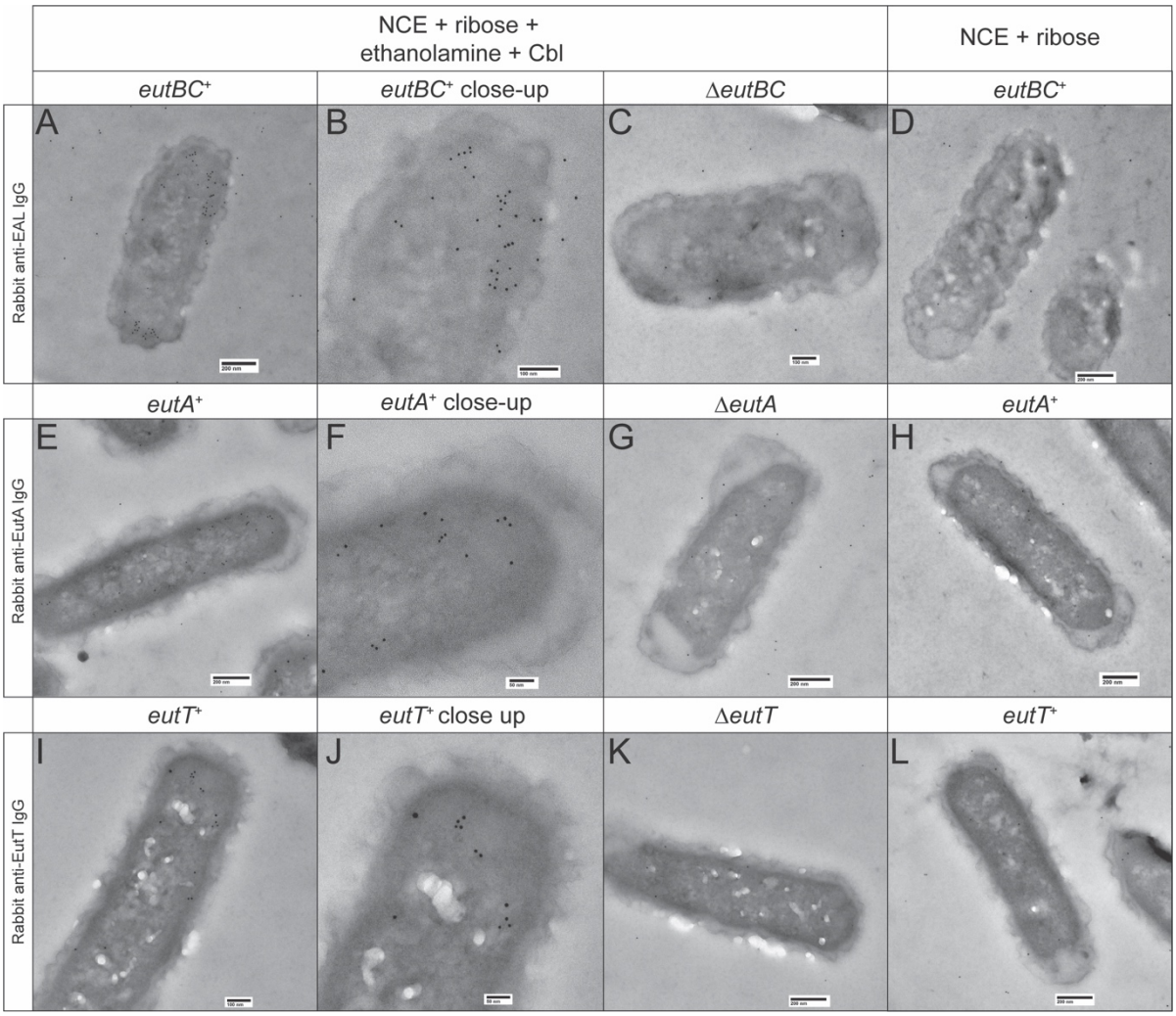

Figure 5.4. Localization of EutT, EutA and EAL in *S. enterica.* Thin sections of fixed and embedded *S. enterica* cells grown in minimal medium supplemented with ribose, ethanolamine and CNCbl (panels A, B, D, E, G, and H), or minimal medium supplemented with ribose (panels C, F, and I). Sections were incubated with rabbit antibodies that bind to EAL (panels A-D), EutA (panels E-H), or EutT (panel I-L). This was followed by incubation with goat anti-rabbit IgG-5nm gold antibody. EAL and EutA were detected within metabolosome structures in the presence of ethanolamine + CNCbl (panels A and E, respectively, with close-ups in panels B and F). The labeling of these sections was compared to labeling of cells grown with the gene deleted (panels C and G, respectively) or when grown in the absence of ethanolamine and CNCbl (panels D and H, respectively). EutT was detected localized to the metabolosomes when the wild-type strain is grown on ribose minimal medium with ethanolamine and CNCbl (panel I, close-up in panel J). However, it was not clear they were localized to the inside of the metabolosome (panel J). Labeling was reduced when *eutT* is deleted (panel K) or when the inducers ethanolamine and CNCbl are absent (panel L).

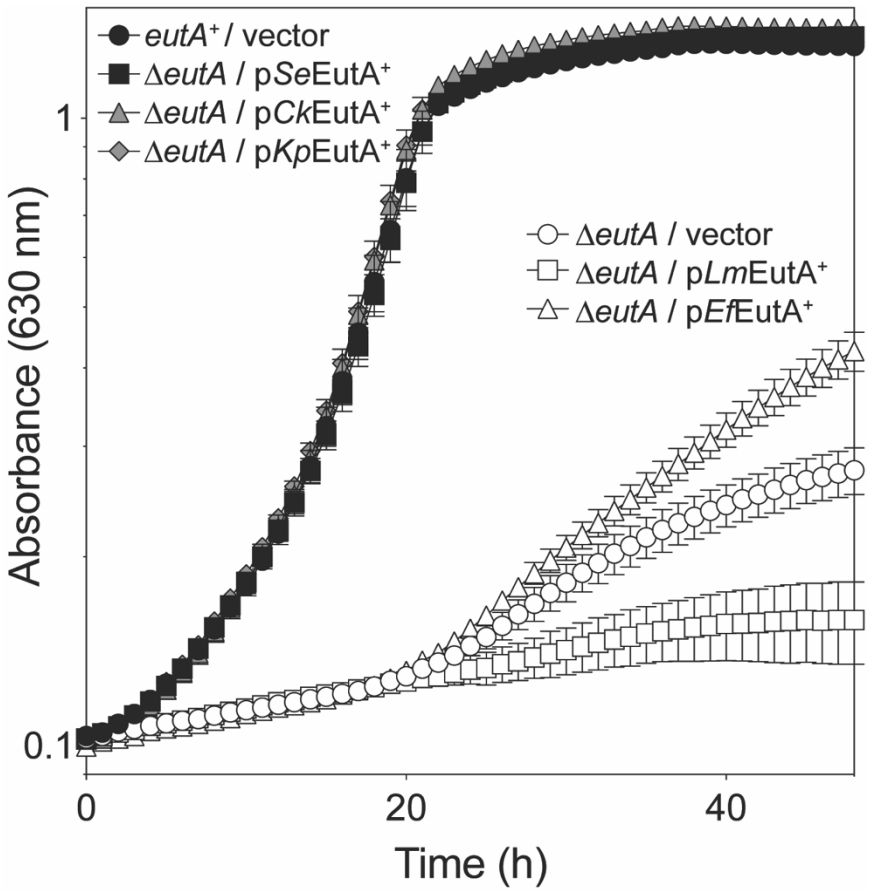

Figure 5.5. EutA homologues from organisms belonging to the *Firmicutes* do not complement a *S. enterica eutA* strain. Strains were grown in NCE minimal medium containing ethanolamine (90 mM), and CNCbl (200 nM) at 37 °C with shaking. Expression of the genes *in trans* was induced with 100 μM IPTG. In *S. enterica*, a *eutA* deletion produces a growth defect on ethanolamine (white circles) that can be complemented by introducing *eutA* from *S. enterica* (*Se_eutA*), *Citrobacter koseri* (*Ck_eutA*), or *Klebsiella pneumoniae* (*Kp_eutA*). The strain expressing *eutA* from *Enterococcus faecalis* (*Ef_eutA*) or *Listeria monocytogenes* (Lm_*eutA*) showed modest growth improvement and no growth improvement over an empty vector control (vector), respectively. Growth was assessed by optical density at 630 nm (OD_{630}). Results are provided as the mean from three biological replicates, where error bars denote standard error of the means.

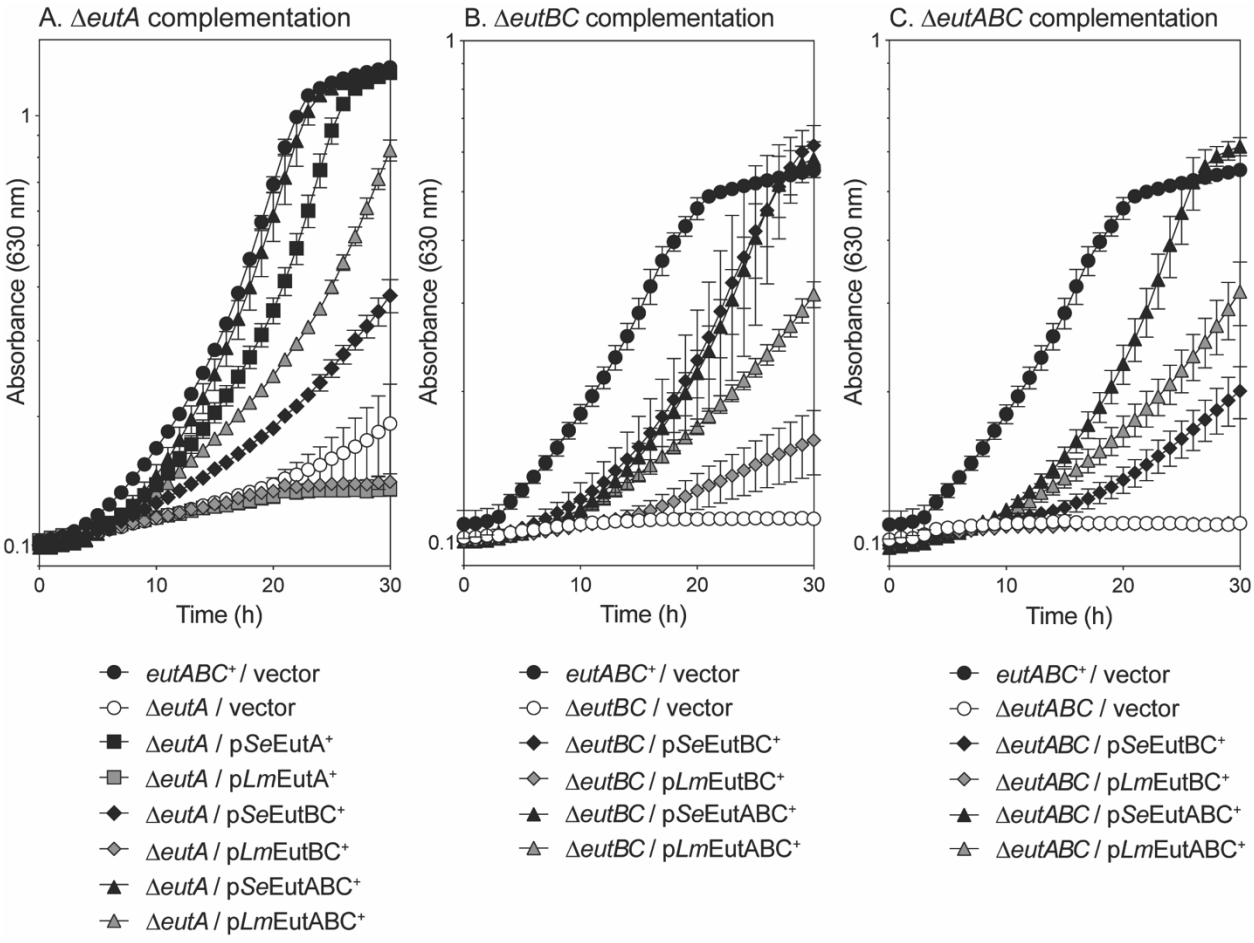

Figure 5.6. *L. monocytogenes eutA* and *eutBC* are both required for complementation of an *S. enterica* Δ*eutA* or Δ*eutBC* mutant strain. *S. enterica* Δ*eutA* (A), Δ*eutBC* (C), and Δ*eutABC* (D) strains expressing combinations of *S. enterica* and *L. monocytogenes eutA* and *eutBC* from a modified pBAD24 expression vector (pCV3) were grown shaking at 37 °C in minimal medium containing 90 mM ethanolamine, 200 nM CNCbl, and 100 μM L-arabinose. Of the *L. monocytogenes* functions expressed *in trans,* only expression of *L. monocytogenes eutABC* could rescue growth on ethanolamine. Growth was assessed by optical density at 630 nm (OD_{630}). Results are provided as the mean from three biological replicates, where error bars denote standard error of the means.

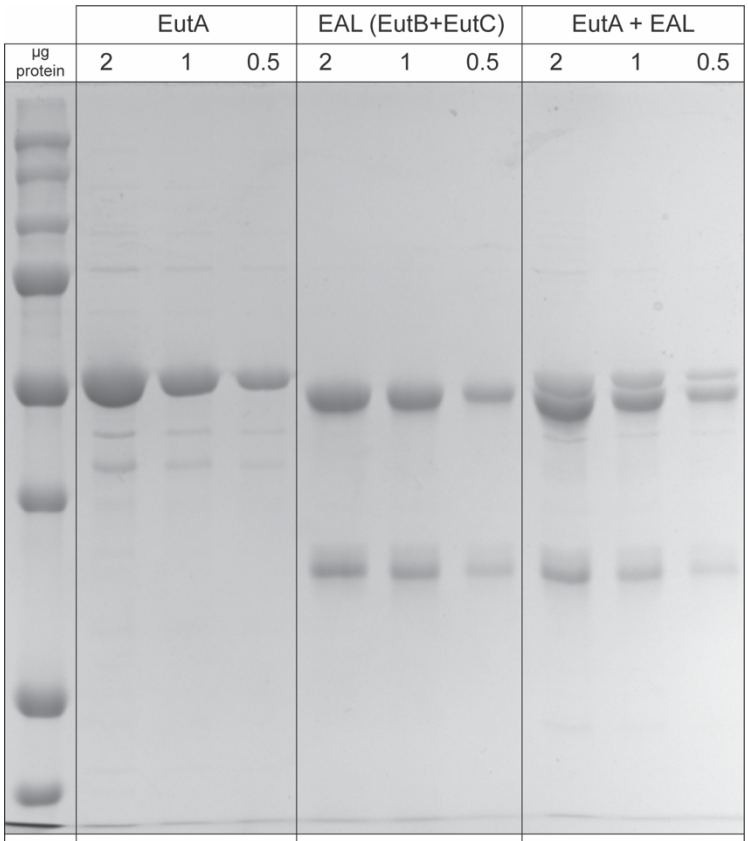

	EutA			EAL (EutB+EutC)			EutA + EAL		
µg protein	2	1	0.5	2	1	0.5	2	1	0.5
% EutA	86	88	88	-	-	-	27	21	19
% EutB	-	-	-	61	65	65	43	50	57
% EutC	-	-	-	38	35	35	27	28	23

Figure 5.7. Homogeneity EutA, EAL, and EutA/EAL purifications. EutA, EAL, or EutA + EAL were purified using a native purification procedure. Each protein preparation was separated by size on a 12% SDS-PAGE gel in 2 µg, 1 µg, and 0.5 µg amounts. The gel was then stained with Coomassie dye and destained with 10% acetic acid. The gel was imaged and the density of the bands was quantified with TotalLab 1000 to determine the purity of the preparation. The relative percentage of EutA (49.5 kDa predicted size), and EAL subunits EutB (49.4 kDa predicted size), and EutC (32.1 kDa predicted size) in each lane is detailed below the gel. EutA has an average purity of 87%, EAL has an average purity of 99%, and EutA + EAL has an average purity of 98%.

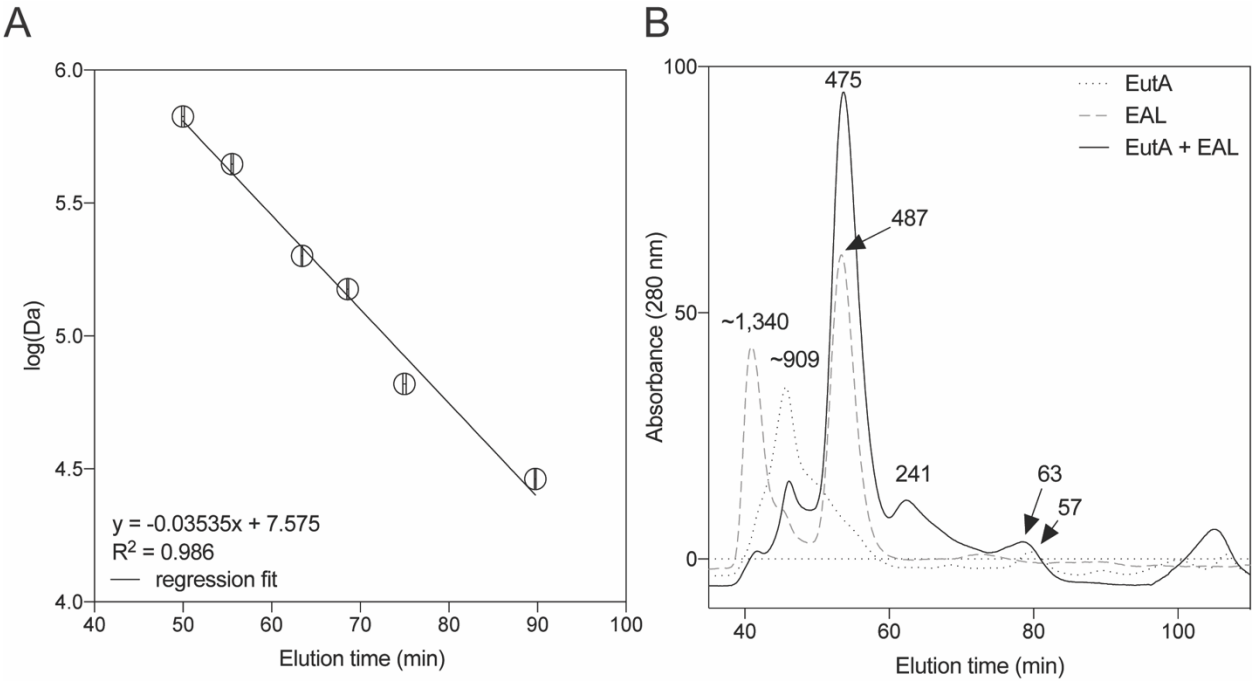

Figure 5.8. Size exclusion chromatography of EutA and EAL. Samples were applied to a HiLoad 16/600 Superdex 200 pg packed column at a rate of 1 mg/mL. (A) The protein standards thyroglobulin (669 kDa), apoferritin (443 kDa), β-amylase (200 kDa), alcohol dehydrogenase (150 kDa), bovine serum albumin (66 kDa), and carbionic anhydrase (29 kDa) were run twice at the beginning and end of experiment for a total of four times. The horizontal error bars represent the 95% CI of the elution time for each protein standard. (B) Elutions of purified EutA (1 mg/mL), EAL (1 mg/mL), and EutA + EAL (1 mg/mL each) were monitored and compared to the standard curve to predict oligomeric size. EutA alone had a predominant peak at ~900 kDa, and an additional minor peak at 57 kDa. EAL alone had a major peak at 487 kDa (95% confidence interval 486.1 – 488.5 kDa), and an additional peak at ~1,340 kDa. When EutA and EAL were combined, the higher molecular mass peaks were reduced in size, and the major peak shifted to 475 kDa (95% confidence interval 474.6 – 476.1 kDa). There were two new peaks, one that formed at 241 kDa (95% confidence interval 225.6 – 257.5 kDa) and another at 63 kDa (95% confidence interval 62.7 – 65.4 kDa).

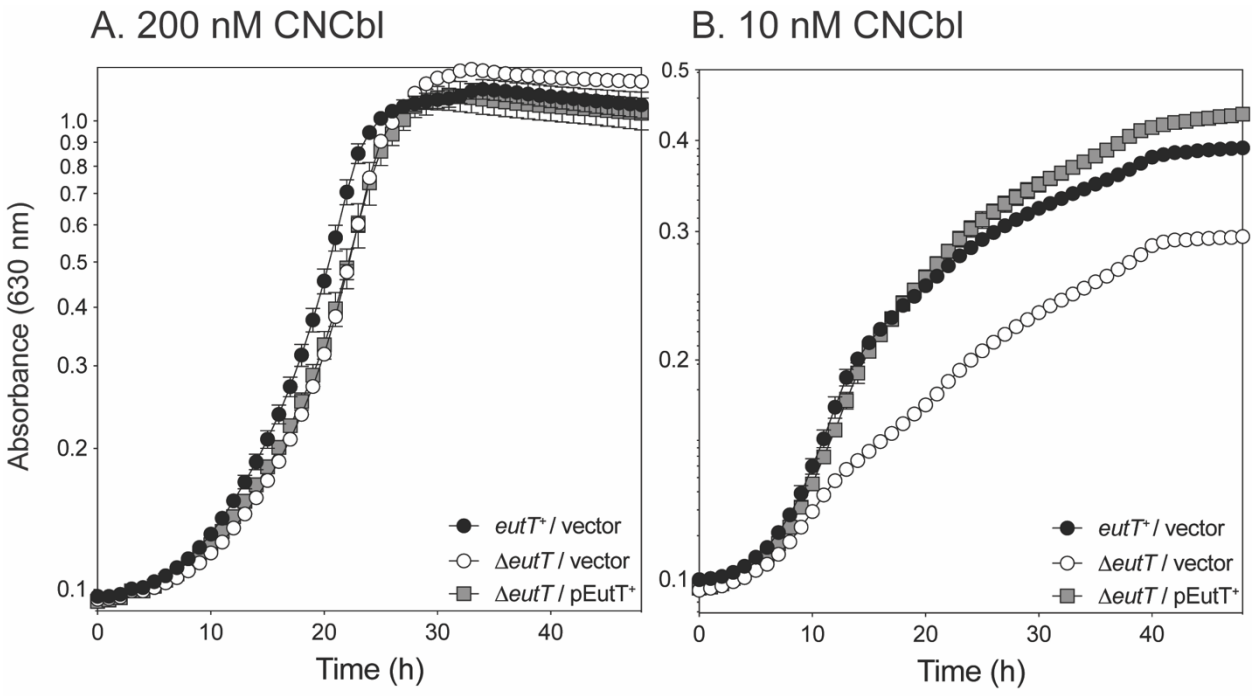

C. Calculated doubling times

[CNCbl]	*eutT*⁺ / vector (h)	Δ*eutT* / vector (h)	Δ*eutT* / pEutT⁺ (h)
200 nM (16 - 23 h)	3.54 (3.33 - 3.78)	3.81 (3.55 - 4.10)	4.11 (3.64 - 4.62)
10 nM (10 - 15 h)	8.89 (8.04 - 9.94)	18.73 (16.92 - 20.96)	8.19 (7.62 - 8.84)
10 nM (15 - 24 h)	21.13 (20.23 - 22.11)	21.43 (20.83 - 22.07)	16.38 (15.37 - 17.53)

Figure 5.9 Confirmation that EutT is conditionally required under limited CNCbl in *S. enterica*. *S. enterica* Δ*eutT* strains were grown in ethanolamine (90 mM) minimal medium supplemented with (A) 200 nM CNCbl or (B) 10 nM CNCbl. The growth rate and overall yield of the Δ*eutT* strain was lower in the 10 nM CNCbl condition, however growth is restored through expression of *eutT in trans*. Growth was assessed by optical density at 630 nm (OD_{630}). Results are provided as the mean from three biological replicates, where error bars denote standard error of the means. (C) Table of doubling times (and 95 % confidence interval) for each strain in each of the conditions. Column 1 denotes time range used for the doubling time calculation. Due to the non-sigmoidal nature of growth curves obtained for the 10 nM CNCbl condition, an initial (10 – 15 h) and secondary (15 - 24 h) doubling time was calculated.

CHAPTER 6

CONCLUSIONS AND FUTURE DIRECTIONS

6.1 SUMMARY AND CONCLUSIONS

Although cobalamin biosynthesis and utilization has been studied in *S. enterica* for decades, key questions remain.[1] Significant progress had been made in understanding the Eut metabolosome, however a detailed understanding of the substrate-binding mechanism of the ATP:Co(II)balamin adenosyltransferase (ACAT) EutT, and the mechanism of adenosylcobalamin delivery to ethanolamine ammonia-lyase (EAL) was not well understood.[2-6] In this work, we sought to advance our understanding of the EutT family of ACATs, and investigate the mechanism of AdoCbl delivery to EAL.

A bioinformatics search for EutT homologues revealed a subset of homologues belonging to *Firmicutes* that lacked the residues critical for binding Fe(II) in *Salmonella enterica* EutT. A EutT homologue from *Listeria monocytogenes* (*Lm*EutT) was selected as a representative of this group of homologues for further analysis. *Lm*EutT demonstrated ACAT activity *in vivo* and *in vitro*, and its activity *in vitro* was not dependent on a divalent cation metal.[7] In addition, further analysis of *Lm*EutT revealed differences in oligomerization state, substrate affinity, and kinetics, compared to *Salmonella enterica* EutT (*Se*EutT).[7] Despite these differences, both homologues shared key characteristics when analyzed spectrophotometrically.[8] Both *Se*EutT and *Lm*EutT can bind cobalamin (Cbl) and cobinamide (Cbi) in the presence of ATP, however both EutT homologues can only convert Cbl to the four coordinate (4C) species required for the reaction to

proceed.[8] In conclusion, the EutT family of ACATs can be split into two classes based on their requirement for a divalent metal cation.

Over the years, efforts to determine the structure of EutT have not been successful, which has hindered our understanding of this family of ACATs. The three ACAT families were previously thought to be evolutionarily divergent because homology was not detected between these ACATs in *Salmonella enterica*. However, in studies with *Lm*EutT, a small amount of homology was detected between LmEutT and PduO from *Lactobacillus reuteri* (*Lr*PduO). Expansion of this alignment with other PduO and EutT homologs revealed similarities between all EutT and PduO sequences. Notably, EutT homologs had an extended (60-70 aa) N-terminus compared to PduO homologs. Many conserved residues in the alignment of EutT and PduO homologues corresponded to the nucleotide substrate binding site. Mutational analysis confirmed that the corresponding residues are also involved in nucleotide substrate binding in *Lm*EutT.[9] Two additional conserved residues in the alignment corresponded to an intersubunit salt bridge in *Lr*PduO. Mutational analysis of these residues in *Lm*EutT determined that the inter-subunit salt bridge stabilized the tetrameric oligomerization of *Lm*EutT.[9] Swapping the position of these salt bridge residues preserved the stability of *Lm*EutT, however like in *Lr*PduO, the variant with the double mutation was not active *in vivo* or *in vitro*. This suggests that like in *Lr*PduO, the argininyl residue in the intersubunit salt bridge plays a key role in the adenosylation reaction.[10] These data demonstrated that EutT and PduO enzymes share a common substrate binding site, and inter-subunit salt bridge, supportive of a common evolutionary origin for PduO and EutT ACATs.

Like CobA, PduO utilizes a hydrophobic residue (in the case of PduO, a phenylalanyl residue) to displace the alpha ligand of the corrinoid, resulting in 4C-Co(II)Cbl.[11] This residue was not conserved in any of the EutT homologues, and systematic mutation of the phenylalanyl,

tryptophanyl and tyrosyl residues of *Lm*EutT did not reveal a similar mechanism for formation of 4C-Co(II)Cbl. This suggested that EutT enzymes utilize a unique method for displacement of the lower ligand of the cobalamin substrate.

With an improved understanding of the mechanism of EutT, we wanted to better understand its role in *S. enterica* physiology. It is remarkable that *S. enterica* encodes three separate ACATs, when one would be sufficient for the AdoCbl requirements in the cell. PduO is localized to the Pdu metabolosome, possibly for the purpose of regenerating AdoCbl in the Pdu metabolosome.[12] Similar studies had not been carried out for the Eut metabolosome, due to difficulties in obtaining purified, intact Eut metabolosomes. To determine if EutT, along with EutA, are localized in the Eut metabolosome with EAL, immunogold-labeling studies of *Salmonella enterica* cells expressing Eut metabolosomes showed localization of EutT, EutA and EAL to the Eut metabolosomes. However, there were limitations in our interpretation of these data. While we observed localization patterns that corresponded to metabolosome localization, we were not able to determine with certainty if these enzymes were localized to the inside or to the outside of the metabolosome.

With these limitations, we sought to identify direct protein-protein interactions to support the observation that these functions are localized to the metabolosome. *In vivo* data using a heterologous expression system, and *in vitro* data demonstrated changes in oligomerization, showed that EutA and EAL interacted directly, supporting the observation that both EutA and EAL were localized to the metabolosome. EutT was necessary for optimal growth on ethanolamine when cobalamin was a limitation of growth, however interactions were not detected between EutT and EutA + EAL *in vitro*, and *Lm*EutT was not required for the function of *Lm*EAL in *S. enterica.* Thus, the question of how EutT is recruited to the metabolosome remains.

In summary, this work advanced our understanding of the EutT family of ACATs, and provided a foundation from which to explore how AdoCbl is generated and delivered to EAL in the Eut metabolosome.

6.2 FUTURE DIRECTIONS

Although this work describes advancements in our understanding of the diversity and mechanism of EutT ACATs, there are some questions remaining regarding the structure and mechanism of EutT. Primarily, the mechanism of displacement of the alpha ligand is still unknown in EutT. In *Se*EutT, it is clear the metal is somehow involved in this step. In *Lm*EutT, a phenylalanine residue (F72) that aligns to the same position in the amino acid sequence as the metal-binding motif (CCXXC) of *Se*EutT, affected access to the substrate-binding site. The threaded model of *Se*EutT and *Lm*EutT to the *Lr*PduO structure placed the CCXXC motif and F72 residue, respectively, at the entrance of the substrate binding site, supporting those observations.

The key to answering this question may lie in the N-terminus of EutT. The N-terminus of EutT homologues did not align with PduO homologues, and was not included in the threaded models of *Se*EutT and *Lm*EutT. Additionally, no residues critical for activity were identified in this region during these studies. It was suggested in the spectroscopic analysis of *Se*EutT that the alpha ligand of Co(II)Cbl may be sequestered to a binding pocket, and this possibility should be pursued further by screening for loss of function mutations in the N-terminal portion of EutT.[13]

As opposed to the Pdu metabolosome, which has been studied extensively, the Eut metabolosome is not understood in as much detail. The primary challenge has been in obtaining purified, intact, metabolosomes for further investigation. Despite this, significant advancements were made using genetic and biochemical approaches. In this work, we sought to understand where EutA and EutT were located in relation to the metabolosome, and how AdoCbl was delivered to

the Eut metabolosome. The immunogold labeling experiments suggested EutA was was localized to the metabolosome, and subsequent genetic and *in vitro* analyses demonstrated direct binding of EutA to EAL, supporting the immunogold labeling observations. Knowing that the solubility and stability of EutA and EAL are drastically improved when co-purified, spectroscopic approaches such as circular dichroism, should be used to better understand the mechanism of EutA reactivation of EAL. Additionally, structural determination of the complex should be undertaken, as structural information of the complex would further our understanding of this mechanism.

The immunogold-labeling experiments suggested EutT also localized to the metabolosome, however direct protein-protein interactions were not elucidated between EutT and EutA or EAL. Again, the N-terminus of EutT may serve a currently unknown function in this capacity, such as localizing EutT to the metabolosome. This should be investigated using co-immunoprecipitation methods to determine the interacting partners of EutT.

6.3 REFERENCES

1. Banerjee, R., *Chemistry and Biochemistry of B_{12}*. John Wiley & Sons: 1999; p 3-6.

2. Thiennimitr, P.; Winter, S. E.; Winter, M. G.; Xavier, M. N.; Tolstikov, V.; Huseby, D. L.; Sterzenbach, T.; Tsolis, R. M.; Roth, J. R.; Baumler, A. J., Intestinal inflammation allows *Salmonella* to use ethanolamine to compete with the microbiota. *Proc. Natl. Acad. Sci. U.S.A.* **2011,** *108*, 17480-17485.

3. Akita, K.; Hieda, N.; Baba, N.; Kawaguchi, S.; Sakamoto, H.; Nakanishi, Y.; Yamanishi, M.; Mori, K.; Toraya, T., Purification and some properties of wild-type and N-terminal-truncated ethanolamine ammonia-lyase of *Escherichia coli*. *J. Biochem.* **2010,** *147*, 83-93.

4. Huseby, D. L.; Roth, J. R., Evidence that a metabolic microcompartment contains and recycles private cofactor pools. *J. Bacteriol.* **2013,** *195*, 2864-2879.

5. Moore, T. C.; Mera, P. E.; Escalante-Semerena, J. C., the EutT enzyme of *Salmonella enterica* is a unique ATP:Cob(I)alamin adenosyltransferase metalloprotein that requires ferrous ions for maximal activity. *J. Bacteriol.* **2014,** *196*, 903-910.

6. Pallares, I. G.; Moore, T. C.; Escalante-Semerena, J. C.; Brunold, T. C., Spectroscopic studies of the EutT adenosyltransferase from *Salmonella enterica*: Evidence of a tetrahedrally coordinated divalent transition metal cofactor with cysteine ligation. *Biochemistry* **2017,** *56*, 364-375.

7. Costa, F. G.; Escalante-Semerena, J. C., A new class of EutT ATP:Co(I)rrinoid adenosyltransferases found in *Listeria monocytogenes* and other *Firmicutes* does not require a metal ion for activity. *Biochemistry* **2018,** *57* (34), 5076-5087.

8. Stracey, N. G.; Costa, F. G.; Escalante-Semerena, J. C.; Brunold, T. C., Spectroscopic study of the EutT adenosyltransferase from *Listeria monocytogenes*: Evidence for the formation of a four-coordinate cob(II)alamin intermediate. *Biochemistry* **2018,** *57* (34), 5088-5095.

9. Costa, F. G.; Greenhalgh, E. D.; Brunold, T. C.; Escalante-Semerena, J. C., Mutational and functional analyses of substrate binding and catalysis of the *Listeria monocytogenes* EutT ATP:Co(I)rrinoid adenosyltransferase. *Biochemistry* **2020,** *59*, 1124-1136.

10. Mera, P. E.; Maurice, M. S.; Rayment, I.; Escalante-Semerena, J. C., Structural and functional analyses of the human-type corrinoid adenosyltransferase (PduO) from *Lactobacillus reuteri*. *Biochemistry* **2007,** *46*, 13829-13836.

11. Mera, P. E.; St Maurice, M.; Rayment, I.; Escalante-Semerena, J. C., Residue Phe112 of the human-type corrinoid adenosyltransferase (PduO) enzyme of *Lactobacillus reuteri* is critical

to the formation of the four-coordinate Co(II) corrinoid substrate and to the activity of the enzyme. *Biochemistry* **2009,** *48*, 3138-3145.

12. Havemann, G. D.; Bobik, T. A., Protein content of polyhedral organelles involved in coenzyme B_{12}-dependent degradation of 1,2-propanediol in *Salmonella enterica* serovar Typhimurium LT2. *J. Bacteriol.* **2003,** *185*, 5086-5095.

13. Park, K.; Mera, P. E.; Moore, T. C.; Escalante-Semerena, J. C.; Brunold, T. C., Unprecedented mechanism employed by the *Salmonella enterica* EutT ATP:Co(I) rrinoid adenosyltransferase precludes adenosylation of incomplete Co(II)rrinoids. *Angew. Chem.* **2015,** *54*, 7158-7161.

APPENDIX A

SPECTROSCOPIC STUDY OF THE EUTT ADENOSYLTRANSFERASE FROM *LISTERIA MONOCYTOGENES*: EVIDENCE FOR THE FORMATION OF A FOUR-COORDINATE COB(II)ALAMIN INTERMEDIATE[4]

[4] Stracey, N. G., Costa, F. G., Escalante-Semerena, J. C., & Brunold, T. C. (2018). Spectroscopic Study of the EutT Adenosyltransferase from Listeria monocytogenes: Evidence for the Formation of a Four-Coordinate Cob (II) alamin Intermediate. *Biochemistry*, *57*(34), 5088-5095. Copyright (2018) American Chemical Society. Reprinted with permission from ACS.

A.1 ABSTRACT

The EutT enzyme from *Listeria monocytogenes* (*Lm*EutT) is a member of the family of ATP:cobalt(I) corrinoid adenosyltransferase (ACAT) enzymes that catalyze the biosynthesis of adenosylcobalamin (AdoCbl) from exogenous Co(II)rrinoids and ATP. Apart from EutT-type ACATs, two evolutionary unrelated types of ACATs have been identified, termed PduO and CobA. Although the three types of ACATs are nonhomologous, they all generate a four-coordinate cob(II)alamin (4C Co(II)Cbl) species to facilitate the formation of a supernucleophilic Co(I)Cbl intermediate capable of attacking the 5′-carbon of cosubstrate ATP. Previous spectroscopic studies of the EutT ACAT from *Salmonella enterica* (*Se*EutT) revealed that this enzyme requires a divalent metal cofactor for the conversion of 5C Co(II)Cbl to a 4C species. Interestingly, *Lm*EutT does not require a divalent metal cofactor for catalytic activity, which exemplifies an interesting phylogenetic divergence among the EutT enzymes. To explore if this disparity in the metal cofactor requirement among EutT enzymes correlates with differences in substrate specificity or the mechanism of Co(II)Cbl reduction, we employed various spectroscopic techniques to probe the interaction of Co(II)Cbl and cob(II)inamide ($Co(II)Cbi^+$) with *Lm*EutT in the absence and presence of cosubstrate ATP. Our data indicate that *Lm*EutT displays a similar substrate specificity as *Se*EutT and can bind both Co(II)Cbl and $Co(II)Cbi^+$ when complexed with MgATP, though it exclusively converts Co(II)Cbl to a 4C species. Notably, *Lm*EutT is the most effective ACAT studied to date in generating the catalytically relevant 4C Co(II)Cbl species, achieving a >98% 5C → 4C conversion yield on the addition of just over one mol equiv of cosubstrate MgATP.

A.2 INTRODUCTION

Ethanolamine and 1,2-propanediol can be utilized by bacteria as a source of carbon, energy and nitrogen for metabolic function.[1-4] Pathogenic bacteria such as *Listeri*a, *Escherichia*, *Clostridium*, and *Salmonella* obtain ethanolamine from phosphatidylethanolamine, a phospholipid found in cell membranes[5, 6], where it is broken down by phosphodiesterases into ethanolamine and glycerol.[1, 7, 8] The primary step in ethanolamine catabolism is catalyzed by ethanolamine ammonia-lyase (EAL) enzymes that convert ethanolamine into ammonia and acetaldehyde.[9] These molecules can then serve as a source of reduced nitrogen and a precursor to metabolically active acetyl-CoA, respectively.[10] Ethanolamine degradation by EAL involves a radical-based 1-2 elimination reaction mediated by adenosylcobalamin (AdoCbl), a corrinoid cofactor (Figure A.1).[11-13] AdoCbl is supplied to apo-EAL by an ATP:Co(I)rrinoid adenosyltransferase (ACAT) enzyme encoded by the *eutT* gene.[1]

ACATs catalyze the biosynthesis of AdoCbl from exogenous Co(II)rrinoids and ATP.[14] Apart from EutT-type ACATs, two evolutionary unrelated types of ACATs have been identified, referred to as PduO and CobA. PduO-type ACATs are reported to play a similar role as EutT does in bacterial growth, supplying AdoCbl to the diol dehydratase associated with 1,2-propanediol metabolism.[15-17] CobA-type ACATs serve a housekeeping role and are responsible for adenosylating corrinoid precursors in *de novo* cobalamin biosynthesis and maintaining adequate intracellular levels of AdoCbl.[18, 19] Unlike the PduO- and CobA-type ACATs, EutT from *Salmonella enterica* (*Se*EutT) requires a divalent metal ion [Fe(II) or Zn(II)] for activity that is postulated to reside in a tetrahedral coordination environment provided by four Cys residues, which are part of a conserved $HX_{11}CCX_2C(83)$ motif.[20-22] Although the three types of ACATs are non-homologous, they all generate a four-coordinate (4C) cob(II)alamin (Co(II)Cbl) species to

facilitate the formation of a supernucleophilic Co(I)Cbl intermediate. This species is sufficiently potent to attack the 5'-carbon of ATP to generate the Co–C(ATP) bond of AdoCbl.[23-27] The formation of a unique 4C Co(II)Cbl species in the presence of co-substrate ATP was initially proposed on the basis of electron paramagnetic (EPR) and magnetic circular dichroism (MCD) spectroscopic studies,[26, 28-30] and has since been confirmed by X-ray crystallographic studies of PduO from *Lactobacillus reuteri* (*Lr*PduO) and CobA from *Salmonella enterica* (*Se*CobA, Figure A.2).[16, 31] In both structures, the DMB base is solvent exposed and the lower axial position is blocked off by hydrophobic residues in the active site. Thus, even though the reduction potentials of free Co(II)rrinoids are substantially lower than those of biologically available reductants such as dihydroflavins (FMN) [e.g., E^{o}(NHE) for Co(II)Cbl = –610 mV vs –228 mV for FMN at pH 7.5],[20, 32, 33] the generation of 4C Co(II)rrinoid species in the ACAT active sites raises the Co(II)/Co(I)corrinoid reduction potential to within the physiologically accessible range.[28, 29, 34]

Although thus far no member of the EutT family has been characterized by X-ray crystallography, MCD and EPR studies of *Se*EutT revealed that this enzyme also generates a 4C Co(II) species to facilitate substrate reduction.[27, 35] These studies have also served to highlight key differences in the selectivity and mode of 4C Co(II)rrinoid formation between the different ACAT families. *Lr*PduO and *Se*CobA can convert both Co(II)Cbl and cob(II)inamide (Co(II)Cbi^{+}, which lacks the nucleotide loop with the terminal DMB base and therefore binds a water molecule in the "lower" axial position) to 4C species that are readily reduced to the Co(I) state. In contrast, EutT is only able to convert Co(II)Cbl to a 4C species. This is surprising considering that the Co–OH_2 bond of Co(II)Cbi^{+} is significantly weaker than the Co–DMB bond of Co(II)Cbl.[25, 27, 35-37] Spectroscopic studies of *Se*EutT revealed that the divalent metal ion is essential for the conversion of Co(II)Cbl to a 4C species, presumably by properly organizing a putative DMB binding pocket.[35]

However, the EutT enzyme from *Listeria monocytogenes* (*Lm*EutT) lacks this divalent metal-binding motif, which exemplifies an interesting phylogenetic divergence amongst the EutT enzymes. As *Lm*EutT does not require a divalent metal cofactor for activity, we sought to expand our understanding of the catalytic mechanisms employed by ACATs through spectroscopic studies of this enzyme. Specifically, we have employed electronic absorption (Abs), MCD, and EPR spectroscopic techniques to probe the interaction of Co(II)Cbl and Co(II)Cbi^+ with *Lm*EutT in the absence and presence of co-substrate ATP.

A.3 MATERIALS AND METHODS

Cofactors and Chemicals. Dicyanocobinamide [$(CN)_2$Cbi], hydroxocobalamin hydrochloride [HOCbl•HCl], sodium borohydride ($NaBH_4$), and potassium formate (HCOOK) were purchased from Sigma-Aldrich and used without further purification. Diaquacobinamide [$(H_2O)_2Cbi_2^+$] was prepared from $(CN)_2$Cbi according to the following procedure. About 3−5 mg of $(CN)_2$Cbi was dissolved in 5 mL of Milli-Q water and sparged for 60 min with N_2. The red-purple solution was then transferred via cannula to a sealed vial containing ∼27 mg of $NaBH_4$ and left stirring overnight under a slow stream of N_2. The resulting brown-purple solution was reoxidized in air over several hours. Once fully oxidized, the solution was loaded onto a C18 Sep Pak column, washed with (i) ultrapure water (30 mL), (ii) a 20% methanol solution until the orange-colored band moved toward the eluting end of the column, and (iii) again with ultrapure water (10 mL), and finally eluted with 100% methanol. Purified $(H_2O)_2Cbi_2^+$ was collected under vacuum. Co(II)Cbl and Co(II)Cbi^+ were generated anaerobically by the reduction of aqueous solutions of HOCbl and $(H_2O)_2Cbi_2^+$ with ∼40−60 μL of a saturated aqueous solution of HCOOK. The progress of the reduction was monitored spectrophotometrically.

Protein preparation and purification. *Lm*EutT was prepared as described elsewhere.[38] BL21-CodonPlus cells (Agilent) containing pEUT140 (pTEV18 with *Lm*EutT) were grown at 37 °C in 4 L flasks with metal springs containing 2 L of Terrific Broth media.[39] At an OD_{600} = 0.5-0.6, *eutT* gene expression was induced with 1 mM *β*-D-1-thiogalactopyranoside, and the culture was incubated at 15 °C for 30 hours. The harvested cells were pelleted at 6,000*g* in a refrigerated Avanti J-20 XPI with a JLA 8.1 rotor and re-suspended at 4 °C in buffer A [50 mM, 2-[4-(2-hydroxyethyl)piperazin-1-yl]ethanesulfonic acid (HEPES), 500 mM NaCl, 1 mM tris(2-carboxyethyl)phosphine (TCEP), and 20 mM imidazole, pH 7.5] with 1 mg/mL lysozyme and 0.1 mg/mL DNase. The suspension was subsequently passed through a cell press at 1.91 kPa and phenylmethysulfonyl fluoride (PMSF, 1 mM) was added immediately after lysis. This sample was centrifuged in an Avanti J-25I centrifuge equipped with a JA 25.50 rotor at 40,000*g* for 30 min at 4 °C and filtered with a 0.45 μm filter. The collected lysate was loaded onto a 5 mL HisTrap Fast Flow (GE) column equilibrated with buffer A. Protein was eluted with an imidazole gradient (20-500). The His_6-tag was cleaved by incubating the solution with recombinant tobacco etch virus (rTEV) protease[40] for 3 hours at room temperature, and the resulting protein sample was dialyzed three times against 1 L of buffer A. Further purification was achieved by loading protein onto the same column re-equilibrated with buffer A and collecting the flow-through. The collected fractions were concentrated to a protein concentration of 1.1 mM and dialyzed three times against storage buffer (20 mM phosphate buffer, 200 mM NaCl, pH 7.5) at 4 °C. The purity of the protein was determined using an SDS-PAGE gel and by analyzing the data with a 1D gel analysis software. For magnetic circular dichroism (MCD) spectroscopy, equivolume protein and 100% glycerol were mixed to produce a final sample containing 550 μM *Lm*EutT, 50% glycerol, 10 mM

phosphate buffer, 100 mM NaCl, pH 7.5. For electron paramagnetic resonance (EPR) spectroscopy, *Lm*EutT was diluted to ~500 μM in the same phosphate buffer.

Sample preparation. Under anoxic conditions in a glove box, purified protein samples (300-700 μM) in 20 mM phosphate buffer with 200 mM NaCl at pH 7.5 in 55-60% (v/v) glycerol were complexed with Co(II)Cbl or $Co(II)Cbi^+$ at a cofactor to protein ratio of 0.9:1 (for MCD) and 0.7:1 (for EPR). Varying equivalents of MgATP were added to the different MCD and EPR samples, as noted in the corresponding figure captions. The solutions were then injected into MCD sample cells or EPR tubes and frozen in liquid nitrogen (LN_2) either immediately (EPR samples) or after collecting room temperature Abs data (MCD samples).

Spectroscopy. X-band EPR spectra were collected on a Bruker ESP 300E spectrometer equipped with an Oxford ESR 900 continuous-flow liquid helium cryostat and an Oxford ITC4 temperature controller. All spectra were collected at 20 K using the following instrument settings: frequency = 9.38 GHz, microwave power = 2.0 mW, gain = 40-60 dB, modulation amplitude = 5 G, conversion time = 87 ms, time constant = 327.68 ms, range = 600-4598 G, resolution = 2048 points and modulation frequency = 100kHz. Simulated EPR spectra were fitted using the SIMPOW program written by Dr. Mark Nilges.[41]

Room temperature Abs spectra were obtained using a Varian Cary 5e spectrophotometer. The sample compartment was purged with $N_2(g)$ for 40 min prior to data collection. Frozen solution Abs and MCD spectra were collected with a JASCO J-715 spectropolarimeter in conjunction with an Oxford Instruments SM-4000 8 T superconducting magnetocryostat. Circular dichroism and glass-strain contributions to the MCD spectra were removed by taking the difference between spectra obtained with the magnetic field oriented parallel and anti-parallel to the light of propagation axis. Sample conditions are listed in the caption of each figure.

A.4 RESULTS

Abs and MCD Data. To probe the interaction between the corrinoid substrate and the *Lm*EutT active site, we have conducted a series of Abs, MCD and EPR spectroscopic studies of Co(II)Cbl and Co(II)Cbi$^+$ in the absence and presence of *Lm*EutT both before and after the addition of co-substrate MgATP. The 4.5 K Abs spectrum of free, 5C base-on Co(II)Cbl in aqueous solution is dominated by intense features associated primarily with $\pi \rightarrow \pi^*$ transitions localized on the corrin ring (Figure A.3, panel A). The prominent feature at ~21 000 cm^{-1} (~476 nm), referred to as the α band, was previously assigned as the lowest energy corrin-based $\pi \rightarrow \pi^*$ transition, while the steady increase in Abs intensity between 17 000 and 19 000 cm^{-1} was attributed to metal-to-ligand charge transfer (MLCT) transitions involving the occupied Co(II) 3d- and empty corrin π^*-based molecular orbitals (MOs).[42, 43] In the corresponding MCD spectrum, at least two positively signed features are present this region. Additionally, several derivative-shaped MCD features are observed between 14 000 and 17 000 cm^{-1} that were assigned as electronic excitations from the doubly occupied Co $3d_{xz}$ and $3d_{yz}$ based-MOs to the singly occupied, redox active Co-$3d_z2$-based MO based on time-dependent density functional theory (TD-DFT) calculations.[42, 44, 45]

When a small excess of *Lm*EutT was added to a sample of Co(II)Cbl, the low-temperature (LT) Abs and MCD spectra changed minimally (Figure A.3, panel B), indicating that Co(II)Cbl may not bind to the *Lm*EutT active site in the absence of co-substrate MgATP. In contrast, upon the addition of a slight excess (1.3 equiv.) of MgATP to a sample containing Co(II)Cbl and *Lm*EutT in a 0.9:1.0 molar ratio, an immediate color change (from orange-red to yellow) was observed that correlates with the blue-shift of the α band in the LT Abs spectrum by ~500 cm^{-1} (to 464 nm, Figure A.3, panel C). As the donor MO for the α band transition has a significant

antibonding contribution from the Co $3d_z2$ and N(DMB) $2p_z$ orbitals, a blue shift of the α band is symptomatic of a weakening of the axial Co-ligand bond.[29, 35, 45] The magnitude of this blue-shift is marginally smaller (by ~33 cm^{-1}) than the corresponding shift observed when Co(II)Cbl binds to the *Se*EutT/MgATP complex, but larger (by ~100 cm^{-1}) than those reported for Co(II)Cbl binding to *Lr*PduO/MgATP and *Se*CobA/MgATP.

The MCD spectrum of Co(II)Cbl bound to the *Lm*EutT/MgATP complex is characteristic of 4C Co(II)rrinoid species. On the basis of previous studies,[26, 27, 35, 36] the sharp features below 15 000 cm^{-1} can be attributed to the electronic origin (δ band at 12 560 cm^{-1}) and a vibrational sideband (β band at 14 014 cm^{-1}) associated with the $3d_x2\text{-}_y2 \rightarrow 3d_z2$ LF transition of 4C Co(II)Cbl.[36] The weak feature at 13 144 cm^{-1} (highlighted by *) likely corresponds to the first member of a vibrational progression involving a ~575 cm^{-1} corrin mode.[46] Conversely, the high energy (> 20 000 cm^{-1}) region is characterized by broad, both positively and negatively signed features that can be attributed to MLCT and $\pi \rightarrow \pi^*$ transitions.[25, 29] The lack of any residual features from 5C base-on Co(II)Cbl in these spectra reveals that nearly full (> 98%) conversion of the 5C base-on Co(II)Cbl to a 4C species occurred. Intriguingly, this near complete conversion at just over 1 equiv of MgATP observed for *Lm*EutT is unprecedented, as neither *Se*EutT nor any of the other ACATs studied to date achieve such a high conversion yield even in the presence of excess MgATP.

Because the Abs spectra of corrinoids are dominated by features originating from corrin-based $\pi \rightarrow \pi^*$ transitions, it is unsurprising that the Abs spectrum of free Co(II)Cbi^+ is similar to that of Co(II)Cbl (Figure A.4, panel A). Yet, the MCD spectra of free Co(II)Cbi^+ and Co(II)Cbl are markedly different, which reflects differences in the Co 3d orbital splittings and highlights the power of this technique to probe geometric changes around the metal center of Co(II)rrinoid

species. Upon incubation of Co(II)Cbi$^+$ with *Lm*EutT, no changes to the MCD spectrum are apparent, indicating that *Lm*EutT, like *Se*Eut*T*,[35] is unable to bind Co(II)Cbi$^+$ in the absence of ATP (Figure A.4, panel B). Even when a large excess (10 equiv.) of MgATP was added to a Co(II)Cbi$^+$ sample incubated with *Lm*EutT, the color remained unchanged and minimal changes to the Abs spectrum were observed (Figure A.4, panel C). However, close inspection of the corresponding MCD spectra reveals that the Co(II)Cbi$^+$ does in fact interact with the enzyme, as evidenced by the modest (~295 cm^{-1}) red-shift of the lowest energy feature centered at 16 388 cm^{-1} (Figure A.4, panel C) that can be attributed to a slight elongation of the lower axial Co – OH_2 bond.[29] Overall, these data provide compelling evidence that *Lm*EutT, similar to *Se*EutT,[35] is unable to convert Co(II)Cb$^+$ to a 4C species.

EPR Data. To complement our electronic Abs and MCD data, we performed parallel studies using X-band EPR spectroscopy. As the unpaired electron of Co(II)Cbl and Co(II)Cbi$^+$ resides in the Co $3d_z2$–based MO, EPR spectroscopy is uniquely sensitive to changes in the axial ligation of the Co(II) ion.[25, 42, 47] Consistent with our MCD data, the EPR spectra of Co(II)Cbl in the absence and the presence of *Lm*EutT are essentially identical (Figure A.5, panel A and B), with small *g* spreads and a broad, derivative-shaped feature centered at 2973 G. Fine structure arising from both ^{59}Co hyperfine coupling [A(Co) = 30, 40 and 305 Hz] and axial ^{14}N superhyperfine coupling [A_z(N^{14}) = 40 MHz] are clearly visible between 3000 and 3700 G. Upon addition of 1.3 equiv. MgATP to Co(II)Cbl incubated with *Lm*EutT, large changes to the EPR spectrum are observed, with numerous weak features appearing in the range between 600 and 4600 G (Figure A.5, panel C and Table A.1). On the basis of previous studies of other ACATs, these changes can be attributed to the loss of the axial DMB ligand from the Co(II) ion, which leads to enhanced spin-orbit mixing between the ground state and ligand field excited states and thus an increase in *g* anisotropy, as

well as a greater localization of the unpaired electron density on the Co(II) ion as reflected in the large A(Co) values.[26, 29, 35]

Interestingly, the small contributions from residual 5C Co(II)Cbl to the EPR spectrum of Co(II)Cbl in the presence of *Lm*EutT and MgATP between 2600 and 3700 G are characteristic of a base-off rather than a base-on Co(II)Cbl species (cf. Figure A.5, panel C and E). Base-off Co(II)Cbl (which is indistinguishable from Co(II)Cbi$^+$ by EPR spectroscopy) displays a larger g spread than base-on Co(II)Cbl (g_x = 2.48 vs g_x =2.26) and lacks axial superhyperfine coupling due to the substitution of the DMB base by a more weakly electron donating water molecule.[29] Consistent with these EPR data, a closer inspection of the MCD spectrum of Co(II)Cbl in the presence of *Lm*EutT and excess MgATP (Figure A.6) also reveals minor contributions from a small fraction of base-off Co(II)Cbl to the spectral region between 16 000 and 19 000 cm^{-1}. Addition of a larger excess (>10 equiv.) of MgATP did not noticeably change the relative populations of the 4C and 5C Co(II)Cbl species in the presence of *Lm*EutT and MgATP (Figure A.5, panel C and D; Table A.1), though the exact proportions are difficult to determine due to the large spread of the EPR features associated with 4C Co(II)Cbl.

The EPR spectra of Co(II)Cbi$^+$ in the absence and presence of *Lm*EutT are almost superimposable, which provides further evidence that this substrate analogue does not bind to the protein in the absence of MgATP (Figure A.7, panel A and B). Yet, the EPR spectrum of Co(II)Cbi$^+$ incubated with *Lm*EutT in the presence of a large excess of MgATP is slightly different from that of free Co(II)Cbi$^+$, with the most notable difference being the distinctly smaller hyperfine splittings compared to those observed for free Co(II)Cbi$^+$ (Table A.1). This result indicates that Co(II)Cbi$^+$ can bind to *Lm*EutT in the presence of MgATP (Figure A.7, panel C and Table A.1), as inferred from our MCD data. Notably, this enzyme-bound Co(II)Cbi$^+$ species is characterized

by *g* and *A* values that are more similar to those of the 5C base-off Co(II)Cbl species contributing to the EPR spectrum of Co(II)Cbl in the presence of *Lm*EutT and MgATP than of free Co(II)Cbi$^+$ (Table A.1).

A.5 DISCUSSION

Generation of 4C Co(II)rrinoid Species. ATP:Co(I)rrinoid adenosyltransferases are a group of enzymes involved in the *de novo* synthesis and scavenging of corrinoids to maintain adequate cellular levels of AdoCbl, a biological cofactor used in a variety of enzyme-mediated organic rearrangement and elimination reactions.[11, 12, 48 14, 18] The supernucleophilic 4C Co(I)rriniod species is the precursor for the formation of the Co–C bond of AdoCbl, and while the reductive environment of the cell can reduce Co(III) → Co(II), the Co(II) → Co(I)Cbl redox potential is too low for cellular reductants. To accomplish this, ACATs must be capable of performing the thermodynamically challenging Co(II) → Co(I)Cbl reduction. All ACATs studied to date have been shown to facilitate this reduction by converting the 5C Co(II)Cbl species, normally found in solution, to a unique 4C Co(II)Cbl intermediate in the presence of ATP.[14, 18, 26, 33, 34, 45, 49]

In the present study we have used MCD and EPR spectroscopies to investigate if the EutT-type ACAT from *Listeria monocytogenes* uses the same strategy for Co(II)→ Co(I)rrinoid reduction and to assess the substrate scope of this enzyme. Our data indicate that *Lm*EutT complexed with MgATP can bind Co(II)Cbl as well as Co(II)Cbi$^+$; however, similar to *Se*EutT,[35] this enzymes exclusively converts Co(II)Cbl, and not the Co(II)Cbi$^+$, to a 4C species. Compared to the other ACATs investigated thus far, *Lm*EutT more readily forms a 4C Co(II)Cbl species (>99% 5C→4C conversion yield) on addition of just over one molar equivalent of co-substrate MgATP.[26, 35, 36] In the case of the *Se*EutT, the inability to convert Co(II)Cbi$^+$ to a 4C species was attributed to the presence of a putative binding pocket for the nucleotide loop of Co(II)Cbl to

enhance its affinity for the native substrate and promote axial ligand dissociation.[22, 35] The EPR spectrum of Co(II)Cbl in the presence of the *Lm*EutT/MgATP complex reveals that in addition to the major 4C form, a minor 5C, base-off Co(II)Cbl species is generated (Figures A.5 and A.6). However, this species is unlikely to be catalytically relevant, as its relative population remained constant on addition of excess MgATP. Thus, unlike *Se*EutT, *Lm*EutT does not appear to generate a 5C, base-off intermediate in the process of 4C Co(II)Cbl formation.[35] This difference in substrate activation mechanism is unsurprising given that *Se*EutT requires a divalent metal cofactor for 4C Co(II)Cbl formation,[22, 35] while *Lm*EutT lacks this cofactor.

Table A.2 summarizes the 5C→ 4C Co(II)rrinoid conversion yields for various ACATs as determined by MCD spectroscopy. The most striking difference among the three ACAT families is that the EutT-type enzymes are unable to convert Co(II)Cbi$^+$ to a 4C species.[26, 29, 35, 36] The crystal structures of 4C Co(II)Cbl bound to *Se*CobA/MgATP and *Lr*PduO/MgATP revealed that these types of ACATs lack specific binding pockets for the DMB base (Figure A.2), which allows them to convert both Co(II)Cbl and Co(II)Cbi$^+$ to 4C species.[31, 45] The higher conversion yields with Co(II)Cbi$^+$ (~50% *Lr*PduO, ~70% *Se*CobA) compared to the substrate Co(II)Cbl (~40% *Lr*PduO, 8% *Se*CobA) can be attributed to the more facile removal of the weakly bound water ligand in Co(II)Cbi$^+$ compared to the DMB base in Co(II)Cbl. The high substrate promiscuity displayed by CobA-type ACATs is consistent with the role of these enzymes as part of the machinery used in the *de novo* biosynthesis of AdoCbl, where scavenging of incomplete corrinoids is likely.[19]

Nature of 4C Co(II)rrinoid Species. All ACATs studied to date raise the Co(II)/Co(I)rrinoid reduction potential to within the physiologically accessible range by generating 4C species, which leads to a stabilization of the "redox-active" Co $3d_z2$ -based MO.[29, 42] Experimental evidence for

this orbital stabilization is provided by large shifts of the g_x and g_y values from the free electron value (2.0233) due to enhanced spin-orbit coupling between the ground state and low lying LF (Co $3d_{xz} \rightarrow 3d_z2$ and $3d_{yz} \rightarrow 3d_z2$) excited states.[25, 29] Additionally, the increased localization of the unpaired electron spin density on the Co(II) ion is reflected in the larger $A(^{59}Co)$ hyperfine coupling constants for the 4C Co(II)rrinoid species compared to their 5C counterparts.[35] Interestingly, the 4C Co(II)Cbl species produced in the active sites of *Lm*EutT and *Se*EutT are characterized by much larger $A(^{59}Co)$ hyperfine coupling constants and *g* shifts than those generated by the PduO and CobA type ACATs [$A(^{59}Co)$ EutT ≈ 600–1300 MHz vs $A(^{59}Co)$ PduO/CobA ≈ 600-800 MHz) and g_x (EutT) ≈ 3.6 vs g_x (PduO/CobA) ≈ 2.7].[26, 35, 36] Furthermore, compared to the CobA and PduO-type ACATs, the *g*-tensors of the 4C Co(II)Cbl species generated in the EutT enzymes are much more rhombic ($g_x >> g_y > g_z$), signifying a unique active site environment in the EutT-type ACATs.[35]

In the crystal structures of 4C Co(II)Cbl bound to *Lr*PduO/MgATP and *Se*CobA/MgATP, the corrin ring is relatively planar.[16, 31] Computational studies suggested that for a planar corrin ring conformation, the unpaired electron of 4C Co(II)Cbl resides in the Co $3d_z2$ -based MO that has large and roughly equal contributions from the Co $3d_{xy}$ and Co $3d_{yz}$ orbitals. This prediction is consistent with the relatively axial *g*-tensors displayed by the 4C Co(II)Cbl species in the *Lr*PduO and *Se*CobA active sites.[29] Thus, the rhombic *g*-tensors exhibited by the EutT-bound 4C Co(II)Cbl species likely reflect a severely constrained conformation of the corrin ring in these enzymes, which would lift the near degeneracy of the Co $3d_{xz}$ and Co $3d_{yz}$-based MOs and result in very different g_x and g_y values. This finding suggests that the corrinoid substrate is firmly locked in place in the EutT active site, which is expected to facilitate the removal of the nucleotide loop during 4C Co(II)Cbl formation.

The results obtained in this study indicate that *Lm*EutT employs a different mechanism than *Se*EutT for controlling the timing of Co(II)Cbl binding and its subsequent conversion to a 4C species. While *Se*EutT can bind Co(II)Cbl in the absence of ATP and convert it to a 5C base-off species with an axial water ligand (Figure A.8, panel A), *Lm*EutT must first bind ATP and then Co(II)Cbl, which is directly converted to a 4C species (Figure A.8, panel B). Given the identical substrate specificities of *Lm*EutT and *Se*EutT, it is reasonable to suggest that both enzymes possess similar nucleotide binding pockets, though in the case of *Se*EutT the architecture of this putative binding pocket appears to change in response to Fe(II) or Zn(II) ion binding.[35] While the exact role of the divalent metal cofactor of *Se*EutT remains unclear, the fact that the Fe(II)-bound enzyme is deactivated in the presence of molecular oxygen suggests that it may serve as a redox sensor to control the levels of AdoCbl generated under aerobic and anaerobic conditions. The absence of this metal cofactor in LmEutT exemplifies an interesting phylogenetic divergence among the EutT enzymes investigated so far.

A.6 REFERENCES

1. Garsin, D. A., Ethanolamine utilization in bacterial pathogens: roles and regulation. *Nature Reviews Microbiology* **2010,** *8* (4), 290-295.

2. Chang, G. W.; Chang, J. T., Evidence for the B12-dependent enzyme ethanolamine deaminase in Salmonella. *Nature* **1975,** *254* (5496), 150-151.

3. Del Papa, M. F.; Perego, M., Ethanolamine activates a sensor histidine kinase regulating its utilization in Enterococcus faecalis. *Journal of bacteriology* **2008,** *190* (21), 7147-7156.

4. Blackwell, C. M.; Scarlett, F. A.; Turner, J. M., Ethanolamine catabolism by bacteria, including Escherichia coli. Portland Press Limited: 1976.

5. Randle, C. L.; Albro, P. W.; Dittmer, J. C., The phosphoglyceride composition of Gram-negative bacteria and the changes in composition during growth. *Biochimica et Biophysica Acta (BBA)-Lipids and Lipid Metabolism* **1969,** *187* (2), 214-220.

6. Ansell, G. B.; Hawthorne, J. N.; Dawson, R. M. C., Form and function of phospholipids. **1973**.

7. Larson, T. J.; Ehrmann, M.; Boos, W., Periplasmic glycerophosphodiester phosphodiesterase of Escherichia coli, a new enzyme of the glp regulon. *Journal of Biological Chemistry* **1983,** *258* (9), 5428-5432.

8. Proulx, P.; Fung, C. K., Metabolism of phosphoglycerides in E. coli IV. The positional specificity and properties of phospbolipase A. *Canadian journal of biochemistry* **1969,** *47* (12), 1125-1128.

9. Bradbeer, C., The clostridial fermentations of choline and ethanolamine I. Preparation and properties of cell-free extracts. *Journal of Biological Chemistry* **1965,** *240* (12), 4669-4674.

10. Jones, P. W.; Turner, J. M., Interrelationships between the enzymes of ethanolamine metabolism in Escherichia coli. *Microbiology* **1984,** *130* (2), 299-308.

11. Banerjee, R., Ed., Chemistry and Biochemistry of B_{12}. John Wiley & Sons, INC: New York, NY, 1999.

12. Banerjee, R., Radical peregrinations catalyzed by B-12 enzymes. *Biochemistry* **2001,** *40* (29), 8634-8634.

13. Banerjee, R.; Ragsdale, S. W., The many faces of vitamin B_{12}: Catalysis by cobalamin-dependent enzymes. *Annual Review of Biochemistry* **2003,** *72*, 209-247.

14. Mera, P. E.; Escalante-Semerena, J. C., Multiple roles of ATP: cob (I) alamin adenosyltransferases in the conversion of B12 to coenzyme B12. *Applied microbiology and biotechnology* **2010,** *88* (1), 41-48.

15. Mera, P. E.; St Maurice, M.; Rayment, I.; Escalante-Semerena, J. C., Structural and functional analyses of the human-type corrinoid adenosyltransferase (PduO) from Lactobacillus reuteri. *Biochemistry* **2007,** *46* (48), 13829-13836.

16. Mera, P. E.; St Maurice, M.; Rayment, I.; Escalante-Semerena, J. C., Residue Phe112 of the Human-Type Corrinoid Adenosyltransferase (PduO) Enzyme of Lactobacillus reuteri Is Critical to the Formation of the Four-Coordinate Co(II) Corrinoid Substrate and to the Activity of the Enzyme. *Biochemistry* **2009,** *48* (14), 3138-3145.

17. Johnson, C. L. V.; Pechonick, E.; Park, S. D.; Havemann, G. D.; Leal, N. A.; Bobik, T. A., Functional genomic, biochemical, and genetic characterization of the Salmonella pduO gene, an ATP: cob (I) alamin adenosyltransferase gene. *Journal of bacteriology* **2001,** *183* (5), 1577-1584.

18. Warren, M. J.; Raux, E.; Schubert, H. L.; Escalante-Semerena, J. C., The biosynthesis of adenosylcobalamin (vitamin B12). *Natural product reports* **2002,** *19* (4), 390-412.

19. Escalante-Semerena, J. C.; Suh, S. J.; Roth, J. R., cobA Function is required for both de novo cobalamin biosynthesis and assimilation of exogenous corrinoids in Salmonella typhimurium. *Journal of Bacteriology* **1990,** *172*, 273-280.

20. Moore, T. C.; Mera, P. E.; Escalante-Semerena, J. C., The EutT enzyme of Salmonella enterica is a unique ATP: cob (I) alamin adenosyltransferase metalloprotein that requires ferrous ions for maximal activity. *Journal of bacteriology* **2014,** *196* (4), 903-910.

21. Buan, N. R.; Suh, S.-J.; Escalante-Semerena, J. C., The eutT gene of Salmonella enterica encodes an oxygen-labile, metal-containing ATP: corrinoid adenosyltransferase enzyme. *Journal of bacteriology* **2004,** *186* (17), 5708-5714.

22. Pallares, I. G.; Moore, T. C.; Escalante-Semerena, J. C.; Brunold, T. C., Spectroscopic Studies of the EutT Adenosyltransferase from *Salmonella enterica*: Evidence for a Tetrahedrally Coordinated Divalent Transition Metal Cofactor with Cysteine Ligation. *Biochemistry* **2016,** *under review*.

23. Pallares, I. G.; Moore, T. C.; Escalante-Semerena, J. C.; Brunold, T. C., Spectroscopic Studies of the Salmonella enterica Adenosyltransferase Enzyme SeCobA: Molecular-Level Insight into the Mechanism of Substrate Cob(II)alamin Activation. *Biochemistry* **2014,** *53* (50), 7969-7982.

24. Pallares, I. G.; Moore, T. C.; Escalante-Semerena, J. C.; Brunold, T. C., Spectroscopic Studies of the EutT Adenosyltransferase from *Salmonella enterica*: Mechanism of Four-Coordinate Co(II)Cbl Formation. *Journal of the American Chemical Society* **2016,** *138* (1), 3694-3704.

25. Brunold, T. C.; Conrad, K. S.; Liptak, M. D.; Park, K., Spectroscopically validated density functional theory studies of the B 12 cofactors and their interactions with enzyme active sites. *Coordination Chemistry Reviews* **2009,** *253* (5), 779-794.

26. Park, K.; Mera, P. E.; Escalante-Semerena, J. C.; Brunold, T. C., Kinetic and spectroscopic studies of the ATP: corrinoid adenosyltransferase PduO from Lactobacillus reuteri: substrate specificity and insights into the mechanism of Co (II) corrinoid reduction. *Biochemistry* **2008,** *47* (34), 9007.

27. Park, K.; Mera, P. E.; Moore, T. C.; Escalante-Semerena, J. C.; Brunold, T. C., Unprecedented Mechanism Employed by the Salmonella enterica EutT ATP: CoIrrinoid Adenosyltransferase Precludes Adenosylation of Incomplete CoIIrrinoids. *Angewandte Chemie International Edition* **2015,** *54* (24), 7158-7161.

28. Liptak, M. D.; Fleischhacker, A. S.; Matthews, R. G.; Telser, J.; Brunold, T. C., Spectroscopic and Computational Characterization of the Base-off Forms of Cob (II) alamin. *The journal of physical chemistry. B* **2009,** *113* (15), 5245.

29. Stich, T. A.; Buan, N. R.; Escalante-Semerena, J. C.; Brunold, T. C., Spectroscopic and computational studies of the ATP : Corrinoid adenosyltransferase (CobA) from Salmonella enterica: Insights into the mechanism of adenosylcobalamin biosynthesis. *Journal of the American Chemical Society* **2005,** *127* (24), 8710-8719.

30. Stich, T. A.; Yamanishi, M.; Banerjee, R.; Brunold, T. C., Spectroscopic evidence for the formation of a four-coordinate Co2+ cobalamin species upon binding to the human ATP: cobalamin adenosyltransferase. *Journal of the American Chemical Society* **2005,** *127* (21), 7660-7661.

31. Moore, T. C.; Newmister, S. A.; Rayment, I.; Escalante-Semerena, J. C., Structural Insights into the Mechanism of Four-Coordinate Cob(II)alamin Formation in the Active Site of the Salmonella enterica ATP:Co(I)rrinoid Adenosyltransferase Enzyme: Critical Role of Residues Phe91 and Trp93. *Biochemistry* **2012,** *51* (48), 9647-9657.

32. Faure, D.; Lexa, D.; Savéant, J.-M., Electrochemistry of vitamin B_{12}. *Journal of Electroanalytical Chemistry and Interfacial Electrochemistry* **1982,** *140*, 297-309.

33. Mera, P. E.; Escalante-Semerena, J. C., Dihydroflavin-driven Adenosylation of 4-Coordinate Co (II) Corrinoids ARE COBALAMIN REDUCTASES ENZYMES OR ELECTRON TRANSFER PROTEINS? *Journal of Biological Chemistry* **2010,** *285* (5), 2911-2917.

34. Liptak, M. D.; Brunold, T. C., Spectroscopic and computational studies of Co^{1+}cobalamin: Spectral and electronic properties of the "superreduced" B12 $cofacto_r$. *Journal of the American Chemical Society* **2006,** *128* (28), 9144-9156.

35. Pallares, I. G.; Moore, T. C.; Escalante-Semerena, J. C.; Brunold, T. C., Spectroscopic studies of the EutT adenosyltransferase from Salmonella enterica: Mechanism of four-coordinate Co (II) Cbl formation. *Journal of the American Chemical Society* **2016,** *138* (11), 3694.

36. Pallares, I. G.; Moore, T. C.; Escalante-Semerena, J. C.; Brunold, T. C., Spectroscopic Studies of the Salmonella Enterica Adenosyltransferase Enzyme Se CobA: Molecular-Level Insight into the Mechanism of Substrate Cob (II) alamin Activation. *Biochemistry* **2014,** *53* (50), 7969-7982.

37. Park, K.; Mera, P. E.; Escalante-Semerena, J. C.; Brunold, T. C., Kinetic and spectroscopic studies of the ATP: Corrinoid adenosyltransferase PduO from Lactobacillus reuteri: Substrate specificity and insights into the mechanism of Co(II)corrinoid reduction. *Biochemistry* **2008,** *47* (34), 9007-9015.

38. Costa, F. G.; Escalante-Semerena, J. C., A new class of EutT ATP:Co(I)rrinoid adenosyltransferases found in *Listeria monocytogenes* and other *Firmicutes* does not require a metal ion for activity. *Biochemistry* **2018,** *57* (34), 5076-5087.

39. Sambrook, J.; Fritsch, E. F.; Maniatis, T., *Molecular Cloning: A Laboratory Manual*. Second ed.; Cold Spring Harbor Laboratory: Cold Spring Harbor, N.Y., 1989.

40. Blommel, P. G.; Becker, K. J.; Duvnjak, P.; Fox, B. G., Enhanced bacterial protein expression during auto-induction obtained by alteration of *lac* repressor dosage and medium composition. *Biotechnol. Prog.* **2007,** *23*, 585-598.

41. Nilges, M. J. in Chemistry. University of Illinois, Urbana-Champaign, Il, 1979.

42. Stich, T. A.; Buan, N. R.; Brunold, T. C., Spectroscopic and computational studies of Co^{2+}corrinoids: Spectral and electronic properties of the biologically relevant base-on and base-off forms of Co^{2+}cobalamin. *Journal of the American Chemical Society* **2004,** *126* (31), 9735-9749.

43. Pratt, J. M., *Inorganic chemistry of vitamin B12*. London, UK, Academic Press Inc.(London) Ltd.: 1972.

44. Brooks, A. J.; Vlasie, M.; Banerjee, R.; Brunold, T. C., Co-C bond activation in methylmalonyl-CoA mutase by stabilization of the post-homolysis product Co^{2+}cobalamin. *Journal of the American Chemical Society* **2005,** *127* (47), 16522-16528.

45. Park, K.; Mera, P. E.; Escalante-Semerena, J. C.; Brunold, T. C., Spectroscopic Characterization of Active-site Variants of the PduO-type ATP: Corrinoid Adenosyltransferase from Lactobacillus reuteri: Insights into the Mechanism of four-coordinate Co (II) corrinoid formation. *Inorganic chemistry* **2012,** *51* (8), 4482.

46. Andruniow, T.; Zgierski, M. Z.; Kozlowski, P. M., Vibrational analysis of methylcobalamin. *The Journal of Physical Chemistry A* **2002,** *106* (7), 1365-1373.

47. in:, P. G.; (Ed)., Q. L. J., In *Physical Methods in Bioinorganic Chemistry*, Books, U. S., Ed. Sausalito, CA, 2000; p 121.

48. Banerjee, R., Radical carbon skeleton rearrangements: Catalysis by coenzyme B-12-dependent mutases. *Chemical Reviews* **2003,** *103* (6), 2083-2094.

49. Fonseca, M. V.; Escalante-Semerena, J. C., Reduction of cob(III)alamin to cob(II)alamin in Salmonella enterica serovar typhimurium LT2. *Journal of Bacteriology* **2000,** *182* (15), 4304-4309.

A.7 TABLES

Table A.1. Spin-Hamiltonian Parameters for Co(II)Cbl and Co(II)Cbi$^+$ in the Absence and Presence of *Lm*EutT and MgATP. Parameters for 4C species generated by *Lr*PduO[26], *Se*CobA[36],

Species	*g* values			*A* (^{59}Co)/MHz			*A* (^{14}N)/MHz
	g_x	g_y	g_z	A_x	A_y	A_z	A_{iso}
A) Co(II)Cbl							
base-on	2.269	2.232	2.004	40	30	302	49
B) Co(II)Cbl + *Lm*EutT							
base-on	2.269	2.233	2.001	40	30	306	49
C) Co(II)Cbl + *Lm*EutT + 1.3/10 equiv. MgATP							
4C species >80%	3.530	2.583	1.800	1265	558	700	n/a
Base-off <20%	2.438	2.300	1.990	210	195	386	
D) Co(II)Cbi$^+$							
Base-off	2.423	2.314	1.994	226	210	402	n/a
E) Co(II)Cbi$^+$ + *Lm*EutT							
Base-off	2.432	2.322	1.990	226	210	405	n/a
F) Co(II)Cbi$^+$ + *Lm*EutT + 10 equiv. MgATP							
Base-off	2.438	2.300	1.990	210	195	386	n/a
G) Co(II)Cbl + *Se*EutT(Zn) + MgATP							
4C species ~58%	3.610	2.553	1.800	1362	625	760	n/a
H) Co(II)Cbl + *Lr*PduO + MgATP							
4C species	2.720	2.700	1.900	595	755	770	n/a
I) Co(II)Cbl + *Se*CobA + MgATP							
4C species	2.730	2.670	2.060	635	590	805	n/a

and *Se*EutT[35] (G–I) are shown for comparison.

Table A.2. . 5C→ 4C Co(II)rrinoid conversion yields for various ACATs as determined by MCD Data taken from references as noted: *Lr*PduO[26], *Se*CobA[36], and *Se*EutT[35].

Species	% conversion (5C→ 4C)
Co(II)Cbl + *Lm*EutT + 1.2 equiv. ATP	>99
Co(II)Cbl + *Se*EutT (Fe/WT) + >10 equiv. ATP	>85
Co(II)Cbl + *Lr*PduO + ATP	~40
Co(II)Cbi^{+}+ *Lr*PduO + ATP	~50
Co(II)Cbl + *Se*CobA + ATP	~8
Co(II)Cbi^{+}+ *Se*CobA + ATP	~70

A.8 FIGURES

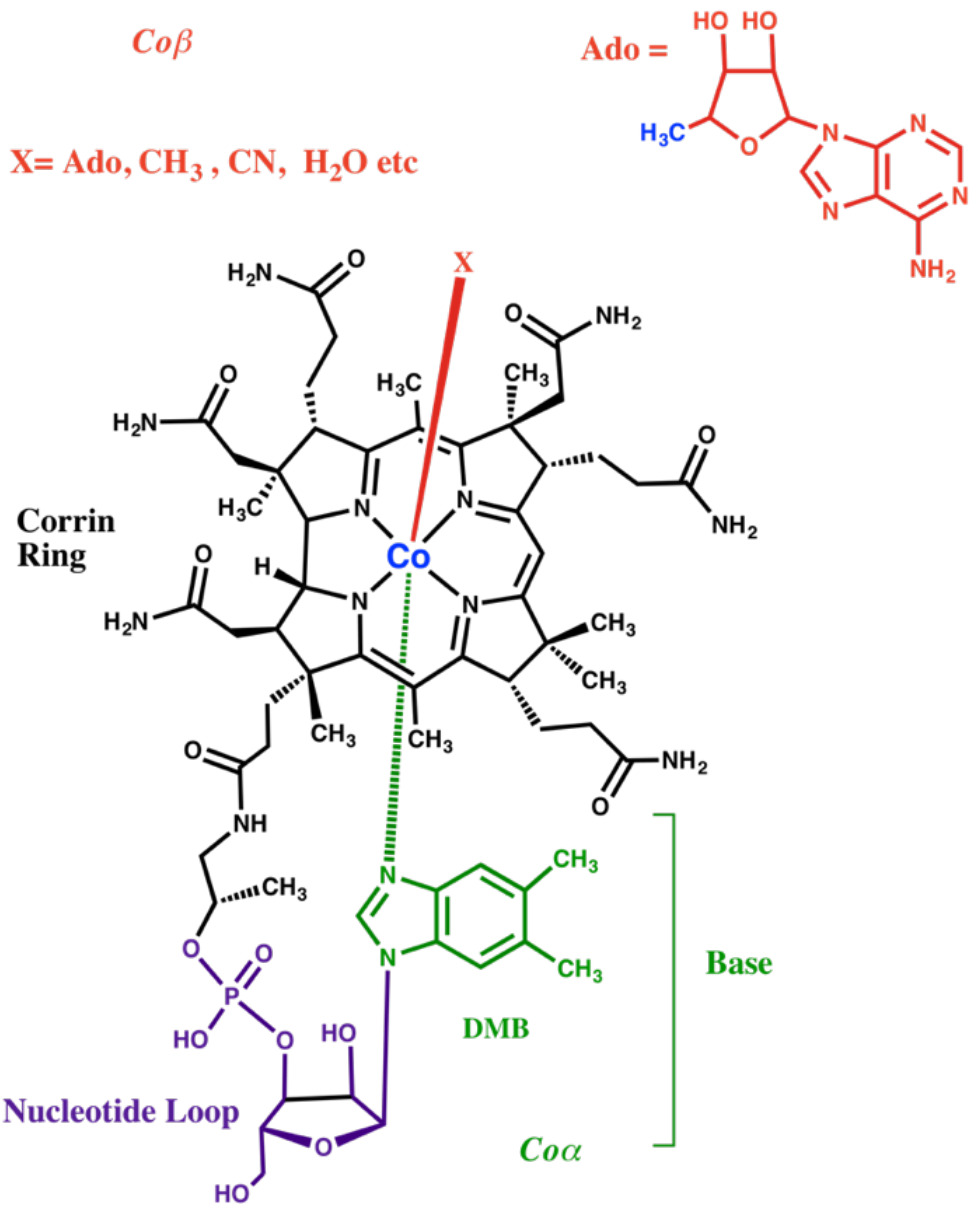

Figure A.1. Chemical structure of Cob(III)alamin species. In AdoCbl, the variable upper axial ligand, X, is Ado as indicated.

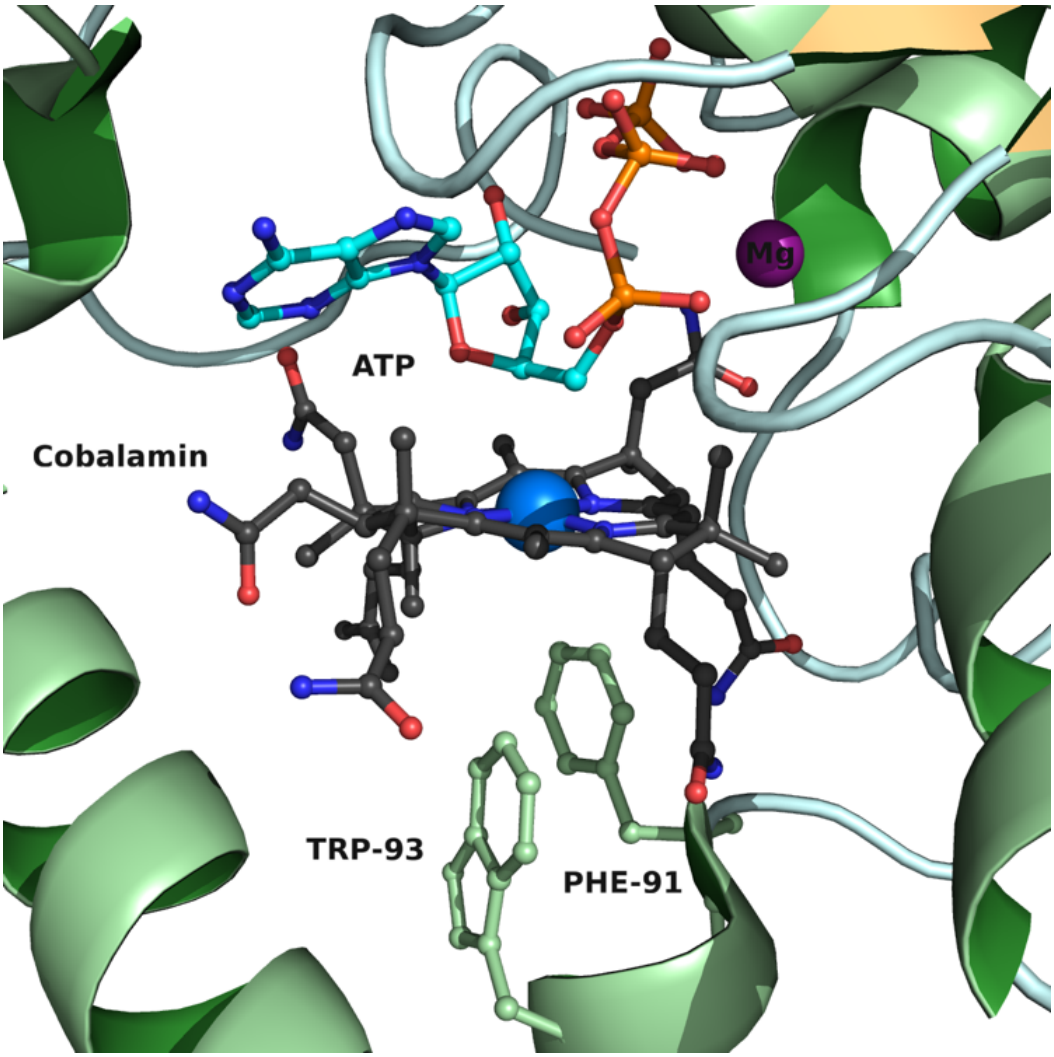

Figure A.2. X-ray crystal structure of 4C Co(II)Cbl (black) in the active site of *Se*CobA, with Mg-ATP (light blue) located above the corrin ring. Key hydrophobic residues are indicated (pale green) that block off the lower axial position. Note that the DMB base, aminopropanol linkage and nucleotide loop are not resolved in the crystal structure as they are likely solvent exposed.[31]

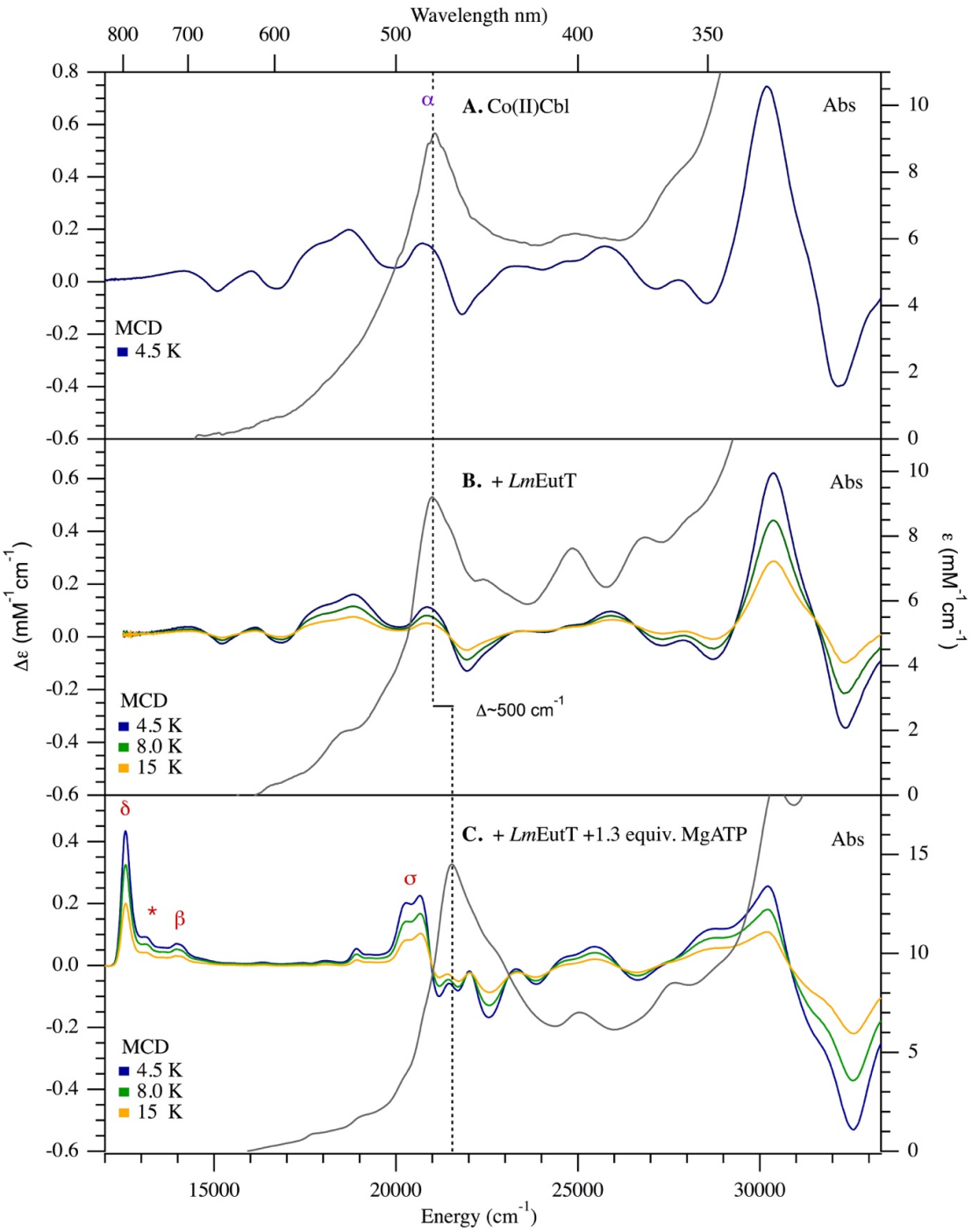

Figure A.3. Abs spectra at 4.5 K (gray traces) and variable temperature MCD spectra at 7 T of (A) free Co(II)Cbl, B) Co(II)Cbl in the presence of *Lm*EutT and C) Co(II)Cbl with 1.3 equiv. MgATP in the presence of *Lm*EutT. The dashed vertical line indicates the position of the α band.

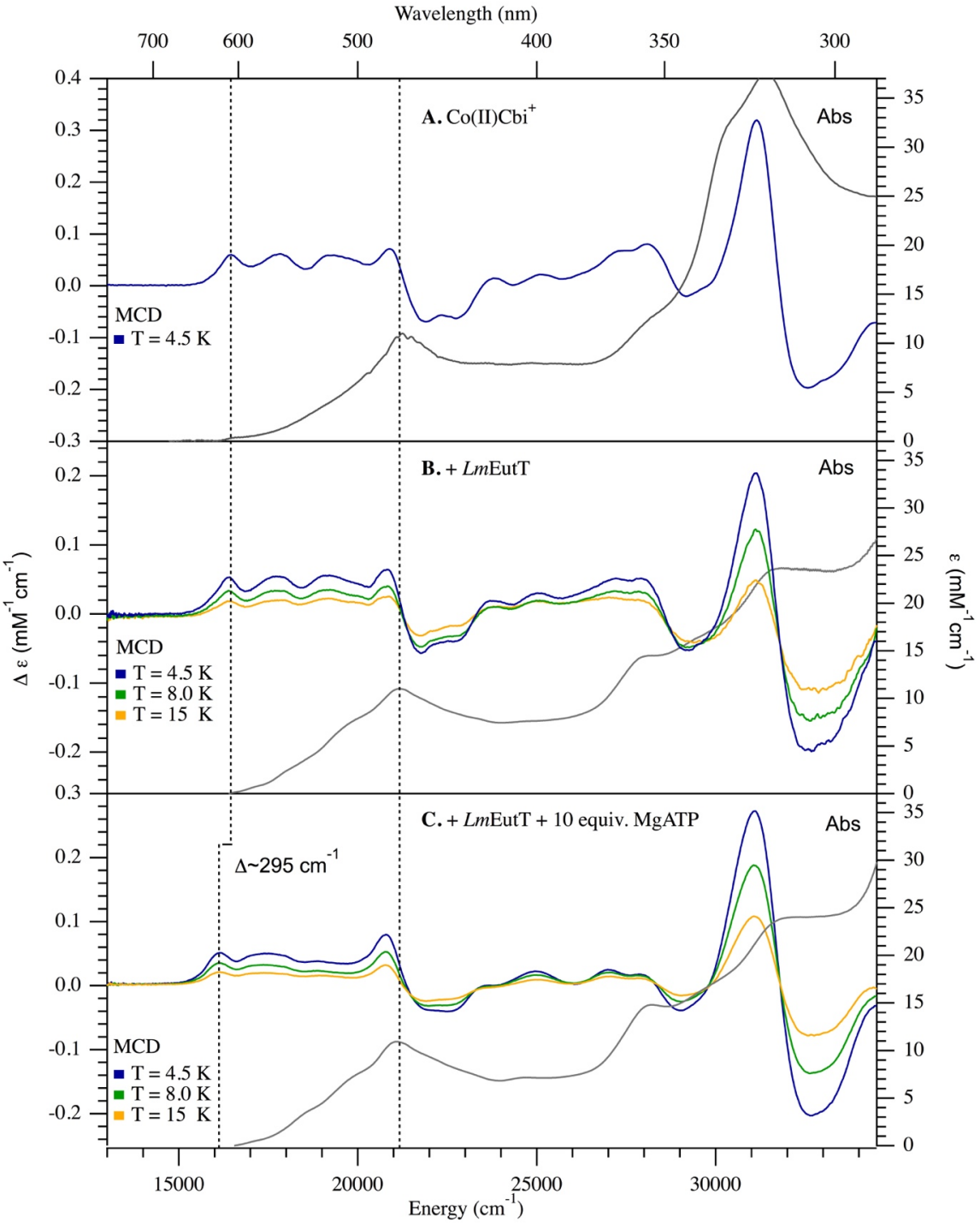

Figure A.4. Abs spectra at 4.5 K (gray traces) and variable temperature MCD spectra at 7 T of (A) free Co(II)Cbi$^+$, (B) Co(II)Cbi$^+$ in the presence of *Lm*EutT (C) Co(II)Cbi$^+$ in the presence of *Lm*EutT with 1.3 equiv. MgATP. The vertical lines indicate the position of the α band in the Abs spectra and the shift of the lowest energy feature in the MCD spectra.

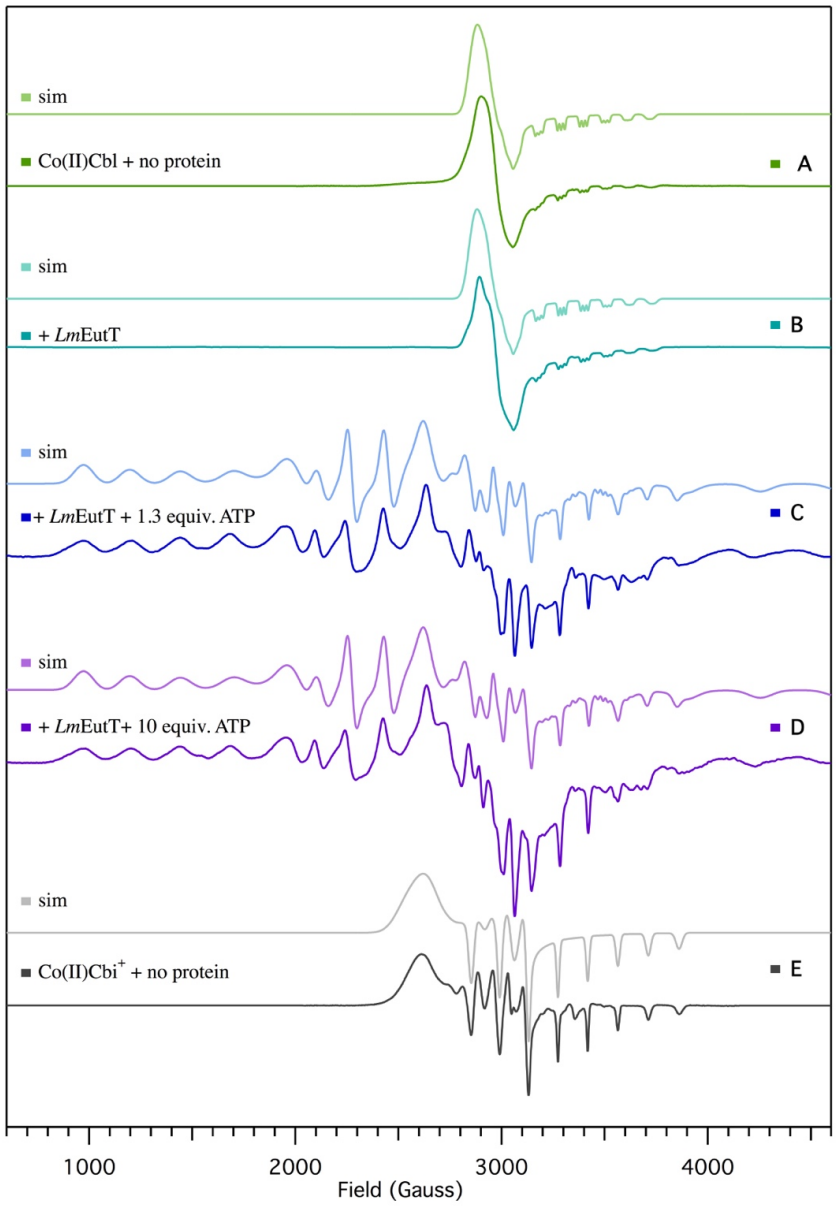

Figure A.5. EPR spectra collected at 20 K of A) free Co(II)Cbl (green), B) Co(II)Cbl incubated with *Lm*EutT (teal), C) Co(II)Cbl in the presence of *Lm*EutT and 1.3 equiv. MgATP (blue) or D) >10 equiv. MgATP (purple), and E) free Co(II)Cbi^{+} (gray). Spectra were simulated using the fit parameters provided in Table 1 (lighter colors).

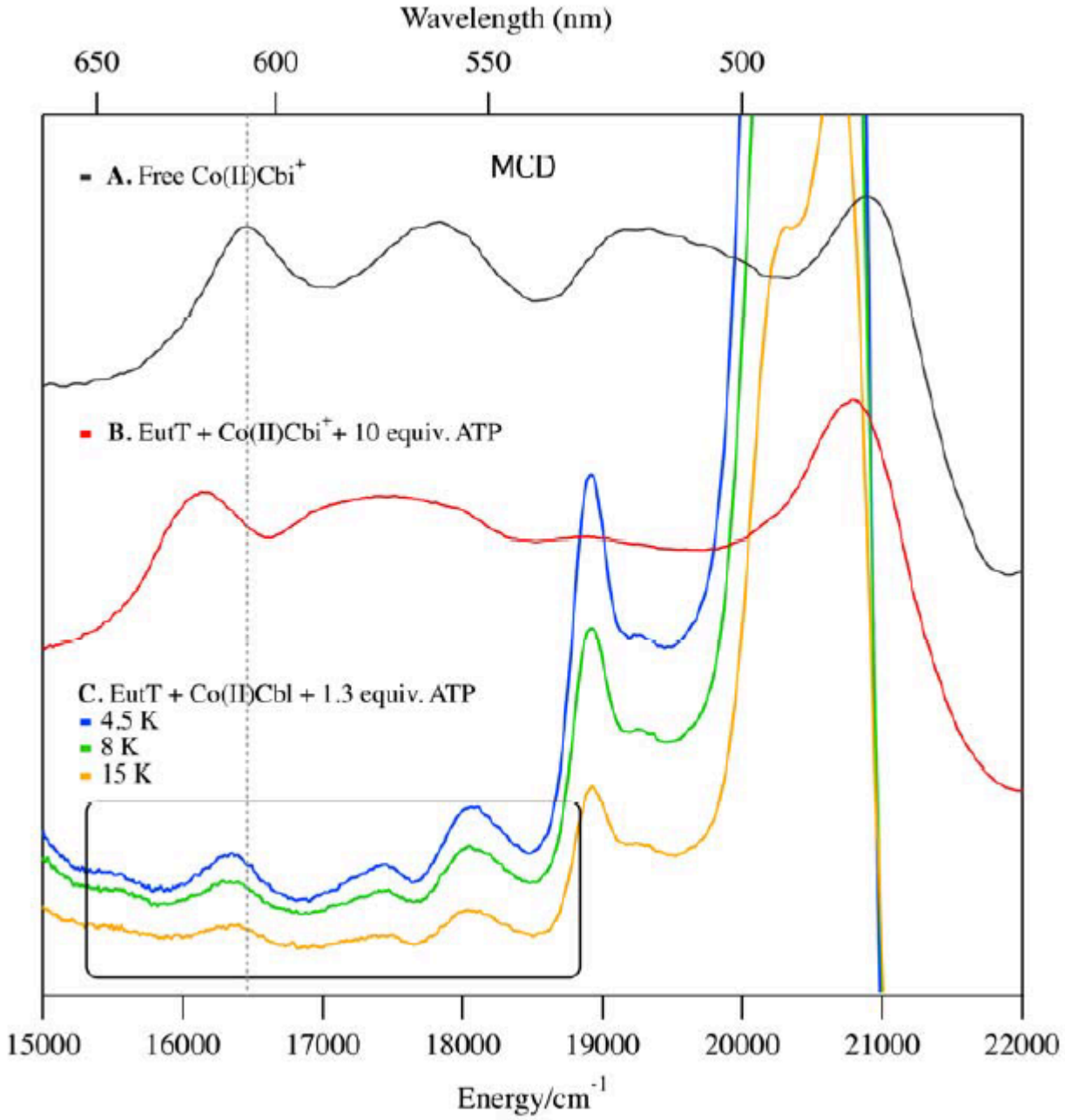

Figure A.6. MCD spectra at 4 K and 7 T of A) free Co(II)Cbi$^+$ (top, gray) and B) Co(II)Cbi$^+$ in the presence of *Lm*EutT and 10 equiv. MgATP (middle, red). The position of the lowest-energy feature in the spectrum of free Co(II)Cbi+ is indicated by a dashed vertical line. The variable temperature MCD spectra at 7 T of C) Co(II)Cbl complexed with LmEutT and 1.3 equiv. MgATP (bottom) reveal that a small fraction of base-off species is present under these conditions (boxed region)

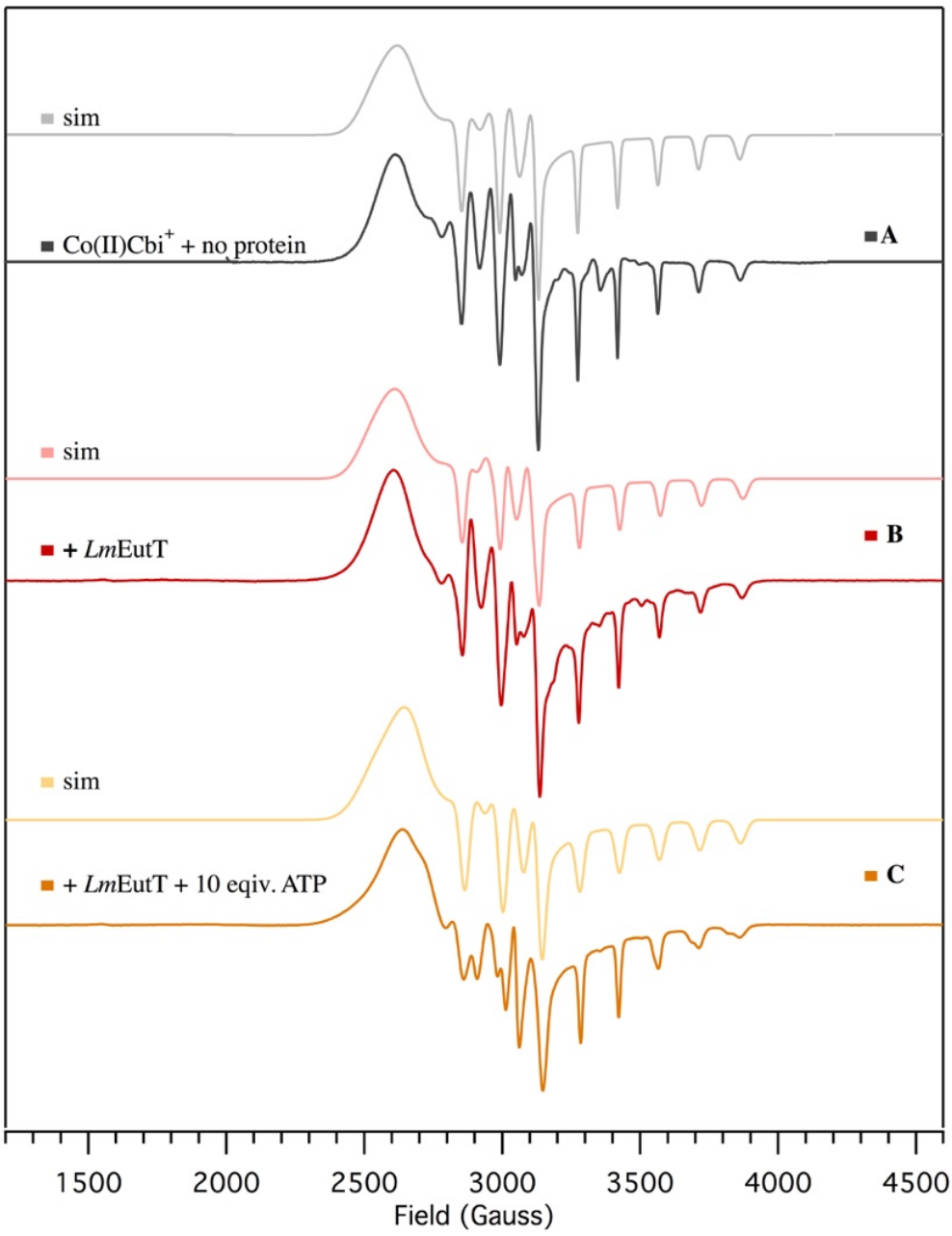

Figure A7. EPR spectra collected at 20 K of A) Co(II)Cbi$^+$ (gray), B) Co(II)Cbi$^+$ in the presence of *Lm*EutT (red), and C) Co(II)Cbi$^+$ in the presence of *Lm*EutT and 10 equiv. MgATP (gold). Spectra were simulated using the fit parameters provided in Table 1 (lighter colors).

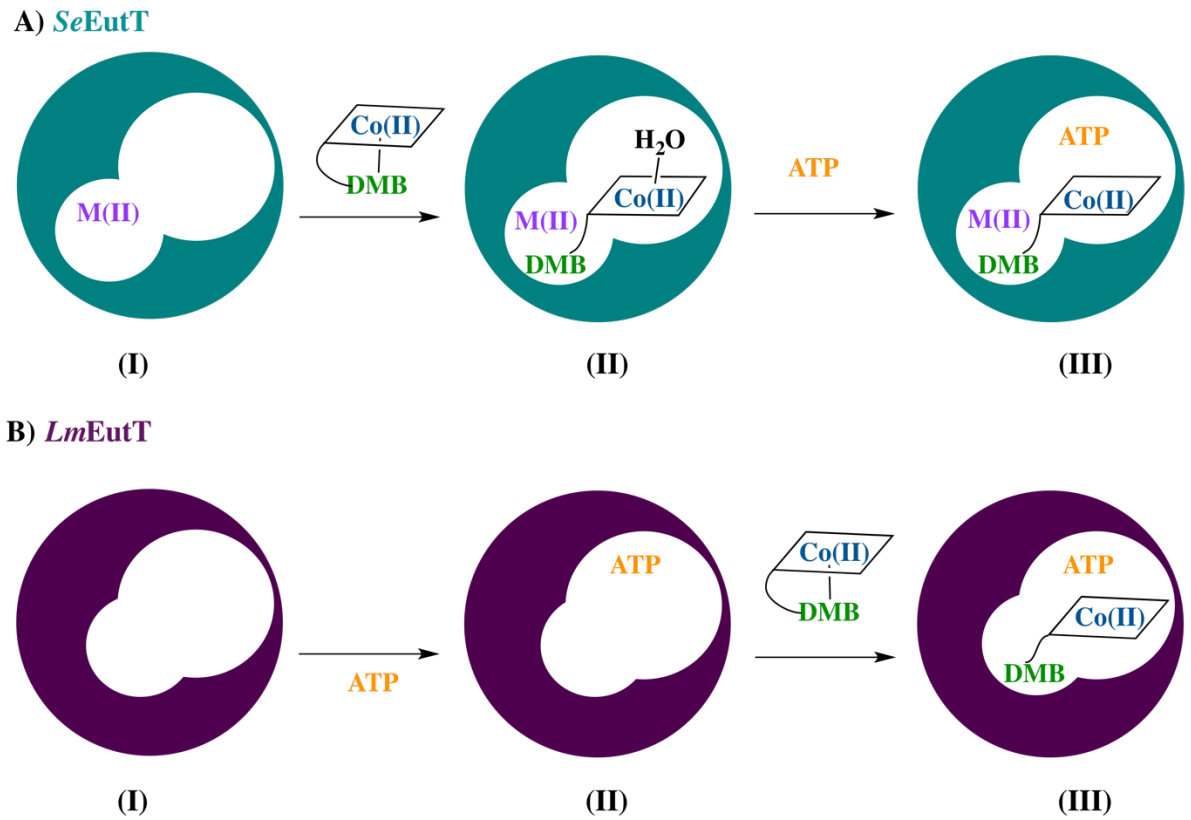

Figure A.8. Proposed mechanisms for generation of 4C Co(II)Cbl in the EutT ACATs. In the case of *Se*EutT (A) Co(II)Cbl can bind to the active site in the absence of ATP as long as the divalent metal cofactor is present (I) to yield a base-off species with an axial water ligand (II). This process is facilitated by the binding of the DMB tail to a specific protein pocket. The subsequent binding of ATP then triggers the formation of 4C Co(II)Cbl (III). For *Lm*EutT (B) that lacks a divalent metal cofactor (I), the enzyme must first bind ATP (II) and then Co(II)Cbl, which is directly converted to a 4C species whereby the DMB base is sequestered in a binding pocket (III).